THE SMALL GTPASE RAB35 IS A NOVEL ONCOGENIC REGULATOR OF PI3K/AKT SIGNALING

A Dissertation

Presented to the Faculty of the Weill Cornell Graduate School

of Medical Sciences

in Partial Fulfillment of the Requirements for the Degree of

Doctor of Philosophy

by

Douglas B. Wheeler

May 2015

THE SMALL GTPASE RAB35 IS A NOVEL ONCOGENIC REGULATOR OF PI3K/AKT SIGNALING

Douglas Berg Wheeler, Ph.D.

Cornell University 2015

The phosphatidylinositol 4,5-bisphosphate 3'-OH kinase (PI3K) is a lipid kinase that regulates cell survival, proliferation and metabolism in response to external growth factors. PI3K signaling regulates a diverse set of effectors via the phosphoinositide dependent kinase 1 (PDK1), AKT/PKB, and the mechanistic target of rapamycin complexes 1 and 2 (mTORC2). The components of this pathway are frequently mutated in human cancers, which give rise to oncogenic signals that drive tumorigenesis. As such, the proteins involved in PI3K/AKT signaling are attractive targets for targeted therapies.

It is thought that most tumors upregulate PI3K/AKT signaling in some way. However, a large portion of tumors do not have any identifiable genetic lesions in the genes that code for proteins that regulate this pathway. Thus, we reasoned that there are likely to be many proteins that regulate PI3K/AKT signaling that are currently unappreciated. To identify novel regulators of the PI3K axis, we undertook an arrayed loss-of-function RNAi screen using a library of shRNA reagents that targeted all known human kinases and GTPases to identify proteins whose depletion altered AKT phosphorylation. Further, we triaged genes from this screen using oncogenomic databases to identify screen hit genes that were mutated in human tumor samples or cell

lines. We reasoned that this approach could identify novel components of PI3K/AKT signaling that also play a role in tumorigenesis.

This screen identified the small GTPase RAB35 as a novel positive regulator of PI3K/AKT signaling. Depletion of RAB35 in a variety of human and murine cell lines suppressed phosphorylation of PI3K-dependent proteins like AKT, FOXO1/3A and NDRG1. Moreover, stable expression of a GTPase-deficient, constitutively active allele of RAB35—but not wildtype RAB35—potently activated AKT signaling in the absence of growth factors. Further, we identified two *RAB35* mutations in human tumor genome sequence databases that activated PI3K signaling and transformed NIH-3T3 cells *in vitro* in a PI3K-dependent manner. Finally, we find that RAB35 is likely regulating PI3K signaling by trafficking the platelet derived growth factor receptor (PDGFR) to a RAB7-positive compartment in the cell where the receptor actively signals PI3K. Thus, RAB35 is a novel oncogenic regulator of PI3K/AKT signaling.

BIOGRAPHICAL SKETCH

Douglas Berg Wheeler was born in 1981 in Utica, NY to Nancy Berg and Albert Charles Wheeler. Doug attended Poland Central School in Poland, NY for elementary, middle and high school. During high school, he participated annually in the Poland Central School and Utica College Science Fairs, which gave him an early taste for both biology and failure. After high school, Doug attended Hamilton College in Clinton, NY from 1999 to 2001, where he worked in the endocrinology lab of Dr. David A. Gapp. After two years at Hamilton, he transferred to Cornell University in Ithaca, NY in the fall of 2001. During his time at Cornell, he taught undergraduate Biochemistry (BIOBM 330) and worked in the lab of yeast geneticist Dr. Susan A. Henry. He graduated from Cornell in May, 2003 with a Bachelors of Science in Biology.

After his time at Cornell, Doug moved to Cambridge, MA and began working as a research technician in the lab of Dr. David M. Sabatini at the Whitehead Institute for Biomedical Research at the Massachusetts Institute of Technology. While at the Whitehead, he developed a tool for rapid, high-throughput loss-of-function RNA interference screens in *Drosophila* cells [3-4]. This technology—where RNA reagents are printed onto glass slides and cells seeded on these spots could be assayed for loss of gene function—spurred Doug's interest in high-throughput technology and the examination of gene function. Further, his time in the Sabatini lab sparked in Doug a desire to study the genes that regulate survival and growth in cancer cells.

After two years at the Whitehead, Doug moved to New York City in July of 2005 to begin his time at the Tri-Institutional MD/PhD program. During the two preclinical years of medical school, Doug decided that he wanted to start his graduate work with an RNAi screen to discover new components the PI3K/AKT signaling pathway. In July of 2007 he began his graduate work in the lab of Dr. Charles L. Sawyers at Memorial Sloan-Kettering Cancer Center. With the cooperation of Dr. Sawyers and Dr. Olaf S. Andersen, Doug was fortunate enough to concoct a thesis that allowed him to be mentored jointly by Dr. Sawyers and his previous mentor, Dr. Sabatini. Doug spent the first two and a half years of his graduate training primarily working at the Whitehead and Broad Institutes. While there, he performed the RNAi screens that nucleate this thesis. After finishing these screens, Doug returned to New York City in the beginning of 2010 to continue his thesis work full time in the Sawyers laboratory.

After six years in the lab, Doug will ultimately defend his Ph.D. in December of 2013, after which he will begrudgingly put down his pipettes and return to medical school. He is looking forward to spending the rest of his days studying cancer.

This dissertation is dedicated to my parents, Nancy Berg Wheeler and Albert Charles Wheeler. Without the two of them I would not have had the inquisitiveness or stubbornness that science demands. They have been very patient.

ACKNOWLEDGEMENTS

I would first like to thank the director of the Tri-Institutional MD/PhD program, Dr. Olaf Sparre Andersen. Without Dr. Andersen's willingness to allow me to pursue my interests, I would not have been able to design and carry out my thesis work the way I wanted to. In the middle of my second year of medical school, I approached Dr. Andersen with the idea for my thesis project—which involved me moving to Boston for an indeterminate amount of time. Rather than turn down my request, Dr. Andersen allowed me to return to the Whitehead Institute without any hesitation. I thank Dr. Andersen for his flexibility in allowing me to pursue my scientific interests.

I would also like to thank my two thesis advisors: Dr. David M. Sabatini and Dr. Charles L. Sawyers. I have known David since 2003, when I joined his lab as a technician. David has always encouraged my pursuit of science, and his passion and excitement for biology are contagious. Moreover, his sense of humor taught me that science can be fun, even when the results are not. I also thank my MSKCC mentor, Dr. Charles Sawyers, for being willing to take me on as a graduate student when I approached him to ask if I could be in his lab, but from a distance. In the years that Dr. Sawyers has been my thesis advisor, I have come to admire his sense of humor, his patience, and his dedication to helping cancer patients with translational science and medicine.

Further, I would like to extend my thanks to my thesis committee members for their patience, scientific insights, and flexible schedules: Dr.

Scott C. Blanchard, Dr. Robert Darnell, Dr. Timothy E. McGraw, Dr. Neal Rosen and Dr. Agata Smogorzewska. Each member of my committee has been generous in sharing their time and wisdom with me. They stand as examples of busy faculty who are nevertheless willing to selflessly extend themselves to trainees. I am in their debt and will seek to emulate their generosity throughout my career.

I would also like to acknowledge the many people who have encouraged my pursuit of science at various stages of my life. During middle and high school, I was privileged to have teachers like William Newman and Edward Rosenburgh, my biology and earth science teachers, respectively. Both Mr. Newman and Mr. Rosenburgh encouraged my science fair projects all throughout my time at Poland Central School—despite the fact that not one of my projects *ever* succeeded. They helped me to learn very early on that science is not about proving one's hypothesis right, but rather about asking interesting questions. Without their involvement in the PCS Science Fair, it is unlikely that I would have chosen the training path that I have.

I was very fortunate during my undergraduate years to have a number of teachers who encouraged me to take risks and try new things. In particular, my advisor from Hamilton College—Dr. David A. Gapp—was instrumental in my early years at the bench. Another of my mentors at Hamilton—my organic chemistry professor Dr. Ian Rosenstein—helped to stoke my passion for biochemistry at an early age. While at Cornell, I was lucky enough to teach undergraduate biochemistry under the guidance of

James E. Blankenship and Dr. Helen T. Nivison. Their enthusiasm for teaching left an indelible mark on me. My time at the bench at Cornell was overseen by Dr. Stephen Jesch in the lab of Dr. Susan A. Henry. I thank both Steve and Susan for their commitment to teaching and their patience for my marginal skills at yeast genetics.

I have been lucky to have been a part of two wonderful labs during my graduate training, and was blessed with many friends from these two groups. From the Sabatini laboratory I would like to thank Dr. Siraj M. Ali, Dr. Timothy R. Peterson, Heather Keyes, Dr. Peggy Hsu, Dr. Yoav Shaul, Dr. Brian Grabiner, Dr. Mathieu LaPlante, Dr. Alejo Efeyan, Dr. Carson Thoreen, Stephanie Kinkel, Dr. Steve Bailey, and Dr. Caitlin Higgins Bailey. I would also like to thank the director of the Broad Institute's RNAi Consortium, Dr. David E. Root. From the Sawyers laboratory I extend my gratitude to my bay-mate Dr. Phil Watson, our lab manager John Wongvipat, my friends Dr. Michael J. Evans, Dr. Minna Balbas, Dr. Rohit Bose, and the technicians that keep the Sawyers lab running: Taslima Ishmael, Mandy Lee, Emily Schenkein, and Jacqueline Wanjala. Dr. Watson has been particularly patient in tolerating my feigned aggression and sarcasm throughout the years.

I wish to also thank a number of close friends who have encouraged me, listened to me, supported me and often offered their honest criticisms at the (many) times when I have been wrong. First and foremost among these are Matthew A. Domser and his parents Celia and Dr. Mark Domser. The

Domsers have been a part of my life since before I can remember, and I cannot imagine having pursued science without their encouragement. I must particularly acknowledge Matt, who has always been there to listen to my scientific and personal travails and has never hesitated to offer his friendship, encouragement, and honest criticism.

I have also been privileged to have shared my time with a number of friends and classmates. I would like to thank my “medical school crew”—Dr. Dennis Spencer, Dr. Selom Gasinu, Dr. Irina Chaikhoutdinov, Dr. Anand Nataraj and Dr. Malikah Latmore—for their time, friendship, and especially their encouragement in pursuing thesis work that would take me to Boston and unfortunately away from them. Further, my medical school and MD/PhD program classmates Dr. Natasha D. Novikov, Dr. Sandeep Kishore, Dr. Ankit B. Patel, Dr. Kirti Magudia, Dr. Nicole Ramsey, Corynn Kasap, and Dr. Svetlana Pavlovic. Everyone listed here—and many that I am likely forgetting—have at one point or another offered their advice, friendship and listened to me talk about cancer and protein phosphorylation *ad nauseum*. In particular, Dr. Novikov has been a pillar of support and friendship in the final year of our training together. Я люблю тебя , мой дорогой Наталья Дмитриевна Новикова.

Although this paragraph will lack sentimentality, I must certainly acknowledge and thank the United States taxpayers for funding my work. In particular, the National Institutes of Health Medical Scientist Training Program grant GM07739, which helps to fund the Tri-Institutional MD/PhD

program. I would also like to thank the Department of Defense Prostate Cancer Research Program and the Office of Congressionally Directed Medical Research Programs for awarding me Predoctoral Prostate Cancer Training Award PC094483. Lastly, the Starr Cancer Consortium generously awarded us Starr Cancer Consortium Award #I2-A117, which allowed me to perform the RNAi screens that began my thesis work.

I must extend my deepest and most heartfelt gratitude to my family: my parents Nancy B. and Albert C. Wheeler, my sister Marie N. Cotier, and my brother Edward S. Wheeler. My mother and father were my first teachers, and their influence is evident in my work, if only just to me. Specifically, I thank my mother for her passion for teaching, learning and science. As an elementary school science and math teacher, my mother always led by example with her commitment to teaching. Further, I must thank my father. My father has been an electrical engineer for most of his life, and I used to presume that my work as a biologist was as far from electrical engineering as one could get. However, after years in the lab, I can see that I primarily inherited my stubbornness and attention to detail from my Father, and our hours of working together on Gracie often parallel my efforts that I put forth at the bench.

I must also acknowledge my siblings—Marie Cotier and Edward S. Wheeler. My sister and brother have always served as examples to the kind of person that I aspire to be. They are both compassionate and intelligent human beings that have put up with a lot of annoying behavior from their

younger brother. They have been unwavering supporters of my work, and I am boundlessly grateful to them.

Finally, I acknowledge a gene who barely even appears in this thesis, but who was instrumental in the work presented here: *RAB25*. From December 2009 to March 2012, most of my work in the lab focused on the GTPase RAB25. Despite many experiments, I finally came to the conclusion that RAB25—although a tantalizing hit from my RNAi screens—was not regulating growth factor signaling the way I initially thought it was. Although none of my efforts with RAB25 are directly evident in this thesis, the time spent on this protein taught me how to rigorously design experiments and execute methods in a way that I could trust my data. Ultimately, this protein taught me that one must be ready to discard one's favorite theories in favor of pursuing biology that is more likely to be real. Thus, the attention to detail that RAB25 taught me bore fruit immediately when I turned my efforts to RAB35.

TABLE OF CONTENTS

LIST OF FIGURES

LIST OF TABLES

LIST OF ABBREVIATIONS

4EBP1	eIF4e-binding protein 1
aa	amino acid
ABL	Abelson kinase
AGC	protein kinase A, G and C
AKT/PKB	AK thymoma/Protein Kinase B
ADP	adenosine diphosphate
AMP	adenosine monophosphate
AMPK	AMP-activated kinase
APC	adenomatous polyposis coli
ATM	ataxia telangiectasia, mutated
ATP	adenosine triphosphate
BCS	bovine calf serum
BCR	breakpoint cluster region homology domain
BCR-ABL	breakpoint cluster region-Abelson kinase
BH	BCR homology domain
bp	base pair
CCLE	cancer cell line encyclopedia
CD	cluster of differentiation
cDNA	complementary DNA
CLIP-170	CAP-GLY domain containing linker protein 170 kDa
CML	chronic myelogenous leukemia
COSMIC	catalogue of somatic mutations in cancer

Da	Dalton
DEP	dishevelled, egl-10 and pleckstrin domain
DEPTOR	DEP domain-containing protein 6
DMEM	Dulbecco's modified eagles media
DMSO	dimethylsulfoxide
DNA	deoxyribonucleic acid
DNA-PK	DNA-dependent protein kinase
EDTA	ethylenediaminetetraacetic acid
EE	early endosome
EEA1	early endosomal antigen 1
EGF	epidermal growth factor
EGFR	epidermal growth factor receptor
eIF4e	eukaryotic translation initiation factor 4e
EMT	epithelial to mesenchymal transition
EPI64A-C	EBP50–PDZ interactor of 64 kDa (also known as TBC1D10A-C)
ERK	extracellular signal-regulated kinase(s)
ESC	embryonic stem cell
ESCRT	endosomal sorting complexes required for transport
FAT	FRAP, ATM and TRRAP domain
FBS	fetal bovine serum
FGF	fetal growth factor
FGFR	fetal growth factor receptor

FK506	fujimycin (also known as tacrolimus)
FKBP12	FK506 binding protein, 12 kDa
FOXO1/3A	forkhead box O 1/3A
FRAP1	FKBP12 and rapamycin associated protein 1 (also known as mTOR, RAFT1)
FRB	FKBP12 and rapamycin binding domain
GAP	GTPase activating protein
GβL	g beta-like protein, aka “gable” (see mLST8)
gDNA	genomic DNA
GDI	guanine nucleotide dissociation inhibitor
GDP	guanine diphosphate
GEF	guanine nucleotide exchange factor
GFP	green fluorescent protein
GF	growth factor
GPCR	G-protein coupled receptor
GRB1	growth factor receptor-bound protein 1 (p85 subunit of PI3K)
GRB2	growth factor receptor-bound protein 2
GSK3	glycogen synthase kinase 3
GST	glutathione S-transferase
GTP	guanine triphosphate
GTPγS	guanosine 5’-3-*O*-(thio)triphosphate
HEAT	Huntingtin, EF3, PP2A, and TOR1
HGF	hepatocyte growth factor

HGFR	hepatocyte growth factor receptor
HSP	heat shock protein
ICGC	international cancer genome consortium
IF	immunofluorescence
IFN	interferon
IGF-I	insulin-like growth factor I
IGF-IR	insulin-like growth factor receptor
IgG	immunoglobulin G
IκB	nuclear factor of kappa light polypeptide gene enhancer in B-cells inhibitor
IKK	IκB kinase
IL	interleukin
ILK	integrin-linked kinase
IP	immunoprecipitation
IP/MS	immunoprecipitation/mass-spectroscopy
IR	insulin receptor
IRS-1	insulin receptor substrate 1
IRS-2	insulin receptor substrate 2
IVK assay	*in vitro* kinase assay
kDa	kilodalton
KD	kinase dead
KDR	kinase-insert domain receptor (also known as VEGFR)
LE	late endosome

LKB1	liver kinase B1
M	molar
MAPK	mitogen-activated protein kinase
MDM2	mouse double minute 2 homolog
MEK	MAP kinase/ERK kinase
MERLIN	Moesin-Ezrin-Radixin-Like Protein (also known as neurofibromin 2)
miRNA	micro RNA
μg	microgram
μm	micrometer
μM	micromolar
μL	microliter
mL	milliliter
mLST8	mammalian lethal with SEC13 protein 8 (see GβL)
mM	millimolar
mRNA	messenger RNA
MTM	myotubularin
mTOR	mechanistic target of rapamycin (also known as FRAP1 and RAFT1)
mTORC1	mechanistic target of rapamycin complex 1
mTORC2	mechanistic target of rapamycin complex 2
MS	mass spectroscopy
NDRG1	n-myc downstream regulated 1

NF1	neurofibromin 1
NF2	neurofibromin 2 (also known as MERLIN)
NF-κB	nuclear factor kappa-light-chain-enhancer of activated B cells
NIH-3T3	NIH, 3-day transfer, inoculum $3x10^5$ cells
NIK	NF-kappa-B-inducing kinase
nM	nanomolar
nt	nucleotides
OCRL	Lowe oculocerebrorenal syndrome protein
OMIM	online Mendelian inheritance in man
PA	phosphatidic acid
PBS	phosphate buffered saline
PCR	polymerase chain reaction
PDGF	platelet derived growth factor
PDGFR	platelet derived growth factor receptor
PDK1	phosphoinositide dependent kinase 1
PDZ	PSD-95/DlgA/ZO-1–like
PGC1	peroxisome proliferator-activated receptor gamma coactivator 1-alpha
PH	pleckstrin homology
PI	phosphatidylinositol
PI3K	phosphatidylinositol 4, 5-bisphosphate 3'-OH kinase
PI4K	phosphatidylinositol 4'-OH kinase
PI5K	phosphatidylinositol 5'-OH kinase

PIKK	phosphatidylinositol 3'-kinase like kinase family
PIP	phosphatidylinositol phosphate
PIP2	phosphatidylinositol 4, 5-bisphosphate
PIP3	phosphatidylinositol 3, 4, 5-trisphosphate
PKA	protein kinase A
PKB	protein kinase B (also known as AKT)
PKC	protein kinase C
PLD1	phospholipase D1
PP2A	phosphatase 2A
PPARγ	peroxisome proliferator-activated receptor
PRAS40	proline-rich AKT substrate, 40 kDa
Protor-1	protein observed with RICTOR-1 (see PRR5)
Protor-2	protein observed with RICTOR-2 (see PRR5L)
PRR5	proline rich 5 (renal) (see Protor-1)
PRR5L	proline rich 5 (renal)-like (see Protor-2)
PTEN	phosphatase and tensin homologue
PX	P40phox and p47phox domain
RAF	rapidly activated fibrosarcoma
RAFT1	rapamycin and FKBP12 target 1 (also known as mTOR and FRAP1)
RAG	Ras-related GTP-binding protein
Raptor	regulatory-associated protein of mTOR
RB	retinoblastoma

RE	recycling endosome
REDD1	regulated in development and DNA damage responses 1
RHEB	ras homologue expressed in brain
RICTOR	rapamycin insensitive companion of TOR
RISC	RNA-initiated silencing complex
RHOK1	RHO kinase 1
RNA	ribonucleic acid
RNAi	RNA interference
RSK	ribosomal S6 kinase
RTK	receptor tyrosine kinase
RT-PCR	reverse transcription polymerase chain reaction
S6	Ribosomal protein subunit, 6 Svedbergs
S6K1	(ribosomal) S6 kinase 1
S6K2	(ribosomal) S6 kinase 2
SDS-PAGE	sodium dodecylsulfate polyacrylamide gel electrophoresis
SGK1	serum and glucocorticoid-induced kinase 1
SH2	src homology domain 2
SH3	src homology domain 3
SHIP1	SH2-domain containing phosphatidylinositol- 3, 4, 5-trisphosphate 5'-phosphatase 1
SHIP2	SH2-domain containing phosphatidylinositol 3, 4, 5-trisphosphate 5'-phosphatase 2
shRNA	short hairpin RNA

SIN1	SAPK-interacting protein 1
siRNA	short interfering RNA
SOS	son of sevenless
SREBP1	Sterol regulatory element-binding protein 1
TBC1D10C	TBC1 domain family member 10C (also known as EPI64)
TGFβ	transforming growth factor beta
TKI	tyrosine kinase inhibitor
TNFα	tumor necrosis factor, alpha
TOP	tract of pyrimidines
TOR	target of rapamycin
TRC	the RNAi consortium
TRRAP	transformation/transcription domain-associated protein
TSC	tuberous sclerosis complex
TSC1	tuberous sclerosis complex 1 (hamartin)
TSC2	tuberous sclerosis complex 2 (tuberin)
Ub	ubiquitin
VEGF	vascular endothelial growth factor
VEGFR	vascular endothelial growth factor receptor (see KDR)
VHL	Von-Hippel Lindau
WB	western blot

CHAPTER ONE:

INTRODUCTION: PI3K/AKT SIGNALING IN HUMAN CANCERS AND RNAi SCREENS TO IDENTIFY NOVEL REGULATORS OF THE PI3K/AKT AXIS

1.1 EXTRACELLULAR SIGNALS REGULATE INTRACELLULAR SIGNALING

1.1.1 Growth factor receptor tyrosine kinases initiate phosphoinositide-dependent signaling

Growth factors and other extracellular factors regulate intracellular signal transduction networks by transmitting their signals through the cell membrane via transmembrane receptors. While many mechanisms for transducing extracellular signals to the inside of cells exist, most growth factors (e.g. insulin and similar signaling molecules) bind to transmembrane growth factor receptor tyrosine kinases (RTKs). The family of transmembrane RTKs is diverse, but most RTKs share a common mechanism: once bound by their cognate growth factors, RTKs form homodimers, and their tyrosine kinase activity is upregulated. RTKs then auto-phosphorylate themselves *in trans*, which forms phosphotyrosine sites that can serve as docking sites to recruit a diverse array of proteins that transduce signals in response to growth factor stimulation.

Activated RTKs can initiate signaling through a number of different transduction pathways, and one of the most well studied of these is the phosphatidylinositol 3-OH kinase (PI3K)/AKT pathway, which is responsible

for a large portion of the cellular processes that lie downstream of RTK activation (Figure 1.1). Because signaling through RTKs typically suppresses apoptosis and activates cell growth, it is not surprising that RTKs and the signaling machinery they regulate are often altered in human tumors.

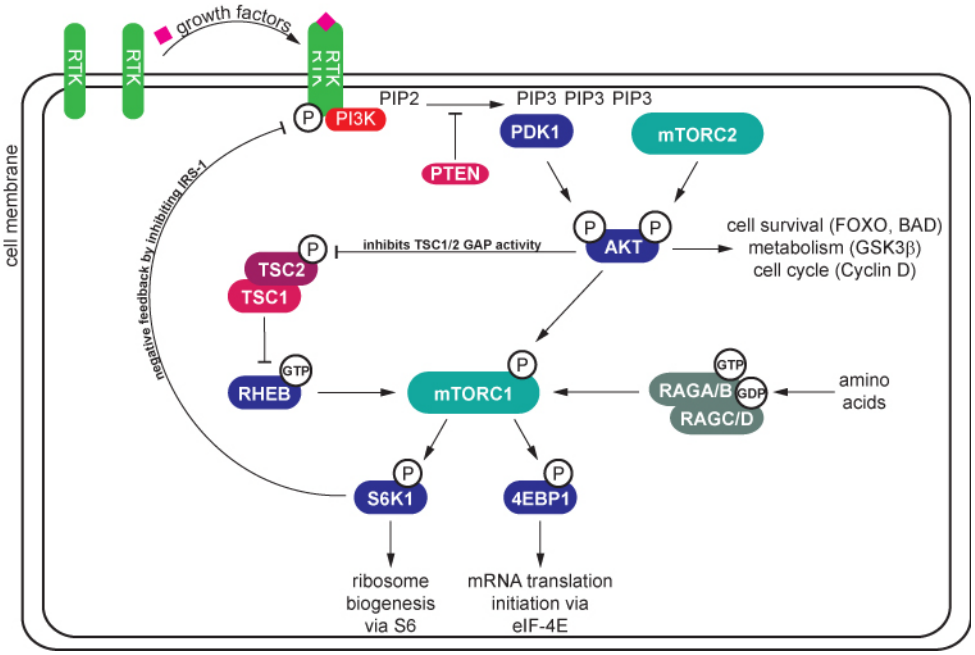

Figure 1.1: The PI3K/AKT/mTOR Pathway. Growth factor signaling is initiated at the cell membrane when growth factor ligands bind to their receptor tyrosine kinases (RTKs). RTKs then dimerize, phosphorylate one another *in trans*, and can recruit effectors to the cell membrane. One effector—phosphatidylinositol 3'-OH kinase (PI3K)—is recruited either directly or by adaptor proteins like the insulin receptor substrate 1 (IRS-1, not shown). PI3K is then proximal to phosphatidylinositol bisphosphate (PIP2), a lipid membrane that PI3K phosphorylates to convert to phosphatidylinositol trisphosphate (PIP3). PIP3 can then recruit effectors such as phosphatidylinositol-dependent kinase 1 (PDK1) or mammalian target of rapamycin complex 2 (mTORC2), which phosphorylate the kinase AKT on distinct sites. Once activated by these phosphorylations, AKT regulates a number of physiological processes such as cell survival, metabolism, and the cell cycle (listed).

1.1.2 Phosphatidylinositol 3'-OH kinases phosphorylate membrane lipids to transduce growth factor signals

The Class I PI3 kinases are medium-sized lipid kinases that were initially identified to have *in vitro* lipid kinase activity that was activated in response to growth factors like insulin and the platelet derived growth factor (PDGF) [5-11]. Once activated, PI3Ks phosphorylate the 3' hydroxyl (3'-OH) group of the inositol ring on phosphatidylinositol 4, 5-bisphosphate (PIP_2) to form phosphatidylinositol 3, 4, 5-trisphosphate (PIP_3) [10]. PIP_3 is a potent second messenger that can then activate an array of signaling molecules. Thus, growth factor stimulation of RTKs activates PI3K signaling to accumulate PIP_3, which in turn activates pro-growth signaling (Figure 1.1). Several isoforms—α, β, δ and γ—of Class I PI3Ks exist. Further, other PI3Ks—such as Class II and Class III PI3Ks—are also present in cells, but their lipid substrates and products do not play as central a role in growth factor signal transduction [12-14].

PI3Kα is thought to be the PI3K that is primarily responsible for transducing signals from activated RTKs [15]. PI3Kα exists as an obligate heterodimer of two proteins: the p110α catalytic subunit, and a regulatory subunit such as p85α, p55α or p50α (three different products of the *PIK3R1* gene) [16]. In resting cells, p110α-p85α heterodimers exist as a tightly bound complex within the cytosol that are recruited to the cell membrane upon the activation of growth factor RTKs. PI3Kα then interacts with RTKs via SRC homology 2 (SH2) domains on p85 [17-18], which bind

phosphotyrosine motifs (pYXXM) on either the RTK itself or on adapter molecules like the insulin receptor substrates IRS1 and IRS2 [19]. Once recruited to RTKs, PI3Kα is in close proximity to its substrate PIP_2 and is able to generate PIP_3. Interestingly, while the p85/p55 adapter subunits are necessary to link PI3Kα to RTKs, it is clear that p85 actually negatively regulates the lipid kinase activity of p110α [20-23]. Thus, although the p85/p55 adapter subunits are necessary to link p110α to RTKs,

The PI3Kβ isoform is distinct in that it can transduce signals downstream of either RTKs or G-protein coupled receptors (GPCRS) [24-26]. Interestingly, some data suggest that PI3Kβ is the PI3K isoform that is primarily responsible for oncogenic signaling in the context of PTEN inactivation [27-28], which may suggest a complex spatial and temporal regulation of phosphoinositide pools by the PI3Ks and PTEN. However, this concept remains controversial, as several groups have published data which suggests that the loss of PTEN can utilize either PI3Kα or PI3Kβ to drive transformation [29-30]. The development of isoform specific inhibitors of the different PI3Ks should help to clarify which genetic contexts (PTEN loss, etc.) are dependent on which PI3Ks.

While PI3Kα and PI3Kβ are the most well studied class I PI3Ks, signaling by PI3Kγ and PI3Kδ occurs under various contexts. Dysregulation of PI3Kγ and PI3Kδ is not a common event in tumors, but overexpression of these kinases can indeed drive transformation *in* vitro [31]. PI3Kδ—encoded by the gene *PIK3CD*—is primarily expressed in immune cells [32]. Like the

other Class IA PI3Ks, PI3Kδ is associated with p85α, p55α, p50α or p85β regulatory subunits. Although the function of PI3Kδ is not completely understood, it appears that in leukocytes PI3Kδ is involved in B and T cell development and antigen receptor signaling [33-36]. The first PI3Kδ isoform-specific inhibitors were recently approved for chronic lymphocytic leukemia and may have an additional role in autoimmune and inflammatory disorders [37-42].

PI3Kγ is the sole member of the Class IB group of PI3Ks [13]. Rather than being regulated by RTKs, PI3Kγ is activated mostly by G-protein coupled receptors (GPCRs) [43-44]. Further, PI3Kγ does not interact with the p85α, p55α, p50α or p85β regulatory subunits, but is instead tightly associated with either p101 or $p87^{PIKAP}$ [45-46]. Similar to PI3Kβ, PI3Kγ kinase signaling is activated by the Gβ and Gγ subunits of heterotrimeric GTPases [47-48]. PI3Kγ is thought to function primarily in cardiac muscle and immune cells, but these functions are poorly defined.

1.1.3 PTEN and lipid phosphatases negatively regulate PI3K signaling

Signaling events downstream of RTKs and PI3Ks are exquisitely regulated under normal physiological conditions. Because prolonged growth factor signaling would result in aberrant growth, there exist a multitude of negative regulatory mechanisms that are set in motion after signal cascades are initiated. One mechanism of negative regulation of PI3K/AKT signaling is the breakdown of PIP_3 by lipid phosphatases like PTEN and SHIP2.

The phosphatase and tensin homologue (PTEN) protein is coded for by the gene *PTEN*, and was originally identified as a tumor suppressor that is frequently altered in human cancers [49-53]. PTEN was originally thought to be a protein tyrosine phosphatase [53], but it is now understood that it is a lipid phosphatase that dephosphorylates PIP_3 at the 3' hydroxyl group of the inositol ring to form phosphatidylinositol 4,5-bisphosphate (PIP_2) [54]. Genetic studies have verified that *PTEN* is a tumor suppressor, while clinical studies have implicated *PTEN* deletion or mutation in tumorigenesis [55-59]. The PTEN protein is localized to the inner leaf of the cell membrane by virtue of its C2 domain, which allows the phosphatase to reside in proximity to its substrate PIP_3 [60].

Another less commonly mutated lipid phosphatase and tumor suppressor is the SH2-domain containing phosphatidylinositol-3, 4, 5-trisphosphate 5'-phosphatase 2 (SHIP2) protein, which is coded for by the gene *INPPL1* [61-62]. Unlike PTEN, SHIP2 dephosphorylates PIP_3 at the 5'-OH group of the inositol ring [61, 63]. Further, rather than being targeted to membrane lipids, SHIP2 is localized to the cell membrane by recruitment to growth factor receptors via its phospho-tyrosine binding SH2 domains, where it is phosphorylated at tyrosine residues by the RTK [64-68]. Its phosphatase activity is activated by these phosphorylation events, thus allowing SHIP2 to locally dephosphorylate PIP_3 to form phosphatidylinositol 3, 4-bisphosphate. The closely related phosphatase phosphatidylinositol- 3,

4, 5-trisphosphate 5'-phosphatase 1 (SHIP1) functions similarly to SHIP2, but is less well characterized.

In addition to PTEN and the SHIP phosphatases, there exist a number of other lipid phosphatases: 1.) the Lowe oculocerebrorenal syndrome protein (OCRL), an inositol polyphosphate 5-phosphatase [69-70], 2.) the phosphatidylinositol 3-phosphate and phosphatidylinositol 3, 5-bisphosphate 3'-OH phosphatase myotubularin (MTM) [71], and several others. These proteins are less well characterized within the context of PI3K/AKT signaling, although it is clear that they may play a role in spatial and temporally specific regulation of signal transduction. Because their roles as tumor suppressors are less prominent, they will not be further discussed here.

1.1.4 The Ras/Raf/MAPK/ERK signaling axis

Although numerous signaling pathways intersect with the PI3K/AKT axis, one other well-studied signal transduction axis is the Ras/Raf/mitogen activated protein kinase (MAPK)/extracellular regulated kinase (ERK) pathway [72]. Although the Ras/Raf/MAPK/ERK signaling axis is a distinct pathway from the PI3K/AKT axis, because of the interrelationship between the two, Ras/Raf/MAPK/ERK signaling will be very briefly reviewed here.

Like PI3K/AKT signaling, Ras/Raf/MAPK/ERK signaling is initiated at the cell membrane when growth factors activate RTKs. Unlike PI3K/AKT signaling, however, the RAS cascade does not rely upon the generation of

the lipid second messenger PIP_3. Instead, tyrosine phosphorylation of growth factor receptors promotes the recruitment of the adapter protein growth factor receptor 2 (GRB2) [73], which interacts with the guanine nucleotide exchange factor (GEF) son of sevenless (SOS) [74]. SOS then facilitates the exchange of guanine diphosphate (GDP) for guanine triphosphate (GTP) on the RAS GTPases (HRas, KRAS and NRas). Thus, growth factor receptor activation leads to activated, GTP-bound RAS GTPases.

Once loaded with GTP, the RAS proteins regulate a number of signaling molecules. Key among these is the serine/threonine protein kinases a-Raf, b-Raf and c-Raf [75-76]. When bound to RAS proteins that are loaded with GTP, the Raf kinases are activated and phosphorylate the MAPK or ERK kinases 1 and 2 (MEK1/2) [77]. MEKs are dual-specificity protein kinases that—when activated by Raf—phosphorylate the extracellular regulated kinases (ERK1/2) on tyrosine residues [78-80]. ERK—also known as MAPK—then regulates a set of effectors to encourage cell division and survival. The best characterized of these are ETS family transcription factors like Elk-1 [81-82], the p90 ribosomal S6 kinase (RSK) [83-84], and mitogen-and stress-activated protein kinase 1(MSK1) [85].

While they are two distinct signaling cascades, the PI3K and MAPK pathways are by no means unconnected. Indeed, they intersect at many points. In some instances, they serve to downregulate the activity of one another. For example, Raf is phosphorylated at several sites by AKT, which

inhibits Raf activity [86], while activated $BRAF^{V600E}$ can inhibit AKT signaling by inhibiting mTORC2 activity [87]. Moreover, treatment with specific small molecule inhibitors of MEK1 can induce AKT phosphorylation, while inhibition of PI3K, mTORC1, mTORC1/2 or AKT can upregulate ERK phosphorylation in many contexts [88].

However, there exist a number of cooperative circuits between MAPK and PI3K pathway. Phosphorylation of the TSC1/2 complex by ERK and RSK at multiple sites can activate mTORC1 [89-93]. A particularly interesting example of cooperation between PI3K and MAPK lies upstream, where KRAS can interact with and activate PI3K isoforms [94-100]. Although this finding was initially controversial, genetic evidence suggests that this interaction is indeed meaningful in tumors as well as some regular physiological contexts [101]. Thus, the interaction between the PI3K/AKT and Ras/MAPK pathways are numerous and complex.

1.2 SIGNALING DOWNSTREAM OF PIP3

1.2.1 PDK1 activates AKT in a phosphoinositide dependent manner

The generation of PIP_3 initiates a cascade of signaling events that positively regulates cell growth, metabolism and survival. One direct effector of PIP_3 is the phosphoinositide-dependent kinase 1 (PDK1) [102-104], which was originally identified from tissue extracts as a kinase that could phosphorylate AKT at threonine 308 (T308). This threonine resides in the catalytic domain of AKT, and its phosphorylation is necessary for AKT kinase

activity [105-106]. Interestingly, the inherent kinase activity of PDK1 is very high regardless of growth factor stimulation or PIP_3 levels in the cell [102]. Rather than being catalytically activated by growth factors, the key determinant in PDK1 signaling to downstream effectors is its localization to the cell membrane, which is accomplished via PDK1's C-terminal pleckstrin homology (PH) domain [107], which binds to PIP_3 and the PIP_2 phosphatidylinositol 3, 4-bisphosphate with high affinity. At the membrane, the constitutively active PDK1 can phosphorylate its substrates. The most well studied PDK1 substrates are the AGC family member kinases AKT/PKB and PKC.

Unequivocal genetic evidence for PDK1's role in activating AKT arrived when murine embryonic stem (ES) cells null for the *PDK1* gene were generated [108]. In *PDK1*$^{-/-}$ ES cells the phosphorylation of AKT's kinase domain residue at T308 was completely absent after growth factor stimulation. Further, the homologous residue in the catalytic domain of other AGC kinases (SGK1 and PKC isoforms) was not phosphorylated in these cells. Lastly, PDK1 is also necessary for activation of a Ras/Raf/MEK/ERK regulated kinase, the 90 kDa ribosomal S6 kinase (p90 RSK) [109-111]. Unlike S6K1/2, RSK phosphorylates the ribosomal S6 protein in a rapamycin-independent manner and largely takes its cues through the ERK signaling cascade. Therefore, although PDK1 is important in PI3K dependent signaling, it is also able to signal to other effectors outside of the PI3K/AKT signaling axis.

1.2.2 AKT/PKB is a major effector of PI3K signaling

As mentioned above, one of the most well characterized effectors of PI3K signaling is AKT (also known as protein kinase B (PKB)). AKT was originally discovered as a viral oncogene that was found to be transforming in a mouse thymoma model [112-114]. Higher eukaryotes have at least one conserved homologue of the viral AKT gene. Indeed, mice and humans have three distinct versions of AKT, coded for by the genes *AKT1*, *AKT2*, and *AKT3* [115]. These isoforms are similar in their structure, but the functional outputs of the signaling by each kinase are unique as well as overlapping. Nevertheless, the signaling events downstream of AKT—i.e. anti-apoptotic, pro-metabolic, pro-growth, and pro-cell division—are generally shared by the AKT isoforms.

The three AKT isoforms are similar in their structure in that they contain an N-terminal PH domain, a kinase domain similar to other AGC kinase family members in the middle, and an inhibitory C-terminal domain that contains a hydrophobic motif (Figure 1.2) [116]. Similar to PDK1, the PH domain on AKT serves to localize the kinase to the cell membrane when PIP_3 is generated [117]. At the membrane, the kinase activity of AKT is upregulated by phosphorylation of its catalytic domain at residue T308 by PDK1, a step which is required for AKT to exhibit enzymatic activity [118].

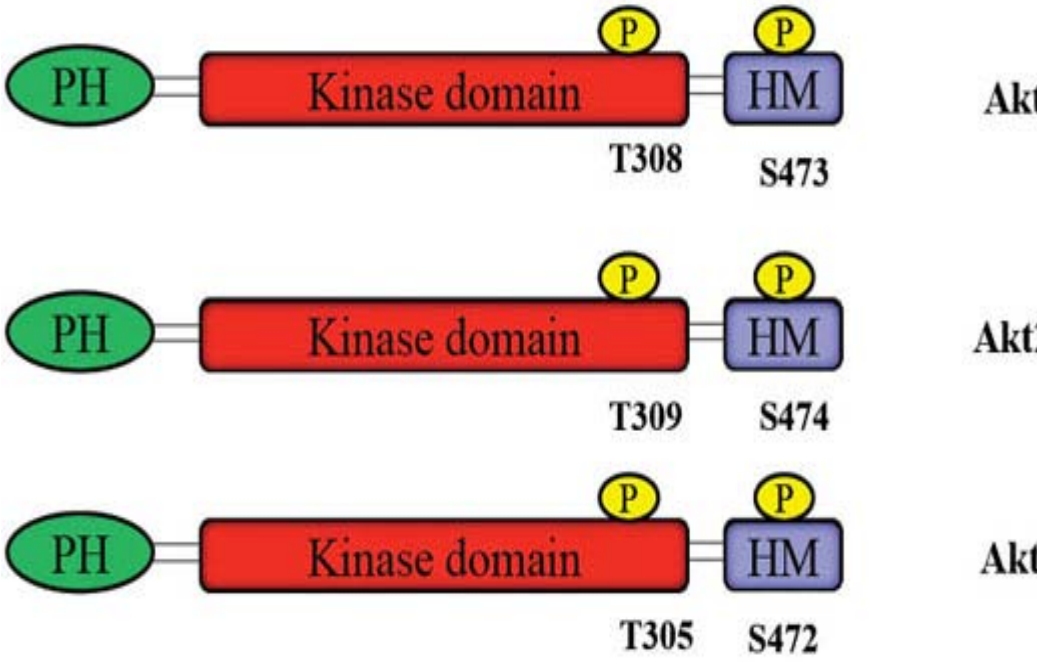

Figure 1.2: Structure of the AKT1, AKT2 and AKT3 isoforms. The AKT1, AKT2 and AKT3 isoforms are structurally similar in that they consist of an N-terminal pleckstrin homology (PH) domain (green), an AGC-kinase like kinase domain (red), and a C-terminal hydrophobic motif (blue). The catalytic domain threonine (T308, T309 and T305 in AKTs1, 2 and 3, respectively) is phosphorylated by PDK1, while the hydrophobic motif serine (S473, S474 and S472) is phosphorylated by mTORC2. Image adapted from Viglietto et. al [2].

However, maximal kinase activity of AKT towards its substrates is only achieved after phosphorylation at serine 473 (S473) by the mammalian target of rapamycin complex 2 (mTORC2) [119]. These two phosphorylation events occur concomitantly and are PIP_3-dependent, and the phosphorylation of some AKT substrates depend on S473 phosphorylation more than others [120-121]. Once activated, AKT signals to a variety of effectors to encourage cell growth and survival.

1.2.3 AKT/PKB positively regulates cell metabolism, growth and survival

Activated AKT transmits a pro-metabolic signal by regulating several steps in glucose metabolism. Importantly, AKT plays a critical step in the insulin-dependent internalization of glucose by the glucose transporter GLUT4 [122]. Once insulin has activated PI3K, AKT phosphorylates the AKT Substrate of 160 kDa (AS160), which is a RAB GTPase-activating protein (RabGAP) [123] that is required for the translocation of GLUT4 to the cell membrane, where it facilitates glucose uptake into the cell [124]. AKT also regulates glycogen metabolism by phosphorylating and inhibiting the glycogen synthase kinase 3 (GSK3) [125-126]. By inhibiting GSK3—which itself inhibits glycogen synthase—AKT upregulates the incorporation of glucose into glycogen.

AKT also negatively regulates apoptosis to encourage cell survival. This is thought to primarily occur through the Forkhead family of transcription factors, particularly FOXO1 and FOXO3a (referred to here collectively as FOXO) [127]. FOXO is a transcription factor that activates the expression of apoptotic proteins like BIM-1, bNIP3, Bcl-6, FasL, and TRAIL [128-129]. AKT directly phosphorylates FOXO at threonine 24 (T24), serine 256 (S256) and serine 319 (S319) which prevents FOXO from entering the nucleus and regulating gene expression. Thus, the phosphorylation of FOXO by AKT sequesters FOXO in the cytosol, which inhibits the expression of members of the apoptotic machinery. Further, AKT can regulate the apoptotic

machinery more directly by phosphorylating targets like Bad, which AKT phosphorylates to inhibit the apoptotic functions of Bad [130-131].

The discovery and elucidation of the mechanistic target of rapamycin (mTOR) signal transduction network has revealed several mechanisms through which AKT regulates cell growth and protein synthesis. Briefly, AKT negatively regulates two inhibitors of mTOR signaling, which upregulate ribosome biogenesis, protein synthesis, and the accumulation of cell mass. These mechanisms will be reviewed in the section below that discusses mTORC1 signaling.

In addition to AKT, other members of the AGC kinase family regulate survival signaling in a PI3K-dependent manner. This is not surprising considering that AGC kinases share a remarkable amount of overlapping characteristics in terms of protein structure [132-133]. One prominent example of a kinase with a similar signaling role to AKT is the serum and glucocorticoid-induced kinase 1 (SGK1) [134]. Interestingly, SGK1 can phosphorylate AKT substrates like FOXO1/3A [135]. Further, recent evidence suggests that SGK1 might take over the PI3K-dependent survival that is usually regulated by AKT in certain tumors and cell lines [136]. The reason for this shift in signaling is unclear, but it highlights the fact that tumors with activated PI3K may not all respond equally to small molecules that target AKT.

1.2.4 The mechanistic target of rapamycin (mTOR) is a master regulator of cell growth that is downstream of PI3K/AKT

One of the more recently well studied members of PI3K/AKT signaling is the mechanistic target of rapamycin (mTOR). Rapamycin is a small molecule (~900 Da) product of *Streptomyces hygroscopicus* that was discovered from soil samples collected on Rapa Nui (Easter Island) [137-140]. The molecular mechanism of rapamycin was initially unclear, but early studies demonstrated that rapamycin blocks the activation of T and B cells by interleukin-2 (IL-2) [140-141]. Thus, even before the target of rapamycin was known, it was appreciated that rapamycin could function as a potent immunosuppressant.

The precise molecular target was elusive until genetic experiments in yeast and affinity purification approaches in mammalian cells identified the kinase mTOR (TOR in yeast) as the binding partner of rapamycin when rapamycin is bound to the prolyl-isomerase FK506 binding protein, 12 kDa (FKBP12) [142-146]. mTOR is a large (~289 kDa) protein kinase that is very similar to the yeast proteins TOR1 (42% homology) and TOR2 (39% homology), which were identified as the yeast targets of rapamycin prior to the identification of mammalian mTOR [147]. The mTOR protein shares a large degree of homology to PI3K family members, and is the founding member of the phosphatidylinositol kinase-like kinase (PIKK) family [148]. Indeed, it was originally thought to phosphorylate phospholipids at the 4'-OH group of the inositol ring [149-150]. Despite its amino acid sequence

similarity to PI-kinases, mTOR is indeed a serine/threonine kinase [151]. The most well characterized effectors of mTOR are the protein kinase ribosomal S6 kinase1/2 (S6K1 and S6K2), and the translation initiation inhibitor 4E-BP1.

1.2.5 mTOR Complex 1 (mTORC1) is a nutrient and growth factor sensitive protein kinase that regulates cell size and cell growth through S6K1 and 4EBP1

For some time after the discovery of mTOR, it was apparent that mTOR phosphorylation of S6K1/2 is regulated by growth factors, amino acids, and glucose. However, interacting proteins remained elusive until gentler purification conditions and chemical crosslinking approaches were used to identify the regulatory associated protein of mTOR (Raptor) [152-153]. Together with mTOR, Raptor can be considered the founding member of a protein complex that is now referred to as the mammalian target of rapamycin complex 1 (mTORC1). mTORC1 is comprised of mTOR, Raptor, the G-beta like protein GβL, the proline-rich AKT substrate of 40 kDa (PRAS40), and the mTOR kinase inhibitor protein DEP-domain containing protein DEPTOR. mTORC1 is a rapamycin-sensitive complex that positively controls protein translation, cell size, and cell growth. mTORC1 is itself regulated by several inputs, such as growth factors, redox conditions within the cell, and glucose and amino acid availability.

By far, the most well understood mTORC1 substrates are the AGC family kinase ribosomal S6 kinase 1/2 (S6K1/2) and eIF4e-binding protein 1 (4EBP1) [151, 154-157]. Both of these proteins are positive regulators of cell growth, primarily through their regulation of mRNA translation [158]. S6K1 and S6K2 phosphorylate the ribosomal S6 protein to positively regulate mRNA translation [159-161]. One important consequence of activated S6K1/2 regulation of S6 is an increase in protein synthesis. Further, S6K-S6 positively regulates both cellular and organismal size [158, 162-164]. In addition to regulating signaling to the ribosome machinery, S6K1 can negatively control growth factor RTK signaling in a negative feedback circuit that will be described below.

mTORC1 is activated by growth factor signaling via AKT through at least two different mechanisms. The first of these to be described is a circuit where AKT signals through a GTPase activating protein (GAP) complex comprised of Tuberous Sclerosis Complex 1 and 2 (TSC1 and TSC2) [165-166]. Phosphorylation of TSC2 by AKT destabilizes the interaction of the two subunits and compromises the GAP activity of TSC1/2 towards the small RAS-like GTPase RHEB (Ras homolog enhanced in brain) [167-172]. When bound to GTP and in its active state, RHEB catalytically activates the kinase activity of mTORC1 towards its substrates S6K1 and 4E-BP1 [173-176]. Thus, activated AKT phosphorylates TSC2, which inhibits the GAP activity of the TSC complex, which allows GTP-bound RHEB to catalytically activate mTORC1 signaling.

A second route through which AKT regulates mTORC1 is the mTORC1 inhibitor Proline Rich AKT Substrate, 40 kDa (PRAS40). PRAS40 was initially identified as a component of mTORC1 that eluded detection because the PRAS40-mTORC1 interaction is disrupted by lysis buffers that contain NaCl [177-178]. Once identified, it was demonstrated that PRAS40 binds mTORC1 via Raptor to suppress mTORC1 kinase activity both *in vivo* and *in vitro*. Phosphorylation of PRAS40 by AKT at threonine 246 (T246) destabilizes the mTORC1-PRAS40 interaction to allow for mTORC1 activation. PRAS40 has also been described as an mTORC1 substrate [179-180]. Activated mTORC1 phosphorylates PRAS40 at serine 183 (S183), which further destabilizes the ability of PRAS40 to interact with Raptor. Thus, mTORC1 is able to activate itself in response to growth factors via a mTORC1-PRAS40 feed-forward circuit.

One of the major signaling inputs that regulate mTORC1 signaling is intracellular amino acids [181]. mTORC1 activity towards S6K1 and 4E-BP1 is tightly regulated by the availability of amino acids. The past several years have seen a flurry of studies that describe an elegant mechanism for amino acid sensing by mTORC1 [182]. First, the Rag GTPases were found to be necessary for amino acid induced activation of mTORC1 [183]. The Rags exist as heterodimers (RAGA/RAGC and RAGB/RAGD) anchored on the surface of the lysosome by the Ragulator complex, the whole of which serves to localize mTORC1 to the lysosome by interacting with Raptor [184]. Once there, mTORC1 is in proximity to the aforementioned GTPase RHEB,

which then catalytically activates mTORC1. In a step that is only partially understood, this sensing of amino acids by the machinery upstream of mTORC1 relies upon a vacuolar (H+)-ATPase on the lysosome surface [185]. These data suggest that amino acid sensing by mTORC1 might actually be initiated within the lumen of the lysosome. Finally, the recently described GATOR complexes act as Rag GAPs to downregulate mTORC1 signaling at the lysosome [186].

1.2.6 mTOR Complex 2 (mTORC2) is a PI3K-dependent kinase that regulates AKT/PKB and other AGC kinases

One of the long-missing pieces of phosphoinositide-dependent signaling was the kinase that phosphorylates AKT at the hydrophobic motif—PDK2 [132, 187-191]. Whereas PDK1 had been well documented as an AKT-phosphorylating, phosphoinositide-dependent kinase, PDK2 remained elusive for several years. In fact, it had been speculated at several points that PDK2 was one of any number of kinases: PDK1 [187], DNA-dependent protein kinase (DNA-PK) [192], integrin-linked kinase (ILK) [193-194], or even AKT itself [118].

The identity of PDK2 was clarified when it was found that mTOR—in a second, rapamycin-insensitive kinase complex—is the hydrophobic motif kinase that phosphorylates AKT at S473 [119, 195]. Examination of immunopurified mTOR complexes revealed the existence of a second mTORC (mTORC2) that is defined by the presence of the rapamycin-

insensitive companion of mTOR, or RICTOR [196]. mTORC2 was initially described as the hydrophobic-motif kinase for several Protein Kinase C (PKC) isoforms, but was subsequently found to phosphorylate other AGC kinases such as AKT and serum and glucocorticoid-induced kinase 1 (SGK1) [197].

Like mTORC1, mTORC2 is a protein complex of several subunits. It shares with mTORC1 the mTOR kinase itself and GβL (also known as mLST8) [198], but is distinct from mTORC1 in that it contains RICTOR instead of Raptor. Further, mTORC2 contains MAP kinase-associated protein 1 (MAPKAP1)/mammalian stress-activated protein kinase (SAPK)-interacting protein (mSIN1), a protein that is necessary for mTORC2 stability and activity towards its substrates [199-201]. It has been recently appreciated that mSIN1 likely functions to provide substrate specificity for mTORC2, as it is apparently necessary for mTORC2 to interact with substrates like AKT and SGK1 [202-204]. mTORC2 also contains one of two proline-rich proteins—PRR5 and PRR5L—which are also known as Protor-1 and Protor-2 [177, 205-206]. The physiological role of these proteins was initially unclear, as they are not required for mTORC2 complex stability or activity towards AKT [206]. Studies of Protor-1 and the similar Protor-2 have revealed that they can suppress apoptosis through PDGFRβ-dependent signaling [177, 205], and that Protor-1 is important in regulating SGK1 function and sodium channel activation in the kidney [207].

Recently, mTORC2 has been found to share another component with mTORC1—the previously mentioned DEPTOR, which is a negative regulator of mTORC1 and mTORC2 kinase activity [208]. Although DEPTOR intrinsically inhibits mTORC2 activation, increased expression of DEPTOR in a cell can lead to a somewhat paradoxical *increase* in mTORC2 signaling, as the inhibition of mTORC1 triggers activation of PI3K-dependent signaling, which then activates mTORC2. Thus, DEPTOR could potentially be a context-dependent tumor suppressor or oncogene. Indeed, elevated expression of DEPTOR in certain forms of multiple myeloma appears to be required for elevated PI3K/AKT signaling and survival of these cells [208]. Under normal physiological conditions, DEPTOR appears to positively regulate adipogenesis [209].

Although many proteins have been described as parts of both the mTORC1 and mTORC2 complexes, it is likely that even more binding partners, adapter proteins, and regulators will be described for both of these large signaling complexes. Interestingly, because of a complex web of feedback circuits within and around the PI3K/AKT/mTOR axis, the mTOR kinase can be considered to be both upstream *and* downstream of itself.

1.2.7 Feedback signaling within the PI3K/AKT/mTOR pathway

As with many biological signaling networks, there exist within the PI3K/AKT/mTOR axis several mechanisms for downregulation of signaling once it has been initiated. One of the first circuits to be appreciated was an

inhibitory circuit where activation of insulin signaling leads to the degradation of the IRS1/2 adapter subunits [210-211]. It is now understood that both S6K1 and mTORC1 phosphorylate IRS1/2 at several residues [212-215], and that—unlike tyrosine phosphorylation of IRS1/2—these phosphorylation events serve to destabilize the protein and facilitate its degradation by the

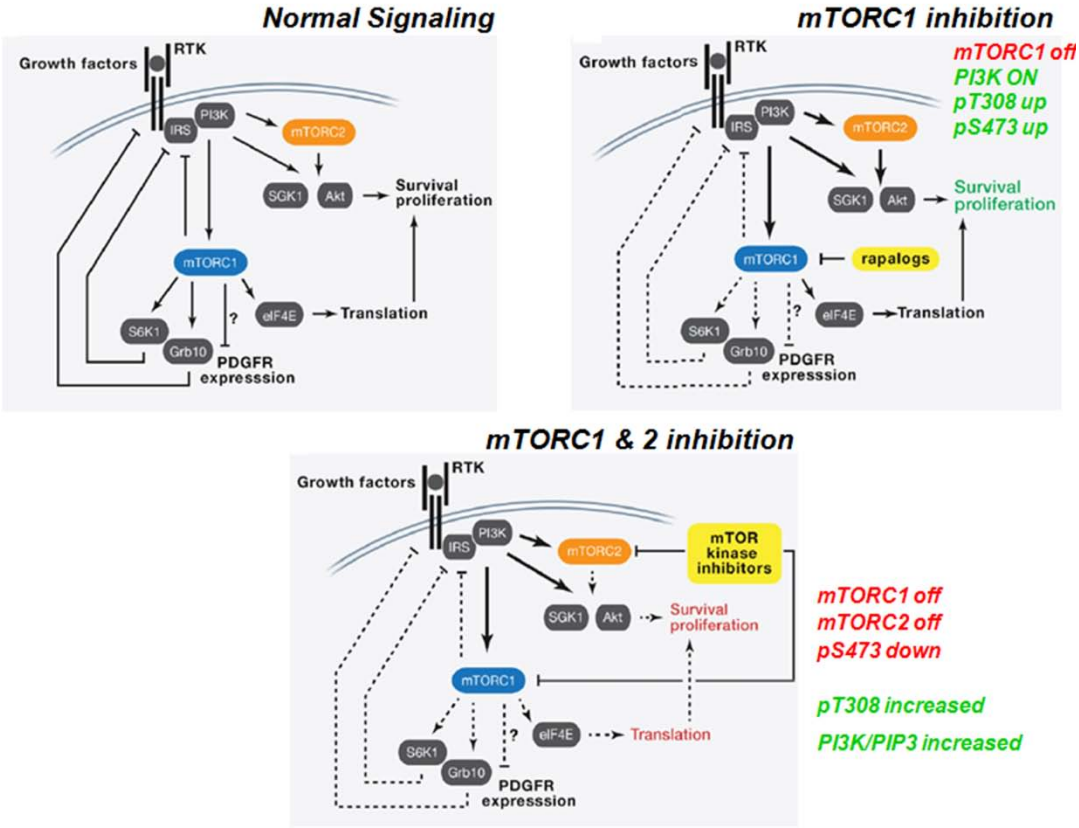

Figure 1.3: mTORC1 or mTORC1/2 inhibition activate PI3K/AKT signaling by relieving negative feedback circuits to upstream RTK signaling machinery. (A) Under normal signaling conditions, RTK activation is inhibited by a negative regulatory circuit where S6K1 inhibits IRS1 stability. (B) mTORC1 inhibition prevents S6K1 phosphorylation of IRS1, which activates mTORC2, PI3K, and AKT. (C) ATP-competitive inhibitors of mTOR potently relieve the aforementioned negative regulatory circuits, which upregulates IRS1/RTK signaling to PI3K, and hyperphosphorylates AKT at T308 despite an ablation in S473 phosphorylation. Adapted from Laplante and Sabatini, 2012 [1].

proteasome. Thus, mTORC1 inhibition with rapamycin leads to accumulation of IRS1/2, activates PI3K, and leads to an increase in membrane PIP_3 and phosphorylation of AKT at T308 and S473 (Figure 1.3). Similarly, the development of ATP-competitive mTOR kinase inhibitors has demonstrated that dual mTORC1/2 inhibition also potently de-engages the negative regulatory circuits between downstream and upstream signaling, despite the inactivation of mTORC2 by these inhibitors [208]. Thus, simultaneous inhibition of mTORC1/2 can potently hyperactivate PI3K activity and AKT T308 phosphorylation, thus upregulating AKT.

Phosphoproteomic approaches have recently uncovered yet another feedback inhibitory mechanism between mTORC1 and the upstream growth factor machinery. The recently described mTORC1 substrate GRB10 serves to inhibit insulin and IGF-I signaling under normal conditions, but this effect is blunted when mTORC1 is inhibited with rapamycin or ATP-competitive inhibitors like Torin1 [216-218]. Further, GRB10 is downregulated in some tumors [218], which suggests that these patients may respond better to therapies that utilize PI3K inhibitors, rather than ones that rely on mTOR inhibitors.

These feedback circuits are likely to have consequences for the efficacy of small molecule inhibitors in the clinic. Indeed, immunohistochemistry from tumors of rapamycin treated patients has demonstrated that rapamycin can potently upregulate AKT phosphorylation *in vivo* [219-220]. Thus, while certain tumors—for examples, cancers with

activating mTOR mutations or inactivating TSC1/2 mutations—may respond ideally to mTOR inhibitors, great caution should be exercised in determining which patients would respond best to these therapies [221-222].

1.3 THE PI3K/AKT SIGNALING AXIS IS FREQUENTLY ALTERED IN HUMAN CANCERS

A number of dysregulations in regular cellular physiology are necessary in the course of tumorigenesis [223]. For example, cells typically respond to a number of cues that encourage regular apoptosis, restrict inappropriate growth, maintain genomic integrity, and keep interactions with surrounding cells physiologically regular. However, in deregulating one or several of these characteristics—typically by genetic or epigenetic mechanisms—cancer cells can escape the normal life and fate of regular cells and become “masters of their own destinies” [223]. Given the central role of PI3K/AKT signaling in regular cellular and organismal physiology, it is unsurprising that a variety of mutations within this pathway are found in human tumors.

It is now appreciated that direct gain-of-function mutations in *PIK3CA*—such as mutations that code for amino acid changes E545K and H1047R in the p110α protein, among others—are found relatively frequently in certain tumor types [31, 224]. Indeed, mutations such as these activate the inherent kinase activity of p110α, which activates downstream kinases like AKT and mTOR. Further, mutations in the regulatory p85 subunit of PI3K

can serve to activate the pathway in tumors [225-227]. The oncogenicitiy of certain hotspot mutations make possible the specific targeting of mutant PI3K proteins with small molecule inhibitors [228]. This work is in relatively early stages, but could be a promising way to target PI3K/AKT signaling in patients.

The most commonly mutated and well understood tumor suppressor within the PI3K pathway is the lipid phosphatase *PTEN*. As described above, PTEN is a lipid phosphatase that plays a critical role in downregulating PI3K/AKT signaling by dephosphorylating the 3'-OH of PIP_3. Loss of PTEN function can occur in tumors a number of ways—methylation of the *PTEN* promoter can silence *PTEN* mRNA expression [229], missense or nonsense mutations can lead to loss-of-function mutant proteins [230-231], and heterozygous or homozygous deletions of *PTEN* can give cells a selective growth advantage [52, 232]. Strikingly, depending on the cancer type, loss of PTEN function can be found in up to 40-80% of tumors. Further, conditional knockout studies in the mouse have confirmed that *PTEN* loss is sufficient to drive tumorigenesis in the prostate and other tissues [233]. Interestingly, even haploinsufficiency of *PTEN* in some systems is sufficient to dysregulate PI3K/AKT signaling and drive tumor growth [234]. PTEN loss poses a significant challenge in the clinic because reconstituting the lost function of a tumor suppressor within diseased cells is far less straightforward than drugging an oncoprotein that is a kinase or transcription factor. However, the

recent description of a soluble PTEN protein that is excreted by cells may suggest interesting therapeutic approaches available in the future [235].

In addition to mutations in *PIK3CA* and *PTEN*, mutations in the receptor tyrosine kinases upstream of PIP_3 generation are able to potently activate PI3K signaling and drive tumorigenesis. The most commonly deranged RTK is EGFR, which is found amplified or mutated in a variety of tumors, most typically in various subtypes of lung and brain tumors [225]. Copy number amplification of the *EGFR* gene is sufficient to drive oncogenic signaling [236], and oncogenic mutations in the *EGFR* gene can arise in the kinase domain itself, the extracellular domain of the receptor [237], or by heterozygous deletion of an autoinhibitory domain of the kinase (the so-called EGFRviii variant) [238-239]. Indeed, these alterations—copy number gain, activating point mutations, and deletion of inhibitory domains—are themes that are repeated with other receptor tyrosine kinases in various tumors (c-Kit, c-Met, PDGFR, etc.).

Finally, several kinases downstream of PIP_3 generation can activate tumorigenic signaling as well. Mutations in *AKT1* have recently been described, where an E17K mutation in the PH domain results in an increased affinity for the phospholipid membrane, thus localizing AKT to the membrane even in the absence of accumulated PIP_3 [240-243]. Although once thought rare, the E17K AKT1 mutation is now found relatively regularly in multiple tumor types. Downstream of AKT, mutations in *MTOR* have recently been identified in tumor samples that confer increased kinase

activity to mTORC1 and in some cases mTORC2 [244][245]. Interestingly, many of these *MTOR* mutants render mTORC1 signaling exquisitely sensitive to rapamycin, which suggests that tumors harboring these mutations may be ideal candidates for mTOR inhibitor-based therapies.

1.4 TARGETING THE PI3K/AKT PATHWAY IN HUMAN CANCERS

1.4.1 From chemotherapy to targeted therapy

The elucidation of the various genetic derangements within growth regulating pathways that can drive tumorigenesis has led to the development of therapies that can specifically target the causative lesion in a tumor [246]. The prospect of identifying the genetic lesions of an individual's tumor and then drugging those lesions has offered a welcome alternative to traditional radiation- and chemotherapy-based treatments for cancer. Rather than targeting all growing cells, targeted inhibition of the oncoprotein(s) that drive the growth of a tumor could ostensibly provide greatly diminished toxicity and better clinical responses. Indeed, some of the first targeted therapies—Gleevec® (imatinib) for chronic myelogenous leukemia (CML) and Herceptin® (trastuzumab) for ERBB2-driven breast cancers—have proved themselves to be superior to the previous therapies for those tumors. However, the hope of targeted therapies has been tempered by the emergence of many mechanisms of resistance. A more complete understanding of the complex balance of survival signal transduction within

the cell (and the mutations that alter these pathways) would greatly improve the design and deployment of targeted therapies for cancer.

1.4.2 Strategies for targeting tyrosine kinases

As mentioned above, the development of kinase inhibitors like Imatinib demonstrated the possibility that small molecules targeting specific signaling proteins could be effectively deployed in the clinic. In the clinic, the most successful type of small molecule kinase inhibitor for cancer therapy have been tyrosine kinase inhibitors. Although it was originally developed to target the BCR-ABL fusion protein, imatinib is also useful for targeting tumors with other activated tyrosine kinases such as PDGFR. Further, several imatinib derivatives—like dasatinib, nilotinib and bosutinib—have been developed to counter the different imatinib-resistant mutations that arise in BCR-ABL [247-249].

Beyond BCR-ABL, several tyrosine kinase inhibitors have also found some success in the clinic. The first of these was monoclonal antibody—trastuzumab—that targets the human epidermal growth factor receptor 2 (HER-2) [250-251]. Trastuzumab was approved by the FDA for use against breast cancer in 1998, and has also found use as a treatment for some types of gastric tumors [252-253]. Other antibodies that target HER-2 or EGFR, like pertuzumab [254], cetuximab [255], and panitumumab [256] are also FDA approved, mostly for use in different types of HER-2 or EGFR-positive breast cancers. EGFR and HER-2 are also targeted by a number of small

molecule inhibitors such as lapatinib [257], erlotinib [258] and gefitinib [259]. These molecules are typically deployed against various breast tumors, non-small cell lung cancers, or pancreatic tumors.

1.4.3 PI3K inhibitors

Considering the central role that PI3Ks play in survival signaling, it is unsurprising that many inhibitors targeting PI3K isoforms are in either preclinical or clinical development [260]. Many groups and private companies have developed isoform-specific inhibitors for p110α [261], p110β [262]. Further, a potentially attractive method for specifically targeting the aberrant PI3K signaling within tumors that harbor activating *PIK3CA* mutations is the use of mutant-specific small molecule inhibitors [228]. These inhibitors are, however, in their early stages of development and it remains unclear how clinically useful they will prove.

PI3K inhibitors have great potential as anti-tumor tools in the clinic [263]. However, that they have yet to gain FDA approval suggests that more effort must be put into properly identifying which patients are most likely to respond favorably to treatment with PI3K inhibitors. For example, while patients with activating *EGFR* or *PIK3CA* mutations may both have hyperactive PI3K/AKT signaling, PI3K blockade would likely be most advantageous to the patient with the *PIK3CA* mutant tumor. Since not all clinical trials evaluating PI3K inhibitors have triaged patients based on the mutational status of the genes in the PI3K/AKT pathway, it is quite possible

that the antitumor benefits of several of these molecules has been masked by tumors predestined by their genotypes to be refractory to PI3K inhibition.

1.4.4 Serine/threonine kinase inhibitors: targeting AKT and mTOR

Because the genetic lesions that drive tumors can occur at multiple points within a given pathway, it may not always be advantageous or even useful to target upstream regulators like RTKs and PI3Ks. For example, some tumors are likely driven by mutations in *AKT* or *MTOR*, and thus inhibiting PI3K signaling would pose little to no benefit. Indeed, several groups have described both ATP-competitive and allosteric inhibitors of AKT1-3 [264-267]. These inhibitors have either shown little advantage over current therapies in the clinic—like perifosine [268]—or are in very early stages of clinical evaluation [269]. However, AKT inhibitors could be very advantageous for patients with tumors driven by oncogenic *AKT* mutations.

As mentioned above, the mTOR inhibitor rapamycin has been deployed in the clinic as an immunosuppressant, an anti-restenotic agent, and most recently as an anti-tumor agent. Although rapamycin and its "rapalogue" derivatives have been clinically evaluated for activity against a variety of tumors, mTORC1 inhibitors like CCI-779 (temsirolimus) were first FDA approved for the treatment of renal cell carcinoma [270-271]. Subsequent studies have led to approval in breast cancer in combination with hormone therapy [272-275]. As is the case for the other small molecule inhibitors discussed above, it is likely that clinical trials that specifically target

patients based on which genetic lesions are present in their tumors (e.g. activating *MTOR* mutations or inactivating *TSC1*/*TSC2* mutations) will be useful in identifying which patient populations would benefit most from molecules that inhibit mTOR.

1.4.5 The promises and risks of targeted therapies

The successes of targeted therapies like Gleevec® and Herceptin has often been heralded as a harbinger of a new era of "personalized medicine" driven by targeted therapies [276-277]. It should be kept in mind that despite the early successes of drugs like BCR-ABL inhibitors (Gleevec, etc.) in treating CML, most cancers are dauntingly complex in the number of genetic lesions that may drive a tumor. Much of the success of BCR-ABL inhibitors is likely due to the fact that oncogenesis in CML is driven primarily by the BCR-ABL fusion protein. In contrast, tumorigenesis in solid tumors and non-CML liquid tumors is typically driven by a number of genetic lesions [223].

The development of resistance to targeted therapies by tumors is a complex challenge. For example, CML often develops resistance to BCR-ABL inhibitors through mutations within or near the ATP-binding pocket of the kinase domain [276, 278-280]. Similarly, EGFR and ERBB2-driven tumors can easily develop resistant kinase mutations in response to treatment with inhibitors like erlotinib or lapatinib [278]. Beyond mutations in the targeted signaling molecule, resistance to EGFR inhibitors can arise from compensatory upregulation of ERK/MAPK signaling [281] or downregulation

of NF-κB signaling [282]. Finally, as mentioned above, mTORC1 inhibition in the clinic should be pursued with caution, as it is likely that the anti-growth properties of rapamycin are blunted by the fact that mTORC1 inhibitors activate PI3K/AKT [219-220].

It is tempting to wish that the success of drugs like Gleevec® could be generalizable to other tumor types. Unfortunately, the signal transduction pathways that regulate tumorigenesis are complex, as is the scope of the genomic alterations that activate these pathways. Thus, the emphasis of the cancer research community should be focused on the discovery of as many regulatory steps, circuits and nodes as possible. This would allow for the design of multitudes of specific inhibitors that could be used to tailor targeted therapies to each individual tumor with an eye towards circumventing resistance to targeted therapies.

1.5 RNAi SCREENS TO IDENTIFY NOVEL COMPONENTS OF ONCOGENIC SIGNALING

1.5.1 RNA interference (RNAi) as a loss-of-function tool to study gene function

RNA interference (RNAi) is a relatively new technology in the toolkit of the modern molecular biologist that takes advantage of an evolutionary conserved mechanism of the regulation of mRNA through the micro RNA (miRNA) pathway [283-286]. miRNAs are small (22 nt), non-coding RNAs that are endogenous to the cell that serve to regulate the abundance and

translation of mRNA transcripts that code for genes [286-288]. When bound to their target mRNAs, miRNAs down-regulates translation of the mRNA by one of two mechanisms: 1.) blocking the ribosome from translating the mRNA, or 2.) facilitating degradation of the mRNA by the RNA-induced silencing complex (RISC).

The mechanism for RNAi-mediated gene silencing is similar to the miRNA pathway with the exception that RNAi is not an endogenous process. Rather, it simply takes advantage of the miRNA machinery that exists within the cell. Indeed, RNAi has been tremendously advantageous to investigators of biology because it provides a relatively easy—albeit imperfect—method of silencing the mRNA transcript of a gene of interest, thus allowing for loss-of-function studies of proteins. Further, in contrast to miRNAs, RNAi reagents are most always perfectly complementary to their target transcripts, which facilitate destruction of targeted mRNA.

There are many methods of delivering RNAi reagents to mammalian cells. For example, small interfering RNAs (siRNAs) can be readily transfected into some cell types. However, this method can induce unwanted toxicity to the transfected cells [3]. To remedy the issues of transient transfection and transfection toxicity associated with siRNA delivery, several groups designed retroviral or lentiviral approaches to facilitate RNAi studies [289-294]. Although these methods differ in some regards, they are similar in that 1.) they rely upon viral delivery of DNA that stably integrates into the host cell's genome, 2.) stable expression of miRNA-like RNAs or short

hairpin RNAs (shRNAs) is achieved from the integrated DNA, and 3.) suppression of the targeted mRNA transcript can be achieved for longer periods than with siRNA-based approaches.

Not long after the initial characterization of mammalian and *Drosophila* RNAi, several groups undertook efforts to generate large scale RNAi libraries to facilitate loss-of-function genetic screens [289, 295-308]. The most prevalent deployment of these RNAi libraries has been in pooled screens, where each shRNA reagent is administered to a population of cells at a multiplicity of infection (MOI) of <1 [282, 305]. Although well suited for high-throughput RNAi, pooled screens are limited by the fact that their readouts rely on the measurement of shRNA or shRNA barcode abundance within the pool. Hairpin abundance is itself an ersatz readout of the viability of a cell population that has been transduced with an individual shRNA reagent. Thus, this approach has been useful in identifying genes that confer drug resistance [282, 305] or in performing *in vivo* loss-of-function screens [306, 309-312].

Although non-pooled, arrayed shRNA screens were described before pooled approaches were refined, the number of arrayed screens that have successfully identified novel biology is relatively limited. Arrayed screens are less technically straightforward than pooled RNAi screens in that they require resources like plate handling robots and high throughput, often high-content microscopy. However, arrayed screens do not require the deconvolution that is inherent to pooled screening. Further, arrayed formats

allow for more biologically interesting assays than pooled screens. For instance, an arrayed RNAi screen can be used to assay the activity of signaling pathways. Indeed, several groups have used this approach to successfully identify novel components of Ras/ERK signaling in *Drosophila* [298, 313-314] and new regulators of cell division and histone phosphorylation [302-303]. Thus, arrayed screens are useful tools for probing signal transduction in ways that pooled approaches are not.

1.5.2 RNAi screens to identify novel oncogenic regulators of PI3K/AKT signaling

Although discovery of new components of signal transduction pathways can be achieved a number of ways—through proteomics, small molecule inhibitor screens, cDNA microarray studies—we reasoned that a loss-of-function RNAi screen could be a potent tool if combined with a robust signaling assay. We were fortunate that the Broad Institute RNAi Consortium (TRC) platform has undertaken a long-term effort to design, synthesize, and make available lentivirus-delivered shRNAs targeting every known human and mouse gene [302-303, 315]. This collection provides an impressive amount of coverage in that a minimum of 5 shRNAs are provided for gene, and many genes are targeted by 10-20 different, non-overlapping shRNA reagents. In addition to a library of shRNA reagents, the TRC has performed extensive validation with quantitative reverse-transcription PCR (qRT-PCR) to validate which hairpins succeed in depleting their target mRNAs.

While the biochemistry and genetics of PI3K/AKT signaling are both very well studied, we theorized that there are likely a number of unappreciated proteins that regulate this pathway. Our rationale was that while most tumors likely upregulate PI3K/AKT in some way, not all tumors in queried oncogenomic databases display obvious lesions in the genes within this signaling axis. Although the assumption of PI3K upregulation in *all* tumors is not a certain one, we reasoned that tumors with no obvious RTK/PI3K/PTEN/AKT/MTOR pathway lesions must be activating PI3K/AKT signaling via genes that regulate—but are currently not understood to be involved in—this pathway.

This thesis details a set of RNAi screens that we performed at the Broad Institute to identify novel regulators of PI3K/AKT signaling. Our goal was to identify novel proteins that regulate the PI3K/AKT pathway, then to interrogate the mutational status of these genes in oncogenomic databases. We suggest that this approach—targeted loss-of-function screening whose results are prioritized by utilizing oncogenomic data—is a useful tactic to identify proteins that play a role in normal cellular signaling as well as tumorigenesis.

CHAPTER TWO:

AN RNAi SCREEN IDENTIFIES THE SMALL GTPASE RAB35 AS A NOVEL ONCOGENIC REGULATOR OF PI3K/AKT SIGNALING

2.1 ABSTRACT

In an RNAi screen for genes that affect AKT phosphorylation, we identified the RAB35 small GTPase—a protein previously implicated in endomembrane trafficking—as a new regulator of the PI3K pathway. Depletion of RAB35 in human and mouse cells suppresses AKT phosphorylation in response to growth factors, whereas expression of a GTPase-deficient mutant of RAB35 constitutively activates the PI3K/AKT pathway. RAB35 functions downstream of growth factor receptors and upstream of PDK1 and mTORC2, two established regulators of AKT, and interacts with PI3K. We identified two RAB35 mutations in human tumors that activate PI3K/AKT signaling, suppress apoptosis, and transform cells in a PI3K-dependent manner. Thus, we identify RAB35 as a proto-oncogene that is both necessary and sufficient for activating PI3K/AKT signaling. That a RAB GTPase can activate PI3K/AKT signaling and transform cells suggests that there may be latent oncogenic potential in dysregulated endomembrane trafficking.

2.2 INTRODUCTION

The phosphatidylinositol 3'-OH kinase alpha (PI3Kα) is a lipid kinase and a key regulator of cell survival, proliferation and growth that is commonly activated in human cancers [316-317]. PI3Kα is comprised of a 110 kDa catalytic subunit (p110α) and an 85 kDa adapter subunit (p85) that links PI3Kα to activated growth factor receptor tyrosine kinases (RTKs) [318]. At the cell membrane, PI3Kα phosphorylates the membrane lipid phosphatidylinositol (4, 5)-bisphosphate (PIP_2) to form the second messenger phosphatidylinositol (3, 4, 5)-trisphosphate (PIP_3), which then recruits a number of effectors to the lipid membrane. Key among these is the serine/threonine kinase AKT, which regulates an array of cellular processes such as glucose transport, the cell cycle, and anti-apoptotic signaling [133]. Activating mutations in oncogenes (*PIK3CA*, *EGFR*, *AKT1*) or loss-of-function alterations in tumor suppressors (*PTEN*) have been well characterized for their ability to drive tumorigenesis in a PI3K-dependent fashion [225]. Thus, the components of this pathway are attractive targets for cancer therapy, and many small molecules that target components of the PI3K/AKT pathway are either currently deployed in the clinic or in clinical trials [263, 319].

To identify new regulators of the PI3K/AKT pathway, we performed a loss-of-function RNA interference (RNAi) screen using lentiviruses that express short hairpin RNAs (shRNAs) [303]. We reasoned that the proteins most likely to be regulators of PI3K/AKT signaling would be GTPases and

kinases, so we limited the screen to shRNAs targeting genes coding for all known G-proteins and lipid/protein kinases. Because AKT phosphorylation is a faithful indicator of PI3K activity, we used an immunofluourescent approach to quantitatively measure phosphorylation of AKT at serine 473 (S473) in screened HeLa cells. Therefore, we screened a collection of 7,450 shRNAs in an arrayed format to identify kinases or GTPases whose depletion could alter PI3K-dependent AKT phosphorylation.

2.3 METHODS AND MATERIALS

2.3.1 Cell lines and tissue culture

The following cell lines were obtained from American Type Culture Collection (ATCC): 22Rv1 (CRL-2505), 786-O kidney adenocarcinoma (CRL-1932), ACHN kidney adenocarcinoma (CRL-1611), HeLa cervical adenocarcinoma cells (CCL-2), Caki-2 renal adenocarcinoma (HTB-47), HT-29 colon adenocarcinoma (HTB-38), NIH-3T3 murine fibroblasts (CRL-1658), PC3 prostate adenocarcinoma (CRL-1435), SK-CO-1 colorectal adenocarcinoma (HTB-39), and SW620 colorectal adenocarcinoma (CCL-227). SN12C kidney carcinoma cells were obtained from the Developmental Therapeutics Program, NCI/NIH. HEK-293E cells were a generous gift to the Sabatini lab from Dr. John Blenis (Harvard Medical School). All human cells were cultured at 37° C (5% CO_2) in high-glucose Dulbecco's Modified Eagle Medium (DMEM) supplemented with 10% fetal bovine serum (FBS), penicillin-streptomycin and glutamate. NIH-3T3 murine fibroblasts were

cultured in DMEM with 10% bovine calf serum (BCS) from Colorado Serum Company. All cells were passaged every 3 days as previously described [208].

2.3.2 Antibodies

The goat anti-RICTOR S-20 antibody was from Santa-Cruz Biotechnology (sc-50678), the anti-p85 antibody was from Millipore (04-196), the anti-FLAG M2 antibody was from Sigma-Aldrich (F1804), and the anti-RAB35 antibody was from Proteintech (11329-2-AP). All other antibodies were from Cell Signaling Technologies: anti-phospho S473 AKT (4060), anti-phospho T308 AKT (2965), anti-total pan AKT (2920), anti-phospho T346 NDRG1 (5482), anti-phospho T24/32 FOXO1/3A (9464), anti-RICTOR (2140), anti-mTOR (2998), anti-p110α (4249), anti-p85 (4257), anti-PARP (9532), anti-cleaved Caspase 3 (9664), and anti-HA (3724). Secondary antibodies used for quantitative immunoblotting were obtained from LiCor Biosciences: IRDye 800CW goat anti-rabbit IgG (926-32211), IRDye 800CW goat anti-mouse IgG (926-32210), IRDye 680RD goat anti-mouse (926-68170).

2.3.3 Chemicals, ligands and small molecules

Insulin (I9278) and polybrene (AL-118) were purchased from Sigma-Aldrich. Dimethylsulfoxide (DMSO, BP231-4) was purchased from Fisher Scientific. Puromycin (ant-pr-1) and Hygromycin B (ant-hm-1) were from

InvivoGen. Epidermal Growth Factor (EGF, AF-100-15), Platelet Derived Growth Factor AA (PDGF-AA, 100-13A), Insulin-like Growth Factor I (IGF-I, 100-11) and Vascular Endothelial Growth Factor (VEGF, 100-20) were purchased from Peprotech. Torin1 (S2827), rapamycin (S1039), PIK-90 (S1187) and GDC-0941 (S1065) were all purchased from Sellekchem. Each drug was resuspended to 10 mM in DMSO, aliquoted and stored at -20° C until use. 100% Triton TX-100 was purchased from Roche (11 332 481 001).

2.3.4 RNAi screens

High-throughput lentiviral-short hairpin RNA (shRNA) screens were performed at The RNAi Consortium (TRC) at the Broad Institute as previously described [303]. The shRNA library screened contained shRNAs targeting control genes (*LUC*, *GFP*, *RFP* and *LACZ*), and between 5-15 individual shRNAs targeting each human kinase or GTPase for a total of 7,774 shRNAs targeting 1,012 genes (Table 1). 1 day before infection, 300 HeLa cells were seeded in each well of glass bottomed 384-well plates (Costar 9120) in 50 μL of regular DMEM. 24 hours later, the medium was removed and replaced with 50 μL DMEM containing 8 μg/mL polybrene. 1 hour later, 1μL of viral supernatant containing one individual shRNA-expressing lentivirus was aliquoted into each well, and the plates were incubated at 37° C. Each individual plate was performed in triplicate, and each plate contained 15-20 control hairpins (sh*LUC*, sh*GFP*, sh*RFP*, sh*LACZ*) distributed throughout each plate, 2 sh*RAPTOR*_65 and 2

sh*RICTOR*_25 control hairpins, 4 or more empty wells as selection controls and ~350 shRNA reagents targeting human kinases or GTPases. 24h later, the media in each well was gently aspirated and replaced with DMEM supplemented with 1 μg/mL puromycin. Screen plates were incubated at 37° C for 3 days, treated for 15 minutes with DMEM containing 100 ng/mL insulin, then immediately processed for immunofluorescence.

2.3.5 Immunofluorescence for RNAi screens

After treatment with insulin, plate media was aspirated, and the cells were fixed for 15 min. at room temperature with 50 μL 4% paraformaldehyde. Plates were then washed with PBS 3 times, then permeabilized with 50 μL 0.1% Triton X-100 in PBS for 15 min, and washed once again with PBS 3 times. The last rinse was aspirated, and 12.5 μL of anti-phospho-S473 AKT antibody mix was added to each well (Cell Signaling Technology #4060, diluted 1:100 in 0.1% TX-100 PBS). Plates were briefly centrifuged, then incubated overnight at 4° C. The next day, primary antibody buffer was aspirated, the plates were washed 3 times with PBS, and the plates were then incubated at room temperature for 2 hours with a secondary immunofluorescence cocktail of goat anti-rabbit 800 nm antibody (1:1000) and Sapphire 700 nm whole cell stain (LiCor 928-40022 , 1:1000) in 0.1% TX-100 PBS. Finally, secondary reagents were aspirated, the wells were washed 3 times with PBS, and each well was filled with 50 μL PBS after the final wash. Plates were then imaged at 700 nm and 800 nm

wavelengths using a LiCor Odyssey near-infrared scanner and LiCor Odyssey software. For each well, the integrated signal intensity in the 700 nm (nuclear and whole-cell stain) and 800 nm (phospho-S473 AKT) channels were quantified using the LiCor Odyssey software, and a normalized phospho-AKT signal of each well was calculated by dividing the signal value for the 800 nm channel by that of the 700 nm channel. These values were then used to calculate Z-scores for each well within its plate as compared to control shRNA reagents.

2.3.6 Phospho-AKT and viability Z-score calculation

In order to compare phospho-AKT levels between different plates, we converted the normalized phospho-AKT from each well to a Z-score [320] with the formula $\mathbf{z = (x - \mu)/\sigma}$ (**x**, normalized phospho-AKT signal for a well; μ and σ, mean and standard deviation (respectively) of the normalized phospho-AKT values for all sh*LUC*, sh*RFP*, sh*GFP* and sh*LACZ* shRNAs in an individual plate). Once normalized, we averaged the values of each well for replicate plates to generate a mean phospho-AKT Z-score for every screened shRNA reagent. The same calculation was used to score viability/cell count for each well using the 700 nm whole-cell stain values. Viability and phospho-AKT Z-scores for each screened shRNA are listed in Appendix A.

2.3.7 RNAi screen data analysis and hit selection

After generating averaged phospho-AKT Z-scores for each hairpin as described above, we ranked our entire dataset from smallest to largest average phospho-AKT Z-score. We chose -1.50 and +1.50 as cutoff points to call shRNAs as hits, thus we discarded from this list any shRNA reagents with a phospho-AKT Z-score greater than -1.50 and less than +1.50. We chose to impose a 40% shRNA hit-rate requirement for each gene. Thus, for a gene represented by 5 hairpins, 2 of those average hairpins must return phospho-AKT Z-scores below -1.50 or above +1.50 to be considered a hit. Similarly, genes with 10 screened hairpins must return 4 shRNAs as hits. shRNAs were only considered for our 40% hit-rate if they scored in the same direction. Further, to exclude shRNAs that induced undue toxicity, we excluded shRNAs that caused a decrease of -6.0 or greater in the viability Z-score. Thus, our primary hit list was comprised of shRNAs that were both non toxic and scored as hits at a rate of 40% or greater per gene, which are listed in Appendix B. We next used quantitative RT-PCR data generated by The RNAi Consortium to further curate our hits. A secondary hit-list was generated by removing any shRNA that failed to knock down its target mRNA by more than 50%. Genes that retained a 40% shRNA hit-rate after this step are listed as secondary hits in supplemental Table 3. We next excluded from our hits any gene that has been linked to PI3K/AKT signaling in the literature. This was accomplished by searching NCBI PubMed for PI3K or AKT and the name of each gene. For example, a PubMed search for

"AKT and RAB35" returns no publications and *RAB35* would therefore be retained in our tertiary list of hits. Genes with no prior link to PI3K/AKT signaling thus comprised our tertiary list of hits and are reported in Table 4. Finally, tertiary hits were curated for alterations in human tumors and cancer cell lines as described in the next section.

2.3.8 Identification of hit gene mutations and genomic alterations in human cancers

To identify genes with mutations or alterations in human cancers we utilized the MSKCC cBio genomics portal (http://www.cbioportal.org/public-portal) [321-322], the Sanger Catalog of Somatic Mutations in Cancer (COSMIC) (http://cancer.sanger.ac.uk/cancergenome/projects/COSMIC/) [323-326], and the Broad Institute/Novartis Cancer Cell Line Encyclopedia (CCLE) (http://www.broadinstitute.org/ccle/home) [327-329]. To identify hit genes mutated in cancers within these databases, we considered meaningful mutations to be either 1.) recurrent mutations, or 2.) mutations that resembled known mutations in similar genes that altered protein function. For example, a Q->L mutation in the catalytic domain of an uncharacterized hit GTPase that resembles the canonical transforming $KRAS^{Q61L}$ mutation would be considered meaningful even if it was not recurrent. For copy number alterations, we considered genes to be altered if they were focally amplified or deleted. For example, a hit gene was not considered to be "altered" in its copy number if the deletion containing it was

comprised of the loss of an entire chromosome arm. We did not inspect genes for alterations in their mRNA expression levels. Tertiary hits that were found to be altered in human tumors or cancer cell lines and their respective alterations comprised our list of prioritized hits and are reported in Table 5.

2.3.9 Cell lysis

Cell lysis and immunoprecipitations were performed as previously described with some modifications [208]. All cells were rinsed once with ice-cold PBS before lysis. Unless otherwise noted, cells were lysed with Triton X-100 lysis buffer (40 mM HEPES [pH 7.4], 2 mM ethylenediaminetetraacetic acid [EDTA], 10 mM sodium pyrophosphate, 10 mM sodium glycerophosphate, 50 mM NaF, 150 mM NaCl, 1% Triton X-100). 25 mL of lysis buffer was supplemented with one cOmplete EDTA-free protease inhibitor chip (Roche, 13971800). The lysates were incubated at 4° C for 15 minutes, the insoluble fraction was spun in a microcentrifuge at 14,000 rpm for 15 minutes at 4° C, and lysates were collected. The protein concentrations of cell lysates were then determined using Bio-Rad Bradford assay reagent (500-0001) and an Eppendorf Biophotometer by reading the absorption of each sample at 600 nm. Lysates were then mixed with Laemmli's buffer (50 mM Tris-HCl [pH 6.8], 2% SDS, 10% glycerol, 100 mM 2-mercaptoethanol, 0.1% bromophenol blue) so that the final protein concentration in each sample was 1-3 μg/μL, boiled for five minutes, and

used for sodium dodecylsulfate polyacrylamide gel electrophoresis (SDS-PAGE) as described below.

2.3.10 Immunoprecipitations

Cells were lysed in CHAPS-containing lysis buffer (40 mM HEPES [pH 7.4], 5 mM $MgCl_2$, 10 mM sodium pyrophosphate, 10 mM sodium glycerophosphate, 50 mM NaF, 0.3% CHAPS). 25 mL of lysis buffers were supplemented with one EDTA-free protease inhibitor chip. Proteins were immunoprecipitated from 1000 μg of cell lysates with 1 μg of primary antibody for 2 hours or overnight at 4° C. 15 μL of a 50% slurry of Protein G-agarose beads (Pierce) was then added to each tube, and the immunoprecipitations were incubated for another hour at 4° C with rotation. Immunoprecipitates were then centrifuged at 5,000 rpm for one minute and washed 3 times with CHAPS lysis buffer. On the final wash, the lysis buffer was aspirated completely and 15 μL 1X SDS loading buffer was added to the beads, which were then boiled for 5 minutes. The immunoprecipitates were then analyzed by SDS-PAGE as described below.

2.3.11 SDS-PAGE

10-20 μg of protein lysates or immunoprecipitates were loaded onto 4-12% Bis-Tris gels (Novex) and resolved by sodium dodecylsulfate-polyacrylamide gel electrophoresis (SDS-PAGE) as previously described [330]. Proteins were then transferred to Immobilon-FL nitrocellulose

membranes (0.45 μm pore size) from Millipore (IPFL00010), and then processed for immunoblotting.

2.3.12 Immunoblotting

All western blots were processed using the LiCor Odyssey near-infrared system. After transferring to membranes, blots were rinsed for 1 hour in Odyssey blocking buffer (927-40000) diluted in 50% PBS, then incubated with primary antibody (1:1000) in antibody incubation buffer (Odyssey blocking buffer, 50% PBS-T) overnight at 4° C or 2 hours at room temperature. Blots were then washed 3 times (5 minutes each) in PBS-T (Tween, 0.1%), and incubated with secondary antibodies (1:10,000, goat anti-rabbit or mouse conjugated to 700 nm or 800 nm IR-dye) in secondary antibody incubation buffer (Odyssey blocking buffer, 50% PBS-T, 0.01% SDS) for 1 hour at room temperature. The blots were rinsed 3 more times in PBS-T, rinsed with deionized H_2O, washed for 5 minutes in PBS, and then imaged on the LiCor Odyssey near-infrared scanner (resolution 84 μm, intensity of 7 on both 700 and 800 nm channels). Images were saved, processed, and quantitated using the LiCor Odyssey software.

2.3.13 Plasmids, cDNA manipulations and mutagenesis

The following plasmids were purchased from Addgene: lentiviral (psPAX2) and retroviral (pUMVC) packaging plasmids (12260 and 8449, respectively), pVSV-G (8454), pBabe HA-*PIK3CA* H1047R (12524), and

pBabe *KRAS* G12V (9052). pMSCV plasmids coding for murine *AKT1* (wildtype and S473D) were generous gifts from Dr. Dos Sarbassov (M.D. Anderson Cancer Center, Houston TX). *RAB35* was synthesized by Genscript (Piscataway, NJ) and subcloned into the SalI-NotI sites in the pLJM60 vector to generate a plasmid that would express N-terminal FLAG-tagged RAB35 protein [208], then transformed into TOP10 *E. coli* cells (Invitrogen). Mutagenesis of pLJM60 FLAG-*RAB35* and pMSCV mAkt1 cDNAs was performed as previously described using the Stratagene QuickChange II XL site-directed mutagenesis kit (200521) [330].

2.3.14 Lentiviral and retroviral production

Lentiviral particles expressing shRNA hairpins or cDNAs were generated as previously described using HEK-293CT cells (Clontech). 500,000 HEK-293CT cells were seeded in 5 mL of DMEM containing 10% IFS and 0.1X penicillin-streptomycin in 6 cm dishes. The next day, each plate was transfected with 1 μg of pLKO or pLJM60 plasmid expressing the desired shRNA or gene, 100 ng of pVSV-G plasmid, and 900 ng of psPAX2 packaging plasmid mixed with 6 μL FugeneHD transfection reagent (Promega, E2311). Retroviral particles expressing cDNAs were generated similarly, except that 900 ng pUMVC was used for packaging 1 μg pBabe or pMSCV reagents. 24 hours after transfection, the media on each plate was aspirated and replaced with regular DMEM supplemented with 10% FBS and 1.1% BSA. Media containing viruses was harvested 24 and 48 hours

afterwards. This supernatant was then clarified of cells by filtration through a 0.22 μm Steri-Flip filter (Millipore). Supernatants containing virus were frozen at -80° C until use or concentrated as described below.

2.3.15 Lentivirus and Retrovirus concentration

Because viral titers from lentiviruses and retroviruses expressing genes are often low, we concentrated each using Lenti-X and Retro-X reagents from Clontech (631231 and 631455, respectively). Briefly, viral supernatants were mixed 4:1 with the appropriate concentration reagent and incubated at 4° C overnight. The next day, virus was spun at 1,500g for 45 minutes, and the clarified supernatant was gently aspirated. Viral pellets were resuspended to 1/50th their original volume in fresh DMEM (with 10% FBS and 1.1% BSA), aliquoted, and stored at -80° C until use.

2.3.16 Lentiviral shRNA experiments

Lentiviral transduction of cells for shRNA experiments was performed as previously described [119, 291, 303, 331]. Human or mouse cells were seeded at 50,000 cells per well in 2 mL of media in 6 well plates. The next day, media was removed and replaced with media containing 8 μg/mL polybrene. 1 mL of unconcentrated shRNA-expressing lentivirus was then added to each well. 24 hours later, the media and virus was removed and replaced with fresh medium containing 1 μg/mL puromycin. Cells were then cultured for 3 to 5 days, then treated as necessary and lysed.

2.3.17 Human and mouse stable cell line generation

HEK-293E, HeLa and NIH-3T3 cell lines stably expressing FLAG-RHEB^{wt}, FLAG-RAB35^{wt}, FLAG-RAB35^{Q67L}, FLAG-RAB35^{S22N}, FLAG-RAB35^{A151T}, FLAG-RAB35^{F161L}, HA-p110α^{H1047R}, mAkt1^{wt}, mAkt1^{S473D}, mAkt1^{T308D}, or FLAG-AKT1^{myr} were generated as previously described [332]. Briefly, 10,000 cells were seeded into one well of a 6-well plate in 2 mL media. The next day, the media in each well was supplemented with 8 μg/mL polybrene. 1 mL of concentrated lentivirus (FLAG-RHEB or the FLAG-RAB35 alleles) or retrovirus (HA-p110α^{H1047R}, mAkt1^{wt}, mAkt1^{S473D}, mAkt1^{T308D}, KRAS^{G12V} or FLAG-AKT1^{myr}) was then added to each well. 24 hours later, the media was aspirated and replaced with fresh media containing the appropriate selection reagent (1 μg/mL puromycin or 100 ng/mL hygromycin B). Cells were grown to 80% confluence, then passaged, expanded further, and preserved at -80° C as frozen aliquots in media containing 10% DMSO and 40% serum.

2.3.18 Lentiviral RNAi reagents

We found that the sh*LUC*_221 hairpin served as the best control hairpin for our experiments because it was not toxic towards cells and did not alter protein levels or phosphorylation under a number of different conditions. Thus, we used sh*LUC*_221 as the preferred shRNA control hairpin for our low-throughput shRNA experiments.

sh*LUC*: sh*LUC*_221: TRCN0000072246; promegaLuc_221s1c1

The human sh*RICTOR*_25 and sh*RAPTOR*_65 shRNAs used as control hairpins in the RNAi screen and throughout this paper can be obtained from Addgene (Plasmids 1853 and 1857, respectively).

Human sh*RICTOR*_25: Sense:

CCGGTACTTGTGAAGAATCGTATCTTCTCGAGAAGATACGATTCTTCAC AAGTTTTTTG

Human sh*RAPTOR*_65: Sense:

CCGGAGGGCCCTGCTACTCGCTTTTCTCGAGAAAAGCGAGTAGCAGGG CCCTTTTTTG

TRC reagents were obtained either directly from the Broad Institute RNAi Consortium or ordered from Sigma-Aldrich. The TRC identifications for the shRNAs used here are as follows and can be used to query individual hairpins in The RNAi Consortium's public data portal (http://www.broadinstitute.org/rnai/public/gene/search):

The five sh*RAB35* reagents screened in our RNAi screen were:

Human sh*RAB35*_207: TRCN0000047796; NM_006861.4-207s1c1

Human sh*RAB35*_451: TRCN0000047793; NM_006861.4-451s1c1

Human sh*RAB35*_486: TRCN0000307737; NM_006861.4-486s1c1

Human sh*RAB35*_649: TRCN0000047794; NM_006861.4-649s1c1

Human sh*RAB35*_709: TRCN0000047797; NM_006861.4-709s1c1

Additionally, we tested the following nine sh*RAB35* reagents that were generated by the TRC more recently and were thus not included in our RNAi screen:

Human sh*RAB35*_207b: TRCN0000291620; NM_006861.4-207s21c1

Human sh*RAB35*_260: TRCN0000331177; NM_006861.4-260s21c1

Human sh*RAB35*_359: TRCN0000331153; NM_006861.4-359s21c1

Human sh*RAB35*_453: TRCN0000380080; NM_006861.4-453s21c1

Human sh*RAB35*_475: TRCN000038033; NM_006861.4-475s21c1

Human sh*RAB35*_486: TRCN0000307737; NM_006861.4-486s21c1

Human sh*RAB35*_537: TRCN0000297015; NM_006861.4-537s21c1

Human sh*RAB35*_565: TRCN0000379410; NM_006861.4-565s21c1

Human sh*RAB35*_601: TRCN0000380003; NM_006861.4-601s21c1

We found that three particular shRAB35 reagents were the most reliable in both depleting RAB35 protein levels and suppressing AKT phosphorylation. The three hairpins used throughout this paper for all experiments after validation of RAB35 as our primary hit are represented with simplified numbers (1, 2, and 3):

sh*RAB35*_1: Human sh*RAB35*_709: TRCN0000047797; NM_006861.4-709s1c1

sh*RAB35*_2: Human sh*RAB35*_475: TRCN000038033; NM_006861.4-475s21c1

sh*RAB35*_3: Human sh*RAB35*_601: TRCN0000380003; NM_006861.4-601s21c1

shRNAs targeting murine *RICTOR* and human *PIK3CA* were purchased from Sigma-Aldrich:

sh*PIK3CA*_1: Human sh*PIK3CA*_3234: TRCN0000010407; NM_006218.x-3234s1c1

sh*PIK3CA*_2: Human sh*PIK3CA*_3254: TRCN0000195304; NM_006218.2-3254s1c1

sh*RICTOR*_1: Mouse sh*RICTOR*_5030: TRCN0000123398; NM_030168.2-5030s1c1

sh*RICTOR*_2: Mouse sh*RICTOR*_5031: TRCN0000123395; NM_030168.2-5031s1c1

2.3.19 mTORC2 in vitro kinase assays

mTORC2 kinase assays were performed *in vitro* as described previously [119, 333]. Briefly, cells grown in 15 cm plates were serum starved overnight, then stimulated, washed once in ice-cold PBS and lysed in 1 mL 0.3% CHAPS lysis buffer. Lysates were incubated at 4° C for 15 minutes, centrifuged at 14,000 rpm for 15 minutes, the soluble fraction was collected and the protein concentration was determined. 1000 μg of protein in a final volume of 750 μL was then used for each immunoprecipitation. 15 μL of goat anti-RICTOR antibody (Santa Cruz) was added to each tube, and tubes were incubated at 4° C overnight with rotation. The next day, 15 μL of a 50% slurry of agarose Protein G beads (Pierce) was added to each tube and incubated for an additional hour with rotation. Immunoprecipitates were then washed three times with CHAPS lysis buffer, and once with 1X mTORC2 kinase buffer (25 mM HEPES [pH 7.5], 100 mM potassium

acetate, 1 mM $MgCl_2$). The kinase buffer was then completely aspirated and the following was immediately added: 7.5 μL 2X mTORC2 kinase buffer, 250 ng inactivated AKT1/PKBα (Millipore, #14-279), 0.75 μL 10 mM ATP, and the reaction volume was then brought up to 15 μL with dH2O. The reactions were then incubated at 37° C for 20 minutes with gentle agitation (300 rpm). Every five minutes, the tubes were gently flicked to resuspend the agarose beads within the reactions. The kinase assay was then stopped with the addition of 200 μL of 1X Laemmli's loading buffer, the tubes were boiled for five minutes, and 20 μL of each reaction was then analyzed by SDS-PAGE.

2.3.20 PI3-kinase in vitro kinase assays

We used Echelon Biosciences PI3K kinase assay ELISA "pico" kits (K-1000s) for *in vitro* PI3K reactions using purified p85-p110α. Cells were lysed in 0.3% CHAPS lysis buffer as described above and PI3K was immunopurified from 1000 μg of clarified cell lysates using 20 μL agarose-conjugated anti-p85 antibody (Millipore, 16-107) overnight at 4° C. Immunoprecipitates were then washed three times in CHAPS lysis buffer and once in KBZ buffer (Echelon). After the final wash, KBZ buffer was completely aspirated and 30 μL of KBZ buffer supplemented with 5 mM DTT and 150 μM ATP was immediately added to the immunoprecipitates. 30 μL of 100 μM phosphatidylinositol 4, 5-bisphosphate (PIP_2) and either DMSO or PIK-90 were then added to the reaction. Final kinase assay buffer was thus comprised of KBZ buffer, 50 μM PIP_2, 2.5 mM DTT, 75 μM ATP, DMSO or

500 μM PIK-90, and 20 μL of agarose anti-p85 beads. Reactions were then incubated at 37° C and tubes were gently tapped every 15 minutes to resuspend the agarose beads in the reaction. After 3 hours, reactions were stopped with the addition of 60 μL KBZ buffer supplemented with 4 mM EDTA. The reactions were then centrifuged, and the supernatants were removed and frozen at -20° C. The PIP_3 competitive ELISA assay kit was then used as per the manufacturer's instructions to determine the concentration of PIP_3 generated in each kinase reaction. The supernatant from each reaction was split between two individual ELISA wells and each reaction was run in duplicate, thus each kinase assay condition was assayed in quadruplicate.

2.3.21 Apoptosis assays of NIH-3T3 cell lines

NIH-3T3 cells were assayed for apoptosis by both western blotting of whole cell lysates and by cell counting methods. Briefly, cells were split and each cell line was seeded at 1 million cells per well of a 6-well plate in 2 mL of DMEM supplemented with 10% BCS. After 6 hours at 37° C, 3 wells of each plate were aspirated, washed once with serum-free DMEM, and the media was replaced with serum-free DMEM and the plates were returned to 37° C. 4 hours later, the cells were lysed in TX-100 lysis buffer and cell lysates were analyzed by immunoblotting. For cell count assays, each cell line was seeded and treated as just described. Instead of lysis, after 4 hours of serum withdrawal, cells were rinsed once with PBS, briefly trypsinized with

500 μL of trypsin, dissociated into a single cell suspension, resuspended to 1000 μL with 500 μL of DMEM and collected. 500 μL of each cell suspension was then counted on a Beckman-Dickinson Vi-Cell XR, and the total number of viable cells per mL was recorded. Each condition (serum complete and serum withdrawn) was performed in triplicate (3 wells each). Serum withdrawn cell counts for each cell line were then normalized to their respective serum complete cell count to arrive at a % of viable cells. Mean and standard deviation values for each condition were then calculated and graphed in Microsoft Excel.

2.3.22 NIH-3T3 focus formation assays

Focus formation assays with NIH-3T3 stable cell lines were performed as previously described [334-335]. For each focus formation assay, freshly thawed, low-passage NIH-3T3 stable cell lines were used. Briefly, NIH-3T3 cells stably expressing genes indicated throughout this paper were seeded in 6-well plates in 2 mL of 10% BCS DMEM at 20,000 cells per well. The next day, the media was aspirated and replaced with 2 mL 2% BCS DMEM containing either DMSO or 250 nM GDC-0941. Cells were then cultured at 37° C for 4 weeks with media changes every 3 days. After 4 weeks, cells were fixed and processed for crystal violet staining as follows. Cells were rinsed once with PBS and fixed for 10 minutes at room temperature in 1 mL 70% EtOH. Next, EtOH was aspirated and cells were stained with crystal violet reagent (0.5% crystal violet, 25% EtOH) for 10 minutes. Crystal violet

was then removed, and each well was rinsed gently with dH_2O until background stain was removed. The plates were then imaged using an Oxford Optronix plate imager. Because the qualitative aspects of foci formed by different oncogenes varies widely (i.e. fewer but larger ones for $RAB35^{Q67L}$ and many small ones for AKT^{myr}, etc.) and because colony counting is a subjective process, we chose to quantify the amount of crystal violet stain in each well as a way of objectively measuring the total amount of cells present in our focus formation assays. To extract crystal violet from stained cells, we incubated each well overnight at room temperature in 1 mL of Sorenson's buffer (50 mM sodium citrate, 50 mM citric acid, 50% EtOH) with gentle agitation. The next day, extractions were collected and the absorbance at 590 nm was recorded using a spectrophotometer. These values were tabulated in Microsoft Excel, and the values for all samples were normalized to the average absorbance of DMSO treated FLAG-$RAB35^{wt}$ NIH-3T3 cells.

2.4 RESULTS

2.4.1 A quantitative, immunofluorescent assay for AKT phosphorylation

To quantitatively assess PI3K/AKT signaling in cultured cells, we designed an immunofluorescence-based assay that detects levels of AKT phosphorylation at S473. mTORC2 phosphorylates AKT at this site in a PI3K-dependent manner, a phosphorylation which both reflects PI3K activity and is required for full activation of AKT itself [119]. To probe for AKT

phosphorylation in HeLa cells grown in 384-well plates, we probed fixed cells with a monoclonal rabbit antibody directed against AKT phosphorylated at S473 (Figure 2.1). This antibody was probed with a secondary antibody tagged with an 800 nm

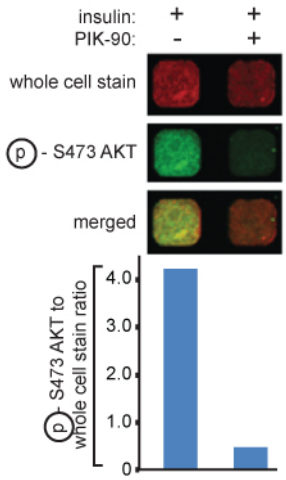

Figure 2.1: An immunofluorescent assay for phospho-S473 AKT quantitatively reflects PI3K activity. HeLa cells grown in 384-well plates were serum starved overnight, treated with PIK-90 and insulin as indicated, then fixed and processed for immunofluorescence with a whole cell stain (red) and an anti-phospho-S473 AKT monoclonal antibody (green) (top). Signals were imaged and quantified with a LiCor Odyssey near-infrared scanner, and the phospho-AKT signal intensity was divided by the whole-cell stain signal intensity to calculate a normalized phospho-AKT value for each well (bottom).

fluorophore (green), and the cells were counterstained with a 700 nm whole cell stain (red). We imaged and quantified these two signals with a near-infrared scanner. These signals could be divided by one another to yield a normalized value for each well that represents phospho-AKT levels (see methods for a more complete description of this assay). This assay was sensitive to inhibition with PI3K and mTOR kinase inhibitors. Thus, we

developed a robust assay for PI3K/AKT activity that we next deployed in a high-throughput screen.

2.4.2 An RNAi screen identifies RAB35 as a novel regulator of PI3K/AKT signaling

We defined phospho-AKT Z-scores -1.50 and +1.50 as the cutoffs beyond which individual shRNAs would be considered as low or high hits, respectively. Fortunately, shRNAs targeting genes whose knockdown should suppress AKT phosphorylation—*RICTOR*, *PIK3CA*, *PIK3CB*, *AKT1*, and

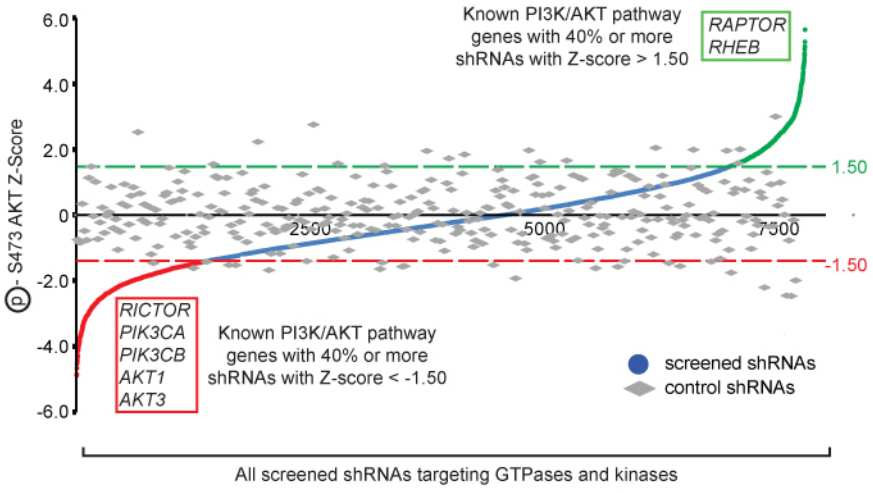

Figure 2.2: An arrayed lentiviral loss-of-function RNA interference screen identifies known and novel regulators of the PI3K/AKT axis. Averaged phospho-AKT Z-scores of screened shRNAs. HeLa cells were plated in 384-well plates, transduced with lentiviral reagents expressing control shRNAs or shRNAs targeting human kinases and GTPases, then processed as in Figure 2.1. Phospho-AKT Z-scores for each shRNA were then calculated, averaged (n=3), and arranged in increasing order. Low hits (Z-score < -1.50) are indicated in red, high hits (Z-score > 1.50) are indicated in green. Hit genes that are known to regulate PI3K/AKT signaling are indicated in red or green boxes. For a full list of non-lethal hit genes please see Appendix B.

AKT3—all diminished AKT phosphorylation and scored as low hits (Figure 2.2, Appendix B). Conversely, shRNAs targeting genes whose protein products inhibit AKT signaling—such as *RAPTOR* and *RHEB*—elevated phospho-AKT levels and scored as high hits. Since this assay successfully identified known regulators of PI3K/AKT signaling, we were confident that our screening approach was a valid method for discovering new members of the this pathway.

To reduce the number of shRNAs and genes in our primary hit list to a manageable number, we discarded shRNAs that were toxic or did not knock down their target mRNA, and considered as hits only genes for which 40% or more of the screened hairpins scored in our assay (Table 2.1, Appendix B). Further, we discarded hit genes that were not ubiquitously expressed or had been previously studied in the context of PI3K/AKT signaling (Appendix D). Finally, we used publicly available oncogenomic databases to annotate the remaining hit genes and discarded any genes that were not altered in human tumor samples or cell lines. Thus we prioritized our hits for validated, non-toxic shRNAs that targeted genes with no previous link to PI3K/AKT signaling that were altered in human cancers. This left us with a manageable list of 29 genes with which we could perform low-throughput loss-of-function experiments (Table 2.2).

Table 2.1: Criteria for selecting hit shRNAs and genes.

	Criteria	Genes	shRNAs	Table
Genes screened	All known human GTPases and kinases	1,012	7,450	Table S1
Primary hits	1. 40% of shRNAs per gene score with an average phospho-AKT Z-score of greater than -/+ 1.50 2. Hit shRNAs are nonlethal	260	755	Table S3
Secondary hits	1. Primary hit genes whose shRNAs knock down target mRNA transcript by 50% or more 2. 40% of shRNAs meet secondary hit criteria #1 (above)	90	218	Table S4
Tertiary hits	1. Secondary hits with no known link to PI3K/AKT signaling in the literature 2. Expression of genes is not cell-line or tissue-specific	48		Table S5
Prioritized hits	Tertiary hits that are altered in human tumors and cancer cell lines	29		Table S6

Table 2.2: RNAi screen hit genes that are widely expressed and altered in human tumor samples or cancer cell lines. We used oncogenomic databases to identify hit genes from Appendix D that are mutated in human tumors or cancer cell lines. See methods for description of data collection from oncogenomic databases

SYMBOL	Recurring mutations from CCLE	Recurring mutations from COSMIC, cBio	Other COSMIC or cBio mutations of interest
Knockdown of the following 3 genes elevated phospho-AKT Z-score			
PRKAR1B	V100M (3), A67V (3)	P87T/fs (5)	

Table 2.2 (continued)

GRK1	L180M, G213S, R19Q (4)	G137E (2), V251M (2), T298M (2)	
OXSR1	E298* (2), p360fs	P433S/T/Q (3), E298*, H391D/Y (3)	
SYMBOL	**Recurring mutations from CCLE**	**Recurring mutations from COSMIC, cBio**	**Other COSMIC or cBio mutations of interest**
Knockdown of the following 26 genes diminished phospho-AKT Z-score			
PKN2	P914, L384del (25)	Q199L/H (2)	
SRP54	no	E34* (2), L69V (2), K373N (2)	
TAF1	A1527, R1034H	R1068H (3), R843W (3), E651G (3), E651K (2), R843Q (2), R854C (2), R996C (2), R1126W (2), R1221Q (2), R1376Q (2), I1741V (2), G626C (2), R539Q (2), P438S (2), R342C (2), G688* (2), K644fs (4), R1022C/G/H (5)	
MAP3K6	R196Q (3), R383H, P848fs (5), K1125del (10)	N622K (7), p848fs (3)	
RAB35	R27H	R27H (2), A151T (2)	A151T, F161L (COSMIC)
RND1	no	C19F (2), E48K (2), D75N (2), R130Q (2)	
GTPBP2	no	E132D (2), D319N (2), E400V (2), R575L/W (3)	
RAB39A	no	R80Q (2), A84C/H (2), R119W (4),	
CABC1 (ADCK3)	F81L (3), P188H (2)	F81L, V85M (3), D117N (2), R137H (2), A279T (2)	
ALPK3	S1597C (2), P648T (2), P1046S (2)	T414S (3), P1299L (2), R1254C (2), P1803L (2)	
TAOK1	none	R492W (2), R562*/Q (2), R605* (2), N639S (2), E719* (2), R759Q (2), R832H (2), R833K (2), V891A (2), G975V/W (2), N639S (2)	
PANK3	no	I301F (3), E233G (2), R260I (2), F121C (2), R126C (2)	

Table 2.2 (continued)

ALPK1	T1150fs (6), S942del (12)	V62M (3), A86T (2), A144S (2), A152S (2), N175D (3), D253N (2), V296M (2), S832F/N/T (4), I1124M (2), K1125E (2), P293L (2)	
RAB1B	no	E35K/Q (2), G42W (2), R79fs (2)	A152T (COSMIC)
ADPGK	no	L176I (2), K450fs (3), R475*/Q (3)	
GSG2	no	R82C (18), K358fs* (2)	
POMK (SGK196)	R15Q, T146N	A13T (5)	
PKDCC	E408G (9)	V131I (2)	
RASEF	no	R262C (2), R332Q (3), H350R (2), R706* (2), G792W (2)	
FUK	no	R235H (2), R767Q (2)	
NRK	S101F, R1387W, P426A, K1409T, E898K	S424C (4), A681E (3), S108P (3), S708P (3), R438*, P389H (2), R1911Q (3)	
STK32C	S392Y (3)	G282W (2), S482L (2)	
TSSK4	T338del (12)	R281C (2)	
NEK8	G602E (2)	A206T (2), L621F (2), G605D (2), V690fs (2)	
RABL3	no	R107C (2)	
NME9	no	E75K (5), R221W (5), G270D (2), E53K (5), G209D (2)	

Next, we were curious as to the types of genes that were present in this enriched hit list, and whether they shared any functional characteristics. Because this list was largely comprised of low hits (26 of 29) and because we were interested in identifying positive (i.e. oncogenic) regulators of PI3K/AKT signaling, we focused on only the 26 low hit genes from Table 2.2. We used literature searches to identify the molecular function—or, failing that, the broader organismal function—of these 26 genes, then asked which molecular function was the most prominently represented (Figure 2.3A).

Interestingly, 5 of these 26 low hit genes were RAB GTPases, which suggested to us that there may be a previously unappreciated role for RAB proteins in oncogenic growth factor signaling.

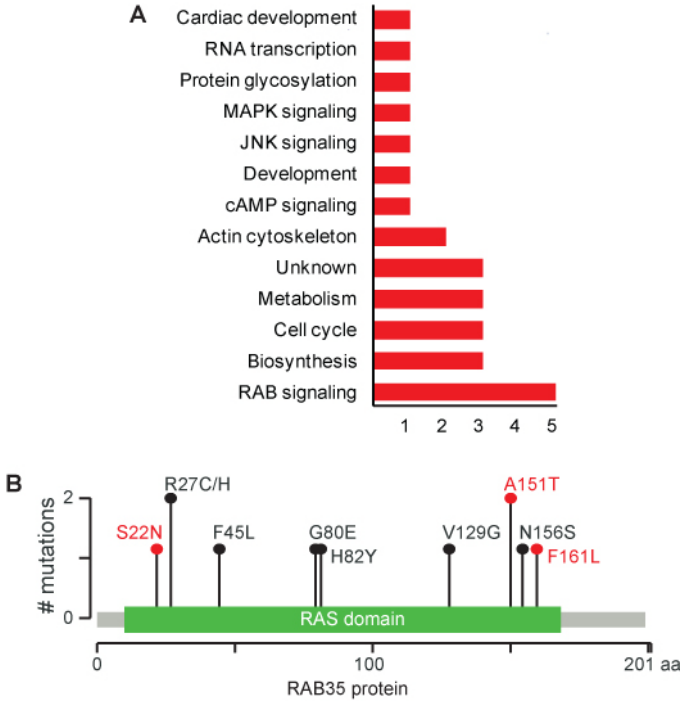

Figure 2.3: RAB proteins are prevalent in the enriched RNAi screen hitlist, and RAB35 is somatically mutated in human cancers. (**A**) The 26 hit genes that reduced AKT phosphorylation, are expressed widely, and are mutated in human cancers were grouped by their annotated function from the literature. (**B**) Mutations found in oncogenomic databases that are predicted to have a medium (black) or high (red) effect on protein function are mapped along the length of the RAB35 protein.

Of the five RAB proteins in this list (RAB1B, RAB35, RAB39, RASEF and RABL3), we prioritized RAB35 for further study because 1.) it is somatically mutated in human cancers (Figure 2.3B) and 2.) it is well-characterized in recycling endosome biology and has widely available reagents and tools. A member of the RAB family of GTPases, RAB35 has

been described as a regulator of cytoskeletal organization and trafficking at the recycling endosome [336-339]. While a number of regulators and effectors of RAB35 have been identified, we did not find any evidence in the literature to suggest that RAB35 plays a central role in growth factor signaling [340]. Further, although several RAS family members have been implicated in cancer, there is little evidence that suggests that RAB proteins possess oncogenic potential. Thus, we reasoned that RAB35 was the most promising candidate for further study.

To confirm that RAB35 depletion with the screened shRNAs could inhibit AKT phosphorylation, we transduced HeLa cells with lentiviruses expressing shRNAs targeting luciferase (as a control), the mTORC2 component RICTOR, or RAB35. Indeed, three of the sh*RAB35* hairpins simultaneously reduced RAB35 protein levels and diminished the phosphorylation of AKT and the AKT substrate FOXO1/3A in response to stimulation with serum (Figure 2.4). Similarly, sh*RAB35* hairpins that were not included in our screen that depleted RAB35 protein levels also suppressed AKT phosphorylation (Data not shown).

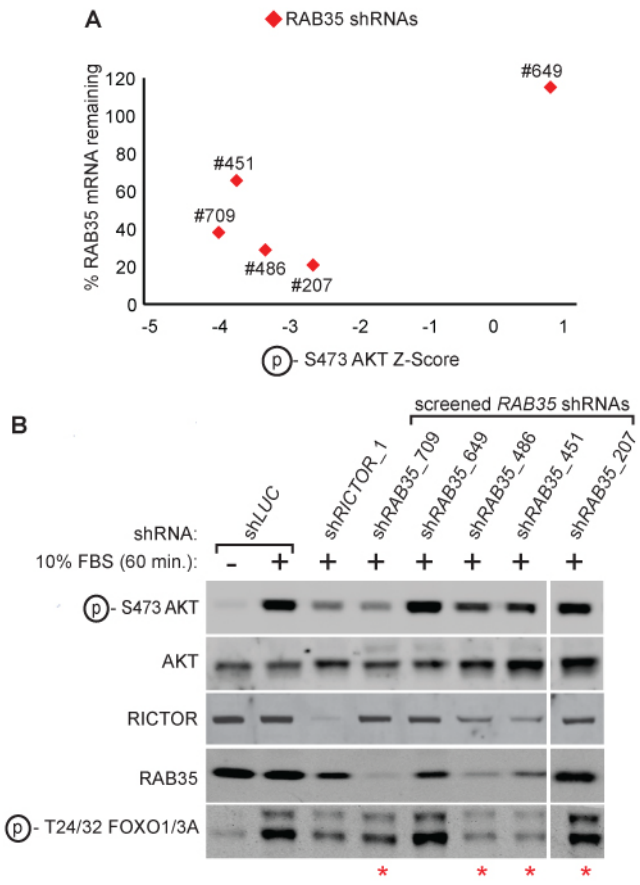

Figure 2.4: Validation of RAB35 as a *bona fide* hit from our RNAi screen. (**A**) Phenotype-knockdown correlation of *RAB35* mRNA levels and phospho-S473 AKT Z-scores. (**B**) shRNAs that deplete RAB35 protein levels also suppress phosphorylation of AKT and the AKT substrate FOXO1/3A. HeLa cells were transduced lentiviruses expressing the indicated shRNAs, starved overnight, stimulated as indicated with medium containing serum, lysed, then lysates were analyzed by immunoblotting.

2.4.3 RAB35 is necessary for full activation of PI3K/AKT signaling in response to serum

To ensure that the effect of RAB35 knockdown on AKT signaling was not cell-type specific, we depleted RAB35 protein in two human (HeLa, HEK-293E) and one mouse (NIH-3T3) cell line(s) (Figure 2.4). Knockdown of

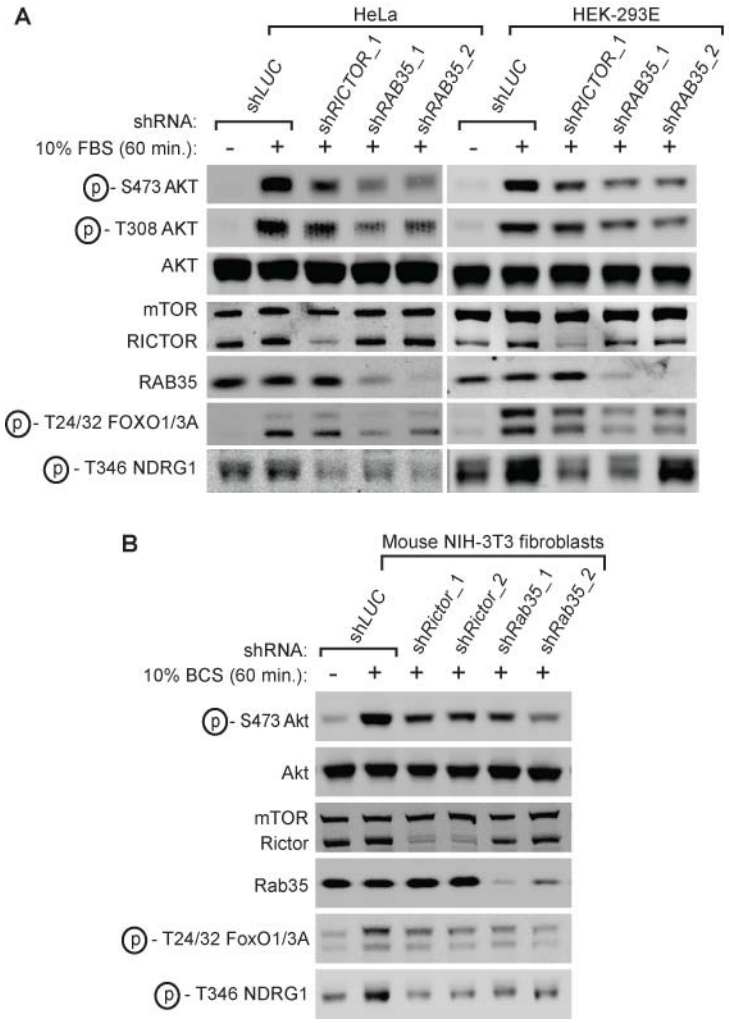

Figure 2.5: RAB35 is necessary for serum-induced PI3K/AKT signaling. (**A, B**) Depletion of RAB35 inhibits serum-induced activation of AKT. (**A**) HeLa and HEK-293E cells were transduced with lentiviral reagents expressing the indicated shRNAs. Cells were serum starved overnight, treated as indicated with fetal bovine serum (FBS), lysed, and cell lysates were then analyzed by immunoblotting. (**B**) Murine NIH-3T3 cells were serum starved then treated as indicated with bovine calf serum (BCS) and analyzed as in (A).

RAB35 protein with two different shRNAs diminished AKT phosphorylation at S473 and T308 more potently than did RICTOR knockdown in both human and mouse cells. Further, the PI3K-dependent phosphorylation of two proteins—the AKT substrate FOXO1/3A and the SGK1 substrate

NDRG1—was also decreased in cells depleted of RAB35. The same experiment performed in a variety of cancer cell lines with different mutational backgrounds (oncogenic *PIK3CA* or *KRAS*, deleted *PTEN*, mutated *NF2* or *TP53*) yielded similar results (Figures 2.6, 2.7). Thus, RAB35 is broadly necessary for the efficient activation of PI3K/AKT signaling in response to serum stimulation.

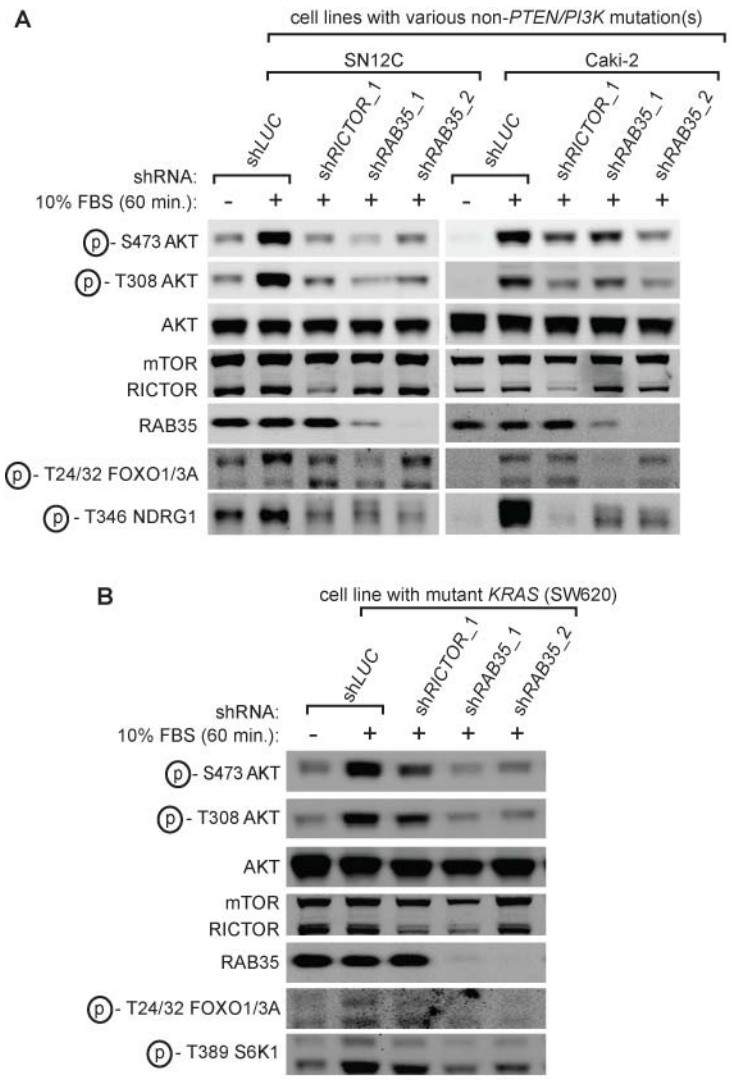

Figure 2.6: Depletion of RAB35 in cell lines with various genetic backgrounds inhibits PI3K/AKT signaling. Cell lines of the indicated mutational backgrounds were transduced with lentiviruses expressing the indicated shRNAs, serum starved overnight, treated as indicated and analyzed as in Figure 2.5. The categories of cell line mutational backgrounds and their relevant cancer gene mutations were obtained from the Sanger COSMIC database and are listed as follows: (A) Cell lines with non-PI3K/PTEN alterations: SN12C (*NF2* and *TP53* mutations) and Caki-2 (*VHL* inactivating nonsense mutation). (B) Cell line with a *KRAS* activating mutation: SW620 (*KRAS* activating mutation, *APC* nonsense substitution, *TP53* mutations).

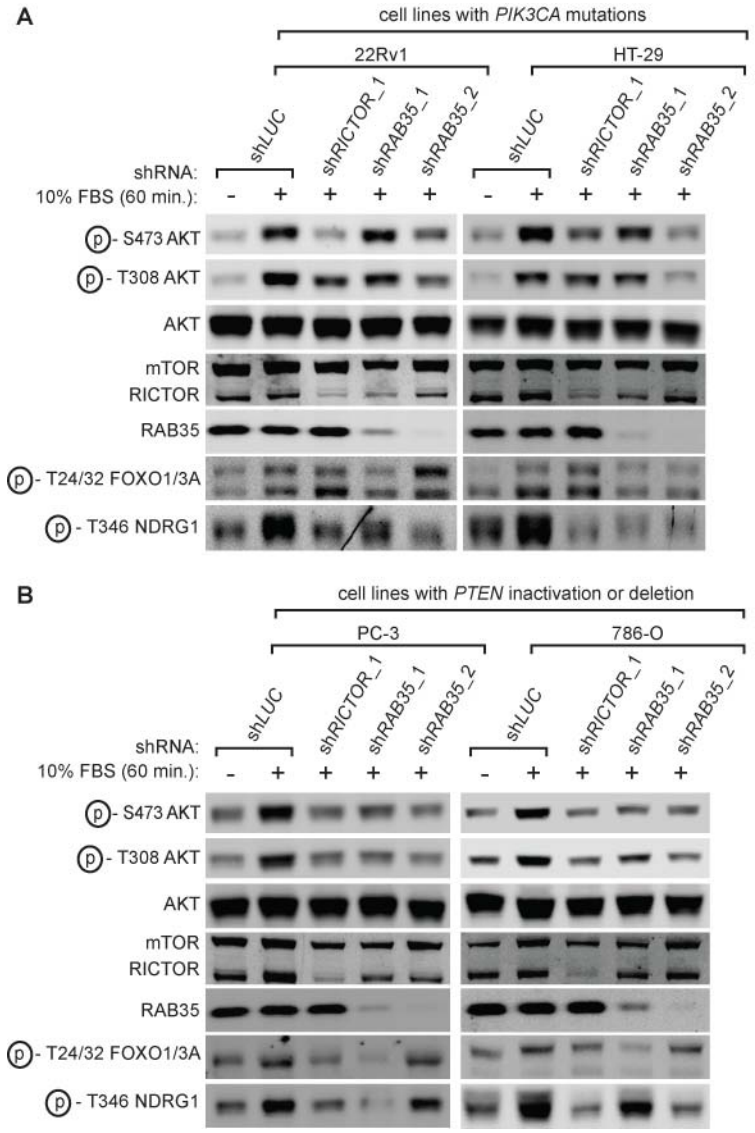

Figure 2.7: Depletion of RAB35 in cell lines with activating *PIK3CA* or inactivating *PTEN* mutations suppresses PI3K/AKT signaling in response to serum. (A) Cell lines with *PIK3CA* mutations: 22Rv1 (*PIK3CA* activating mutation, *TP53* mutation) and HT-29 (*APC* inactivating mutations, *BRAF* activating mutation, *PIK3CA* mutation, *TP53* mutation) (B) cell lines with *PTEN* inactivation: 786-0 (*PTEN* nonsense mutation, *CDKN2A* deletions, *VHL* deletion, *TP53* mutation) and PC-3 (*PTEN* and *TP53* deletions). Cells were treated and analyzed as in Figure 2.5 and 2.6.

2.4.4 RAB35 is sufficient to activate PI3K/AKT signaling

To ask whether RAB35 could activate the PI3K/AKT axis, we generated human cell lines that stably expressed either a wildtype allele of the GTPase RHEB ($RHEB^{wt}$) as a control, wildtype RAB35 ($RAB35^{wt}$), or the dominant active GTPase-deficient, GTP-bound RAB35 Q67L mutant ($RAB35^{Q67L}$). Stable expression of either $RHEB^{wt}$ or $RAB35^{wt}$ did not alter the regulation of growth factor signaling to AKT (Figure 2.8). However, stable

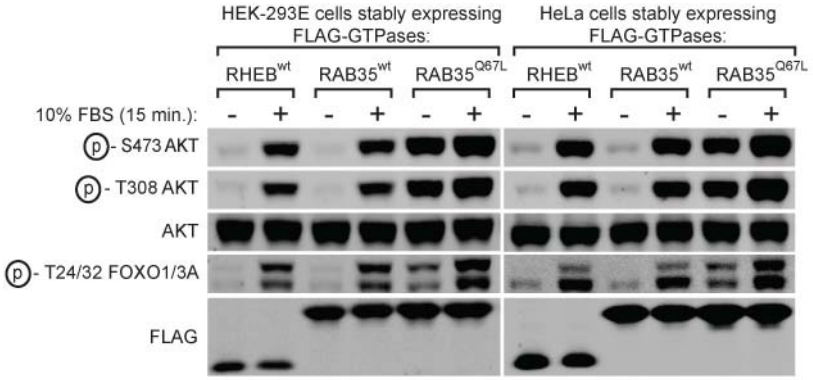

Figure 2.8: GTPase-deficient $RAB35^{Q67L}$ is sufficient to activate PI3K/AKT signaling. GTPase-deficient $RAB35^{Q67L}$ activates PI3K/AKT signaling. HeLa and HEK-293E cells were stably transduced with lentiviruses expressing FLAG-tagged $RHEB^{wt}$, $RAB35^{wt}$ or $RAB35^{Q67L}$. Cells were serum starved overnight, treated as indicated and lysates were analyzed by immunoblotting.

expression of the active $RAB35^{Q67L}$ allele rendered AKT phosphorylation constitutively elevated and refractory to growth factor deprivation. Not surprisingly, the phosphorylation of FOXO1/3A was also elevated in lysates from serum-deprived cells expressing $RAB35^{Q67L}$. Furthermore, neither expression of $RAB35^{wt}$ or $RAB35^{Q67L}$ altered the phosphorylation of the protein kinase ERK (Figure 2.9). Therefore, the expression of GTP-bound

RAB35 is sufficient to activate PI3K/AKT signaling in cells in the absence of growth factors.

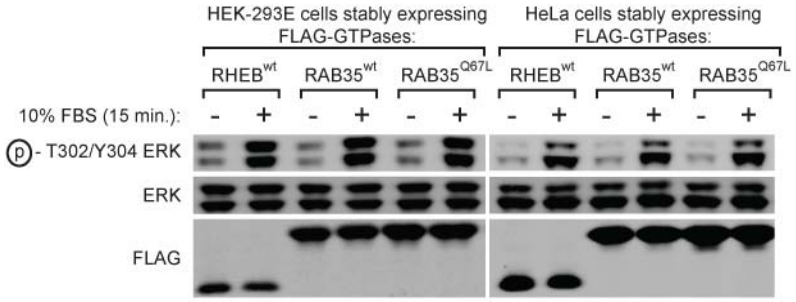

Figure 2.9: Stable expression of dominant active, GTPase-deficient RAB35^{Q67L} does not activate ERK signaling. HEK-293E and HeLa cells transduced with FLAG-tagged RHEB^{wt}, RAB35^{wt}, or RAB35^{Q67L} from Fig. 2C were treated as indicated, lysed, and cell lysates were analyzed by immunoblotting for levels of total ERK protein and ERK phosphorylation.

2.4.5 RAB35 depletion inhibits mTORC2 kinase activity towards AKT/PKB in vitro

Because these data thus far did not indicate where in the pathway RAB35 might be acting, we asked whether RAB35 regulates AKT activation via either of the two kinases that phosphorylate AKT—PDK1 and mTORC2 [341-342]. Because one of our motivations for performing our RNAi screen was to identify regulators of mTORC2, the first question we asked was whether depletion of RAB35 could inhibit mTORC2 kinase activity *in vitro* (Figure 2.10). We generated HeLa cells stably expressing a control shRNA or shRNAs targeting either *RICTOR*, *PIK3CA,* or *RAB35*, then immunopurified mTORC2 with an anti-RICTOR antibody and assayed the *in vitro* kinase activity of mTORC2 against recombinant, inactivated AKT [333, 341, 343-345]. Not surprisingly, the ability of immunopurified mTORC2 to

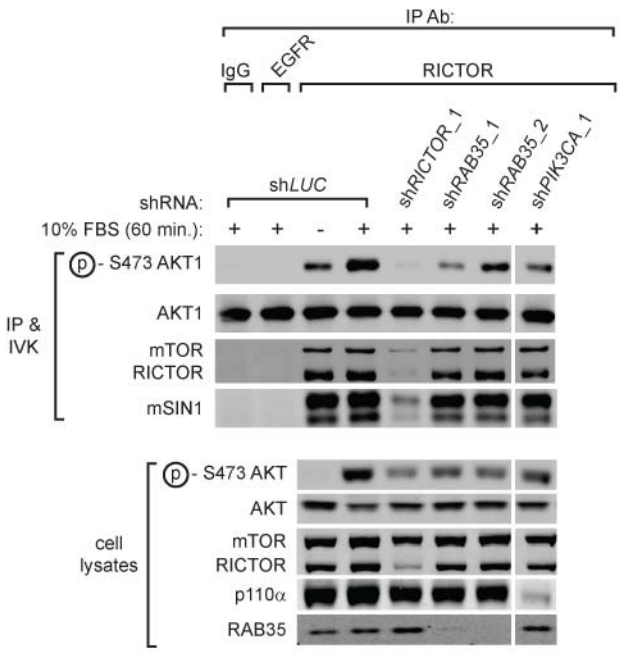

Figure 2.10: RAB35 depletion inhibits the *in vitro* kinase activity of immunopurified mTORC2 towards AKT. HeLa cells were stably transduced with lentiviruses expressing the indicated shRNAs, serum starved overnight, stimulated with serum where indicated, then lysed. Cell lysates were then used for immunoprecipitations with the indicated antibodies, and the immunoprecipitates were used for *in vitro* mTORC2 kinase assays using 100 ng of purified, inactivated AKT1 as a substrate. Kinase reactions were then analyzed by immunoblotting analysis for AKT phosphorylation and mTORC2 components as indicated (top). Whole cell lysates were concomitantly analyzed by immunoblotting (bottom).

phosphorylate AKT *in vitro* was activated by growth factors, ablated by RICTOR depletion, and inhibited by PI3Kα depletion. Further, we found that depletion of RAB35 with two different hairpins also markedly reduced mTORC2's kinase activity *in vitro*. Taken with the data in section 2.3, these data suggest that RAB35 is necessary for full activation of mTORC2. However, this did not indicate whether RAB35 was directly regulating mTORC2 or was acting further upstream of it. Because we were unable to

identify any interaction between endogenous or recombinant RAB35 and components of mTORC2 (data not shown), we reasoned that RAB35 could be regulating mTORC2 indirectly. We next sought to delineate whether RAB35 was regulating both PDK1 and mTORC2 by acting on their common regulator PI3K.

2.4.6 RAB35 functions above PDK1 and mTORC2

To place RAB35 within the pathway, we asked if RAB35 regulates AKT activation via either of the two kinases that phosphorylate AKT—PDK1 on T308 and mTORC2 on S473 [341-342]. Determining whether a particular gene or small molecule functions through either PDK1 or mTORC2 is challenging because the phosphorylation states of T308 and S473 in wildtype cells are influenced by one another [119, 134, 346]. We took advantage of cells that stably expressed alleles of murine Akt1 (mAkt1) where either T308 or S473 were mutated to phosphomimetic aspartate residues [344] (Figure 2.11) to ask whether RAB35 was regulating AKT via either PDK1, mTORC2, or both kinases.

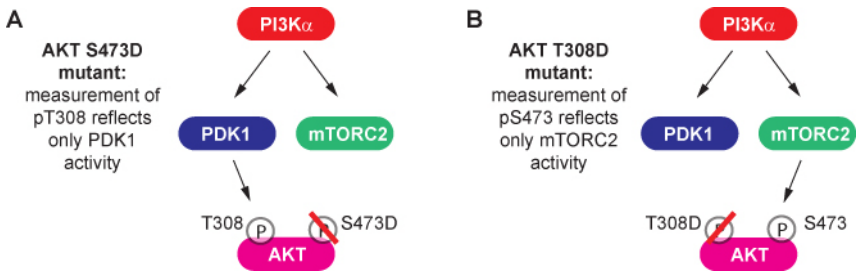

Figure 2.11: AKT phosphomimetic mutants to delineate between regulators of PDK1 and mTORC2. Because phosphorylation of the T308 and S473 sites on AKT can affect one another, determining whether an unknown regulator or perturbogen functions by controlling PDK1, mTORC2, or p110α is challenging. By locking one residue into a phosphomimetic state by mutating it to an aspartate, the phosphorylation state of the other can be probed without concern that it is being influenced by the other site. (**A**) S473D mutation allows measurement of T308 phosphorylation to reflect only PDK1 activity. (**B**) T308D mutation allows measurement of S473 phosphorylation to reflect only mTORC2 activity.

As expected, mTOR blockade with the ATP-competitive inhibitor Torin1 or RICTOR depletion suppressed S473 phosphorylation on mAkt1 that had an intact mTORC2 site (mAkt1^{wt} and mAkt1^{T308D}) (Figure 2.12). Further, in cells without a regulatable mTORC2 site (mAkt1^{S473D}), RICTOR depletion did not depress T308 phosphorylation, and treatment with Torin1 elevated phosphorylation at T308. Interestingly, depletion of RAB35 decreased S473 phosphorylation in mAkt1^{wt} and mAkt1^{T308D} cells as well as T308 phosphorylation in mAkt1^{wt} and mAkt1^{S473D} cells. Together, these data suggested that RAB35 signals to AKT by acting upstream of both PDK1 and mTORC2.

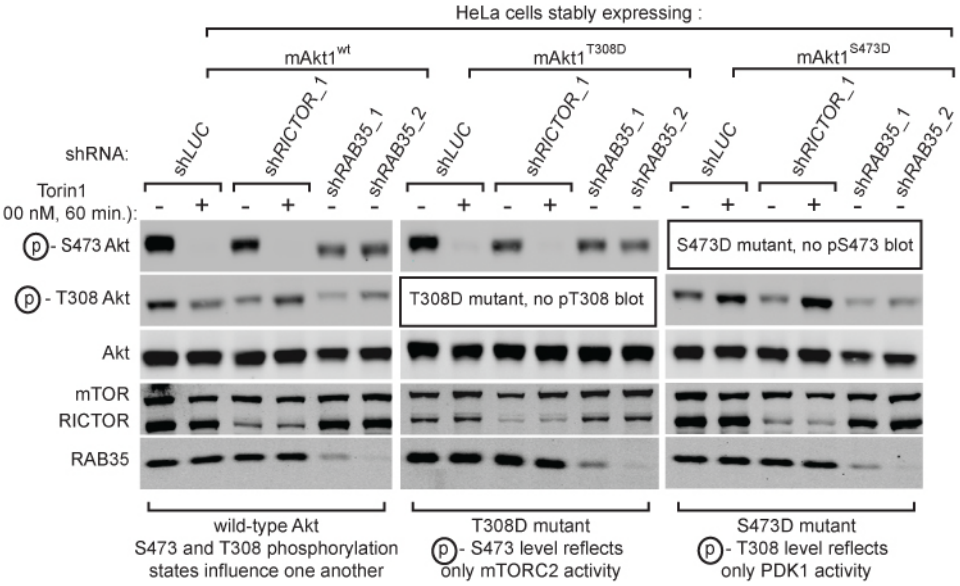

Figure 2.12: RAB35 acts upstream of both PDK1 and mTORC2. HeLa cells stably expressing murine Akt1^{wt}, Akt1^{S473D} or Akt1^{T308D} were treated as indicated with shRNA-expressing lentiviruses and Torin1. Cells were then lysed and cell lysates were analyzed by immunoblotting.

2.4.7 RAB35 depletion upregulates protein levels of the mTORC1/2 inhibitor DEPTOR

In addition to the “biochemical epistasis” experiment described in Figure 2.12, we performed further experiments to confirm that RAB35 was acting upstream of mTOR. One indicator of both mTORC1 and mTORC2 activity is the stability of DEPTOR, a negative regulator of both mTOR complexes [208, 343, 347-349]. In addition to regulating mTOR, DEPTOR is itself an mTOR substrate, and phosphorylation by mTOR reduces the stability of DEPTOR protein. Thus, inhibition of PI3K or mTOR—by pharmacological means or via deprivation of growth factors—leads to accumulation of DEPTOR levels. Similarly, depletion of PI3K/mTOR pathway

components can lead to increased DEPTOR stability. We reasoned that if RAB35 was regulating PI3K and/or mTOR that RAB35 depletion in the presence of growth factors would result in increased DEPTOR protein levels. Indeed, serum deprivation, RICTOR, PI3Kα or RAB35 depletion—in the presence of complete media—all lead to DEPTOR accumulation (Figure 2.13). This further suggested to us that RAB35 regulates PI3K/mTOR signaling upstream of mTOR.

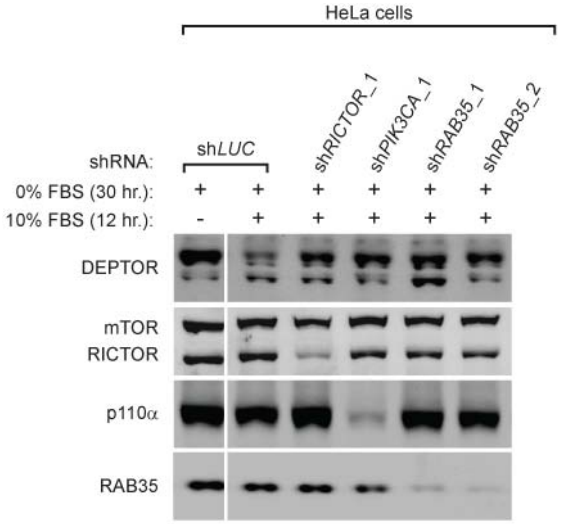

Figure 2.13: Serum deprivation, depletion of RICTOR, p110α, or RAB35 all lead to accumulation of the mTORC1 and mTORC2 inhibitor Deptor. HeLa cells were transduced with lentivirus expressing the indicated shRNAs, then were serum starved for 30 hours and either lysed or re-stimulated with serum for 12 hours, lysed, and lysates were analyzed by immunoblotting.

2.4.8 Depletion of RAB35 blunts mTORC1 inhibitor-induced PI3K/AKT activation

Next, we reasoned that if RAB35 was involved in PI3K/AKT/mTOR signaling, depletion of this protein would blunt the activation of PI3K/AKT

signaling that is induced by rapamycin. As reviewed in chapter 1 of this thesis, there exists a negative feedback circuit between mTORC1/S6K1 and upstream components of PI3K signaling—namely through proteins like IRS-1 and GRB10 [218-220, 350-354]. Under regular conditions, mTORC1 and its substrate S6K1 phosphorylate and inhibit negative regulatory components of PI3K/AKT signaling like GRB10, or destabilize positive regulators like IRS1. Thus, mTORC1 inhibition with rapamycin induces an increase in AKT and AKT substrate phosphorylation. Even mTORC1/2 inhibition with ATP-competitive mTOR kinase inhibitors potently upregulates PI3K activity and leads to activation of PI3K, PIP_3 accumulation, and hyperphosphorylation of T308 on AKT even when mTORC2 is disabled [208, 355-356].

We therefore reasoned that if RAB35 was a positive regulator of signaling from PI3K/AKT to either PDK1 or mTORC2 (or both), then the increase in AKT phosphorylation induced by mTORC1 inhibition with rapamycin should be blunted with RAB35 inactivation (Figure 2.14). Not surprisingly, we found that depletion of the mTORC2 component RICTOR in HeLa cells prevented any increase of AKT phosphorylation at both T308 and S473 after 18 hours of mTORC1 inhibition. Consistent with our data that indicated that RAB35 lay upstream of both mTORC2 and PDK1, depletion of RAB35 blunted AKT activation by rapamycin to the same extent as did RICTOR knockdown. Thus, RAB35 likely functions proximally to RTKs and PI3K rather than at downstream signal nodes like AKT and mTORC2.

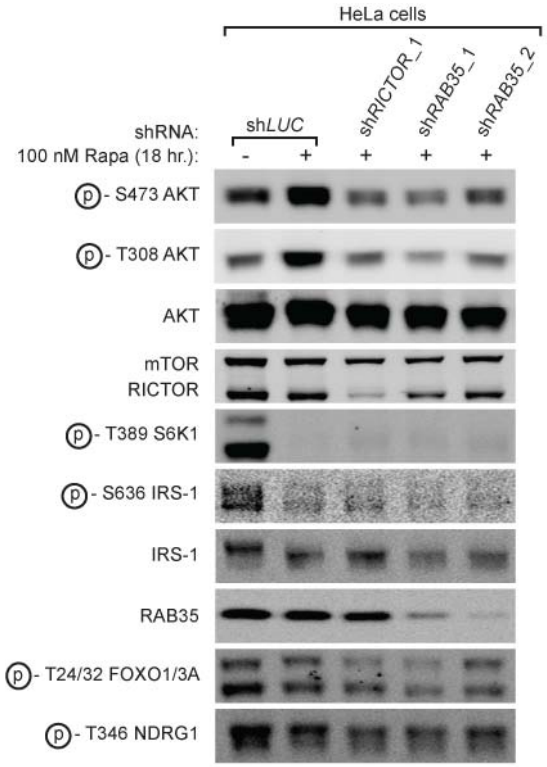

Figure 2.14: Depletion of RAB35 prevents PI3K/AKT activation in response to mTORC1 inhibition. HeLa cells were transduced with lentivirus expressing the indicated shRNAs, treated with 100 nM rapamycin for 18 hours, lysed, and cell lysates were analyzed by immunoblotting.

2.4.9 RAB35 is necessary for full activation of PI3K kinase activity in vitro

We reasoned that if RAB35 acts upstream of both PDK1 and mTORC2, it may be controlling their common regulator PI3K. Therefore, we asked whether RAB35 is necessary for PI3K kinase activity *in vitro* (Figure 2.15). As expected, PI3K immunopurified from cells depleted of PI3Kα—but not RICTOR—had significantly reduced *in vitro* kinase activity towards PIP_2. Further, PI3K purified from cells depleted of RAB35 had approximately 50% less *in vitro* PI3K kinase activity. These data indicate that RAB35 regulates PI3K/AKT signaling upstream of PI3K.

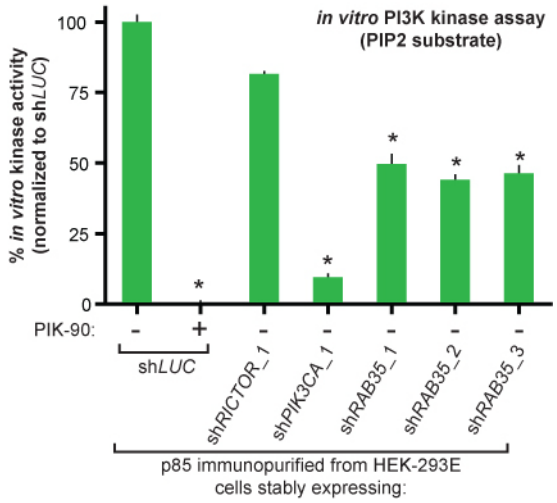

Figure 2.15: RAB35 depletion inhibits the kinase activity of immunopurified PI3K *in vitro.* HEK-293E cells stably expressing shRNAs targeting Luciferase, RICTOR, PI3Kα or RAB35 were treated as indicated. Cells were then lysed, PI3K was immunopurified with an anti-p85 antibody, and purified PI3K was analyzed for *in vitro* kinase activity using PIP_2 as a substrate.

2.4.10 RAB35 is necessary for activation of PI3K/AKT signaling in response to growth factor receptor stimulation

Next, we investigated whether RAB35 acts downstream of any particular growth factor receptor. Not surprisingly, depletion of RICTOR or PI3Kα in cells reduced the phosphorylation of AKT in response to treatment with insulin-like growth factor (IGF-I), epidermal growth factor (EGF), platelet-derived growth factor (PDGF-AA) and vascular endothelial growth factor (VEGF) (Figure 2.16A). Further, depletion of RAB35 also prevented AKT activation by IGF-I, EGF, PDGF-AA or VEGF. Interestingly, RAB35 depletion did not dramatically alter phosphorylation of ERK or tyrosine phosphorylation of IGFR, EGFR, PDGFR or VEGFR (Figure 2.16B). Taken together, the data in Figures 2.10-2.16 suggest that RAB35 functions

upstream of PI3K and downstream of growth factor receptor tyrosine kinases.

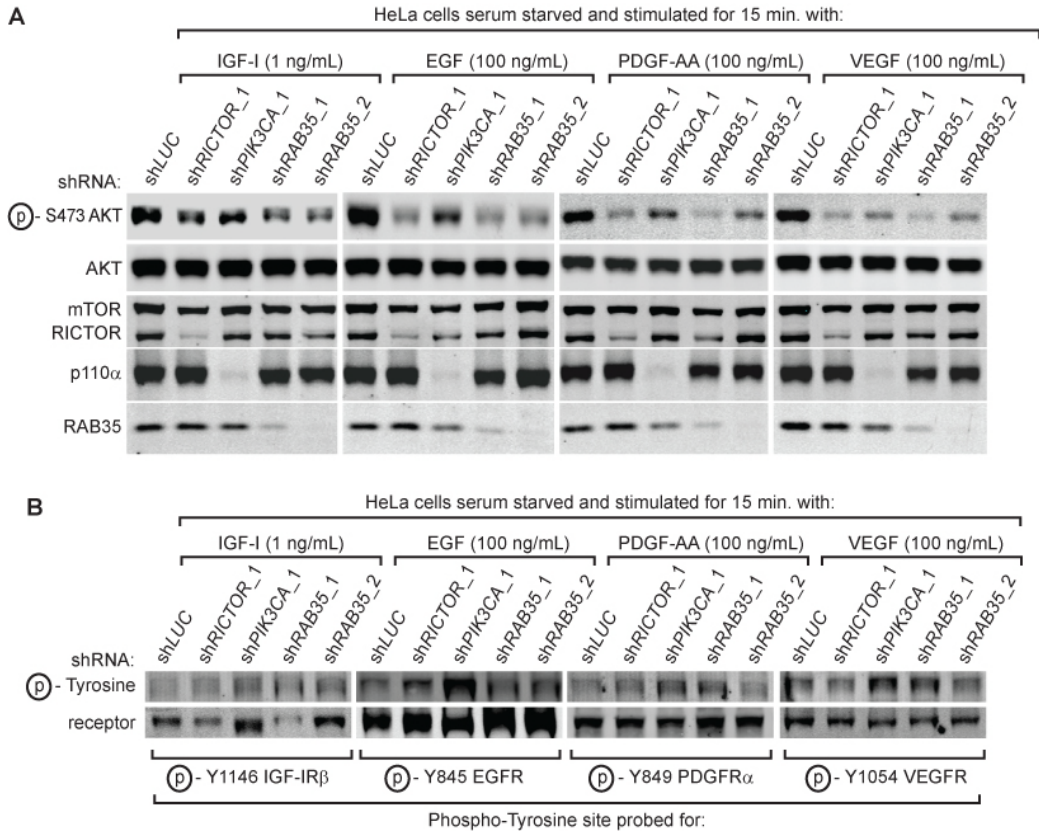

Figure 2.16: RAB35 depletion inhibits PI3K signaling to AKT downstream of multiple growth factor receptors. (**A**) HeLa cells were transduced with the indicated shRNA-expressing lentiviruses, serum starved overnight, treated as indicated with either insulin-like growth factor I (IGF-I), epidermal growth factor (EGF), platelet derived growth factor AA (PDGF-AA) or vascular endothelial growth factor (VEGF), then lysed and analyzed by immunoblotting. (**B**) Lysates from (A) were analyzed by immunoblotting for tyrosine phosphorylation of the indicated growth factor receptors.

2.4.11 RAB35 is mutated in human tumors

Like the other genes on our prioritized hit list in Table 2.2, we found that *RAB35* was mutated in human tumor samples (Table 2.3). Although none of the *RAB35* mutations that we observed were recurrent, two of the

mutations in RAB35—A151T and F161L—occurred at residues that are conserved in RAS-like GTPases. We noticed that the A151T and F161L mutations in RAB35 were strikingly similar to *KRAS* mutations (A146T and F156L) that have been previously identified from human tumor samples (Figure 2.17) [357-358]. While they are not “canonical” KRAS- activating mutations, stable expression of these two KRAS mutants was sufficient to activate ERK signaling and transform NIH-3T3 cells *in vitro*. We therefore reasoned that the two similar mutations in RAB35 might also be gain-of-function mutations that could activate RAB35 signaling.

Table 2.3: The TCGA, COSMIC and MSKCC cBIO databases reveal somatic *RAB35* mutations in human cancers. The Cancer Genome Atlas (TCGA), Catalogue of Somatic Mutations in Cancer (COSMIC), the International Cancer Genomics Consortium (ICGC) and MSKCC computation biology (cBio) data portal web sites were used to search for mutations in *RAB35* in human tumor samples. Mutations are listed in order of the amino acid residue that they occur at. Predicted change in protein function was assessed by the cBio mutational assessor with the exception of F161L, whose change in function was predicted manually by literature survey (asterisk).

Tissue	Database(s)	Amino acid change	Frequency of mutation (%)	Predicted change in function?
Uterus	cBio, COSMIC, TCGA	S22N K35N	1 of 248 (0.4%)	High NP
Colon (HCT-116 cell line)	cBio, COSMIC	R27C	1 of 60 (1.67%)	Medium
Stomach	COSMIC, TCGA	R27H	1 of 386 (0.26%)	Medium
Lung	COSMIC, ICGC	A29V	1 of 488 (0.2%)	Neutral
Breast	cBio, COSMIC, TCGA	F45L	1 of 772 (0.1%)	Medium
Skin	cBio, TCGA	S50F	1 of 413 (0.24%)	NP
Colon (HCT-15 cell line)	cBio, TCGA	T76 splice	1 of 60 (1.67%)	NP
Colon (HCT-116 cell line)	cBio, COSMIC, TCGA	G80E	1 of 60 (1.67%)	Medium
Adrenal	cBio, TCGA	H82Y	1 of 179 (0.56%)	Medium
Medulla	COSMIC, ICGC	V90I	Unknown	NP
Colon	COSMIC, TCGA	E94K	1 of 600 (0.17%)	NP
Skin	cBio	S95F	1 of 228 (0.44%)	NP
Lung	COSMIC, TCGA	R101Q	1 of 173 (0.58%)	Neutral
Breast	cBio	V129G	1 of 1061 (0.09%)	Medium
Liver	cBio	Y136C	1 of 268 (0.37%)	Neutral
Colon	COSMIC	A139V	1 of 2132 (0.05%)	NP
Uterus	cBio, COSMIC, TCGA	E150K	1 of 248 (0.4%)	NP
Lymphoid (MOLT4 cell line)	cBio, COSMIC	A151T	1 of 60 (1.67%)	High
Uterus	COSMIC, ICGC	A151T	1 of 815 (0.12%)	High

Table 2.3 (continued)

Prostate	cBio, COSMIC, TCGA	N156S	1 of 425 (0.24%)	Medium
Lung	cBio, COSMIC	F161L	1 of 183 (0.5%)	High*
Stomach	cBio, TCGA	K173fs	1 of 295 (0.34%)	NP
Stomach	cBio, TCGA	R196*	1 of 295 (0.34%)	NP

Tissue	Tumor type	Amino acid change	Frequency of mutation (%)
Uterus	carcinoma	A151T	1 of 815 (0.12%)
Lung	adenocarcinoma	F161L	1 of 183 (0.55%)

Figure 2.17: RAB35 mutants identified in human tumors are similar to known activating mutations in KRAS. Two mutations in *RAB35* that code for amino acid changes A151T and F161L were identified in the MSKCC cBio and COSMIC datasets. Alignment of RAB35 with KRAS was performed using ClustalW2.

2.4.12 Mutant RAB35 from human tumors can activate PI3K/AKT signaling

To ask whether stable expression of RAB35 with the A151T and F161L substitutions could activate PI3K/AKT signaling, we generated NIH-3T3 cells stably expressing either RAB35^{wt}, GTPase-deficient RAB35^{Q67L}, or the RAB35^{A151T} or RAB35^{F161L} alleles identified from the COSMIC database. While expression of RAB35^{wt} did not activate AKT phosphorylation during serum deprivation, stable expression of the GTPase-deficient RAB35^{Q67L} or the naturally occurring RAB35^{A151T} and RAB35^{F161L} mutants elevated AKT phosphorylation levels even in the absence of growth factors (Figure 2.18). Thus, stable expression of the GTPase-deficient RAB35^{Q67L} mutant or the two RAB35 mutants from human tumors is sufficient to activate PI3K/AKT signaling.

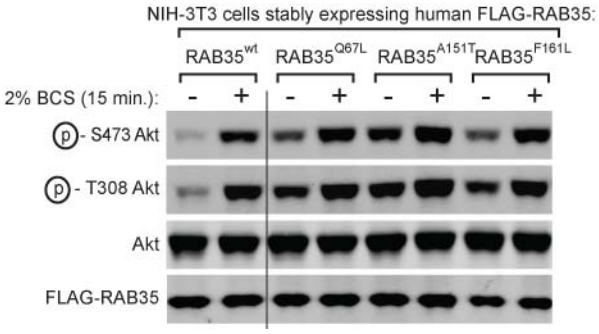

Figure 2.18: Mutant RAB35 alleles from human tumors can activate PI3K/AKT signaling. NIH-3T3 mouse fibroblasts stably expressing the indicated RAB35 alleles were serum starved for 4 hours, left unstimulated or treated with bovine calf serum (BCS), lysed, and cell lysates were analyzed by immunoblotting for the indicated proteins.

2.4.13 Stable expression of mutant alleles of RAB35 suppresses apoptosis

Because PI3K/AKT signaling inhibits apoptosis, we next examined whether cells expressing mutant alleles of RAB35 were resistant to apoptosis triggered by growth factor withdrawal. 4 hours of serum deprivation of NIH-3T3 cells stably expressing $RAB35^{wt}$ was sufficient to elevate cleaved levels of the apoptotic markers PARP and Caspase3 (Figure 2.19A). In comparison, cells stably expressing all three RAB35 mutants or oncogenic $p110\alpha^{H1047R}$ had decreased levels of cleaved PARP and cleaved Caspase3 following serum withdrawal. Further, while cells expressing $RAB35^{wt}$ were sensitive to cell death in response to serum deprivation, cells expressing mutant alleles of RAB35 or $p110\alpha^{H1047R}$ exhibited significantly improved cell viability when deprived of growth factors (Figure 2.19B). Together, these data suggest that mutant RAB35 proteins can suppress cell death in response to growth factor deprivation.

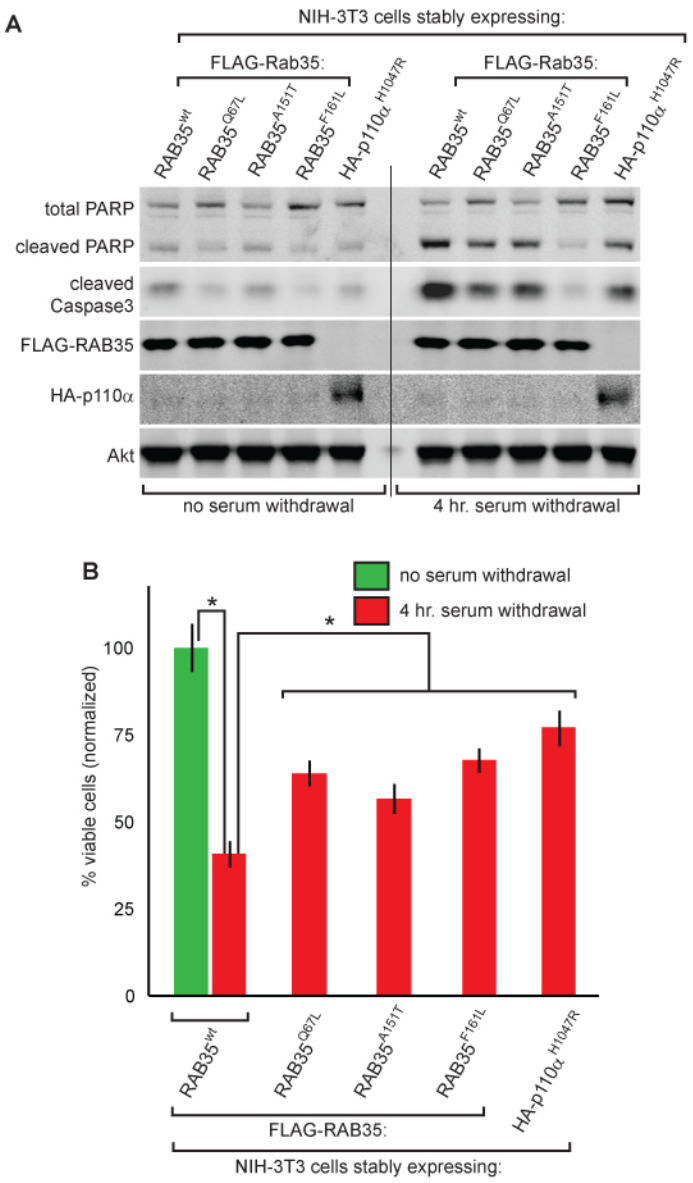

Figure 2.19: Expression of RAB35 mutants suppresses apoptosis. (**A**) NIH-3T3 cells stably expressing the indicated proteins were plated then treated as indicated for 4 hours with or without serum-containing medium. Cells were then lysed and the cell lysates were immunoblotted for the indicated proteins. (**B**) NIH-3T3 cells were treated as in (A), trypsinized and the number of viable cells was counted. Cell counts for each cell line were normalized to the number of viable cells for each cell line from non serum starved conditions. Asterisks indicate *p*-value <0.05.

2.4.14 Mutant alleles of RAB35 transform NIH-3T3 cells in vitro *in a PI3K-dependent manner*

To determine if the mutant alleles of RAB35 are oncogenic, we asked whether they could transform non-cancerous NIH-3T3 cells in a focus-formation assay—a standard *in vitro* model of density-independent growth and thus tumorigenicity [334-335]. Indeed, NIH-3T3 cells expressing oncogenic $p110\alpha^{H1047R}$, $AKT1^{myr}$ or the three mutant alleles of RAB35—but not $RAB35^{wt}$—formed foci (Figure 2.20). Moreover, we found that when cultured in medium containing 250 nM of the pan-class I PI3K inhibitor GDC-0941 [359], cells expressing RAB35 mutants and $p110\alpha^{H1047R}$ were unable to form foci. Not surprisingly, GDC-0941did not inhibit the growth of cells transduced with $AKT1^{myr}$. Thus, expression of RAB35 mutants identified from human cancers can transform NIH-3T3 cells *in vitro* in a PI3K-dependent manner.

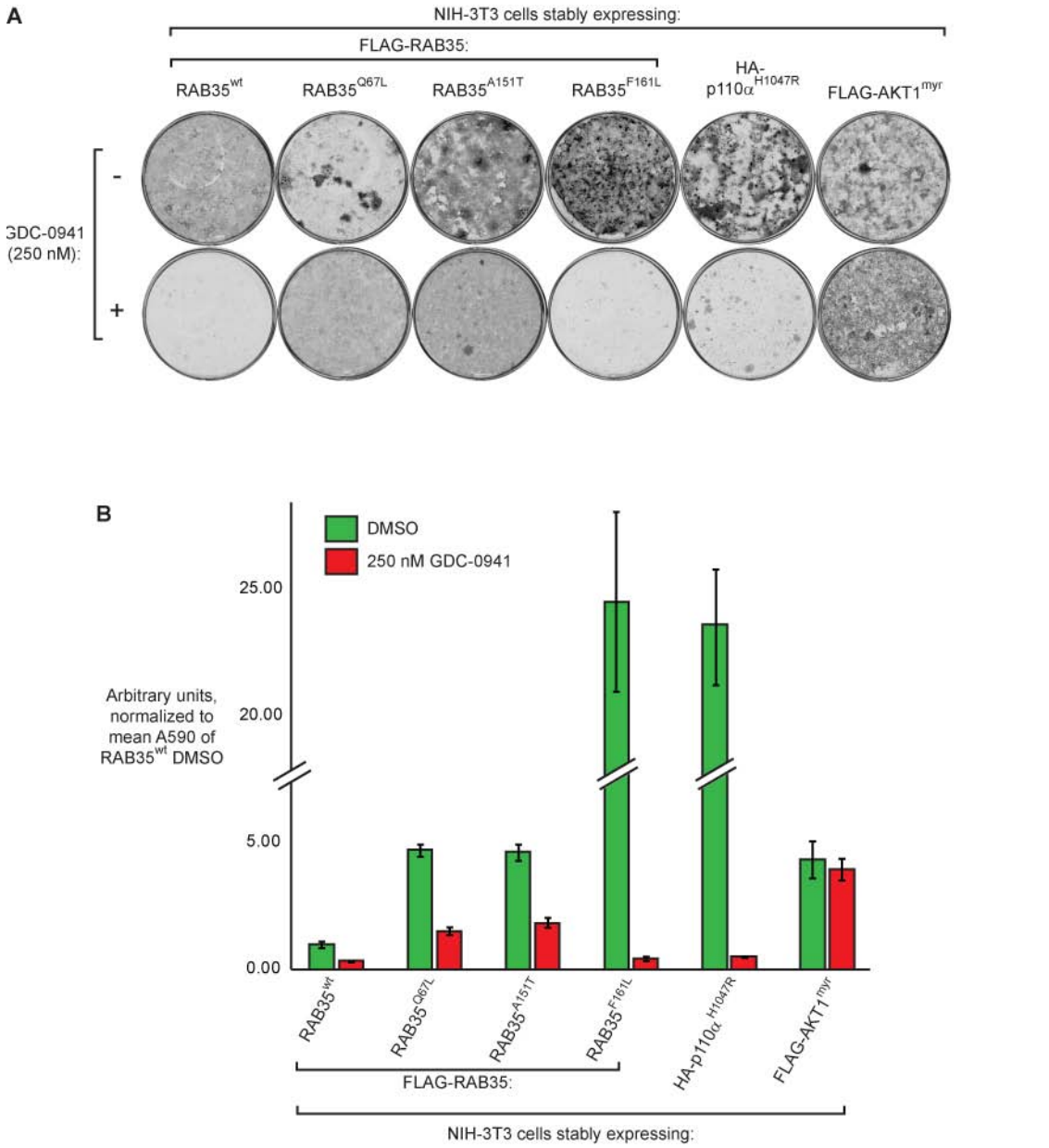

Figure 2.20: RAB35 mutants can transform cells *in vitro* in a PI3K-dependent manner. (**A**) NIH-3T3 cells stably expressing the indicated RAB35 alleles, HA-p110α^{H1047R}, or myristoylated FLAG-AKT1^{myr} were cultured for 4 weeks in medium containing 2% BCS with either DMSO or 250 nM GDC-0941, then fixed, stained with crystal violet, and imaged. (**B**) Crystal violet stain from each well was then solubilized in Sorenson's Buffer and the absorbance at 590 nm for each was determined.

2.5 DISCUSSION

We identify here the small GTPase RAB35 as a positive regulator of PI3K signaling (Figure 2.21). Although the precise mechanism of how RAB35 transduces upstream signals to PI3K remains unclear, our data demonstrate a previously unappreciated role for RAB35 in regulating growth

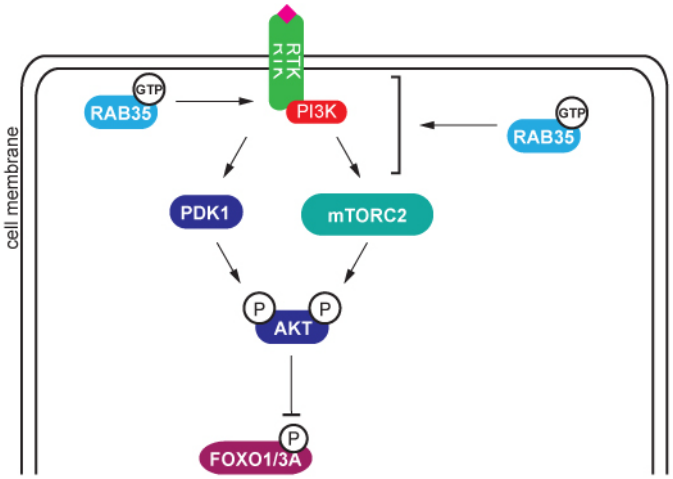

Figure 2.21: RAB35 regulates PI3K signaling to AKT either through PI3K or growth factor receptors. The data presented in this chapter suggest that RAB35 controls PI3K signaling by regulating signaling at the level of growth factor receptor tyrosine kinases (RTKs, left) or at the level of PI3K (right).

factor signaling to PI3K/AKT. Further, the ability of mutant alleles of RAB35 found in human cancers to activate PI3K/AKT signaling, protect cells from apoptosis and transform cells *in vitro* suggests that RAB35 may be a proto-oncogene. Finally, that a RAB protein that regulates endomembrane trafficking possesses oncogenic potential suggests that dysregulation of membrane trafficking in cells could itself serve as a driver in the development and survival of tumor cells.

CHAPTER THREE:

RAB35 REGULATES THE PI3K/AKT PATHWAY VIA THE PLATELET-DERIVED GROWTH FACTER RECEPTOR TYROSINE KINASE

3.1 ABSTRACT

The data described in Chapter 2 of this thesis suggest that RAB35 is a *bona fide* positive regulator of PI3K signaling. Here, we suggest that RAB35 regulates this pathway specifically via the platelet-derived growth factor receptor α (PDGFRα). GTPase-deficient RAB35 ^{Q67L} potently activates PI3K/AKT signaling by specifically activating PDGFRα. Further, dominant active RAB35 constitutively localizes PDGFRα—but not receptor tyrosine kinases like EGFR—to RAB7-positive late endosomes, which is the same compartment that active, liganded PDGFRα localizes to after internalization in cells that express wildtype RAB35. Finally, blockade of PDGFRα kinase activity with the PDGFRα-specific inhibitor Crenolanib suppresses AKT activation in cells that express dominant active RAB35Q^{67L}. Thus, RAB35 signals to PI3K/AKT primarily through PDGFRα, likely by serving to traffic PDGFRα to a RAB7-positive endomembrane where it is active.

3.2 INTRODUCTION

Thus far, our data suggest that RAB35 is a positive regulator of PI3K/AKT signaling (Chapter 2) [360]. We used loss-of-function studies to demonstrate that RAB35 is necessary for activation of the PI3K/AKT pathway. Further, our gain-of-function experiments with a constitutively

activated allele of RAB35 provided evidence that RAB35 is a positive regulator of PI3K/AKT signaling. Finally, biochemical epistasis experiments strongly suggest that RAB35 functions upstream of PI3K itself.

Because 1.) our data strongly implicate RAB35 as a positive regulator of PI3K signaling, 2.) RAB35 is well documented to be involved in the trafficking of several cargoes between endocytic compartments and the cell membrane, and 3.) growth factor receptors and their associated signaling machinery are known to actively signal after internalization to endomembranes, we reasoned that RAB35 might serve to activate or retain RTK-PI3K complexes in a cellular compartment where they transmit signaling to PI3K/AKT effectors. Thus, we asked whether RAB35 signaling is transduced through any particular RTK-PI3K complexes. We investigated whether these complexes were altered in their trafficking by activated RAB35 proteins. Interestingly, the data we describe in this chapter suggests that RAB35 activates PI3K through a particular RTK and at a specific endomembrane within the cell.

3.3 METHODS

3.3.1 In vitro *PI3K-RAB35 interaction assays*

In vitro interaction assays between immunoprecipitated PI3K and FLAG-purified RAB35 were adapted from previously described protocols [183-184, 361-362]. First, we affinity purified FLAG-GTPases as follows. HEK-293E cell lines stably expressing either FLAG-tagged $RHEB^{wt}$,

RAB35^{wt}, or RAB35^{Q67L} were lysed in 1% TX-100 lysis buffer as described in Chapter 2.2 of this thesis. The lysates were clarified, and 40 μL of mouse anti-FLAG M2 antibody conjugated to agarose beads was added to tubes containing 2 μg of cell lysates. The lysate/antibody mix was incubated over night at 4° C. The next day, the agarose beads were washed three times with TX-100 lysis buffer, then twice more with RHEB GTPase buffer (20 mM HEPES [pH 8.0], 200 mM NaCl, 5 mM MgCl2) [178]. The GTPase buffer was aspirated completely and 100 μL of 10 mM FLAG peptide in GTPase buffer was added to the beads. This mixture was then incubated at room temperature for 1 hour to elute the FLAG-GTPases from the agarose beads. The eluates were then collected and pooled. To remove the FLAG peptide and concentrate the GTPases, the pooled eluates were filtered with a 10 kDa Amicon Ultra 0.5 mL centrifuge filter (Millipore, UFC501008).

The same day that FLAG-GTPase expressing cells were lysed, wildtype HEK-293E cells cultured in complete medium were lysed in 0.3% CHAPS buffer, and 1 μg of cell lysates were incubated overnight with 20 μL of anti-p85 antibody conjugated agarose beads. The next day, the complex of agarose/antibody and immunoprecipitated PI3K was washed three times with CHAPS lysis buffer.

Prior to combining the immunopurified PI3K and GTPases, FLAG-RHEB or FLAG-RAB35 were loaded with either GDP or guanosine 5'-3-*O*-(thio) triphosphate (GTPγS) as follows [178]. FLAG-RHEB or FLAG-RAB35 GTPases were incubated with 10 mM EDTA and either 1 mM GDP or 0.1

mM GTPγS at 30° C for 10 minutes, then 20 mM MgCl2 was added and the proteins were kept on ice until use.

Once PI3K was immunopurified and washed and FLAG-GTPases were loaded with either GDP or GTPγS, 40 μL of purified, nucleotide loaded GTPase was added to each individual PI3K IP. This mixture was incubated at room temperature for 30 minutes, and then washed three times with GTPase storage buffer. Finally, the last wash was aspirated, beads were resuspended in 20 μL Laemmli's buffer, boiled, resolved by SDS-PAGE and then analyzed by immunoblotting as described in Chapter 2.

3.3.2 Immunofluorescence for microscopy

Immunofluorescence was performed as described previously [363]. Millicell EZ slide 4-well chamber slides (Millipore, PEZGS0416) were coated for 30 minutes with 0.01 mg/mL human fibronectin (Calbiochem, 341635) in PBS, rinsed once with PBS, and seeded with 100,000 HEK-293E cells. Immediately following the indicated treatments and/or stimulations, slides were fixed in 4% paraformaldehyde (Electron Microscopy Sciences, 15714-S) in PBS for 15 minutes at room temperature. The slides were then rinsed 3 times in PBS for 5 minutes each, permeabilized with 0.05% Triton TX-100 in PBS for 1 minute at room temperature, then rinsed three more times in PBS. Next, each well was incubated with primary antibody at a dilution of 1:100 in 5% normal goat serum (Vector Laboratories, S-1000) in PBS overnight at 4° C. When Alexa Fluor 488 conjugated mouse anti-myc antibody (Cell

Signaling Technology, 2279) was necessary, it was used at a 1:50 dilution and incubated as indicated overnight. The next day, the slides were rinsed in PBS 3 times at room temperature, and incubated for 1 hour at room temperature with the following mixture: the appropriate fluorophore-conjugated secondary antibody (either goat anti-rabbit Alexa Fluor 488 nm (Invitrogen, A11070), goat anti-mouse Alexa Fluor 488 nm (Invitrogen, A11029), goat anti-mouse Alexa Fluor 555 nm (Invitrogen, A21424), or goat anti-rabbit Alexa Fluor 555 nm (Invitrogen, A21429)) at a 1:200 dilution, and Hoechst 33342 (Invitrogen, H3570) at a 1:10,000 dilution. When actin staining with fluorophore-conjugated phalloidin was performed, Alexa Fluor 594 conjugated phalloidin (Invitrogen, A12381) was included in the secondary staining mix at a dilution of 1:200. After incubation, the slides were rinsed 4 times in room temperature PBS, the slide chambers were removed, slides were mounted with 100 μL ProLong Gold anti-fade reagent (Invitrogen, P36930) and glass coverslips (Fisher Scientific, 12-545-88). Slides were then sealed with Sally Hansen® “Super Shine” Shiny Top Coat (Sally Hansen, 2290), air dried, then stored at 4° C until imaging. Slides were imaged with an Axio Imager 2 widefield microscope (Zeiss) and AxioVision 4.0 software (Zeiss). Images were exported from AxioVision as TIFF files.

3.3.3 Immunoprecipitation/mass spectroscopy for the identification of PI3K interacting proteins

Immunoprecipitations of PI3K were carried out as described in the previous chapter. Immunoprecipitates were then resolved by SDS-PAGE and the gel was stained with Novex Simply Blue stain (Invitrogen, PART #). The gel was then submitted to the Memorial Sloan-Kettering Cancer Center Microchemistry and Proteomics Core Facility. The lanes of the gel containing the immunoprecipitated proteins were then cut into sections, digested with trypsin, and subjected to mass spectroscopic analysis as previously described [364-366]. Results of the MS run were analyzed using the program Scaffold v4.2.1 (Proteome Software). Only peptides of >90% certainty with 1 or more peptide fragments present were considered in analysis of MS data.

3.4 RESULTS

3.4.1 RAB35 interacts with PI3K in a nucleotide-dependent manner

The data described in Chapter 2 suggest that RAB35 regulates PI3K signaling either 1.) at PI3K itself or 2.) at the interface between growth factor receptor tyrosine kinases and PI3K. However, those data do not delineate whether RAB35 regulates PI3K directly or indirectly. To first ask whether the two proteins interact, we used an anti-p85 antibody to immunopurify PI3K from cells stably expressing FLAG-tagged alleles of RHEB (as a control) or RAB35 (Figure 3.1). Indeed, we found that FLAG-RAB35^{wt}—but not FLAG-

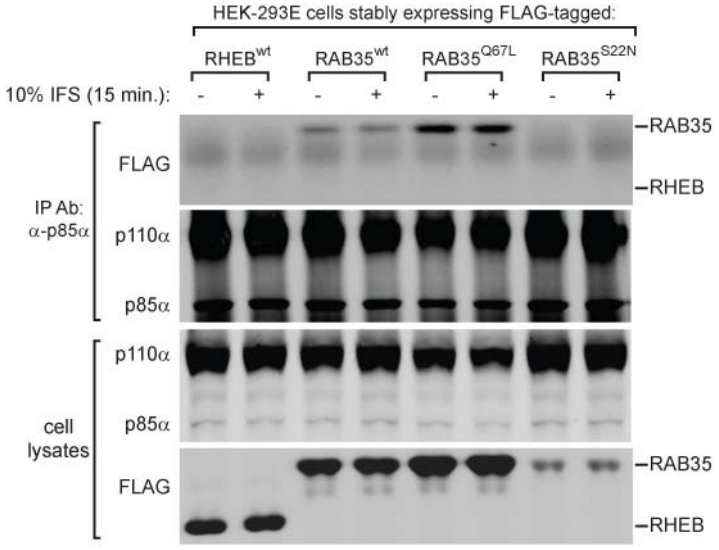

Figure 3.1: Stably expressed RAB35 interacts with endogenous PI3K in a nucleotide-dependent fashion. HEK-293E cells stably expressing the indicated FLAG-GTPases were serum starved overnight, treated with serum, lysed, and PI3K was immunopurified with an anti-p85 antibody. Lysates and immunoprecipitates were then analyzed by immunoblotting.

RHEB—co-immunopurified with PI3K. Further, the dominant active GTPase deficient RAB35^{Q67L} mutant was present in the PI3K immunoprecipitates to a higher extent than was the wildtype allele. Further, the GDP-bound mutant—RAB35^{S22N}—was barely detectable in PI3K immunoprecipitates from HEK-293E cells that stably expressed FLAG-RAB35^{S22N}.

In addition to these data, we also found that transiently expressed myc-tagged RAB35—but not myc-tagged RHEB—immunoprecipitated with endogenous PI3Kα (Figure 3.2). Consistent with the interaction data from the stable cell lines in Figure 3.1, myc-RAB35^{S22N} was nearly undetectable in PI3K IPs. Taken together, these data suggested to us that RAB35 interacts with PI3K. However, whether RAB35 interacts with PI3K directly—as has

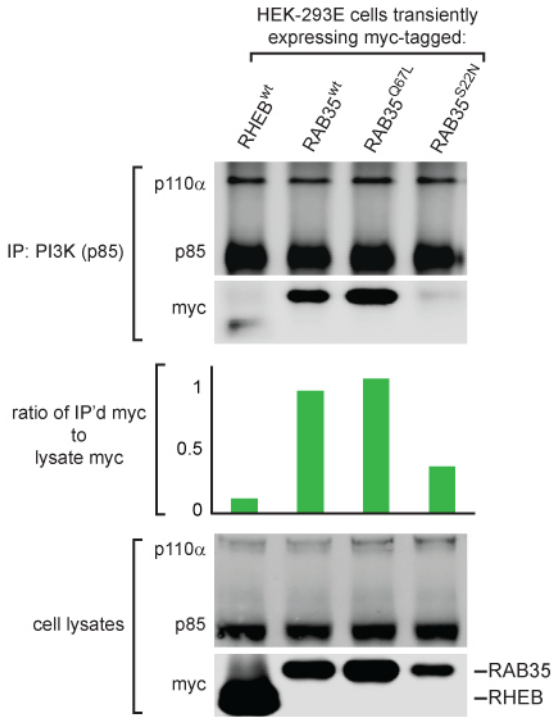

Figure 3.2: Transiently expressed RAB35 interacts with endogenous PI3K in a nucleotide-dependent fashion. HEK-293E cells stably expressing the indicated FLAG-GTPases were serum starved overnight, treated with serum, lysed, and PI3K was immunopurified with an anti-p85 antibody. Lysates and immunoprecipitates were then analyzed by immunoblotting. Signal intensities of the bands were quantified using the LiCor Odyssey software, then the signal intensity of each immunoprecipitated myc band (top) was divided by that of the corresponding myc band in the cell lysates (bottom). These ratios are represented by the green bars (middle).

been demonstrated for GTPases like KRAS—or does so through other proteins remained unclear [94-95, 97-99, 101, 367-370].

We next sought to validate the PI3K-RAB35 interaction with an *in vitro* interaction assay. PI3K immunopurified from HEK-293E cells was incubated with either purified FLAG-tagged RHEB loaded with the GTP-analogue GTPγS or purified FLAG-RAB35 loaded with GDP or GTPγS (Figure 3.3)

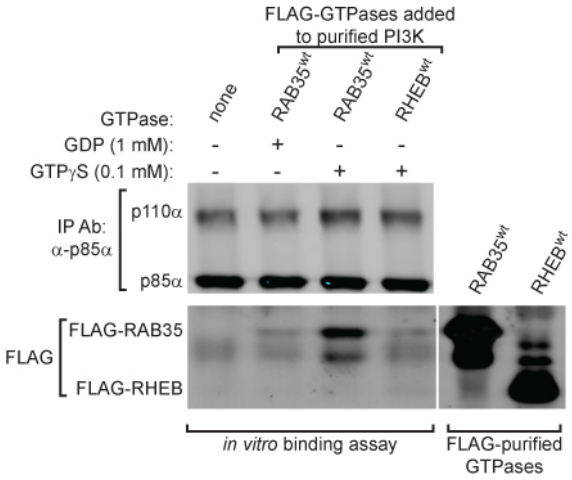

Figure 3.3: Immunopurified PI3K interacts with purified GTPγS-RAB35 but not GDP-RAB35. FLAG-tagged RHEB or RAB35 were affinity purified from lysates of cells stably expressing either GTPase, loaded with either GDP or GTPγS as indicated. Endogenous PI3K was immunopurified from wildtype HEK-293E cells with an agarose-conjugated anti-p85 antibody, washed, and then incubated with the GTPases as indicated above. The GTPase-PI3K complexes were then washed and analyzed by immunoblotting.

[183-184, 361, 371-373]. After incubation together, the agarose beads bound to PI3K were washed and the remaining proteins were analyzed by immunoblotting for the presence of FLAG-RAB35^{wt}. Indeed, the only PI3K immunoprecipitates that retained bound RAB35 were those that had been incubated with GTP-loaded FLAG-RAB35 ^{wt}. These data indicate that PI3K and RAB35 interact in a GTP-dependent manner. However, because the PI3K used in this experiment had been immunopurified from cells, it is possible that adapter proteins or growth factor receptors that associate with PI3K could serve to interact with RAB35. Thus, whether RAB35 interacts directly with PI3K remains unclear.

3.4.2 GTPase-deficient RAB35 specifically activates the platelet-derived growth factor receptor

In probing the interaction of RAB35 with PI3K, we noticed that a prominent phospho-tyrosine signal was present in immunoprecipitates of PI3K from cells stably expressing GTPase-deficient RAB35^{Q67L} (Figure 3.4).

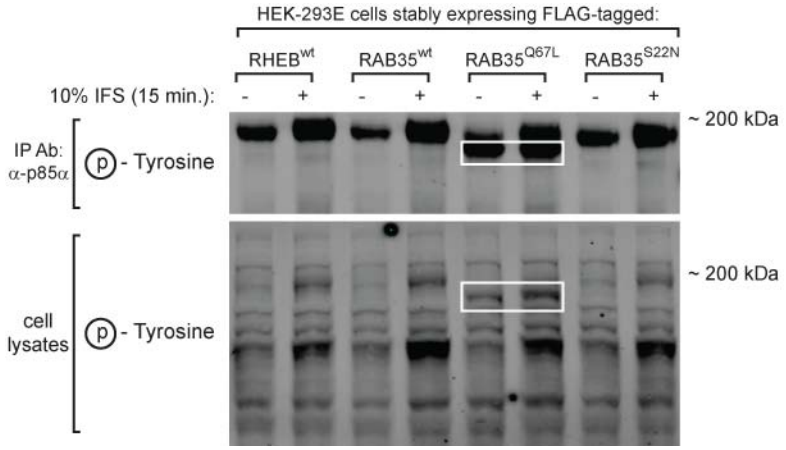

Figure 3.4: PI3K immunoprecipitated from cells stably expressing RAB35^{Q67L} is associated with a constitutively elevated phospho-tyrosine signal. HEK-293E cells stably expressing FLAG GTPases were serum starved overnight, treated as indicated with FBS, lysed, and PI3K was immunopurified from the lysates. Immunoprecipitates and whole cell lysates were then analyzed by immunoblotting. White boxes indicate elevated phosphotyrosine signal in RAB35^{Q67L} lysates.

In cells stably expressing RAB35^{wt}, this signal is strongest in PI3K immunoprecipitates from cells that have been treated with growth factors or serum. Interestingly, this signal is elevated in PI3K immunoprecipitates from cells expressing RAB35^{Q67L} regardless of whether cells had been serum starved or not. Indeed, this signal was apparent even in the lysates of cells expressing RAB35^{Q67L} but not RHEB or RAB35^{wt}.

The protein responsible for the elevated phospho-tyrosine signal in PI3K immunoprecipitates and whole cell lysates from cells expressing

dominant active RAB35 was of a relatively high molecular weight (175-200 kDa). Given the prominence of tyrosine phosphorylation in the activation of receptor tyrosine kinases and their substrates, we thus reasoned that this signal might be emanating from either a receptor tyrosine kinase (EGFR, PDGFR, IGF-IR, etc.) or an RTK substrate of a high molecular weight (such as IRS-1, etc.). Further, we speculated that this was likely one individual protein, as there were not other phosphotyrosine signals present in lysates from cells expressing GTPase-deficient $RAB35^{Q67L}$.

We next asked which growth factor receptor tyrosine kinase might be the source of the phosphotyrosine signal in cells stably expressing GTP-bound $RAB35^{Q67L}$. Once activated, RTKs auto-phosphorylate numerous tyrosine residues *in trans*, and tyrosine phosphorylation of the catalytic domain tyrosines is necessary for activation of most receptor tyrosine kinases [374-378]. In contrast, the other auto-phosphorylation tyrosine sites on RTKs serve as sites for adaptor proteins—such as IRS1/2, p85, GRB2, etc.—to interact with active RTKs. Because each receptor has multiple binding domains that contain phosphorylatable tyrosine residues, we reasoned that the most effective way to identify the source of this elevated phosphotyrosine signal would be to probe lysates for phosphorylation of the catalytic domain tyrosine residues of different growth factor receptors. Thus, we probed for multiple RTK catalytic domain phosphorylation levels in lysates from cells expressing FLAG-tagged $RHEB^{wt}$, $RAB35^{wt}$ and $RAB35^{Q67L}$ that had been either serum starved or stimulated with serum

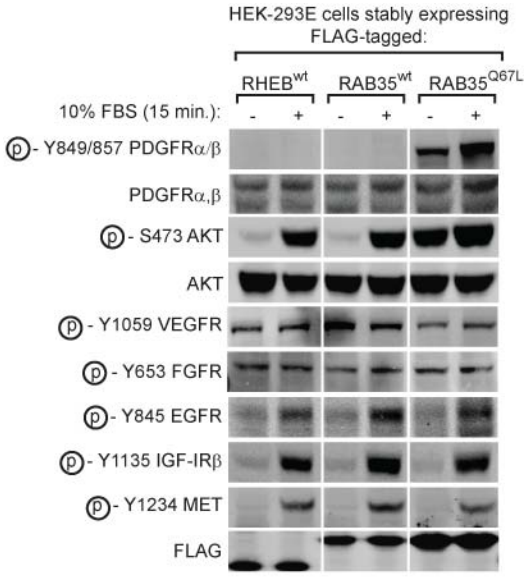

Figure 3.5: The platelet-derived growth factor receptor—but not other growth factor receptors—is hyper-phosphorylated at a catalytic domain tyrosine residue in cells stably expressing GTPase-deficient RAB35^{Q67L}. HEK-293E cells expressing the indicated FLAG-GTPases were starved overnight, stimulated with FBS as indicated, lysed, and lysates were analyzed by immunoblotting with the indicated antibodies.

(Figure 3.5). Interestingly, we found that only the phosphorylation levels of Y849/857 on PDGFRα/β were constitutively elevated in cells expressing RAB35^{Q67L}. The catalytic domain tyrosine phosphorylation sites on other receptors were either normally activated by serum in all three cell lines (IGF-IRβ, EGFR, MET) or equally constitutively active in all three cell lines regardless of serum deprivation/stimulation (VEGFR, FGFR). We also probed for phosphorylation of other tyrosine kinases (c-Kit, SRC, etc.) and did not find any difference in phosphotyrosine levels between the three cell lines examined in Figure 3.5 (data not shown).

3.4.3 Pharmacological inhibition of PDGFRα/β but not PDGFRβ inhibits PI3K/AKT signaling in cells stably expressing GTPase-deficient RAB35^{Q67L}

Because the upregulation of growth factor receptors by dominant active RAB35 seemed so specific to PDGFR, we next asked whether pharmacological blockade of PDGFR could inhibit PI3K/AKT signaling. Our first course of action was to attempt PDGFR inhibition with the well characterized pan-tyrosine kinase inhibitor imatinib/gleevec [278, 379-381], but this molecule failed to suppress PI3K/AKT signaling in cells that expressed GTP-bound RAB35^{Q67L} (data not shown). This could be accounted for by the fact that: 1.) the affinity of imatinib for PDGFR is relatively low, or 2.) the activated PDGFR is locked in an imatinib-resistant conformation.

We next asked whether more potent, isoform specific PDGFR inhibitors could block PDGFR signaling to PI3K/AKT (Figure 3.6A). Indeed, in cells stably expressing RAB35^{Q67L} the phosphorylation of the PDGF receptor, AKT, and FOXO1/3A were not suppressed by treatment with the PDGFRβ-specific small molecule CP-673451[382]. However, an inhibitor that specifically targets PDGFRα and PDGFRβ with similar potency—CP-868596 (Crenolanib®) [383-387]—was more effective at suppressing the phosphorylation of PDGFR, AKT and FOXO1/3A. To ensure that the majority of the signal through the PI3K/AKT

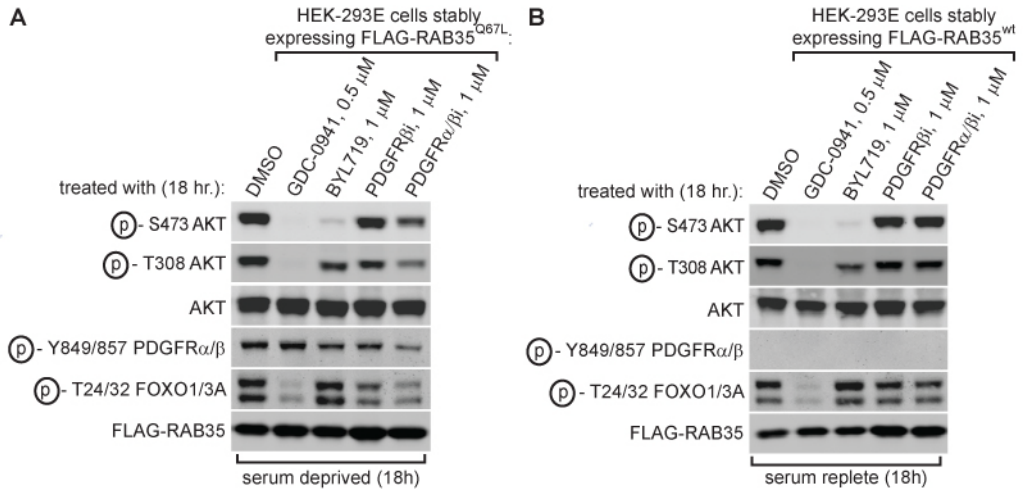

Figure 3.6: Pharmacological blockade of PDGFRα/β inhibits PI3K/AKT signaling in cells stably expressing GTPase-deficient RAB35^{Q67L}. (**A**) Cells stably expressing RAB35^{Q67L} were serum starved and treated overnight with either vehicle (DMSO), the pan-Class I PI3K inhibitor GDC-0941 (0.5 μM), the PI3Kα-specific BYL-719 (1 μM), the PDGFRβ inhibitor CP-673451 (PDGFRβi, 1 μM), or the PDGFRα/β inhibitor CP-868596 (PDGFRα/βi, 1 μM). Cells were then lysed and lysates were analyzed by immunoblotting. (**B**) Cells stably expressing RAB35^{wt} were treated overnight as indicated in serum replete medium, then lysed and analyzed as in (A).

pathway was originating from the mutant allele of RAB35, these experiments were performed in serum-free conditions. Interestingly, in the same experiment performed in cells stably expressing RAB35^{wt} in serum replete conditions, we found that PDGFRα/β inhibition failed to suppress AKT phosphorylation (Figure 3.6B). This suggests that PDGFR inhibition on its own in the presence of serum is not sufficient to inhibit PI3K/AKT signaling (Figure 3.6B).

Finally, to check whether other RTKs might be involved in the regulation of PI3K/AKT by RAB35, we also tested a number of lipid kinase and tyrosine kinase inhibitors (TKI's) on cells expressing GTPase deficient,

dominant active RAB35^{Q67L} (Figure 3.7 and data not shown). As expected, the PI3K inhibitors GDC-0941 and BYL-719 suppressed AKT

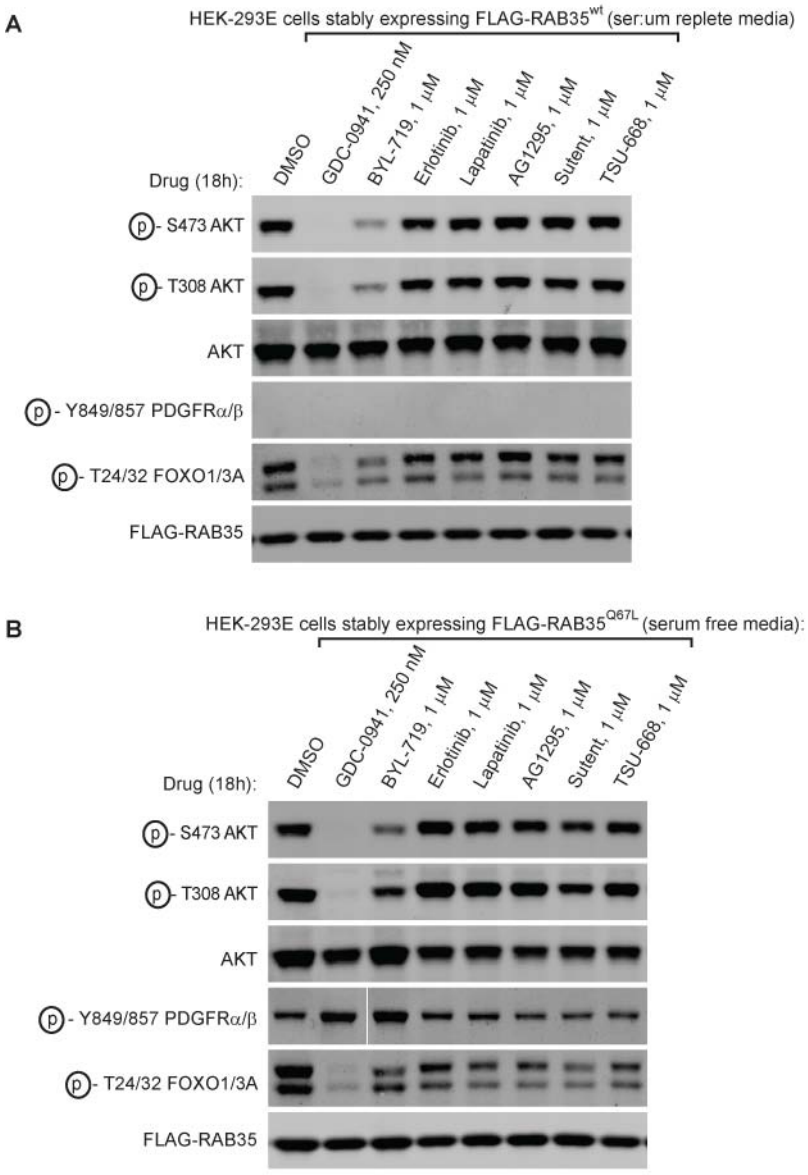

Figure 3.7: Non-PDGFR targeting kinase inhibitors do not reduce PI3K/AKT signaling in cells expressing GTPase-deficient RAB35^{Q67L}. (**A**) Cells stably expressing RAB35^{wt} were serum starved and treated with either DMSO or the indicated drugs overnight as noted. The next day, the cells were stimulated with DMEM containing 10% FBS and the indicated inhibitors. (**B**) Cells stably expressing RAB35^{Q67L} were treated overnight in serum free medium as indicated. Cells were then lysed and lysates were analyzed by immunoblotting.

phosphorylation in cells expressing RAB35^{Qwt} or RAB35^{Q67L}. Further, EGFR inhibitors like Erlotinib and Lapatinib failed to suppress AKT phosphorylation in cells expressing GTPase-deficient RAB35^{Q67L}. Further, VEGFR-specific molecules had little to no effect on AKT phosphorylation in cells expressing RAB35^{Q67L}.

3.4.4 RAB35^{wt} and GTPase-deficient RAB35^{Q67L} interact with PDGFRα and PDGFRβ

As demonstrated earlier in this chapter, we had found that RAB35 interacts with PI3K in a GTP-dependent manner. This led us to wonder whether RAB35 was interacting with PI3K in a manner analogous to how the GTPase KRAS interacts with PI3K—i.e. directly and in a way that activates the kinase activity of PI3K. However, our findings that 1.) the expression of dominant active RAB35^{Q67L} specifically upregulates the tyrosine phosphorylation of PDGFRα/β (Figure 3.5) and 2.) a PDGFRα/β specific kinase inhibitor suppresses RAB35^{Q67L}-driven PI3K/AKT activity suggested to us that RAB35 might be acting directly on PDGFR.

To ask whether RAB35 might be interacting with PDGFR, we transfected cDNAs expressing either myc-tagged PDGFRα or β into cells stably expressing either RHEB^{wt}, RAB35^{wt} or RAB35^{Q67L}. After lysing these cells, we then immunopurified either PI3K (using an anti-p85 antibody) or myc-PDGFR (using an anti-myc antibody) and asked whether FLAG-tagged RAB35 co-immunoprecipitated with these proteins (Figure 3.8). Not

surprisingly, we found that both PDGFRα and β immunoprecipitated with PI3K, and that FLAG-tagged RAB35^{wt} and RAB35^{Q67L}—but not RHEB^{wt}—was also present in these purifications (Figure 3.8A). These data were consistent with 1.) the fact that PDGFRα/β is a well-characterized interaction partner of PI3K and 2.) our RAB35-PI3K interaction studies in Figures 3.1-3.3.

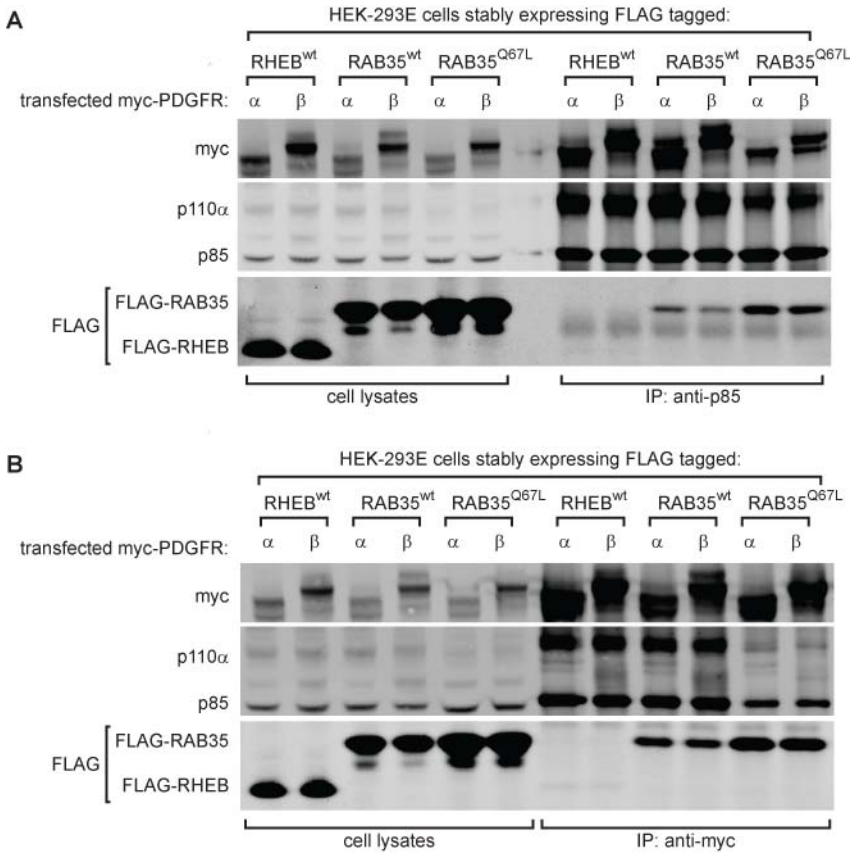

Figure 3.8: RAB35^{wt} and GTPase-deficient RAB35^{Q67L} interact with PDGFRα and PDGFRβ. (**A**) HEK-293E cells stably expressing FLAG-tagged RHEB^{wt}, RAB35^{wt} or RAB35^{Q67L} were transfected with cDNA encoding for either myc-PDGFRα or myc-PDGFRβ. Cells were then lysed and PI3K was immunopurified with an anti-p85 antibody. (**B**) myc-PDGFR was immunopurified with an anti-myc antibody from the same lysates as in (A).

We also immunopurified myc-PDGFRα or β using an anti-myc antibody. As with our PI3K purifications, we found that both the p85 and p110α subunits of PI3K were present in both PDGFRα and β immunoprecipitates (Figure 3.8B). We also found that both alleles of FLAG-tagged RAB35 were also present in these purifications. Interestingly, the FLAG-RAB35 signal present in PDGFR purifications was consistently stronger than the FLAG-RAB35 signal in our PI3K purifications, which suggested to us that the PDGFR-RAB35 interaction may be more robust than the PI3K-RAB35 interaction. This is reinforced by the fact that in cells expressing RAB35^{Q67L}, less p85 and p110α purify with both PDGFRα and β, but the amount of FLAG-RAB35^{Q67L} is not diminished in these immunoprecipitations. This suggests to us that the interaction of PI3K and RAB35 may be indirect and due to the fact that both are interacting with PDGFR. However, whether RAB35 interacts with PDGFR directly or via another protein remains unclear.

3.4.5 GTPase-deficient RAB35^{Q67L} constitutively localizes PDGFRα to an internal compartment

Because RAB35 is a RAB GTPase, we had previously considered that its role in PI3K/AKT signaling could be due to endomembrane trafficking of either PDGFR, PI3K or AKT itself. Since we had evidence that dominant active RAB35^{Q67L} is exerting its effects via PDGFRα—and because trafficking of RTKs is a well documented phenomenon [388-391]—we next

asked whether expression of dominant active, GTPase-deficient RAB35^{Q67L} was altering the localization of PDGFRα (Figure 3.9). We transiently transfected cDNAs coding for myc-tagged PDGFRα into cells that

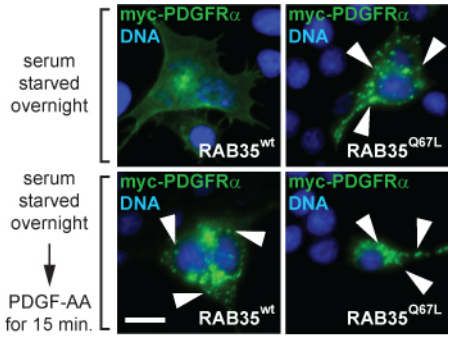

Figure 3.9: Dominant active, GTPase-deficient RAB35^{Q67L} constitutively internalizes PDGFRα. HEK-293E cells stably expressing FLAG-tagged RAB35^{wt} or RAB35^{Q67L} were transiently transfected with cDNAs expressing myc-tagged PDGFRα, then starved, treated with 100 ng/mL PDGF-AA for 15 minutes and processed for immunofluorescence with an anti-myc antibody and stained for actin and DNA/nuclei as indicated. Scale bar represents 10 μm.

stably expressed either RAB35^{wt} or RAB35^{Q67L} and asked whether the localization of the receptor was altered by GTPase-deficient RAB35. Not surprisingly, in cells expressing RAB35^{wt}, PDGFRα was diffusely localized in the absence of growth factors but reorganized into discreet internalized punctate structures after 15 minutes of treatment with PDGF-AA. However, in cells expressing RAB35^{Q67L}, PDGFRα was constitutively internalized regardless of whether the cells had been stimulated with PDGF or not. Thus, GTPase-deficient RAB35^{Q67L} dyslocalizes PDGFRα to compartments inside the cell regardless of growth factor stimulation.

Although our biochemical evidence and experiments with small molecules already suggested that RAB35-mediated activation of PI3K/AKT signaling was explicitly through PDGFRα, we wanted to ask whether trafficking of RTKs was generally deranged in cells with activated RAB35^{Q67L}. The epidermal growth factor receptor (EGFR) is well-characterized in terms of its internalization and recycling after stimulation with EGF. Thus, we performed a similar experiment to the one in Figure 3.9 using myc-tagged EGFR to visualize EGFR trafficking in cells expressing either RAB35^{wt} or RAB35^{Q67L} (Figure 3.10). Unlike our observations with PDGFRα, we did not see any difference in the EGF-stimulated internalization of EGFR between the two cell lines, which suggested to us that the trafficking of EGFR is not affected by the GTP-loading state of RAB35.

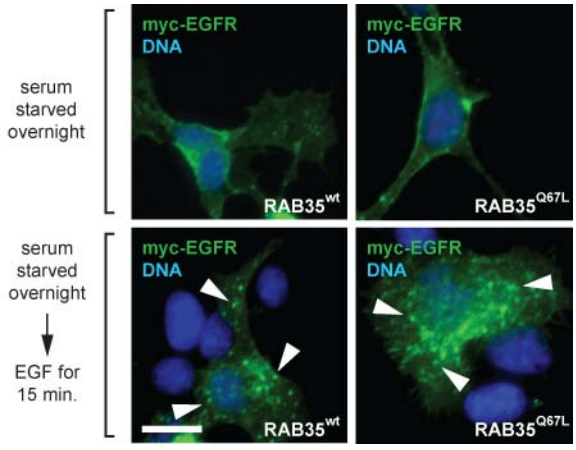

Figure 3.10: Dominant active RAB35^{Q67L} does not alter the localization of the epidermal growth factor receptor (EGFR). HEK-293E cells stably expressing the indicated FLAG-RAB35 alleles were transiently transfected with cDNAs expressing the indicated receptor tyrosine kinases, starved overnight, treated with the indicated ligands then processed for immunofluorescence. Scale bar represents 10 μm.

Interestingly, the localization of other growth factor receptors also did not appear to be grossly altered in cells that stably expressed RAB35^{Q67L} (data not shown). These data are consistent with our biochemical evidence that PDGFR is the only RTK that is hyper-phosphorylated due to expression of RAB35^{Q67L}. This further suggested to us that the influence of RAB35 on PI3K/AKT signaling is transduced by PDGFRα but not other RTKs.

3.4.6 RAB35^{Q67L} sequesters PDGFRα to RAB7-positive endomembranes

We were curious as to whether or not the localization of PDGFRα in cells that expressed GTP-bound RAB35^{Q67L} was either due to 1.) excessive accumulation of the receptor in a compartment that PDGFR normally traffics through, or 2.) aberrant trafficking of the receptor into an abnormal endomembrane compartment. We thus asked two questions: 1.) which endosomal compartment is internalized PDGFRα normally associated with after PDGF-treatment in cells that express RAB35^{wt}? and 2.) which endosomal compartment PDGFRα is localized to in cells expressing activated RAB35^{Q67L}? Although endosomes are a diverse population of endomembrane compartments, they can be roughly functionally categorized by the populations of proteins that they contain [392-395]. For example, early endosomes contain early endosomal antigen 1 (EEA1) and the GTPase RAB5 [396-402], while late endosomes contain RAB7 [403-404], recycling

endosomes are marked by RAB11a and RAB11b [405-411], and lysosomes contain RAB7 and LAMP1 [412-413].

We found that 15 minutes after PDGF-AA treatment in cells expressing wildtype RAB35, transiently expressed myc-tagged PDGFRα is localized in part to a RAB7-positive compartment within the cell (Figure 3.11A). This is not surprising, as RAB proteins (RAB4, in particular) have been implicated in PDGFR trafficking previously [414]. Interestingly, in cells stably expressing $RAB35^{Q67L}$, myc-PDGFRα was also localized to RAB7-positive compartments even in the absence of stimulation with PDGF-AA (Figure 3.11B). These data suggested to us that $RAB35^{Q67L}$ may be retaining active PDGFRα in a RAB7-positive compartment.

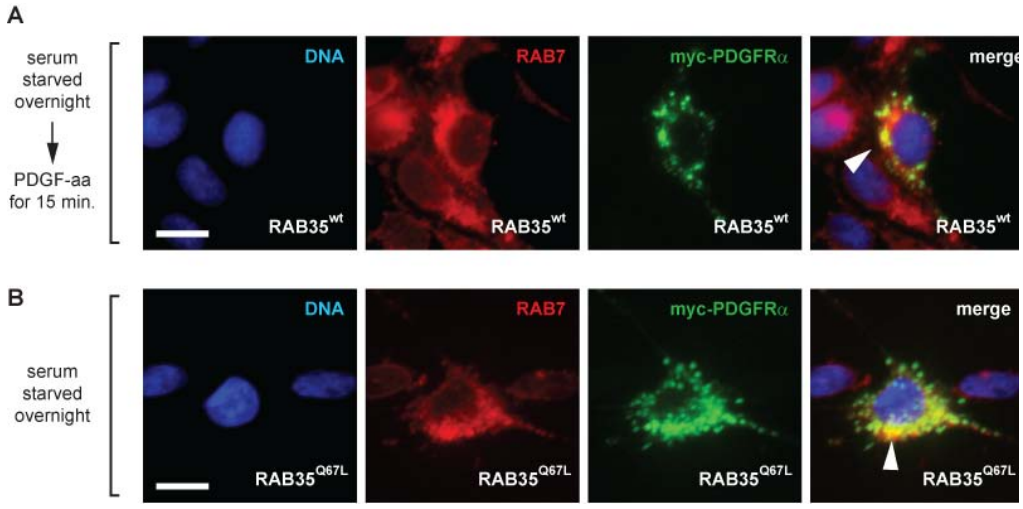

Figure 3.11: PDGF-stimulated PDGFRα localizes to a RAB7-positive compartment in cells stably expressing $RAB35^{wt}$ or in PDGF-deprived cells stably expressing $RAB35^{Q67L}$. HEK-293E cells stably expressing FLAG-$RAB35^{wt}$ were transfected with myc-PDGFRα, treated with PDGF-AA for 15 minutes, then processed for immunofluorescence with anti-myc and antibodies against the indicated GTPases.

We also asked whether PDGFRα localized to other compartments that are marked by the RAB proteins RAB5 (present in early endosomes) or RAB11 (present in recycling endosomes). Interestingly, myc-PDGFRα did not localize to RAB5 or RAB11-containing compartments in RAB35^{wt} cells that had been treated with PDGF-AA or in RAB35^{Q67L} expressing cells that had been deprived of growth factors. This indicated to us that the RAB35^{Q67L}-driven dyslocalization of PDGFRa is likely specific to RAB7-positive endomembranes.

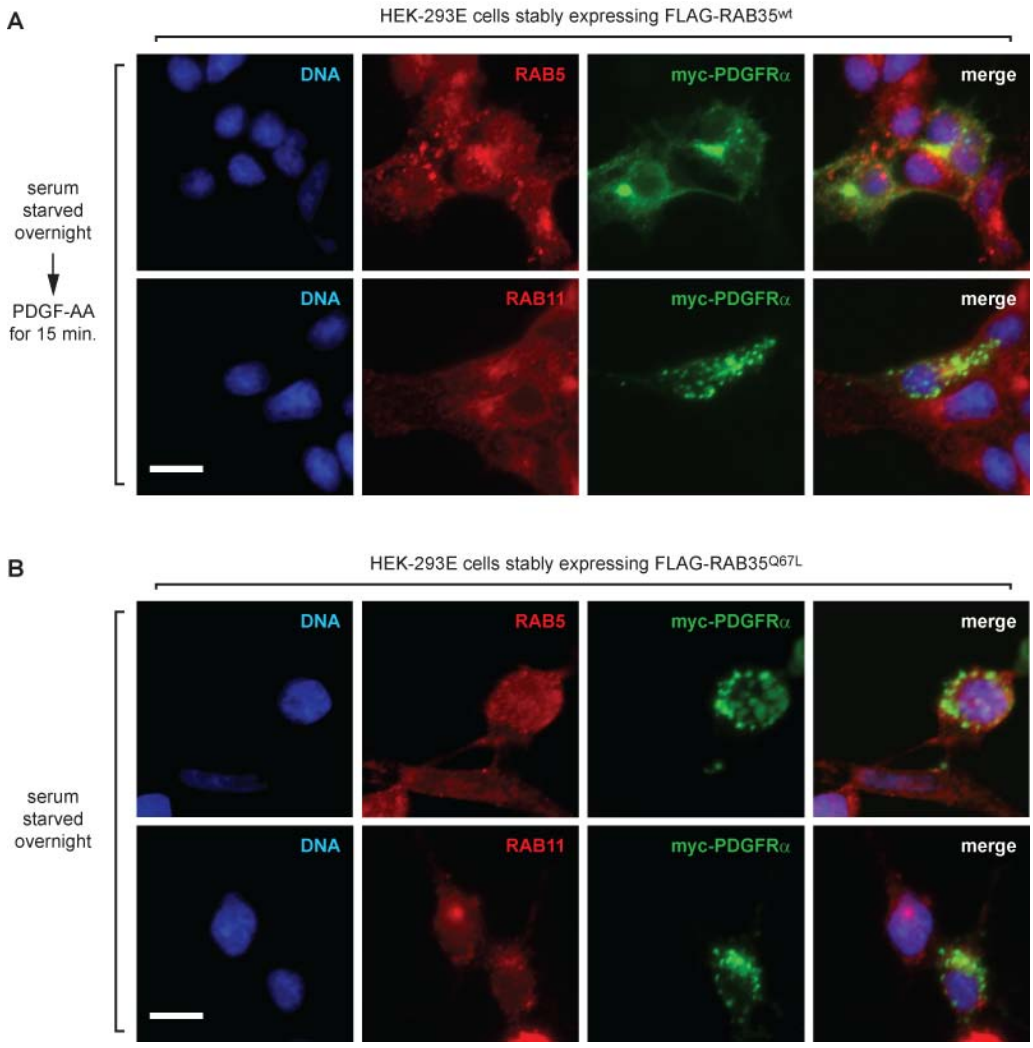

Figure 3.12: PDGFRα does not localize to RAB5 or RAB11-positive endomembranes in cells expressing RAB35^{wt} or RAB35^{Q67L}. (**A**) HEK-293E cells stably expressing FLAG-RAB35^{wt} were transfected with myc-PDGFRα, serum starved overnight, then treated with 100 ng/mL PDGF-AA for 15 minutes and processed for immunofluorescence with the indicated antibodies. (**B**) HEK-293E cells stably expressing FLAG-RAB35^{Q67L} were transfected with cDNA expressing myc-PDGFRα, serum starved overnight, then processed as in (A).

3.5 DISCUSSION

Our data suggest that RAB35 interacts with PI3K, and that this interaction is at least partially GTP-dependent. In searching for mechanisms by which RAB35 regulates PI3K, we identified PDGFR as aberrantly activated in cells that stably express a dominant active allele of RAB35. Further, small molecule inhibitor experiments suggest that RAB35 likely regulates PI3K/AKT signaling through PDGFRα, although the "division of labor" between PDGFRα and β when regulated by RAB35 remains unclear.

In addition to the biochemical evidence that RAB35 regulates PI3K via the PDGFRs, we find that expression of activated RAB35^{Q67L} retains PDGFRα in a RAB7-positive endomembrane compartment. Interestingly, this is similar to the location of liganded PDGFRα in cells expressing wildtype RAB35. Thus, it appears that dominant active RAB35^{Q67L} is not trafficking PDGFRs to an inappropriate or abnormal endomembrane, rather retaining these RTKs in a location that they likely inhabit only temporarily under normal conditions. Whether this RAB7-positive location in the cell is an unidentified endosome, a late endosome [404], or the lysosome [415] is at present unclear.

Rab proteins like RAB35 are primarily thought to regulate endomembrane trafficking, and growth factor receptor trafficking is a mechanism of regulating RTK signaling. Thus, we hypothesize that GTP-loaded RAB35 traffics activated PDGFRs to endomembranes where the PDGFR-PI3K complexes sustain localized PI3K signaling. Although our data

do support such a hypothesis, many questions about the nature of this relationship remain unanswered. For instance, whether—and to what extent—RAB35 is a normal physiological regulator of PDGFRα trafficking is unclear. Further, whether PDGFRα is a direct cargo of RAB35 or merely a "hitchhiker" on RAB35-positive endosomes is also unknown. These questions can be answered as more is learned about the trafficking life cycle of PDGFRα itself and as the relationship between RAB35 and PI3K signaling becomes more clearly defined.

CHAPTER FOUR:

RAB35, CANCER, AND THE ONCOGENIC POTENTIAL OF THE ENDOMEMBRANE TRAFFICKING SYSTEM

4.1 THE SMALL GTPASE RAB35 IS A REGULATOR OF ENDOSOMAL TRAFFICKING AND CYTOSKELETAL ORGANIZATION

4.1.1 RAB35 regulates endomembrane trafficking at the recycling endosome

RAB35 was at first thought to be a member of the RAB1 sub-family of RAB GTPases by virtue of its amino acid sequence, and it was initially called Ray/RAB1C [416-417]. However, it was soon appreciated that despite sequence similarity, RAB35 was functionally distinct from RAB1A and RAB1B, which regulate vesicular trafficking between the endoplasmic reticulum and the golgi apparatus [417-420]. The first endomembrane trafficking function ascribed to RAB35 was fast endocytic recycling, which is necessary for the terminal steps of cytokinesis in dividing cells [421]. Other early studies of RAB35 localization indicated that although RAB35 is localized to recycling endosomes, it is located at other endosomes as well as at the plasma membrane [336, 421-422]. Considering the different effectors of RAB35 that will be reviewed here, it is likely that there exist within the cell many distinct cellular pools of RAB35 that allow for fine-tuning of RAB35's functions. Thus, the functions of RAB35 are very likely to be quite diverse.

In addition to regulating the recycling endosome, RAB35 has also been implicated in exosome regulation. One group recently described

RAB35 as a positive regulator of exosome secretion, where RAB35 is necessary for the normal release of exosomes from oligodendrocytes into the intracellular space [423]. Hsu et. al. further described the proteins TBC1D10A-C as RAB35 GTPase activating proteins that inhibit RAB35 GTP-loading and exosome release. Further, TBC1D10C has been shown to negatively regulate the export of transferrin from the recycling endosome pathway, as well as T-cell receptor (TCR) recycling at the immunological synapse [373]. Recent data also suggest that GTP-bound RAB35 serves to retain cadherin molecules at the surface of cells, which promotes cell-to-cell adhesion [424-426].

RAB35 has also been demonstrated to play a role at the early endosome. Both RAB35 and its positive regulator DENND1A (a guanine nucleotide exchange factor (GEF) [427]) have been shown to regulate trafficking at the early endosome [337]. Specifically, RAB35 and DENND1A recruit the tubular endosome protein EHD1 to EEA1-positive early endosomes. Further, the RAB35 GAP Skylwalker—a *Drosophila* homologue of the TBC1D10A-C proteins in humans—regulates the pool of synaptic endosomes in neurons [428]. Thus, in addition to regulating the recycling of cargoes through the recycling endosome, RAB35 functions at several other endomembrane sites in a variety of different cellular contexts.

Interestingly, RAB35 can regulate the endosomal localization and activation of other small GTPases. For example, GTP-bound RAB35 can activate centaurin-β2 GAPs that negatively regulate the GTPase ARF6 [429],

which in turn downregulates ARF6-dependent recycling of β1-integrins and EGFRs [426]. Conversely, GTP-bound ARF6 can activate the RAB35 GAP TBC1D10B, which downregulates RAB35-dependent signaling and prevents loading of RAB35 into the endocytic pathway [430]. More recent evidence from the Fukuda lab suggests that RAB35 recruits RAB8, RAB13 and RAB36 to recycling endosomes via the scaffold protein MICAL-L1 [431]

It also appears that the recruitment of the Rho GTPases RAC1 and CDC42 to phagosomes is dependent on GTP-bound RAB35 [432]. Further, Shim et. al. suggest that RAB35 is necessary for actin remodeling by RAC1 and CDC42. Thus, the regulation of actin/the cytoskeleton and membrane trafficking can actually be seen as overlapping functions, as RAB35 regulates the localization of several GTPases that directly govern cytoskeletal shape.

4.1.2 RAB35 regulates actin cytoskeletal dynamics and cell shape

In addition to its role in trafficking cargoes through the recycling endosome, RAB35 regulates the shape of the actin cytoskeleton [338]. The same group that described RAB35 as a regulator of cytokinesis has also described RAB35 as a regulator of the 5'-OH phosphatase OCRL, which localizes phosphatidylinositol 4, 5-bisphosphate and F-actin to the cellular bridge during the abscission steps of cytokinesis [336]. Activated RAB35 has also been described as a positive regulator of the actin remodeling that drives neurite outgrowth [433-435]. Indeed, several groups have found that

expression of dominant active GTP-bound RAB35 caused remodeling of the cytoskeleton into spindly, neurite-like portions of cell membrane. Indeed, stable expression of $RAB35^{Q67L}$ in our hands yielded the same phenotype. Interestingly, we found that this was PI3K-dependent, as treatment with PI3K inhibitors reversed this $RAB35^{Q67L}$-dependent spindly actin phenotype (data not shown).

It also appears that RAB35 regulates actin via a direct interaction. In *Drosophila* and mammalian cells, GTP-bound RAB35 interacts with the actin-bundling protein fascin to locally recruit actin [339]. These studies are supported by data from other groups that also identify the DENND1A-C proteins as guanine nucleotide exchange factors (GEFs) that activate the actin-related functions of RAB35 [433].

In summary, RAB35 performs a number of functions in a diverse set of biological pathways. In most cases, these appear to share a similar mechanism, where GTP-bound RAB35 recruits its effectors to various cellular locales. The effectors and regulators of RAB35 discussed in this section are summarized below in Figure 4.1.

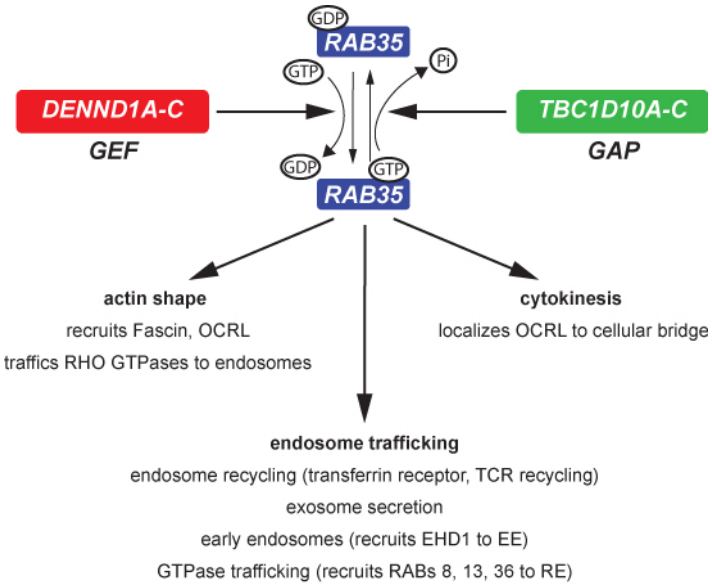

Figure 4.1: RAB35 regulates the recycling endosome and actin cytoskeletal dynamics. GDP-bound RAB35 is inactive and does not bind effectors. GDP is exchanged for GTP on RAB35 by the guanine nucleotide exchange factors (GEFs) DENND1A-C (left), which activates RAB35. RAB35 GTPase activity is activated by the GTPase activating proteins (GAPs) TBC1D10A-C. GTP-bound RAB35 then regulates a diverse set of effectors by recruiting them to different cellular locations. OCRL, oculocerebral syndrome of Lowe; TCR, T-cell receptor; EHD1, EH-domain containing 1; EE, early endosome; RE, recycling endosome.

4.2 PDGFR TRAFFICKING, RAB35, PI3K/AKT SIGNALING, AND CANCER

4.2.1 Growth factor receptor tyrosine kinases are trafficked via the endomembrane system

After growth factor stimulation, RTKs are internalized and either inactivated and returned to the membrane, allowed to signal in various subcellular locations, or targeted for destruction by the lysosome and proteasome system [389]. This mechanism is likely common to most growth factor receptors, but the epidermal growth factor receptor (EGFR) is the most thoroughly investigated receptor with regards to its internalization and trafficking after activation [389]. Because we found that RAB35 regulates the intracellular location of PDGFRα, it is important to consider how RTKs are trafficked by the cell after internalization.

One mechanism by which growth factor receptors are downregulated is through ubiquitinization by the E3 ubiquitin ligase CBL [389, 436-437]. RTKs like EGFR [438], IGFIR [439], PDGFR [440-441], MET [442], KIT [443], VEGFR [444], and the Ephrin receptors [445-446] are all regulated by CBL in a similar process. Activated RTKs are internalized by clathrin-coated pieces of membrane, which often includes the recruitment of CBL to the RTK or its associated proteins. CBL then mono- and di-ubiquitinylates the target RTK, which tags the kinase for degradation at the lysosome and/or proteasome. Alternatively, receptors can be de-liganded, de-ubiquitinylated,

and recycled back to the cell membrane where they can be re-activated later. These scenarios are illustrated in Figure 4.2.

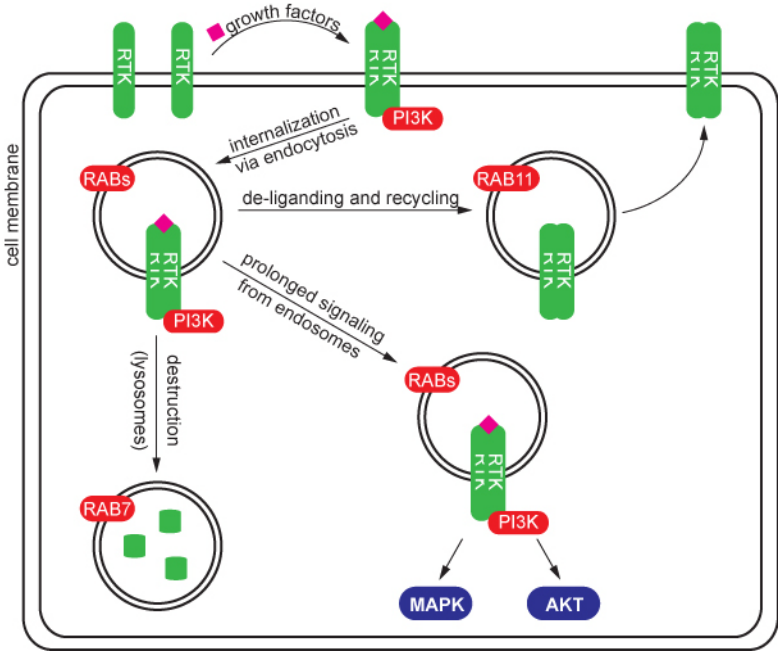

Figure 4.2 The fates of internalized growth factor receptor tyrosine kinases. Once growth factor receptor tyrosine kinases (RTKs) are activated by their growth factor ligands, they initiate signaling at the cell membrane via PI3K and other effectors. They are then trafficked into the cell by endocytosis. Signaling can be attenuated by lysosomal destruction of the RTK, or by de-liganding and recycling the RTK back to the cell membrane. Alternatively, the RTK/PI3K complex can continue to actively signal to effectors like MAPK or AKT while still residing on endomembranes.

The trafficking and degradation of receptors like EGFR has been understood for some time, but recent data have demonstrated that instead of simply being internalized and turned off, EGFR can actively signal while it is associated with endosomes [389, 391, 447-449] (See example in Figure 4.2). The signaling of internalized EGFR from endomembrane compartments suggests a mechanism by which the cell can exquisitely govern the spatial

and temporal activity of signal transduction. Interestingly, similar studies conducted with respect to PDGFR suggest that much of the signaling downstream of this receptor occurs after PDGFR is internalized to endosomes [390].

We speculate that much of the PI3K-dependent signaling by PDGFR actually happens while receptors are trafficked intracellularly. Interestingly, we have found that the inhibition of endocytosis with the dynamin GTPase inhibitor Dynasore [450-453] or N-ethylmaleimide (NEM, which inhibits vesicular trafficking) [454-456] spares the initial activation of PI3K/AKT by growth factors (0-5 minutes), but blocks signaling that occurs 15 minutes to several hours after initial stimulation (data not shown). Given that RTKs are internalized within minutes after their initial stimulation, this suggests to us that RTK signaling to oncogenic pathways such as PI3K/AKT is dependent upon vesicular trafficking.

4.2.2 RAB35 regulates the PI3K/AKT signaling axis by controlling the intracellular location of PDGFRα

With the data presented in Chapters 2 and 3 of this thesis, we have provided evidence that GTP-bound RAB35 retains the PDGFRα in a RAB7-positive endosome where it can drive PI3K/AKT signaling. Because depletion of RAB35 suppressed AKT and FOXO/NDRG1 phosphorylation in response to serum and individual growth factors, our data suggested that RAB35 might function downstream of multiple growth factor receptors. Our

first suspicion was that RAB35 either functioned at PI3K or was a general regulator of RTK activation of PI3K. However, our gain-of-function experiments indicate that RAB35 might function specifically through PDGFRα.

Localization studies in cell lines stably expressing wildtype RAB35 suggested to us that PDGFRα is normally trafficked to RAB7-positive endomembranes after PDGF stimulation. Further, in cells expressing GTPase-deficient $RAB35^{Q67L}$, PDGFRα is trafficked to RAB7-positive endomembranes in the absence of PDGF. Although our data do not indicate whether or not RAB35 is required for the trafficking of PDGFRα to a RAB7-positive compartment, it appears that GTP-bound RAB35 somehow retains PDGFRα at this location, where it actively drives PI3K/AKT signaling in the absence of ligand. Whether RAB35 is necessary for trafficking PDGFRα to a RAB7-positive endomembrane will be addressed with RAB35 loss-of-function studies. Further, it is unclear whether $RAB35^{Q67L}$ is itself driving PDGFRα to RAB7-positive compartments, or preventing the efficient exit from these compartments.

It is also possible that GTP-bound $RAB35^{Q67L}$ inhibits a negative regulator of PDGFR signaling, trafficking, or degradation. For example, $RAB35^{Q67L}$ could inhibit the ability of the protein tyrosine phosphatase Src homology 2 domain-containing phosphatase 1 (SHP-1) to dephosphorylate the phospho-tyrosine residues on PDGFRs [457]. Alternatively—considering that RAB35 has been demonstrated to negatively regulate GTPases such as

ARF6 [426, 430]— RAB35^{Q67L} may inhibit a RAB or ARF GTPase that determines the trafficking fate(s) of PDGFRs. Finally, RAB35^{Q67L} may prevent ubiquitin ligases like CBL or CBL2 from ubiquitinylating PDGFRs [441, 458], which could lead to accumulated, phosphorylated and activated PDGFRs on endomembranes that can sustain signaling to PI3K/AKT.

Although it is interesting to postulate various scenarios by which RAB35 may regulate PDGFRα, we suspect that the indirect scenarios outlined above are less likely, given that we have detected interactions between wildtype and mutant RAB35 and both PI3Kα and PDGFRα. We propose that the PDGFRα/PI3Kα complex is bound directly by RAB35, preferentially when it is loaded with GTP. The data presented in Figure 3.8—where RAB35 co-purified more robustly with PI3K immunoprecipitates than it did with PDGFRα immunoprecipitates—suggest to us that RAB35 interacts with PI3Kα, which interacts with PDGFRα (Figure 4.3). Thus, we suspect that GTP-bound RAB35 directly binds PI3K and serves to localize PDGFRα/PI3Kα to RAB7-containing endomembranes, either by “steering” PDGFRα/PI3Kα to this compartment or “trapping” it there. Whether the exit of PDGFRα from this compartment is dependent on hydrolysis of the GTP of activated RAB35 is an interesting question that could be addressed with loss-of-function experiments that ask whether perturbation of the known RAB35 GAPs (TBC1D10A-C) and GEFs (DENND1A-C) for RAB35.

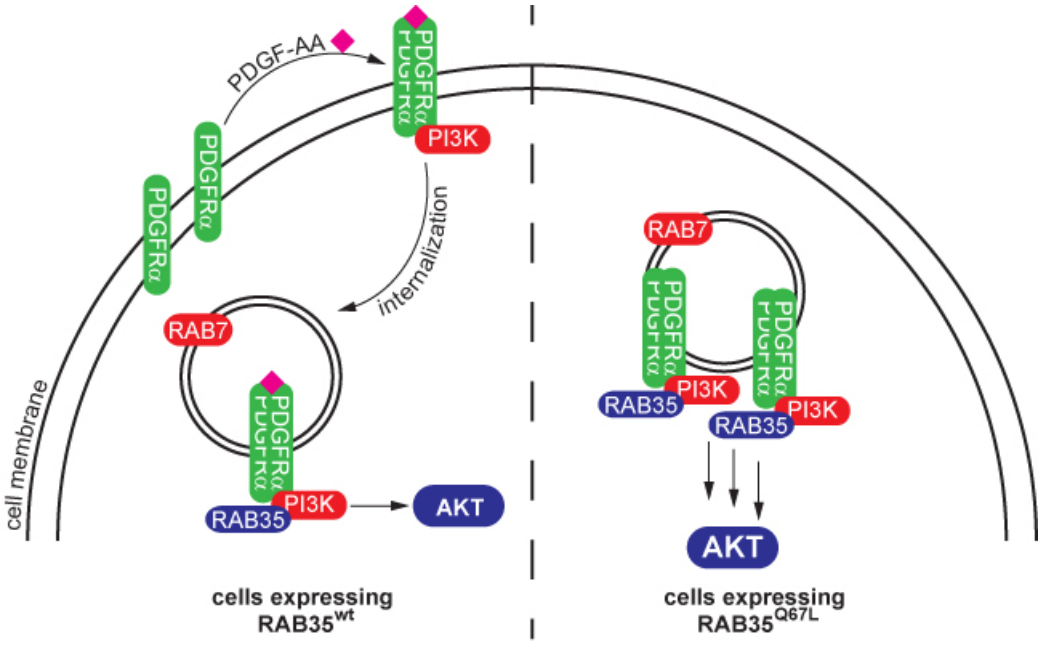

Figure 4.3: A model for regulation of PDGFRα-PI3K signaling by the small GTPase RAB35. Following stimulation with PDGF-AA, actively signaling PDGFRα/PI3K is internalized to RAB7-positive endomembranes. RAB35 interacts with the PDGFRα/PI3K complex, likely by direct interaction with PI3K (left). In cells that express GTPase-deficient, dominant active RAB35^{Q67L}, PDGFRα/PI3K is retained at RAB7-positive endosomes within the cell even in the absence of ligand, where it constitutively signals to AKT (right).

4.2.3 Is RAB35 a physiological regulator of PDGFRα/PI3K signaling, and are oncogenic mutant alleles of RAB35 hypermorphic or neomorphic?

At first glance, our gain-of-function data—that RAB35 signal to PI3K by activating PDGFRα—did not fit with our loss-of-function data, which suggested that RAB35 was required for PI3K/AKT activation in response to non-PDGF ligands like VEGF, IGF-I or EGF (Figure 2.16). However, recent data from the Kwiatkowski lab strongly suggests that these other ligands actually require PDGFRα/β to efficiently signal to the PI3K/AKT machinery

[459]. These findings confirmed earlier ones that indicated that PDGFRs are activated in a “lateral signaling” fashion: stimulation of IGF-IRs with IGF, for example, activates a Src-dependent activation of PDGFRs, which then signal along with IGF-IR to PI3K [460-463]. Further, PDGFR and EGFR can heterodimerize to activate one another in response to EGF stimulation [464]. Thus, the loss-of-function data that suggests that RAB35 is necessary for EGF, IGF, PDGF and VEGF-mediated PI3K/AKT activation do not necessarily conflict with the gain-of-function data that suggest that RAB35 regulation of PI3K/AKT is primarily accomplished via PDGFRα.

It is also interesting to speculate over the nature of the gain-of-function phenotype we observed in the GTPase-deficient allele of RAB35. Mutations that alter protein function can be inactivating (hypomorphic), hyperactivating (hypermorphic), or confer new functions to that protein altogether (neomorphic) [465]. For example, mutations that result in a truncated and inactive PTEN protein are hypomorphic, while mutations that generate constitutively active alleles displaying normal function—like activating mutations in PI3K—are hypermorphic. Occasionally, mutations can confer altogether neomorphic functions on proteins. For example, the PIK3R1/p85 adaptor subunit of PI3K actually serves to inhibit the lipid kinase activity of PI3K. However, mutations in the *PIK3R1* gene have been identified from human tumors that confer a novel, activating capacity of PIK3R1 towards PI3K activity [466].

The data presented in this thesis suggest that RAB35 is a physiological regulator of PDGFR-PI3K-AKT signaling and that the internalization and activation of PDGFRα and PI3K/AKT signaling by dominant active $RAB35^{Q67L}$ is a hypermorphic—not neomorphic—phenomenon. We suspect that if the regulation of PDGFRα/PI3K by $RAB35^{Q67L}$ was non-physiological—i.e. neomorphic—that depletion of wildtype RAB35 in loss-of-function experiments would not block PI3K/AKT signaling. Indeed, as demonstrated in Chapter 2, depletion of RAB35 in a number of contexts serves to blunt the activation of PI3K/AKT as potently as does the depletion of other core PI3K/AKT signaling components.

Further, our gain-of-function experiments using GTPase-deficient $RAB35^{Q67L}$ also suggest that the phenotype demonstrated by $RAB35^{Q67L}$ is an exaggerated and unregulated version of the normal signaling phenotype of $RAB35^{wt}$. The internalization of PDGF-stimulated PDGFRα in cells expressing $RAB35^{wt}$ appears virtually identical to the internalization of unliganded PDGFRα in cells expressing $RAB35^{Q67L}$. In both cases, PDGFRα localizes to RAB7-positive endosomes. If $RAB35^{Q67L}$ were conferring a truly neomorphic function to PDGFRα signaling in cells, we would expect it to be re-trafficked into different compartments from those normally occupied by liganded PDGFRα.

A full assessment of the hypermorphic vs. neomorphic nature of oncogenic alleles of RAB35 will be further clarified by studying the relationship between wildtype RAB35 and PDGFRα trafficking. This would

likely include loss-of-function experiments using both RNAi and small molecule inhibitors.

4.3 CONCLUDING REMARKS

4.3.1 RAB35, cancer and why "private mutations" matter

This thesis began with a desire to use RNAi screens to identify novel regulators of PI3K/AKT signaling. While we used this loss-of-function screening approach to identify candidate genes that might regulate PI3K/AKT signaling, we prioritized hit genes that were mutated in a way that might alter their function (Table 2.2). Although we are interested in identifying any new members of the PI3K/AKT pathway, we hoped that such an approach would allow us to identify novel PI3K/AKT components that play an role in oncogenesis.

As described in Chapter 2 of this thesis, the mutations that we identified and characterized in RAB35 were not recurrent. Indeed, the RAB35 mutations that we identified in human tumors (A151T and F161L) were not canonical mutations that are known to lock RAB35 in a GTP-bound state (e.g. Q67L). Nevertheless, the fact that the $RAB35^{A151T}$ and $RAB35^{F161L}$ mutant proteins could activate PI3K/AKT signaling and transform cells suggests that these mutations are not "passenger" mutations, but that they instead played a role in the development of the tumors in which they were found. Recent findings that the same mutations in *KRAS* at similar residues are transforming suggest further that these two RAB35 mutations

are functionally relevant to tumorigenesis [357-358, 467]. Thus, rare mutations in proteins like RAB35 that regulate growth factor signaling can activate oncogenic signaling.

The possibility that RAB35 mutations in patients are activating PI3K/AKT signaling and aiding in tumor formation or progression could have actionable clinical implications. For example, patients with activating mutations in *PIK3CA* would likely benefit from PI3Kα inhibitors, similar to $BRAF^{V600E}$-positive melanoma patients treated with vemurafenib [468-470]. Thus, given that PDGFRα/PI3K/AKT is hyperactivated by$RAB35^{A151T}$ and $RAB35^{F161L}$, patients with these mutations could benefit from PI3K-inhibitors.

The scenario outlined above underscores the importance of finding, identifying, and characterizing rare but biologically relevant mutations in genes that regulate cell survival pathways. These so-called “private mutations” [471-473] are the subject of considerable discussion within the oncology community [474][475] because the number of patients with them is relatively small. We suggest that the identification of RAB35 as a regulator of PI3K signaling that is mutated in cancers thus serves as an example for why rarer “private” mutations should be investigated and understood.

4.3.2 Endomembrane trafficking as an oncogenic force

The concept of dysregulated endomembrane trafficking in cancer is not a novel one [476]. Indeed, many investigators have documented dysregulated membrane organization and trafficking downstream of various

oncogenic forces. For example, it is well documented that the membrane polarity of tumor cells is deranged in many contexts [477-479]. In addition, it has recently been reported that some oncogenic mutations in MET disrupt the normal trafficking of the receptor [480]. This enhances the oncogenic potential of MET by preventing its degradation and localizing the protein to endosomes where it actively signals. Further, as mentioned earlier, mutations that derange CBL function can also lead to aberrant RTK localization and signaling.

However, the notion that the direct dysregulation of endomembrane trafficking may itself lead to transformation is relatively unexamined. We reason that the oncogenic capability of mutant RAB35 proteins is likely due to dysregulated membrane trafficking of PDGFRα/PI3K signaling machinery, which allows sustained oncogenic signaling. The idea that dysregulation of endomembrane trafficking—in this case by RAB35—could be an oncogenic force is novel and indeed tantalizing. Further, the fact that the majority (5 of 7) of the GTPases that were tertiary hits in our screen were RAB proteins (RAB35, RAB1B, RAB39, RASEF, and RABL3) begs further examination of this idea. If dysregulated endomembrane trafficking possesses tumorigenic capability, it could reveal an entirely new realm of therapeutic targets for combating cancer.

APPENDIX A: Human kinases and GTPases targeted by shRNA screen.

NCBI ID	GENE ID
25	ABL1
27	ABL2
90	ACVR1
91	ACVR1B
92	ACVR2A
93	ACVR2B
94	ACVRL1
132	ADK
156	ADRBK1
157	ADRBK2
203	AK1
204	AK2
205	AK3L1
207	AKT1
208	AKT2
238	ALK
269	AMHR2
369	ARAF
472	ATM
545	ATR
558	AXL
613	BCR
640	BLK
657	BMPR1A
658	BMPR1B
659	BMPR2
660	BMX
673	BRAF
676	BRDT
695	BTK
699	BUB1
701	BUB1B
780	DDR1
801	CALM1
805	CALM2
808	CALM3
814	CAMK4
815	CAMK2A
816	CAMK2B
817	CAMK2D

NCBI ID	GENE ID
818	CAMK2G
914	CD2
983	CDC2
984	CDC2L1
985	CDC2L2
1017	CDK2
1018	CDK3
1019	CDK4
1020	CDK5
1021	CDK6
1022	CDK7
1024	CDK8
1025	CDK9
1111	CHEK1
1119	CHKA
1120	CHKB
1147	CHUK
1152	CKB
1158	CKM
1159	CKMT1B
1160	CKMT2
1163	CKS1B
1164	CKS2
1195	CLK1
1196	CLK2
1198	CLK3
1263	PLK3
1326	MAP3K8
1399	CRKL
1432	MAPK14
1436	CSF1R
1445	CSK
1452	CSNK1A1
1453	CSNK1D
1454	CSNK1E
1455	CSNK1G2
1456	CSNK1G3
1457	CSNK2A1
1459	CSNK2A2
1460	CSNK2B

NCBI ID	GENE ID
1606	DGKA
1607	DGKB
1608	DGKG
1609	DGKQ
1613	DAPK3
1633	DCK
1716	DGUOK
1739	DLG1
1740	DLG2
1741	DLG3
1760	DMPK
1841	DTYMK
1859	DYRK1A
1956	EGFR
1969	EPHA2
2011	MARK2
2041	EPHA1
2042	EPHA3
2043	EPHA4
2044	EPHA5
2045	EPHA7
2046	EPHA8
2047	EPHB1
2048	EPHB2
2049	EPHB3
2050	EPHB4
2051	EPHB6
2064	ERBB2
2065	ERBB3
2066	ERBB4
2081	ERN1
2185	PTK2B
2241	FER
2242	FES
2260	FGFR1
2261	FGFR3
2263	FGFR2
2264	FGFR4
2268	FGR
2321	FLT1

NCBI ID	GENE ID
2322	FLT3
2324	FLT4
2395	FXN
2444	FRK
2475	FRAP1
2534	FYN
2580	GAK
2584	GALK1
2585	GALK2
2645	GCK
2710	GK
2712	GK2
2868	GRK4
2869	GRK5
2870	GRK6
2872	MKNK2
2931	GSK3A
2932	GSK3B
2965	GTF2H1
2984	GUCY2C
2986	GUCY2F
2987	GUK1
3000	GUCY2D
3055	HCK
3098	HK1
3099	HK2
3101	HK3
3480	IGF1R
3551	IKBKB
3611	ILK
3643	INSR
3645	INSRR
3654	IRAK1
3656	IRAK2
3702	ITK
3705	ITPK1
3706	ITPKA
3707	ITPKB
3716	JAK1
3717	JAK2
3718	JAK3
3791	KDR
3795	KHK

NCBI ID	GENE ID
3815	KIT
3932	LCK
3984	LIMK1
3985	LIMK2
4058	LTK
4067	LYN
4117	MAK
4139	MARK1
4140	MARK3
4145	MATK
4214	MAP3K1
4215	MAP3K3
4216	MAP3K4
4217	MAP3K5
4233	MET
4293	MAP3K9
4294	MAP3K10
4296	MAP3K11
4342	MOS
4354	MPP1
4355	MPP2
4356	MPP3
4486	MST1R
4593	MUSK
4598	MVK
4638	MYLK
4750	NEK1
4751	NEK2
4752	NEK3
4830	NME1
4831	NME2
4832	NME3
4833	NME4
4881	NPR1
4882	NPR2
4914	NTRK1
4915	NTRK2
4916	NTRK3
4919	ROR1
4920	ROR2
4921	DDR2
5058	PAK1
5062	PAK2

NCBI ID	GENE ID
5063	PAK3
5105	PCK1
5106	PCK2
5127	PCTK1
5128	PCTK2
5129	PCTK3
5156	PDGFRA
5157	PDGFRL
5159	PDGFRB
5163	PDK1
5164	PDK2
5165	PDK3
5166	PDK4
5170	PDPK1
5207	PFKFB1
5208	PFKFB2
5209	PFKFB3
5210	PFKFB4
5211	PFKL
5213	PFKM
5214	PFKP
5218	PFTK1
5230	PGK1
5232	PGK2
5255	PHKA1
5256	PHKA2
5257	PHKB
5260	PHKG1
5261	PHKG2
5286	PIK3C2A
5287	PIK3C2B
5288	PIK3C2G
5289	PIK3C3
5290	PIK3CA
5291	PIK3CB
5292	PIM1
5293	PIK3CD
5294	PIK3CG
5295	PIK3R1
5296	PIK3R2
5297	PI4KA
5298	PI4KB
5305	PIP4K2A

NCBI ID	GENE ID
5313	PKLR
5315	PKM2
5328	PLAU
5347	PLK1
5361	PLXNA1
5362	PLXNA2
5364	PLXNB1
5365	PLXNB3
5394	EXOSC10
5562	PRKAA1
5563	PRKAA2
5564	PRKAB1
5565	PRKAB2
5566	PRKACA
5567	PRKACB
5568	PRKACG
5571	PRKAG1
5573	PRKAR1A
5575	PRKAR1B
5576	PRKAR2A
5577	PRKAR2B
5578	PRKCA
5579	PRKCB
5580	PRKCD
5581	PRKCE
5582	PRKCG
5583	PRKCH
5584	PRKCI
5585	PKN1
5586	PKN2
5587	PRKD1
5588	PRKCQ
5590	PRKCZ
5591	PRKDC
5592	PRKG1
5593	PRKG2
5594	MAPK1
5595	MAPK3
5596	MAPK4
5597	MAPK6
5598	MAPK7
5599	MAPK8
5600	MAPK11

NCBI ID	GENE ID
5601	MAPK9
5602	MAPK10
5603	MAPK13
5604	MAP2K1
5605	MAP2K2
5606	MAP2K3
5607	MAP2K5
5608	MAP2K6
5609	MAP2K7
5610	EIF2AK2
5613	PRKX
5616	PRKY
5631	PRPS1
5634	PRPS2
5681	PSKH1
5747	PTK2
5753	PTK6
5754	PTK7
5756	TWF1
5832	ALDH18A1
5871	MAP4K2
5891	RAGE
5894	RAF1
5979	RET
5987	TRIM27
6011	GRK1
6041	RNASEL
6046	BRD2
6093	ROCK1
6098	ROS1
6102	RP2
6195	RPS6KA1
6196	RPS6KA2
6197	RPS6KA3
6198	RPS6KB1
6199	RPS6KB2
6259	RYK
6300	MAPK12
6347	CCL2
6351	CCL4
6416	MAP2K4
6446	SGK1
6714	SRC

NCBI ID	GENE ID
6725	SRMS
6732	SRPK1
6733	SRPK2
6787	NEK4
6788	STK3
6789	STK4
6790	AURKA
6792	CDKL5
6793	STK10
6794	STK11
6795	AURKC
6850	SYK
6872	TAF1
6885	MAP3K7
7006	TEC
7010	TEK
7016	TESK1
7046	TGFBR1
7048	TGFBR2
7049	TGFBR3
7075	TIE1
7083	TK1
7084	TK2
7175	TPR
7204	TRIO
7272	TTK
7273	TTN
7294	TXK
7297	TYK2
7301	TYRO3
7371	UCK2
7443	VRK1
7444	VRK2
7465	WEE1
7525	YES1
7535	ZAP70
7786	MAP3K12
7867	MAPKAPK3
8019	BRD3
8295	TRRAP
8317	CDC7
8382	NME5
8394	PIP5K1A

NCBI ID	GENE ID
8395	PIP5K1B
8396	PIP4K2B
8408	ULK1
8428	STK24
8444	DYRK3
8445	DYRK2
8476	CDC42BPA
8491	MAP4K3
8503	PIK3R3
8525	DGKZ
8526	DGKE
8527	DGKD
8536	CAMK1
8550	MAPKAPK5
8558	CDK10
8566	PDXK
8569	MKNK1
8573	CASK
8576	STK16
8621	CDC2L5
8649	MAPKSP1
8711	TNK1
8737	RIPK1
8767	RIPK2
8780	RIOK3
8798	DYRK4
8814	CDKL1
8844	KSR1
8851	CDK5R1
8859	STK19
8877	SPHK1
8895	CPNE3
8899	PRPF4B
8941	CDK5R2
8986	RPS6KA4
8997	KALRN
8999	CDKL2
9020	MAP3K14
9024	BRSK2
9060	PAPSS2
9061	PAPSS1
9064	MAP3K6
9088	PKMYT1

NCBI ID	GENE ID
9113	LATS1
9149	DYRK1B
9162	DGKI
9175	MAP3K13
9201	DCLK1
9212	AURKB
9223	MAGI1
9252	RPS6KA5
9261	MAPKAPK2
9262	STK17B
9263	STK17A
9344	TAOK2
9414	TJP2
9448	MAP4K4
9451	EIF2AK3
9467	SH3BP5
9475	ROCK2
9578	CDC42BPB
9625	AATK
9641	IKBKE
9706	ULK2
9748	SLK
9807	IP6K1
9829	DNAJC6
9833	MELK
9874	TLK1
9891	NUAK1
9942	XYLB
9943	OXSR1
9950	GOLGA5
10000	AKT3
10020	GNE
10087	COL4A3BP
10110	SGK2
10114	HIPK3
10128	LRPPRC
10154	PLXNC1
10188	TNK2
10201	NME6
10221	TRIB1
10290	SPEG
10295	BCKDK
10298	PAK4

NCBI ID	GENE ID
10420	TESK2
10461	MERTK
10494	STK25
10519	CIB1
10595	ERN2
10645	CAMKK2
10654	PMVK
10733	PLK4
10746	MAP3K2
10769	PLK2
10783	NEK6
10922	FASTK
11011	TLK2
11035	RIPK3
11040	PIM2
11113	CIT
11139	
11183	MAP4K5
11184	MAP4K1
11200	CHEK2
11213	IRAK3
11284	PNKP
11329	STK38
11344	TWF2
22848	AAK1
22853	LMTK2
22858	ICK
22868	FASTKD2
22901	ARSG
22928	SEPHS2
22983	MAST1
23012	STK38L
23031	MAST3
23043	TNIK
23049	SMG1
23097	CDC2L6
23129	PLXND1
23139	MAST2
23178	PASK
23227	MAST4
23235	SIK2
23300	ATMIN
23387	

NCBI ID	GENE ID
23396	PIP5K1C
23476	BRD4
23533	PIK3R5
23552	CCRK
23604	DAPK2
23617	TSSK2
23636	NUP62
23654	PLXNB2
23677	SH3BP4
23678	SGK3
23683	PRKD3
23729	SHPK
25778	DSTYK
25865	PRKD2
25989	ULK3
26007	DAK
26289	AK5
26353	HSPB8
26524	LATS2
26576	SRPK3
26750	RPS6KC1
27010	TPK1
27102	EIF2AK1
27148	STK36
27231	ITGB1BP3
27330	RPS6KA6
27347	STK39
28951	TRIB2
28996	HIPK2
29110	TBK1
29904	EEF2K
29922	NME7
29941	PKN3
29959	NRBP1
30811	HUNK
30849	PIK3R4
50488	MINK1
50808	AK3
51086	TNNI3K
51135	IRAK4
51231	VRK3
51265	CDKL3
51314	TXNDC3
51347	TAOK3
51422	PRKAG2
51447	IP6K2
51678	MPP6
51701	NLK
51727	CMPK1
51755	CRKRS
51765	
51776	
53354	PANK1
53632	PRKAG3
53834	FGFRL1
53904	MYO3A
53944	CSNK1G1
54101	RIPK4
54103	PION
54822	TRPM7
54861	SNRK
54899	PXK
54963	UCKL1
54981	C9orf95
54986	ULK4
55224	ETNK2
55229	PANK4
55277	FGGY
55300	PI4K2B
55312	RFK
55351	STK32B
55359	STYK1
55361	PI4K2A
55437	STRADB
55500	ETNK1
55558	PLXNA3
55561	CDC42BPG
55577	NAGK
55589	BMP2K
55681	SCYL2
55728	N4BP2
55750	AGK
55781	RIOK2
55872	PBK
56155	TEX14
56164	STK31
56848	SPHK2
56911	C21orf7
56924	PAK6
56997	CABC1
57118	CAMK1D
57143	ADCK1
57144	PAK7
57147	SCYL3
57172	CAMK1G
57396	CLK4
57410	SCYL1
57538	ALPK3
57551	TAOK1
57729	
57761	TRIB3
57787	MARK4
58538	MPP4
60493	FASTKD5
64080	RBKS
64089	SNX16
64122	FN3K
64149	C17orf75
64398	MPP5
64768	IPPK
64781	CERK
65018	PINK1
65061	PFTK2
65125	WNK1
65220	NADK
65266	WNK4
65267	WNK3
65268	WNK2
65975	STK33
79012	CAMKV
79072	FASTKD3
79646	PANK3
79672	
79675	FASTKD1
79705	LRRK1
79834	
79837	PIP4K2C
79858	NEK11
79877	DCAKD

NCBI ID	GENE ID
79906	MORN1
79934	ADCK4
80025	PANK2
80122	YSK4
80201	HKDC1
80216	ALPK1
80271	ITPKC
80347	COASY
80851	SH3BP5L
81629	TSSK3
81788	NUAK2
83440	ADPGK
83549	UCK1
83694	RPS6KL1
83732	RIOK1
83903	GSG2
83931	STK40
83942	TSSK1B
83983	TSSK6
84033	OBSCN
84197	POMK
84206	MEX3B
84254	CAMKK1
84284	C1orf57
84433	CARD11
84446	BRSK1
84451	
84630	TTBK1
84930	MASTL
85366	MYLK2
85443	DCLK3
85481	PSKH2
89882	TPD52L3
90381	C15orf42
90956	ADCK2
91156	IGFN1
91419	XRCC6BP1
91461	
91584	PLXNA4
91754	NEK9
91807	MYLK3
92335	STRADA
93627	

NCBI ID	GENE ID
112858	TP53RK
114783	LMTK3
114836	SLAMF6
115701	ALPK2
117283	IP6K3
120892	LRRK2
122011	CSNK1A1L
122481	AK7
124923	
127933	UHMK1
130106	CIB4
130399	ACVR1C
131890	GRK7
132158	GLYCTK
136332	LRGUK
138429	PIP5KL1
138474	TAF1L
139189	DGKK
139728	PNCK
140469	MYO3B
140609	NEK7
140803	TRPM6
140901	STK35
143098	MPP7
146057	TTBK2
147746	HIPK4
149420	PDIK1L
150094	SIK1
152110	NEK10
157285	
158067	C9orf98
160851	DGKH
166614	DCLK2
167359	
169436	C9orf96
197258	FUK
197259	MLKL
200576	PIP5K3
202374	STK32A
203054	ADCK5
203447	NRK
204851	HIPK1
220686	

NCBI ID	GENE ID
221823	PRPS1L1
225689	MAPK15
253430	IPMK
255239	ANKK1
256356	GK5
260425	MAGI3
282974	STK32C
283455	KSR2
283629	TSSK4
284086	NEK8
284656	EPHA10
285220	EPHA6
285962	
340156	MYLK4
340371	NRBP2
341676	NEK5
344387	CDKL4
347359	BMP2KL
347736	NME9
374872	C19orf35
375133	PI4KAP2
375298	CERKL
375449	MAST4
378464	MORN2
387851	AK3L2
388228	SBK1
388259	
388957	
389840	MAP3K15
389906	
390877	
391295	
391533	
392226	
392265	
392347	
400301	
402289	
402679	
415116	PIM3
440275	EIF2AK4
440345	
441047	

NCBI ID	GENE ID
441655	
441708	
441777	
441971	
442075	
442313	
442558	
57521	RAPTOR
253260	RICTOR
373	TRIM23
375	ARF1
377	ARF3
378	ARF4
379	ARL4D
381	ARF5
382	ARF6
387	RHOA
388	RHOB
389	RHOC
390	RND3
391	RHOG
399	RHOH
400	ARL1
402	ARL2
403	ARL3
989	39698
998	CDC42
1731	39692
1759	DNM1
1785	DNM2
1819	DRG2
1915	EEF1A1
1917	EEF1A2
1968	EIF2S3
2633	GBP1
2634	GBP2
2635	GBP3
2669	GEM
2767	GNA11
2768	GNA12
2769	GNA15
2770	GNAI1
2771	GNAI2

NCBI ID	GENE ID
2773	GNAI3
2774	GNAL
2775	GNAO1
2776	GNAQ
2778	GNAS
2779	GNAT1
2780	GNAT2
2781	GNAZ
2782	GNB1
2783	GNB2
2784	GNB3
2785	GNG3
2786	GNG4
2787	GNG5
2788	GNG7
2791	GNG11
2792	GNGT1
2793	GNGT2
3265	HRAS
3266	ERAS
3845	KRAS
4218	RAB8A
4261	CIITA
4599	MX1
4600	MX2
4733	DRG1
4735	39693
4893	NRAS
4976	OPA1
5413	39696
5414	39695
5861	RAB1A
5862	RAB2A
5864	RAB3A
5865	RAB3B
5867	RAB4A
5868	RAB5A
5869	RAB5B
5870	RAB6A
5872	RAB13
5873	RAB27A
5874	RAB27B
5878	RAB5C

NCBI ID	GENE ID
5879	RAC1
5880	RAC2
5881	RAC3
5898	RALA
5899	RALB
5901	RAN
5906	RAP1A
5908	RAP1B
5911	RAP2A
5912	RAP2B
6009	RHEB
6014	RIT2
6016	RIT1
6236	RRAD
6237	RRAS
6729	SRP54
6734	SRPR
7284	TUFM
7879	RAB7A
8153	RND2
8766	RAB11A
8934	RAB7L1
9077	DIRAS3
9230	RAB11B
9363	RAB33A
9364	RAB28
9367	RAB9A
9545	RAB3D
9567	GTPBP1
9609	RAB36
9630	GNA14
9886	RHOBTB1
9927	MFN2
10059	DNM1L
10123	ARL4C
10124	ARL4A
10139	ARFRP1
10325	RRAGB
10633	RASL10A
10670	RRAGA
10672	GNA13
10681	GNB5
10801	39700

NCBI ID	GENE ID
10890	RAB10
10966	RAB40B
10981	RAB32
11020	RABL4
11021	RAB35
11031	RAB31
11158	RABL2B
11159	RABL2A
11321	XAB1
22800	RRAS2
22808	MRAS
22931	RAB18
23011	RAB21
23157	39697
23221	RHOBTB2
23433	RHOQ
23551	RASD2
23560	GTPBP4
23682	RAB38
25837	RAB26
26052	DNM3
26164	GTPBP5
26225	ARL5A
26284	ERAL1
27289	RND1
27314	RAB30
28511	NKIRAS2
28512	NKIRAS1
28954	REM1
29984	RHOD
51062	SPG3A
51128	SAR1B
51209	RAB9B
51285	RASL12
51552	RAB14
51560	RAB6B
51655	RASD1
51715	RAB23
51762	RAB8B
51764	GNG13
53916	RAB4B
53917	RAB24
54331	GNG2

NCBI ID	GENE ID
54509	RHOF
54622	ARL15
54676	GTPBP2
54734	RAB39
54769	DIRAS2
55207	ARL8B
55288	RHOT1
55647	RAB20
55669	MFN1
55752	39702
55964	39694
55970	GNG12
56269	IRGC
56681	SAR1A
57111	RAB25
57381	RHOJ
57403	RAB22A
57521	KIAA1303
57580	PREX1
57799	RAB40C
57826	RAP2C
58477	SRPRB
58480	RHOU
58528	RRAGD
59345	GNB4
64121	RRAGC
64223	GBL
64284	RAB17
64792	RABL5
65997	RASL11B
79109	MAPKAP1
79899	FLJ14213
80117	ARL14
81876	RAB1B
83452	RAB33B
83871	RAB34
84084	RAB6C
84100	ARL6
84335	AKT1S1
84705	GTPBP3
84932	RAB2B
85004	RERG
89941	RHOT2

NCBI ID	GENE ID
91608	RASL10B
94235	GNG8
115273	RAB42
115361	GBP4
115362	GBP5
115761	ARL11
115827	RAB3C
116442	RAB39B
116986	CENTG1
116987	CENTG2
116988	CENTG3
121268	RHEBL1
127829	ARL8A
132946	ARL9
142684	RAB40A
148252	DIRAS1
151011	39701
158158	RASEF
161253	REM2
171177	RHOV
200894	ARL13B
221079	ARL5B
285282	RABL3
285598	ARL10
326624	RAB37
338382	RAB7B
339122	RAB43
344988	SAR1P3
347517	RAB41
376267	RAB15
387496	RASL11A
387751	GVIN1
401409	RAB19

APPENDIX B: Non-lethal shRNAs with phospho-AKT Z-scores greater than -/+ 1.50.

NCBI ID	Symbol	TRC Clone Name	mean	%	cell
207	AKT1	NM_005163.x-642s1c1	-2.23	10%	A-431
207	AKT1	NM_005163.x-1044s1c1	-1.52	14%	A-431
207	AKT1	NM_005163.1-1410s1c1	-1.69	48%	A-431
207	AKT1	NM_005163.x-981s1c1	-2.02	17%	A-431
207	AKT1	NM_005163.x-642s1c1d2	-1.55	16%	A431
207	AKT1	NM_005163.x-1044s1c1d1	-1.70	14%	A431
373	TRIM23	NM_001656.3-655s1c1d1	-2.07	37%	Jurkat
373	TRIM23	NM_001656.3-301s1c1d1	-1.67	65%	Jurkat
378	ARF4	NM_001660.2-614s1c1d2	2.55	1%	A549
378	ARF4	NM_001660.2-296s1c1d2	4.14	68%	A549
387	RHOA	NM_001664.1-382s1c1d2	-2.51	16%	A549
387	RHOA	NM_001664.1-616s1c1d2	-2.78	3%	A549
387	RHOA	NM_001664.1-300s1c1d2	-2.67	15%	A549
387	RHOA	NM_001664.1-199s1c1d2	-2.51	5%	A549
388	RHOB	NM_004040.2-839s1c1d2	4.69	5%	A549
388	RHOB	NM_004040.2-452s1c1d2	-1.91	12%	A549
388	RHOB	NM_004040.2-461s1c1d2	-1.80	22%	A549
388	RHOB	NM_004040.2-623s1c1d2	-2.74	65%	A549
389	RHOC	NM_175744.3-539s1c1d3	-1.50	13%	A549
389	RHOC	NM_175744.3-328s1c1d2	-1.77	12%	A549
390	RND3	NM_005168.2-557s1c1d2	-2.61	103%	A549
390	RND3	NM_005168.2-338s1c1d2	-2.61	32%	A549
391	RHOG	NM_001665.2-273s1c1d2	-3.16	#N/A	#N/A
391	RHOG	NM_001665.2-616s1c1d2	-2.47	#N/A	#N/A
391	RHOG	NM_001665.2-192s1c1d2	-1.81	#N/A	#N/A
399	RHOH	NM_004310.2-1177s1c1d2	-2.15	#N/A	#N/A
399	RHOH	NM_004310.2-828s1c1d2	-2.19	#N/A	#N/A
400	ARL1	NM_001177.3-374s1c1d2	-3.57	#N/A	#N/A
400	ARL1	NM_001177.3-190s1c1d2	-2.25	#N/A	#N/A
402	ARL2	NM_001667.1-531s1c1d3	-1.88	54%	A549
402	ARL2	NM_001667.1-182s1c1d3	-2.09	11%	A549
403	ARL3	NM_004311.2-480s1c1d3	-2.65	13%	A549
403	ARL3	NM_004311.2-290s1c1d3	-1.57	3%	A549
472	ATM	NM_000051.2-9211s1c1	-1.81	0%	MCF7
472	ATM	NM_000051.2-9380s1c1	-2.57	0%	MCF7
472	ATM	NM_000051.2-1717s1c1	-1.76	0%	MCF7
472	ATM	NM_000051.2-1974s1c1	-2.39	75%	MCF7
545	ATR	NM_001184.x-3426s1c1	-1.78	33%	A549
640	BLK	NM_001715.x-1031s1c1	-2.41	16%	Jurkat
640	BLK	NM_001715.2-746s1c1	-2.12	30%	Jurkat
640	BLK	NM_001715.2-1626s1c1	-1.66	43%	Jurkat

640	BLK	NM_001715.x-1200s1c1	-2.03	29%	Jurkat
676	BRDT	NM_001726.1-629s1c1	1.98	36%	A549
676	BRDT	NM_001726.2-2905s1c1	2.15	80%	A549
676	BRDT	NM_001726.1-2954s1c1	2.95	36%	A549
780	DDR1	NM_001954.x-961s1c1	2.00	20%	MCF7
780	DDR1	NM_001954.x-3795s1c1	1.64	100%	A549
983	CDC2	NM_001786.x-820s1c1	-1.76	10%	A549
983	CDC2	NM_001786.x-906s1c1	-2.31	52%	A549
983	CDC2	NM_001786.2-748s1c1	-1.92	51%	A549
998	CDC42	NM_001791.2-493s1c1d2	-1.73	73%	A549
998	CDC42	NM_001791.2-328s1c1d2	-2.18	24%	A549
1119	CHKA	NM_001277.1-1557s1c1	1.98	71%	A549
1119	CHKA	NM_001277.1-1136s1c1	2.11	92%	A549
1152	CKB	NM_001823.3-1250s1c1	-2.50	8%	MCF7
1152	CKB	NM_001823.3-877s1c1	-1.70	35%	MCF7
1152	CKB	NM_001823.3-722s1c1	-2.70	34%	MCF7
1152	CKB	NM_001823.3-326s1c1	-1.68	60%	MCF7
1152	CKB	NM_001823.3-1251s1c1	-1.80	20%	MCF7
1453	CSNK1D	NM_139062.x-991s1c1	2.52	74%	A549
1453	CSNK1D	NM_139062.x-1027s1c1	2.11	85%	A549
1453	CSNK1D	NM_001893.x-991s1c1	2.57	58%	A549
1453	CSNK1D	NM_001893.x-1027s1c1	3.61	69%	A549
1606	DGKA	NM_001345.4-592s1c1	2.41	22%	Jurkat
1606	DGKA	NM_001345.4-382s1c1	2.52	42%	Jurkat
1633	DCK	NM_000788.x-252s1c1	-2.09	113%	MCF7
1633	DCK	NM_000788.x-440s1c1	-1.60	0%	MCF7
1915	EEF1A1	NM_001402.4-807s1c1d1	-1.76	2%	A549
1915	EEF1A1	NM_001402.4-338s1c1d1	-2.53	4%	A549
1968	EIF2S3	NM_001415.2-1225s1c1d1	-4.87	136%	A549
1968	EIF2S3	NM_001415.2-646s1c1d1	-1.85	11%	A549
1968	EIF2S3	NM_001415.2-782s1c1d1	-2.28	45%	A549
2041	EPHA1	NM_005232.2-3118s1c1	-1.94	8%	MCF7
2041	EPHA1	NM_005232.2-2176s1c1	-2.01	61%	MCF7
2049	EPHB3	NM_004443.3-3611s1c1	2.14	43%	MCF7
2049	EPHB3	NM_004443.3-1895s1c1	1.58	46%	MCF7
2050	EPHB4	NM_004444.x-459s1c1	-1.76	27%	A549
2050	EPHB4	NM_004444.x-2076s1c1	-1.55	8%	A549
2064	ERBB2	NM_004448.x-1214s1c1	-2.37	0%	A-431
2064	ERBB2	NM_004448.x-1365s1c1	-2.23	37%	A-431
2064	ERBB2	NM_004448.1-466s1c1	-1.78	135%	A549
2260	FGFR1	NM_000604.2-2340s1c1	1.99	56%	MCF7
2260	FGFR1	NM_000604.2-1013s1c1	1.67	121%	MCF7
2260	FGFR1	NM_000604.2-1237s1c1	1.77	38%	MCF7
2321	FLT1	NM_002019.2-5483s1c1	-2.57	#N/A	#N/A

2321	FLT1	NM_002019.2-4063s1c1	-2.92	#N/A	#N/A
2321	FLT1	NM_002019.2-654s1c1	-2.56	#N/A	#N/A
2321	FLT1	NM_002019.x-2722s1c1	2.94	133%	MCF7
2321	FLT1	NM_002019.2-3492s1c1	-3.01	#N/A	#N/A
2321	FLT1	NM_002019.x-1340s1c1	1.91	47%	MCF7
2321	FLT1	NM_002019.x-5356s1c1	1.58	2203%	MCF7
2324	FLT4	NM_002020.x-3875s1c1	1.54	28%	A549
2324	FLT4	NM_002020.x-2503s1c1	-1.70	71%	A549
2324	FLT4	NM_002020.1-3989s1c1	1.57	81%	MCF7
2444	FRK	NM_002031.x-1177s1c1	1.55	0%	A549
2444	FRK	NM_002031.x-1620s1c1	2.68	270%	A549
2475	FRAP1	NM_004958.2-640s1c1	1.72	14%	A549
2475	FRAP1	NM_004958.2-7897s1c1	2.56	21%	A549
2475	FRAP1	NM_004958.2-4662s1c1	2.21	21%	A549
2475	FRAP1	NM_004958.2-3425s1c1	2.73	35%	A549
2475	FRAP1	NM_004958.2-3425s1c1d2	2.54	25%	Jurkat
2710	GK	NM_000167.3-3396s1c1	-1.95	74%	293T
2710	GK	NM_000167.3-814s1c1	-1.64	40%	293T
2770	GNAI1	NM_002069.4-1208s1c1d1	-1.69	#N/A	#N/A
2771	GNAI2	NM_002070.1-870s1c1d1	-1.83	28%	#N/A
2785	GNG3	NM_012202.1-326s1c1d1	1.86	#N/A	#N/A
2785	GNG3	NM_012202.1-288s1c1d1	2.31	#N/A	#N/A
2791	GNG11	NM_004126.2-502s1c1d1	2.49	47%	A549
2791	GNG11	NM_004126.2-437s1c1d1	2.73	32%	A549
2870	GRK6	NM_002082.2-1407s1c1	1.70	52%	Jurkat
2870	GRK6	NM_002082.x-545s1c1	1.87	6%	MCF7
2870	GRK6	NM_002082.2-2152s1c1	1.73	56%	Jurkat
2931	GSK3A	NM_019884.1-1173s1c1	-2.44	9%	MCF7
2931	GSK3A	NM_019884.x-1428s1c1	-2.10	0%	MCF7
2965	GTF2H1	NM_005316.2-1316s1c1	-2.98	40%	MCF7
2965	GTF2H1	NM_005316.2-1755s1c1	-1.78	25%	MCF7
2965	GTF2H1	NM_005316.2-1228s1c1	2.01	38%	MCF7
2965	GTF2H1	NM_005316.2-2502s1c1	3.33	91%	MCF7
2984	GUCY2C	NM_004963.x-3280s1c1	1.87	#N/A	#N/A
2984	GUCY2C	NM_004963.1-2425s1c1	2.66	#N/A	#N/A
2984	GUCY2C	NM_004963.1-1244s1c1	1.68	#N/A	#N/A
3101	HK3	NM_002115.1-1748s1c1	-1.57	#N/A	#N/A
3101	HK3	NM_002115.1-2902s1c1	-1.56	#N/A	#N/A
3101	HK3	NM_002115.1-932s1c1	-1.77	#N/A	#N/A
3611	ILK	NM_004517.2-1136s1c1	-2.55	59%	A549
3611	ILK	NM_004517.x-687s1c1	-1.71	22%	A549
3654	IRAK1	NM_001569.3-2873s1c1	-1.69	18%	MCF7
3654	IRAK1	NM_001569.x-1257s1c1	-1.66	115%	MCF7
3706	ITPKA	NM_002220.1-539s1c1	-2.37	#N/A	#N/A

3706	ITPKA	NM_002220.1-1420s1c1	-1.94	#N/A	#N/A
3706	ITPKA	NM_002220.1-783s1c1	-2.10	#N/A	#N/A
3706	ITPKA	NM_002220.1-808s1c1	1.97	#N/A	#N/A
3706	ITPKA	NM_002220.1-1076s1c1	3.36	#N/A	#N/A
3706	ITPKA	NM_002220.1-368s1c1	3.37	#N/A	#N/A
3717	JAK2	NM_004972.2-3669s1c1	1.66	#N/A	#N/A
3717	JAK2	NM_004972.x-4564s1c1	3.73	23%	A549
3717	JAK2	NM_004972.2-4773s1c1	1.98	#N/A	#N/A
3795	KHK	NM_000221.1-359s1c1	-2.19	#N/A	#N/A
3795	KHK	NM_000221.1-1328s1c1	-2.83	#N/A	#N/A
3795	KHK	NM_000221.1-458s1c1	-3.11	#N/A	#N/A
3984	LIMK1	NM_002314.x-1512s1c1	-2.04	5%	MCF7
3984	LIMK1	NM_002314.x-1374s1c1	-1.78	3%	MCF7
4058	LTK	NM_002344.x-2132s1c1	-2.46	0%	A549
4058	LTK	NM_002344.x-1509s1c1	-2.00	69%	A549
4058	LTK	NM_002344.x-593s1c1	-1.88	99%	A549
4117	MAK	NM_005906.x-982s1c1	2.78	#N/A	#N/A
4117	MAK	NM_005906.x-2562s1c1	4.33	#N/A	#N/A
4139	MARK1	NM_018650.2-1916s1c1	-1.83	86%	A549
4139	MARK1	NM_018650.2-2586s1c1	-1.58	86%	A549
4139	MARK1	NM_018650.2-2974s1c1	4.07	117%	A549
4139	MARK1	NM_018650.2-1564s1c1	1.59	99%	A549
4140	MARK3	NM_002376.x-518s1c1	-2.69	36%	MCF7
4140	MARK3	NM_002376.x-1363s1c1	-2.47	59%	MCF7
4214	MAP3K1	XM_042066.8-5517s1c1	1.73	173%	A549
4214	MAP3K1	XM_042066.11-7305s1c1	1.53	49%	A549
4294	MAP3K10	NM_002446.x-3247s1c1	-3.27	84%	MCF7
4294	MAP3K10	NM_002446.x-1420s1c1	-2.37	83%	MCF7
4294	MAP3K10	NM_002446.2-1329s1c1	-2.30	#N/A	#N/A
4294	MAP3K10	NM_002446.x-2033s1c1	-1.54	94%	MCF7
4354	MPP1	NM_002436.2-1286s1c1	-3.06	26%	A549
4354	MPP1	NM_002436.2-1216s1c1	-1.73	24%	A549
4355	MPP2	NM_005374.2-178s1c1	1.95	46%	Jurkat
4355	MPP2	NM_005374.2-755s1c1	2.84	57%	Jurkat
4486	MST1R	NM_002447.x-4136s1c1	-3.05	58%	A549
4486	MST1R	NM_002447.1-2829s1c1	-2.00	57%	A549
4486	MST1R	NM_002447.1-2397s1c1	-2.14	20%	A549
4733	DRG1	NM_004147.2-665s1c1d1	1.51	18%	A549
4733	DRG1	NM_004147.2-514s1c1d1	1.89	10%	A549
4750	NEK1	NM_012224.1-1427s1c1	1.52	71%	Jurkat
4750	NEK1	NM_012224.1-2206s1c1	2.59	92%	Jurkat
4750	NEK1	NM_012224.1-2620s1c1	1.55	89%	Jurkat
4832	NME3	NM_002513.2-310s1c1	-1.88	11%	293T
4832	NME3	NM_002513.2-414s1c1	-2.96	15%	293T

4976	OPA1	NM_130832.1-435s1c1d1	-4.29	55%	A549
4976	OPA1	NM_130832.1-434s1c1d1	-2.45	12%	A549
5062	PAK2	NM_002577.x-2531s1c1	2.20	9%	MCF7
5062	PAK2	NM_002577.3-1555s1c1	2.63	7%	MCF7
5062	PAK2	NM_002577.x-454s1c1	2.70	15%	MCF7
5062	PAK2	NM_002577.3-4034s1c1	2.77	96%	MCF7
5165	PDK3	NM_005391.1-1322s1c1	-2.02	83%	A549
5165	PDK3	NM_005391.1-440s1c1	-1.96	16%	A549
5165	PDK3	NM_005391.1-1354s1c1	-1.60	106%	A549
5170	PDPK1	NM_002613.1-1373s1c1	-1.88	86%	MCF7
5170	PDPK1	NM_002613.1-542s1c1	-2.46	118%	MCF7
5170	PDPK1	NM_002613.x-1306s1c1	-1.57	110%	MCF7
5211	PFKL	NM_002626.x-1630s1c1	-2.08	10%	A549
5211	PFKL	NM_002626.4-2301s1c1	-1.69	11%	A549
5211	PFKL	NM_002626.4-2309s1c1	-1.69	0%	A549
5213	PFKM	NM_000289.3-1883s1c1	-1.52	35%	MCF7
5213	PFKM	NM_000289.3-429s1c1	-2.57	16%	MCF7
5213	PFKM	NM_000289.3-1708s1c1	-1.71	#N/A	#N/A
5213	PFKM	NM_000289.3-1571s1c1	-3.01	#N/A	#N/A
5291	PIK3CB	NM_006219.x-61s1c1	-1.63	40%	MCF7
5291	PIK3CB	NM_006219.x-2289s1c1	-1.60	25%	MCF7
5291	PIK3CB	NM_006219.x-748s1c1	-1.56	55%	MCF7
5291	PIK3CB	NM_006219.x-1306s1c1	-1.57	29%	MCF7
5291	PIK3CB	NM_006219.x-61s1c1d2	-1.74	40%	MCF7
5291	PIK3CB	NM_006219.x-748s1c1d1	-1.89	56%	MCF7
5347	PLK1	NM_005030.3-1986s1c1	-1.50	48%	MCF7
5347	PLK1	NM_005030.3-1374s1c1	-1.93	35%	MCF7
5347	PLK1	NM_005030.3-1893s1c1	-2.01	25%	MCF7
5347	PLK1	NM_005030.3-1361s1c1	-1.89	0%	MCF7
5361	PLXNA1	NM_032242.2-4255s1c1	2.36	31%	A549
5361	PLXNA1	NM_032242.2-4656s1c1	2.82	38%	A549
5364	PLXNB1	NM_002673.3-6053s1c1	-2.85	43%	Jurkat
5364	PLXNB1	NM_002673.3-1116s1c1	-1.91	66%	Jurkat
5394	EXOSC10	NM_002685.1-1833s1c1	-1.87	24%	A549
5394	EXOSC10	NM_002685.1-1274s1c1	-3.51	7%	A549
5394	EXOSC10	NM_002685.1-2560s1c1	-1.64	25%	A549
5563	PRKAA2	NM_006252.x-2127s1c1	-2.05	#N/A	#N/A
5563	PRKAA2	NM_006252.x-1028s1c1	-2.37	#N/A	#N/A
5575	PRKAR1B	NM_002735.1-157s1c1	3.79	#N/A	#N/A
5575	PRKAR1B	NM_002735.1-593s1c1	2.77	8%	MCF7
5575	PRKAR1B	NM_002735.1-544s1c1	4.01	61%	MCF7
5575	PRKAR1B	NM_002735.1-620s1c1	3.24	7%	MCF7
5580	PRKCD	NM_006254.3-2389s1c1	-2.77	102%	MCF7
5580	PRKCD	NM_006254.x-826s1c1	-2.55	56%	A549

5580	PRKCD	NM_006254.3-1145s1c1	-1.74	57%	MCF7
5586	PKN2	NM_006256.1-2250s1c1	-2.06	39%	A549
5586	PKN2	NM_006256.1-309s1c1	-2.26	28%	A549
5608	MAP2K6	NM_002758.x-592s1c1	1.89	77%	MCF7
5608	MAP2K6	NM_002758.x-503s1c1	1.61	191%	MCF7
5631	PRPS1	NM_002764.x-592s1c1	1.70	42%	MCF7
5631	PRPS1	NM_002764.x-819s1c1	2.05	0%	MCF7
5634	PRPS2	NM_002765.x-871s1c1	1.81	16%	MCF7
5634	PRPS2	NM_002765.x-320s1c1	1.96	13%	MCF7
5832	ALDH18A1	NM_002860.2-568s1c1	-2.13	44%	A549
5832	ALDH18A1	NM_002860.2-658s1c1	-2.59	8%	A549
5861	RAB1A	NM_004161.3-698s1c1d1	-3.70	9%	A549
5861	RAB1A	NM_004161.3-1607s1c1d1	-2.02	57%	A549
5862	RAB2A	NM_002865.1-523s1c1d1	-2.40	143%	A549
5864	RAB3A	NM_002866.3-266s1c1d4	-2.11	161%	Jurkat
5864	RAB3A	NM_002866.3-447s1c1d2	-1.67	132%	Jurkat
5865	RAB3B	NM_002867.x-907s1c1d1	-1.54	6%	A549
5865	RAB3B	NM_002867.x-447s1c1d1	-2.71	8%	A549
5865	RAB3B	NM_002867.x-446s1c1d1	-2.98	5%	A549
5867	RAB4A	NM_004578.2-500s1c1d1	-3.32	71%	Jurkat
5867	RAB4A	NM_004578.2-608s1c1d1	-2.33	69%	Jurkat
5867	RAB4A	NM_004578.2-346s1c1d3	-2.10	56%	Jurkat
5868	RAB5A	NM_004162.3-659s1c1d1	-3.94	46%	#N/A
5868	RAB5A	NM_004162.3-2139s1c1d3	-1.86	16%	#N/A
5868	RAB5A	NM_004162.3-406s1c1d1	-1.53	69%	#N/A
5870	RAB6A	NM_002869.4-824s1c1d3	1.97	103%	Jurkat
5870	RAB6A	NM_002869.4-1073s1c1d3	2.07	42%	Jurkat
5872	RAB13	NM_002870.2-336s1c1d2	-3.60	#N/A	#N/A
5872	RAB13	NM_002870.2-196s1c1d2	-2.18	#N/A	#N/A
5873	RAB27A	NM_004580.3-735s1c1d2	-1.72	5%	A549
5873	RAB27A	NM_004580.3-477s1c1d2	-2.09	25%	A549
5874	RAB27B	NM_004163.3-697s1c1d2	-2.83	24%	A549
5874	RAB27B	NM_004163.3-217s1c1d2	-1.61	72%	A549
5874	RAB27B	NM_004163.3-566s1c1d2	-2.18	133%	A549
5881	RAC3	NM_005052.2-544s1c1d2	-2.77	17%	293T
5881	RAC3	NM_005052.2-664s1c1d2	-3.31	20%	293T
5881	RAC3	NM_005052.2-331s1c1d2	-2.78	14%	293T
6009	RHEB	NM_005614.x-624s1c1d2	2.48	#N/A	#N/A
6009	RHEB	NM_005614.x-754s1c1d2	2.57	#N/A	#N/A
6009	RHEB	NM_005614.2-1100s1c1d2	2.28	#N/A	#N/A
6011	GRK1	NM_002929.x-388s1c1	2.79	#N/A	#N/A
6011	GRK1	NM_002929.x-945s1c1	1.73	#N/A	#N/A
6011	GRK1	NM_002929.2-1682s1c1	2.82	#N/A	#N/A
6011	GRK1	NM_002929.2-463s1c1	1.61	#N/A	#N/A

6046	BRD2	NM_005104.2-2401s1c1	-2.12	40%	293T
6046	BRD2	NM_005104.2-2059s1c1	-2.57	21%	293T
6729	SRP54	NM_003136.2-1839s1c1d1	-2.80	25%	A549
6729	SRP54	NM_003136.2-1903s1c1d1	-2.61	22%	A549
6729	SRP54	NM_003136.2-849s1c1d1	-2.71	15%	A549
6733	SRPK2	NM_003138.1-749s1c1	-1.79	9%	MCF7
6733	SRPK2	NM_003138.1-2730s1c1	-1.61	3%	MCF7
6734	SRPR	NM_003139.2-202s1c1d1	-4.08	4%	A549
6734	SRPR	NM_003139.2-1086s1c1d1	-1.86	5%	A549
7083	TK1	NM_003258.x-530s1c1	-1.74	14%	A549
7083	TK1	NM_003258.x-610s1c1	-1.94	11%	A549
7083	TK1	NM_003258.x-327s1c1	-1.51	3%	A549
7284	TUFM	NM_003321.3-1266s1c1d1	-1.71	2%	A549
7284	TUFM	NM_003321.3-668s1c1d1	-2.68	5%	A549
7297	TYK2	NM_003331.x-3209s1c1	-2.87	13%	A549
7297	TYK2	NM_003331.x-4078s1c1	-2.54	15%	A549
7879	RAB7A	NM_004637.5-347s1c1d1	-1.96	151%	Jurkat
7879	RAB7A	NM_004637.5-781s1c1d1	-2.40	41%	Jurkat
8153	RND2	NM_005440.2-244s1c1d3	-2.11	#N/A	#N/A
8153	RND2	NM_005440.2-189s1c1d2	-2.77	#N/A	#N/A
8153	RND2	NM_005440.2-286s1c1d3	-2.16	#N/A	#N/A
8476	CDC42BPA	NM_014826.x-2749s1c1	2.49	3%	A549
8476	CDC42BPA	NM_014826.x-4292s1c1	1.55	44%	A549
8476	CDC42BPA	NM_003607.x-4535s1c1	2.58	6%	A549
8476	CDC42BPA	NM_003607.x-2992s1c1	2.33	5%	A549
8503	PIK3R3	NM_003629.2-752s1c1d1	3.29	#N/A	#N/A
8503	PIK3R3	NM_003629.2-1826s1c1d1	2.82	#N/A	#N/A
8503	PIK3R3	NM_003629.2-1543s1c1d1	5.15	#N/A	#N/A
8503	PIK3R3	NM_003629.2-3516s1c1	1.56	#N/A	#N/A
8503	PIK3R3	NM_003629.2-1826s1c1	2.56	#N/A	#N/A
8503	PIK3R3	NM_003629.2-1126s1c1	1.95	#N/A	#N/A
8526	DGKE	NM_003647.1-853s1c1	-1.70	20%	MCF7
8526	DGKE	NM_003647.1-952s1c1	-1.54	5%	MCF7
8527	DGKD	NM_003648.x-1118s1c1	-1.82	42%	Jurkat
8527	DGKD	NM_003648.2-2201s1c1	-1.96	81%	Jurkat
8527	DGKD	NM_003648.x-1812s1c1	-1.95	40%	Jurkat
8527	DGKD	NM_003648.x-350s1c1	-1.56	56%	Jurkat
8566	PDXK	NM_003681.x-889s1c1	-1.81	112%	A549
8566	PDXK	NM_003681.x-684s1c1	-1.73	9%	A549
8649	MAPKSP1	NM_021970.2-415s1c1	2.44	40%	A-431
8649	MAPKSP1	NM_021970.2-577s1c1	2.44	69%	A-431
8766	RAB11A	NM_004663.3-209s1c1d1	-2.46	#N/A	#N/A
8766	RAB11A	NM_004663.3-387s1c1d1	-1.52	#N/A	#N/A
8798	DYRK4	NM_003845.1-1163s1c1	-1.99	21%	Jurkat

8798	DYRK4	NM_003845.1-1342s1c1	-2.22	37%	Jurkat
8798	DYRK4	NM_003845.1-814s1c1	-1.84	76%	Jurkat
8798	DYRK4	NM_003845.x-1755s1c1	-1.81	94%	Jurkat
8877	SPHK1	NM_182965.1-1640s1c1	-2.43	36%	293T
8877	SPHK1	NM_182965.1-1116s1c1	-1.68	21%	293T
8877	SPHK1	NM_182965.1-1063s1c1	-3.09	13%	293T
8934	RAB7L1	NM_003929.1-533s1c1d2	-2.70	157%	A549
8934	RAB7L1	NM_003929.1-307s1c1d2	-1.66	33%	A549
9060	PAPSS2	NM_004670.2-177s1c1	-1.83	11%	MCF7
9060	PAPSS2	NM_004670.2-1768s1c1	-1.58	7%	MCF7
9064	MAP3K6	NM_004672.3-2887s1c1	-1.61	#N/A	#N/A
9064	MAP3K6	NM_004672.x-3795s1c1	-2.40	24%	A549
9064	MAP3K6	NM_004672.3-4159s1c1	-1.84	#N/A	#N/A
9064	MAP3K6	NM_004672.3-3541s1c1	-1.64	#N/A	#N/A
9223	MAGI1	NM_004742.2-5513s1c1	1.99	91%	A549
9223	MAGI1	NM_004742.2-1636s1c1	2.34	76%	A549
9230	RAB11B	NM_004218.1-288s1c1d1	-2.40	#N/A	#N/A
9230	RAB11B	NM_004218.1-469s1c1d1	-2.75	#N/A	#N/A
9263	STK17A	NM_004760.x-1998s1c1	-1.55	65%	A549
9263	STK17A	NM_004760.x-854s1c1	-2.64	150%	A549
9363	RAB33A	NM_004794.2-630s1c1d2	-3.23	20%	Jurkat
9363	RAB33A	NM_004794.2-778s1c1d2	-2.14	89%	Jurkat
9363	RAB33A	NM_004794.2-749s1c1d2	-2.79	55%	Jurkat
9364	RAB28	NM_004249.1-265s1c1d2	-2.74	#N/A	#N/A
9364	RAB28	NM_004249.1-75s1c1d2	-2.85	#N/A	#N/A
9545	RAB3D	NM_004283.2-296s1c1d2	-2.10	#N/A	#N/A
9545	RAB3D	NM_004283.2-745s1c1d2	-1.67	#N/A	#N/A
9567	GTPBP1	NM_004286.3-884s1c1d2	-4.45	23%	293T
9567	GTPBP1	NM_004286.3-1015s1c1d2	-1.90	31%	293T
9567	GTPBP1	NM_004286.3-362s1c1d2	-1.92	61%	293T
9641	IKBKE	NM_014002.x-941s1c1	-2.06	40%	MCF7
9641	IKBKE	NM_014002.x-1628s1c1	-2.32	62%	MCF7
9829	DNAJC6	NM_014787.x-355s1c1	-3.04	56%	Jurkat
9829	DNAJC6	NM_014787.x-2453s1c1	-2.01	26%	Jurkat
9891	NUAK1	NM_014840.x-2796s1c1	-2.20	0%	A549
9891	NUAK1	NM_014840.x-1712s1c1	-1.67	56%	A549
9943	OXSR1	NM_005109.x-551s1c1	2.16	#N/A	#N/A
9943	OXSR1	NM_005109.x-1189s1c1	1.52	#N/A	#N/A
9943	OXSR1	NM_005109.x-1969s1c1	2.54	#N/A	#N/A
10000	AKT3	NM_005465.x-569s1c1	-1.82	21%	A549
10000	AKT3	NM_005465.x-770s1c1	-3.04	33%	A549
10000	AKT3	NM_005465.x-1757s1c1	-1.83	47%	A549
10000	AKT3	NM_005465.x-1307s1c1	-1.57	58%	A549
10139	ARFRP1	NM_003224.2-265s1c1d2	4.15	66%	A549

10139	ARFRP1	NM_003224.2-571s1c1d2	3.86	27%	A549
10154	PLXNC1	NM_005761.1-3289s1c1	-2.25	31%	Jurkat
10154	PLXNC1	NM_005761.1-1236s1c1	-2.26	32%	Jurkat
10221	TRIB1	NM_025195.x-1691s1c1	2.66	95%	A549
10221	TRIB1	NM_025195.x-641s1c1	1.67	60%	A549
10519	CIB1	NM_006384.2-504s1c1	-2.80	7%	A549
10519	CIB1	NM_006384.2-376s1c1	-2.04	31%	A549
10783	NEK6	NM_014397.x-445s1c1	-2.40	3%	MCF7
10783	NEK6	NM_014397.x-484s1c1	-2.11	22%	MCF7
10890	RAB10	NM_016131.2-997s1c1d1	-3.78	#N/A	#N/A
10890	RAB10	NM_016131.2-874s1c1d1	-2.49	#N/A	#N/A
10966	RAB40B	NM_006822.1-513s1c1d2	-3.48	40%	A549
10966	RAB40B	NM_006822.1-354s1c1d1	-2.30	7%	A549
10966	RAB40B	NM_006822.1-243s1c1d1	-2.99	53%	A549
11020	RABL4	NM_006860.2-605s1c1d2	-2.14	#N/A	#N/A
11020	RABL4	NM_006860.2-527s1c1d2	-2.69	#N/A	#N/A
11021	RAB35	NM_006861.4-486s1c1d2	-3.27	27%	A549
11021	RAB35	NM_006861.4-451s1c1d2	-3.67	64%	A549
11021	RAB35	NM_006861.4-207s1c1d2	-2.58	19%	A549
11021	RAB35	NM_006861.4-709s1c1d2	-3.93	37%	A549
11035	RIPK3	NM_006871.x-1280s1c1	-3.02	98%	Jurkat
11035	RIPK3	NM_006871.x-612s1c1	-1.59	104%	Jurkat
11158	RABL2B	NM_001003789.1-319s1c1d2	-2.18	#N/A	#N/A
11158	RABL2B	NM_001003789.1-270s1c1d2	-2.83	#N/A	#N/A
11158	RABL2B	NM_001003789.1-418s1c1d2	-3.69	#N/A	#N/A
11158	RABL2B	NM_001003789.1-625s1c1d2	-2.37	#N/A	#N/A
11159	RABL2A	NM_007082.2-312s1c1d2	-1.55	#N/A	#N/A
11159	RABL2A	NM_007082.2-190s1c1d2	-2.63	#N/A	#N/A
11159	RABL2A	NM_007082.2-705s1c1d1	-2.76	#N/A	#N/A
11200	CHEK2	NM_007194.x-2219s1c1	-1.67	110%	A549
11200	CHEK2	NM_007194.x-2394s1c1	-1.70	49%	A549
11321	XAB1	NM_007266.1-835s1c1d2	2.33	4%	A549
11321	XAB1	NM_007266.1-220s1c1d2	2.73	18%	A549
11344	TWF2	NM_007284.3-522s1c1	-2.09	22%	A549
11344	TWF2	NM_007284.3-610s1c1	-1.50	9%	A549
23227	MAST4	XM_291141.3-2703s1c1	-1.95	#N/A	#N/A
23227	MAST4	XM_291141.3-4700s1c1	-2.33	#N/A	#N/A
23433	RHOQ	NM_012249.1-96s1c1d1	-3.06	#N/A	#N/A
23433	RHOQ	NM_012249.1-385s1c1d1	-2.69	#N/A	#N/A
23560	GTPBP4	NM_012341.1-114s1c1d2	-3.01	#N/A	#N/A
23560	GTPBP4	NM_012341.1-485s1c1d2	-1.51	#N/A	#N/A
23636	NUP62	NM_012346.3-302s1c1	-3.18	50%	Jurkat
23636	NUP62	NM_012346.3-925s1c1	-2.62	110%	Jurkat
23636	NUP62	NM_012346.3-533s1c1	-1.97	87%	Jurkat

23729	SHPK	NM_013276.2-3662s1c1	-2.00	85%	Jurkat
23729	SHPK	NM_013276.2-1334s1c1	-1.92	50%	Jurkat
23729	SHPK	NM_013276.2-558s1c1	-1.85	18%	Jurkat
25837	RAB26	NM_014353.4-721s1c1d2	-4.06	40%	A549
25837	RAB26	NM_014353.4-512s1c1d2	-2.21	48%	A549
26007	DAK	NM_015533.2-1015s1c1	-1.70	10%	A549
26007	DAK	NM_015533.2-1597s1c1	-1.51	0%	A549
26164	GTPBP5	NM_015666.2-372s1c1d2	-3.99	#N/A	#N/A
26164	GTPBP5	NM_015666.2-747s1c1d2	-1.77	#N/A	#N/A
26164	GTPBP5	NM_015666.2-1174s1c1d2	-2.10	#N/A	#N/A
26164	GTPBP5	NM_015666.2-1250s1c1d2	-2.00	#N/A	#N/A
26225	ARL5A	NM_177985.1-335s1c1d1	1.95	#N/A	#N/A
26225	ARL5A	NM_177985.1-556s1c1d1	3.44	#N/A	#N/A
26284	ERAL1	NM_005702.1-539s1c1d1	-2.37	#N/A	#N/A
26284	ERAL1	NM_005702.1-1693s1c1d1	-1.59	#N/A	#N/A
27289	RND1	NM_014470.2-741s1c1d2	-2.73	#N/A	#N/A
27289	RND1	NM_014470.2-285s1c1d2	-1.86	#N/A	#N/A
27289	RND1	NM_014470.2-424s1c1d2	-2.72	#N/A	#N/A
27314	RAB30	NM_014488.3-341s1c1d2	-2.92	26%	Jurkat
27314	RAB30	NM_014488.3-571s1c1d2	-3.07	240%	Jurkat
28996	HIPK2	NM_022740.x-1389s1c1	-1.86	104%	A549
28996	HIPK2	NM_022740.x-1940s1c1	-1.63	227%	A549
28996	HIPK2	NM_022740.x-3587s1c1	-1.53	51%	A549
29110	TBK1	NM_013254.x-1212s1c1	-2.46	35%	A549
29110	TBK1	NM_013254.x-1536s1c1	-1.75	33%	A549
29110	TBK1	NM_013254.x-1773s1c1	-1.98	74%	A549
29904	EEF2K	NM_013302.2-281s1c1	-3.44	74%	Jurkat
29904	EEF2K	NM_013302.2-1449s1c1	-3.78	136%	Jurkat
51128	SAR1B	NM_016103.2-267s1c1d2	-3.50	9%	A549
51128	SAR1B	NM_016103.2-569s1c1d2	-1.95	8%	A549
51135	IRAK4	NM_016123.x-2142s1c1	1.64	71%	A549
51135	IRAK4	NM_016123.x-374s1c1	1.88	29%	A549
51135	IRAK4	NM_016123.x-197s1c1	2.81	53%	A549
51135	IRAK4	NM_016123.x-820s1c1	1.53	10%	A549
51209	RAB9B	NM_016370.1-444s1c1d2	-3.12	79%	Jurkat
51209	RAB9B	NM_016370.1-361s1c1d2	-1.83	63%	Jurkat
51231	VRK3	NM_016440.x-354s1c1	1.74	149%	MCF7
51231	VRK3	NM_016440.x-209s1c1	1.70	11%	MCF7
51285	RASL12	NM_016563.2-1552s1c1d1	2.76	#N/A	#N/A
51285	RASL12	NM_016563.2-341s1c1d1	1.58	#N/A	#N/A
51552	RAB14	NM_016322.2-304s1c1d1	1.50	21%	Jurkat
51552	RAB14	NM_016322.2-505s1c1d1	2.84	55%	Jurkat
51678	MPP6	NM_016447.x-528s1c1	-1.89	14%	A549
51678	MPP6	NM_016447.x-527s1c1	-1.57	27%	A549

51701	NLK	NM_016231.2-2245s1c1	-2.56	#N/A	#N/A
51701	NLK	NM_016231.2-3634s1c1	-3.95	#N/A	#N/A
51701	NLK	NM_016231.x-1422s1c1	-3.18	60%	A549
51701	NLK	NM_016231.x-2413s1c1	-2.86	38%	A549
51715	RAB23	NM_016277.3-1262s1c1d2	-1.96	#N/A	#N/A
51715	RAB23	NM_016277.3-762s1c1d2	-1.69	#N/A	#N/A
53632	PRKAG3	NM_017431.2-1075s1c1	1.56	#N/A	#N/A
53632	PRKAG3	NM_017431.1-564s1c1	2.05	#N/A	#N/A
53632	PRKAG3	NM_017431.2-183s1c1	2.52	#N/A	#N/A
53632	PRKAG3	NM_017431.1-156s1c1	1.92	#N/A	#N/A
53834	FGFRL1	NM_001004356.1-2412s1c1	-2.87	136%	Jurkat
53834	FGFRL1	NM_001004356.1-1103s1c1	-2.25	29%	Jurkat
54509	RHOF	NM_019034.2-565s1c1d2	-3.14	#N/A	#N/A
54509	RHOF	NM_019034.2-376s1c1d2	-2.90	#N/A	#N/A
54676	GTPBP2	NM_019096.3-1522s1c1d2	-2.27	#N/A	#N/A
54676	GTPBP2	NM_019096.3-464s1c1d2	-1.74	#N/A	#N/A
54676	GTPBP2	NM_019096.3-1308s1c1d2	-4.43	#N/A	#N/A
54734	RAB39	NM_017516.1-1624s1c1d2	-2.80	#N/A	#N/A
54734	RAB39	NM_017516.1-533s1c1d2	-1.81	#N/A	#N/A
54734	RAB39	NM_017516.1-485s1c1d2	-1.71	#N/A	#N/A
55277	FGGY	NM_018291.2-1232s1c1	1.73	58%	Jurkat
55277	FGGY	NM_018291.2-863s1c1	2.03	45%	Jurkat
55288	RHOT1	NM_018307.2-900s1c1d2	-2.05	17%	Jurkat
55288	RHOT1	NM_018307.2-457s1c1d2	-2.15	71%	Jurkat
55288	RHOT1	NM_018307.2-169s1c1d2	-3.02	23%	Jurkat
55312	RFK	NM_018339.3-731s1c1	1.71	10%	A549
55312	RFK	NM_018339.3-595s1c1	3.05	3%	A549
55312	RFK	NM_018339.3-550s1c1	1.87	5%	A549
55351	STK32B	NM_018401.x-185s1c1	-1.81	12%	A549
55351	STK32B	NM_018401.x-570s1c1	-2.36	34%	A549
55500	ETNK1	NM_018638.x-714s1c1	-1.75	11%	A549
55500	ETNK1	NM_018638.x-581s1c1	2.65	15%	A549
55577	NAGK	NM_017567.1-369s1c1	2.62	65%	A549
55577	NAGK	NM_017567.1-621s1c1	3.09	10%	A549
55577	NAGK	NM_017567.1-999s1c1	2.05	34%	A549
55750	AGK	NM_018238.2-457s1c1	2.72	47%	Jurkat
55750	AGK	NM_018238.2-1634s1c1	2.07	35%	Jurkat
55970	GNG12	NM_018841.2-238s1c1d1	2.21	4%	A549
55970	GNG12	NM_018841.2-272s1c1d1	1.79	32%	A549
56681	SAR1A	NM_020150.3-398s1c1d3	-2.29	34%	A549
56681	SAR1A	NM_020150.3-566s1c1d3	-2.07	9%	A549
56997	CABC1	NM_020247.3-1678s1c1	-1.56	47%	MCF7
56997	CABC1	NM_020247.3-1093s1c1	-1.93	0%	MCF7
56997	CABC1	NM_020247.3-683s1c1	-2.17	35%	MCF7

57111	RAB25	NM_020387.1-571s1c1d1	-2.66	2%	MCF7
57111	RAB25	NM_020387.1-706s1c1d1	-3.05	2%	MCF7
57111	RAB25	NM_020387.1-387s1c1d1	-3.65	14%	MCF7
57381	RHOJ	NM_020663.2-878s1c1d2	-4.05	#N/A	#N/A
57381	RHOJ	NM_020663.2-1007s1c1d2	-2.22	#N/A	#N/A
57403	RAB22A	NM_020673.2-500s1c1d2	5.07	127%	Jurkat
57403	RAB22A	NM_020673.2-356s1c1d2	2.92	84%	Jurkat
57521	Raptor	NM_020761.1-65s1c1	4.06	#N/A	#N/A
57521	Raptor	NM_020761.1-65s1c1	2.38	#N/A	#N/A
57521	Raptor	NM_020761.1-65s1c1	1.76	#N/A	#N/A
57521	Raptor	NM_020761.1-65s1c1	4.59	#N/A	#N/A
57521	Raptor	NM_020761.1-65s1c1	2.14	#N/A	#N/A
57521	Raptor	NM_020761.1-65s1c1	4.78	#N/A	#N/A
57521	Raptor	NM_020761.1-65s1c1	2.05	#N/A	#N/A
57521	Raptor	NM_020761.1-65s1c1	2.72	#N/A	#N/A
57521	Raptor	NM_020761.1-65s1c1	1.55	#N/A	#N/A
57521	Raptor	NM_020761.1-65s1c1	1.53	#N/A	#N/A
57521	Raptor	NM_020761.1-65s1c1	1.65	#N/A	#N/A
57521	Raptor	NM_020761.1-65s1c1	2.01	#N/A	#N/A
57521	Raptor	NM_020761.1-65s1c1	2.05	#N/A	#N/A
57521	Raptor	NM_020761.1-65s1c1	1.60	#N/A	#N/A
57521	Raptor	NM_020761.1-65s1c1	1.75	#N/A	#N/A
57521	Raptor	NM_020761.1-65s1c1	1.71	#N/A	#N/A
57521	Raptor	NM_020761.1-65s1c1	2.42	#N/A	#N/A
57521	Raptor	NM_020761.1-65s1c1	2.03	#N/A	#N/A
57521	Raptor	NM_020761.1-65s1c1	1.66	#N/A	#N/A
57521	Raptor	NM_020761.1-65s1c1	1.67	#N/A	#N/A
57521	KIAA1303	NM_020761.1-4689s1c1d1	2.53	28%	A549
57521	KIAA1303	NM_020761.1-2564s1c1d1	2.52	35%	A549
57521	Raptor	NM_020761.1-65s1c1	2.49	#N/A	#N/A
57521	Raptor	NM_020761.1-65s1c1	1.79	#N/A	#N/A
57521	Raptor	NM_020761.1-65s1c1	2.49	#N/A	#N/A
57521	Raptor	NM_020761.1-65s1c1	2.73	#N/A	#N/A
57521	Raptor	NM_020761.1-65s1c1	2.17	#N/A	#N/A
57521	Raptor	NM_020761.1-65s1c1	2.63	#N/A	#N/A
57521	Raptor	NM_020761.1-65s1c1	1.60	#N/A	#N/A
57521	Raptor	NM_020761.1-65s1c1	1.85	#N/A	#N/A
57538	ALPK3	NM_020778.1-1004s1c1	-2.51	#N/A	#N/A
57538	ALPK3	NM_020778.1-2799s1c1	-1.82	#N/A	#N/A
57538	ALPK3	NM_020778.1-3638s1c1	-1.83	#N/A	#N/A
57799	RAB40C	NM_021168.2-388s1c1d2	-2.25	50%	Jurkat
57799	RAB40C	NM_021168.2-253s1c1d2	-1.66	91%	Jurkat
58480	RHOU	NM_021205.4-972s1c1d2	-3.88	#N/A	#N/A
58480	RHOU	NM_021205.4-1218s1c1d2	-3.20	#N/A	#N/A

60493	FASTKD5	NM_021826.4-1341s1c1	-2.47	7%	A549
60493	FASTKD5	NM_021826.4-1602s1c1	-2.00	5%	A549
64080	RBKS	NM_022128.1-837s1c1	2.12	10%	A549
64080	RBKS	NM_022128.x-101s1c1	2.29	5%	A549
64122	FN3K	NM_022158.2-860s1c1	-1.93	#N/A	#N/A
64122	FN3K	NM_022158.2-413s1c1	-3.33	#N/A	#N/A
64122	FN3K	NM_022158.2-848s1c1	-1.60	#N/A	#N/A
64122	FN3K	NM_022158.2-257s1c1	-2.32	#N/A	#N/A
64792	RABL5	NM_022777.1-178s1c1d1	-3.10	#N/A	#N/A
64792	RABL5	NM_022777.1-626s1c1d1	-2.38	#N/A	#N/A
64792	RABL5	NM_022777.1-451s1c1d1	-1.52	#N/A	#N/A
64792	RABL5	NM_022777.1-439s1c1d1	-2.66	#N/A	#N/A
65018	PINK1	NM_032409.1-785s1c1	-2.37	0%	MCF7
65018	PINK1	NM_032409.1-1601s1c1	-1.84	0%	MCF7
65018	PINK1	NM_032409.1-2473s1c1	-1.98	99%	MCF7
65018	PINK1	NM_032409.1-784s1c1	-2.10	10%	MCF7
65266	WNK4	NM_032387.2-723s1c1	3.60	#N/A	#N/A
65266	WNK4	NM_032387.2-534s1c1	4.00	#N/A	#N/A
65267	WNK3	NM_020922.x-5208s1c1	-2.15	122%	MCF7
65267	WNK3	NM_020922.x-2746s1c1	-1.98	74%	MCF7
65267	WNK3	NM_020922.x-4699s1c1	-1.70	60%	MCF7
65267	WNK3	NM_020922.x-2356s1c1	-2.35	95%	MCF7
65975	STK33	NM_030906.x-2319s1c1	-2.89	37%	A549
65975	STK33	NM_030906.x-3035s1c1	-2.19	95%	A549
65975	STK33	NM_030906.x-1436s1c1	-1.61	60%	A549
65975	STK33	NM_030906.x-2398s1c1	-1.89	49%	A549
79109	MAPKAP1	NM_024117.x-1308s1c1d1	-1.50	19%	MCF7
79109	MAPKAP1	NM_024117.x-526s1c1d1	-1.94	23%	MCF7
79675	FASTKD1	NM_024622.2-770s1c1	-1.65	28%	Jurkat
79675	FASTKD1	NM_024622.2-862s1c1	-1.61	42%	Jurkat
79877	DCAKD	NM_024819.3-590s1c1	3.06	21%	Jurkat
79877	DCAKD	NM_024819.3-419s1c1	3.28	35%	Jurkat
79877	DCAKD	NM_024819.3-420s1c1	3.44	22%	Jurkat
79877	DCAKD	NM_024819.3-997s1c1	1.55	10%	Jurkat
79899	FLJ14213	NM_024841.2-1143s1c1d1	1.96	#N/A	#N/A
79899	FLJ14213	NM_024841.2-963s1c1d1	2.87	#N/A	#N/A
79906	MORN1	NM_024848.1-117s1c1	1.69	#N/A	#N/A
79906	MORN1	NM_024848.1-118s1c1	2.73	#N/A	#N/A
80216	ALPK1	NM_025144.2-3416s1c1	-1.96	#N/A	#N/A
80216	ALPK1	NM_025144.2-1319s1c1	-2.36	#N/A	#N/A
80216	ALPK1	NM_025144.2-4083s1c1	-1.99	#N/A	#N/A
80347	COASY	NM_025233.4-547s1c1	-2.01	37%	A549
80347	COASY	NM_025233.4-2299s1c1	-2.74	7%	A549
81876	RAB1B	NM_030981.1-260s1c1d2	-2.11	2%	A549

81876	RAB1B	NM_030981.1-374s1c1d1	-2.51	3%	A549
81876	RAB1B	NM_030981.1-290s1c1d1	-1.93	47%	A549
83440	ADPGK	NM_031284.3-507s1c1	-3.50	8%	A549
83440	ADPGK	NM_031284.3-995s1c1	-3.55	3%	A549
83440	ADPGK	NM_031284.3-1498s1c1	-2.18	6%	A549
83452	RAB33B	NM_031296.1-801s1c1d1	-1.92	70%	Jurkat
83452	RAB33B	NM_031296.1-2153s1c1d1	-2.66	42%	Jurkat
84100	ARL6	NM_032146.3-445s1c1d3	2.10	#N/A	#N/A
84100	ARL6	NM_032146.3-702s1c1d3	2.88	#N/A	#N/A
84100	ARL6	NM_032146.3-713s1c1d3	1.83	#N/A	#N/A
84206	MEX3B	NM_032246.3-597s1c1	-1.66	165%	Jurkat
84206	MEX3B	NM_032246.3-1299s1c1	-1.91	212%	Jurkat
84284	C1orf57	NM_032324.1-569s1c1	2.68	20%	Jurkat
84284	C1orf57	NM_032324.1-561s1c1	2.66	26%	Jurkat
84451		NM_032435.x-1423s1c1	-3.68	0%	MCF7
84451		NM_032435.x-4199s1c1	-2.02	14%	MCF7
84451		NM_032435.x-2263s1c1	-1.58	26%	MCF7
84705	GTPBP3	NM_032620.1-1158s1c1d2	-1.82	#N/A	#N/A
84705	GTPBP3	NM_032620.1-645s1c1d2	-2.74	#N/A	#N/A
84930	MASTL	NM_032844.x-2725s1c1	-1.93	16%	A549
84930	MASTL	NM_032844.x-1818s1c1	-1.95	17%	A549
84932	RAB2B	NM_032846.2-502s1c1d2	-2.37	92%	Jurkat
84932	RAB2B	NM_032846.2-405s1c1d2	-2.04	88%	Jurkat
89882	TPD52L3	NM_033516.4-396s1c1	-2.17	22%	MCF7
89882	TPD52L3	NM_033516.4-266s1c1	-1.74	40%	MCF7
89882	TPD52L3	NM_033516.4-563s1c1	-1.94	36%	MCF7
89941	RHOT2	NM_138769.1-227s1c1d1	-1.84	32%	A549
89941	RHOT2	NM_138769.1-1585s1c1d1	-2.50	13%	A549
89941	RHOT2	NM_138769.1-499s1c1d1	-3.56	ND	A549
94235	GNG8	NM_033258.1-51s1c1d1	2.13	#N/A	#N/A
94235	GNG8	NM_033258.1-48s1c1d1	1.74	#N/A	#N/A
115273	RAB42	NM_152304.1-586s1c1d2	-2.48	#N/A	#N/A
115273	RAB42	NM_152304.1-472s1c1d2	-1.95	#N/A	#N/A
115273	RAB42	NM_152304.1-336s1c1d2	-2.70	#N/A	#N/A
115827	RAB3C	NM_138453.2-361s1c1d2	-1.83	#N/A	#N/A
115827	RAB3C	NM_138453.2-683s1c1d1	-2.89	#N/A	#N/A
115827	RAB3C	NM_138453.2-566s1c1d1	-1.72	#N/A	#N/A
116442	RAB39B	NM_171998.1-594s1c1d2	-1.60	47%	Jurkat
116442	RAB39B	NM_171998.1-393s1c1d2	-2.02	61%	Jurkat
116442	RAB39B	NM_171998.1-468s1c1d2	-2.27	53%	Jurkat
127829	ARL8A	NM_138795.2-535s1c1d1	3.04	93%	Jurkat
127829	ARL8A	NM_138795.2-208s1c1d1	1.78	67%	Jurkat
130106	CIB4	XM_059399.4-218s1c1	2.51	#N/A	#N/A
130106	CIB4	XM_059399.4-491s1c1	1.58	#N/A	#N/A

130106	CIB4	XM_059399.4-101s1c2	1.51	#N/A	#N/A
132158	GLYCTK	NM_145262.2-178s1c1	-1.91	55%	A549
132158	GLYCTK	NM_145262.2-1501s1c1	-2.15	36%	A549
132158	GLYCTK	NM_145262.2-1510s1c1	-1.85	59%	A549
139728	PNCK	NM_198452.1-229s1c1	2.22	21%	MCF7
139728	PNCK	NM_198452.1-1391s1c1	1.64	27%	MCF7
143098	MPP7	NM_173496.2-493s1c1	-1.87	37%	MCF7
143098	MPP7	NM_173496.2-610s1c1	-2.44	44%	MCF7
158067	C9orf98	NM_152572.2-1877s1c1	-1.56	73%	Jurkat
158067	C9orf98	NM_152572.2-700s1c1	-2.17	14%	Jurkat
158067	C9orf98	NM_152572.2-1099s1c1	-2.30	10%	Jurkat
158158	RASEF	NM_152573.2-907s1c1d2	-1.79	#N/A	#N/A
158158	RASEF	NM_152573.2-1153s1c1d2	-2.06	#N/A	#N/A
158158	RASEF	NM_152573.2-2189s1c1d2	-2.12	#N/A	#N/A
197258	FUK	NM_145059.1-1966s1c1	-2.54	23%	Jurkat
197258	FUK	NM_145059.1-3135s1c1	-2.34	9%	Jurkat
197258	FUK	NM_145059.1-525s1c1	-3.21	16%	Jurkat
200894	ARL13B	NM_182896.1-656s1c1d1	-2.40	37%	Jurkat
200894	ARL13B	NM_182896.1-1057s1c1d1	-1.80	102%	Jurkat
203447	NRK	NM_198465.1-2037s1c1	-1.51	#N/A	#N/A
203447	NRK	NM_198465.1-6369s1c1	-1.81	#N/A	#N/A
203447	NRK	NM_198465.1-3444s1c1	-1.79	#N/A	#N/A
203447	NRK	NM_198465.1-1263s1c1	-1.94	#N/A	#N/A
204851	HIPK1	NM_152696.3-3218s1c1	-1.62	#N/A	#N/A
204851	HIPK1	NM_152696.3-2649s1c1	-1.78	29%	MCF7
204851	HIPK1	NM_152696.3-3011s1c1	-2.07	#N/A	#N/A
204851	HIPK1	NM_152696.3-2105s1c1	-2.60	#N/A	#N/A
220686		NM_199283.4-2143s1c1	-1.58	#N/A	#N/A
220686		NM_199283.4-1290s1c1	-1.82	#N/A	#N/A
220686		NM_199283.4-699s1c1	1.99	#N/A	#N/A
221079	ARL5B	NM_178815.2-272s1c1d2	5.15	76%	Jurkat
221079	ARL5B	NM_178815.2-589s1c1d2	3.83	249%	Jurkat
253260	RICTOR	NM_152756.3-25s1c1	-1.60	#N/A	#N/A
253260	RICTOR	NM_152756.3-25s1c1	-2.01	#N/A	#N/A
253260	RICTOR	NM_152756.3-25s1c1	-2.20	#N/A	#N/A
253260	RICTOR	NM_152756.3-25s1c1	-1.50	#N/A	#N/A
253260	RICTOR	NM_152756.3-25s1c1	-2.30	#N/A	#N/A
253260	RICTOR	NM_152756.3-25s1c1	-1.51	#N/A	#N/A
253260	RICTOR	NM_152756.3-25s1c1	-1.73	#N/A	#N/A
253260	RICTOR	NM_152756.3-25s1c1	-2.19	#N/A	#N/A
253260	RICTOR	NM_152756.3-25s1c1	-2.09	#N/A	#N/A
253260	RICTOR	NM_152756.3-25s1c1	-2.06	#N/A	#N/A
253260	RICTOR	NM_152756.3-25s1c1	-1.67	#N/A	#N/A
253260	RICTOR	NM_152756.3-25s1c1	-2.24	#N/A	#N/A

253260	RICTOR	NM_152756.3-25s1c1	-1.75	#N/A	#N/A
253260	RICTOR	NM_152756.3-25s1c1	-2.59	#N/A	#N/A
253260	RICTOR	NM_152756.3-25s1c1	-2.19	#N/A	#N/A
253260	RICTOR	NM_152756.3-25s1c1	-1.90	#N/A	#N/A
253260	RICTOR	NM_152756.3-25s1c1	-1.64	#N/A	#N/A
253260	RICTOR	NM_152756.2-5035s1c1d1	-1.59	26%	A549
253260	RICTOR	NM_152756.3-25s1c1	-1.52	#N/A	#N/A
253260	RICTOR	NM_152756.3-25s1c1	-1.83	#N/A	#N/A
253260	RICTOR	NM_152756.3-25s1c1	-1.60	#N/A	#N/A
253260	RICTOR	NM_152756.3-25s1c1	-2.34	#N/A	#N/A
253260	RICTOR	NM_152756.3-25s1c1	-1.67	#N/A	#N/A
253260	RICTOR	NM_152756.3-25s1c1	-1.69	#N/A	#N/A
253260	RICTOR	NM_152756.3-25s1c1	-1.86	#N/A	#N/A
253260	RICTOR	NM_152756.3-25s1c1	-1.54	#N/A	#N/A
253260	RICTOR	NM_152756.3-25s1c1	-2.02	#N/A	#N/A
253260	RICTOR	NM_152756.3-25s1c1	-1.71	#N/A	#N/A
253260	RICTOR	NM_152756.3-25s1c1	-1.52	#N/A	#N/A
253260	RICTOR	NM_152756.3-25s1c1	-2.05	#N/A	#N/A
253260	RICTOR	NM_152756.3-25s1c1	-2.64	#N/A	#N/A
253260	RICTOR	NM_152756.3-25s1c1	-2.05	#N/A	#N/A
253430	IPMK	NM_152230.2-691s1c1	2.46	#N/A	#N/A
253430	IPMK	NM_152230.2-1075s1c1	2.44	#N/A	#N/A
253430	IPMK	NM_152230.2-1502s1c1	2.43	#N/A	#N/A
256356	GK5	NM_152776.1-1237s1c1	-4.51	69%	Jurkat
256356	GK5	NM_152776.1-356s1c1	-2.65	60%	Jurkat
260425	MAGI3	NM_020965.2-2984s1c1	-3.05	15%	A549
260425	MAGI3	NM_020965.2-1964s1c1	-2.08	8%	A549
282974	STK32C	NM_173575.2-311s1c1	-2.72	16%	A549
282974	STK32C	NM_173575.2-1898s1c1	-1.84	23%	A549
282974	STK32C	NM_173575.2-839s1c1	-2.04	29%	A549
282974	STK32C	NM_173575.2-1386s1c1	-1.93	21%	A549
283629	TSSK4	NM_174944.x-1134s1c1	-1.79	#N/A	#N/A
283629	TSSK4	NM_174944.2-217s1c1	-1.56	#N/A	#N/A
283629	TSSK4	NM_174944.2-408s1c1	-1.95	#N/A	#N/A
283629	TSSK4	NM_174944.x-495s1c1	-1.80	#N/A	#N/A
284086	NEK8	NM_178170.2-2231s1c1	-3.55	#N/A	#N/A
284086	NEK8	NM_178170.2-84s1c1	-3.78	#N/A	#N/A
284086	NEK8	NM_178170.2-2321s1c1	-2.08	#N/A	#N/A
284086	NEK8	NM_178170.2-1734s1c1	-1.77	#N/A	#N/A
284086	NEK8	NM_178170.2-210s1c1	-1.89	#N/A	#N/A
284086	NEK8	NM_178170.2-1494s1c1	-2.72	#N/A	#N/A
284656	EPHA10	NM_173641.1-546s1c1	-2.39	64%	Jurkat
284656	EPHA10	NM_173641.1-199s1c1	-2.30	107%	Jurkat
285282	RABL3	NM_173825.1-253s1c1d1	-1.66	#N/A	#N/A

285282	RABL3	NM_173825.1-288s1c1d1	-2.69	#N/A	#N/A
285282	RABL3	NM_173825.1-511s1c1d1	-1.57	#N/A	#N/A
326624	RAB37	NM_175738.2-1059s1c1d2	-2.67	36%	Jurkat
326624	RAB37	NM_175738.2-711s1c1d2	-3.07	36%	Jurkat
339122	RAB43	NM_198490.1-326s1c1d1	3.32	106%	Jurkat
339122	RAB43	NM_198490.1-323s1c1d1	1.72	72%	Jurkat
344988	SAR1P3	XM_293671.3-48s1c1d2	1.73	#N/A	#N/A
344988	SAR1P3	XM_293671.3-90s1c1d2	4.57	#N/A	#N/A
347359	BMP2KL	XM_293293.1-316s1c1	-1.56	#N/A	#N/A
347359	BMP2KL	XM_293293.1-829s1c1	-2.68	#N/A	#N/A
347736	TXNDC6	NM_178130.2-862s1c1	-1.81	#N/A	#N/A
347736	TXNDC6	NM_178130.2-695s1c1	-2.86	#N/A	#N/A
347736	TXNDC6	NM_178130.2-1004s1c1	-2.14	#N/A	#N/A
374872	C19orf35	NM_198532.1-1942s1c1	-2.13	#N/A	#N/A
374872	C19orf35	NM_198532.1-163s1c2	-2.77	#N/A	#N/A
374872	C19orf35	NM_198532.1-2156s1c1	-1.74	#N/A	#N/A
375133	PI4KAP2	NM_199345.1-570s1c2	-1.67	#N/A	#N/A
375133	PI4KAP2	NM_199345.1-721s1c1	-2.02	#N/A	#N/A
375133	PI4KAP2	NM_199345.2-868s1c1	-1.52	#N/A	#N/A
387751	GVIN1	XM_495863.1-787s1c1d2	-2.09	#N/A	#N/A
387751	GVIN1	XM_495863.1-3014s1c1d2	-2.37	#N/A	#N/A
390877		XM_372705.1-33s1c1	1.80	#N/A	#N/A
390877		XM_372705.1-306s1c1	1.91	#N/A	#N/A
392226		XM_498286.1-954s1c1	-2.73	#N/A	#N/A
392226		XM_498286.1-166s1c1	-2.51	#N/A	#N/A
392226		XM_498286.1-790s1c1	1.69	#N/A	#N/A
392265		XM_498294.1-79s1c1	-2.42	#N/A	#N/A
392265		XM_498294.1-502s1c1	-2.77	#N/A	#N/A
392347		XM_373298.2-623s1c1	2.46	#N/A	#N/A
392347		XM_373298.2-598s1c1	-3.01	#N/A	#N/A
392347		XM_373298.2-411s1c1	-1.88	#N/A	#N/A
392347		XM_373298.2-94s1c1	3.29	#N/A	#N/A
402679		XM_380022.4-429s1c1	-2.18	#N/A	#N/A
402679		XM_380022.2-441s1c1	-3.15	#N/A	#N/A
402679		XM_380022.4-298s1c1	-3.98	#N/A	#N/A
402679		XM_380022.4-27s1c1	-2.35	#N/A	#N/A
440275	EIF2AK4	XM_496066.1-495s1c1	2.55	73%	A549
440275	EIF2AK4	XM_496066.1-405s1c1	2.05	56%	A549
440275	EIF2AK4	XM_496066.1-304s1c1	4.62	21%	A549
440345		XM_496125.1-7371s1c1	2.08	#N/A	#N/A
440345		XM_496125.1-7211s1c1	2.60	#N/A	#N/A
440345		XM_496125.1-352s1c1	1.96	#N/A	#N/A
441655		XM_497366.1-217s1c1	-2.37	#N/A	#N/A
441655		XM_497366.1-331s1c1	-1.55	#N/A	#N/A

441971		XM_497790.1-98s1c1	-1.63	#N/A	#N/A
441971		XM_497790.1-373s1c1	-1.56	#N/A	#N/A
441971		XM_497790.1-446s1c1	-3.89	#N/A	#N/A
441971		XM_497790.1-119s1c1	-3.04	#N/A	#N/A
442313		XM_498204.1-610s1c1	-1.73	#N/A	#N/A
442313		XM_498204.1-650s1c1	-2.39	#N/A	#N/A
442558		XM_499301.1-934s1c1	-1.58	#N/A	#N/A
442558		XM_499301.1-514s1c1	-1.84	#N/A	#N/A
442558		XM_499301.1-568s1c1	2.11	#N/A	#N/A
442558		XM_499301.1-496s1c1	2.09	#N/A	#N/A

APPENDIX C: shRNAs from Appendix B with greater than 50% target mRNA knockdown.

NCBI ID	Symbol	TRC Clone Name	mean pAKT Z-score	% mRNA	cell line
207	AKT1	NM_005163.x-642s1c1	-2.23	10%	A-431
207	AKT1	NM_005163.x-981s1c1	-2.02	17%	A-431
207	AKT1	NM_005163.x-1044s1c1d1	-1.70	14%	A431
207	AKT1	NM_005163.1-1410s1c1	-1.69	48%	A-431
207	AKT1	NM_005163.x-642s1c1d2	-1.55	16%	A431
207	AKT1	NM_005163.x-1044s1c1	-1.52	14%	A-431
387	RHOA	NM_001664.1-616s1c1d2	-2.78	3%	A549
387	RHOA	NM_001664.1-300s1c1d2	-2.67	15%	A549
387	RHOA	NM_001664.1-382s1c1d2	-2.51	16%	A549
387	RHOA	NM_001664.1-199s1c1d2	-2.51	5%	A549
388	RHOB	NM_004040.2-452s1c1d2	-1.91	12%	A549
388	RHOB	NM_004040.2-461s1c1d2	-1.80	22%	A549
389	RHOC	NM_175744.3-328s1c1d2	-1.77	12%	A549
389	RHOC	NM_175744.3-539s1c1d3	-1.50	13%	A549
403	ARL3	NM_004311.2-480s1c1d3	-2.65	13%	A549
403	ARL3	NM_004311.2-290s1c1d3	-1.57	3%	A549
640	BLK	NM_001715.x-1031s1c1	-2.41	16%	Jurkat
640	BLK	NM_001715.2-746s1c1	-2.12	30%	Jurkat
640	BLK	NM_001715.x-1200s1c1	-2.03	29%	Jurkat
640	BLK	NM_001715.2-1626s1c1	-1.66	43%	Jurkat
1152	CKB	NM_001823.3-722s1c1	-2.70	34%	MCF7
1152	CKB	NM_001823.3-1250s1c1	-2.50	8%	MCF7
1152	CKB	NM_001823.3-1251s1c1	-1.80	20%	MCF7
1152	CKB	NM_001823.3-877s1c1	-1.70	35%	MCF7
1606	DGKA	NM_001345.4-592s1c1	2.41	22%	Jurkat
1606	DGKA	NM_001345.4-382s1c1	2.52	42%	Jurkat
1915	EEF1A1	NM_001402.4-338s1c1d1	-2.53	4%	A549
1915	EEF1A1	NM_001402.4-807s1c1d1	-1.76	2%	A549
1968	EIF2S3	NM_001415.2-782s1c1d1	-2.28	45%	A549
1968	EIF2S3	NM_001415.2-646s1c1d1	-1.85	11%	A549
2049	EPHB3	NM_004443.3-1895s1c1	1.58	46%	MCF7
2049	EPHB3	NM_004443.3-3611s1c1	2.14	43%	MCF7
2050	EPHB4	NM_004444.x-459s1c1	-1.76	27%	A549
2050	EPHB4	NM_004444.x-2076s1c1	-1.55	8%	A549
2475	FRAP1	NM_004958.2-640s1c1	1.72	14%	A549
2475	FRAP1	NM_004958.2-4662s1c1	2.21	21%	A549
2475	FRAP1	NM_004958.2-3425s1c1d2	2.54	25%	Jurkat
2475	FRAP1	NM_004958.2-7897s1c1	2.56	21%	A549

2475	FRAP1	NM_004958.2-3425s1c1	2.73	35%	A549
2791	GNG11	NM_004126.2-502s1c1d1	2.49	47%	A549
2791	GNG11	NM_004126.2-437s1c1d1	2.73	32%	A549
2931	GSK3A	NM_019884.1-1173s1c1	-2.44	9%	MCF7
2931	GSK3A	NM_019884.x-1428s1c1	-2.10	0%	MCF7
2965	GTF2H1	NM_005316.2-1316s1c1	-2.98	40%	MCF7
2965	GTF2H1	NM_005316.2-1755s1c1	-1.78	25%	MCF7
3717	JAK2	NM_004972.x-4564s1c1	3.73	23%	A549
3984	LIMK1	NM_002314.x-1512s1c1	-2.04	5%	MCF7
3984	LIMK1	NM_002314.x-1374s1c1	-1.78	3%	MCF7
4354	MPP1	NM_002436.2-1286s1c1	-3.06	26%	A549
4354	MPP1	NM_002436.2-1216s1c1	-1.73	24%	A549
4733	DRG1	NM_004147.2-665s1c1d1	1.51	18%	A549
4733	DRG1	NM_004147.2-514s1c1d1	1.89	10%	A549
4832	NME3	NM_002513.2-414s1c1	-2.96	15%	293T
4832	NME3	NM_002513.2-310s1c1	-1.88	11%	293T
5211	PFKL	NM_002626.x-1630s1c1	-2.08	10%	A549
5211	PFKL	NM_002626.4-2301s1c1	-1.69	11%	A549
5211	PFKL	NM_002626.4-2309s1c1	-1.69	0%	A549
5213	PFKM	NM_000289.3-429s1c1	-2.57	16%	MCF7
5213	PFKM	NM_000289.3-1883s1c1	-1.52	35%	MCF7
5291	PIK3CB	NM_006219.x-61s1c1d2	-1.74	40%	MCF7
5291	PIK3CB	NM_006219.x-61s1c1	-1.63	40%	MCF7
5291	PIK3CB	NM_006219.x-2289s1c1	-1.60	25%	MCF7
5291	PIK3CB	NM_006219.x-1306s1c1	-1.57	29%	MCF7
5347	PLK1	NM_005030.3-1893s1c1	-2.01	25%	MCF7
5347	PLK1	NM_005030.3-1374s1c1	-1.93	35%	MCF7
5347	PLK1	NM_005030.3-1361s1c1	-1.89	0%	MCF7
5347	PLK1	NM_005030.3-1986s1c1	-1.50	48%	MCF7
5361	PLXNA1	NM_032242.2-4255s1c1	2.36	31%	A549
5361	PLXNA1	NM_032242.2-4656s1c1	2.82	38%	A549
5394	EXOSC10	NM_002685.1-1274s1c1	-3.51	7%	A549
5394	EXOSC10	NM_002685.1-1833s1c1	-1.87	24%	A549
5394	EXOSC10	NM_002685.1-2560s1c1	-1.64	25%	A549
5575	PRKAR1B	NM_002735.1-593s1c1	2.77	8%	MCF7
5575	PRKAR1B	NM_002735.1-620s1c1	3.24	7%	MCF7
5586	PKN2	NM_006256.1-309s1c1	-2.26	28%	A549
5586	PKN2	NM_006256.1-2250s1c1	-2.06	39%	A549
5631	PRPS1	NM_002764.x-592s1c1	1.70	42%	MCF7
5631	PRPS1	NM_002764.x-819s1c1	2.05	0%	MCF7
5634	PRPS2	NM_002765.x-871s1c1	1.81	16%	MCF7
5634	PRPS2	NM_002765.x-320s1c1	1.96	13%	MCF7

5832	ALDH18A1	NM_002860.2-658s1c1	-2.59	8%	A549
5832	ALDH18A1	NM_002860.2-568s1c1	-2.13	44%	A549
5865	RAB3B	NM_002867.x-446s1c1d1	-2.98	5%	A549
5865	RAB3B	NM_002867.x-447s1c1d1	-2.71	8%	A549
5865	RAB3B	NM_002867.x-907s1c1d1	-1.54	6%	A549
5868	RAB5A	NM_004162.3-659s1c1d1	-3.94	46%	#N/A
5868	RAB5A	NM_004162.3-2139s1c1d3	-1.86	16%	#N/A
5873	RAB27A	NM_004580.3-477s1c1d2	-2.09	25%	A549
5873	RAB27A	NM_004580.3-735s1c1d2	-1.72	5%	A549
5881	RAC3	NM_005052.2-664s1c1d2	-3.31	20%	293T
5881	RAC3	NM_005052.2-331s1c1d2	-2.78	14%	293T
5881	RAC3	NM_005052.2-544s1c1d2	-2.77	17%	293T
6046	BRD2	NM_005104.2-2059s1c1	-2.57	21%	293T
6046	BRD2	NM_005104.2-2401s1c1	-2.12	40%	293T
6729	SRP54	NM_003136.2-1839s1c1d1	-2.80	25%	A549
6729	SRP54	NM_003136.2-849s1c1d1	-2.71	15%	A549
6729	SRP54	NM_003136.2-1903s1c1d1	-2.61	22%	A549
6733	SRPK2	NM_003138.1-749s1c1	-1.79	9%	MCF7
6733	SRPK2	NM_003138.1-2730s1c1	-1.61	3%	MCF7
6734	SRPR	NM_003139.2-202s1c1d1	-4.08	4%	A549
6734	SRPR	NM_003139.2-1086s1c1d1	-1.86	5%	A549
7083	TK1	NM_003258.x-610s1c1	-1.94	11%	A549
7083	TK1	NM_003258.x-530s1c1	-1.74	14%	A549
7083	TK1	NM_003258.x-327s1c1	-1.51	3%	A549
7284	TUFM	NM_003321.3-668s1c1d1	-2.68	5%	A549
7284	TUFM	NM_003321.3-1266s1c1d1	-1.71	2%	A549
7297	TYK2	NM_003331.x-3209s1c1	-2.87	13%	A549
7297	TYK2	NM_003331.x-4078s1c1	-2.54	15%	A549
8476	CDC42BPA	NM_014826.x-4292s1c1	1.55	44%	A549
8476	CDC42BPA	NM_003607.x-2992s1c1	2.33	5%	A549
8476	CDC42BPA	NM_014826.x-2749s1c1	2.49	3%	A549
8476	CDC42BPA	NM_003607.x-4535s1c1	2.58	6%	A549
8526	DGKE	NM_003647.1-853s1c1	-1.70	20%	MCF7
8526	DGKE	NM_003647.1-952s1c1	-1.54	5%	MCF7
8877	SPHK1	NM_182965.1-1063s1c1	-3.09	13%	293T
8877	SPHK1	NM_182965.1-1640s1c1	-2.43	36%	293T
8877	SPHK1	NM_182965.1-1116s1c1	-1.68	21%	293T
9060	PAPSS2	NM_004670.2-177s1c1	-1.83	11%	MCF7
9060	PAPSS2	NM_004670.2-1768s1c1	-1.58	7%	MCF7
9064	MAP3K6	NM_004672.x-3795s1c1	-2.40	24%	A549
9567	GTPBP1	NM_004286.3-884s1c1d2	-4.45	23%	293T
9567	GTPBP1	NM_004286.3-1015s1c1d2	-1.90	31%	293T

10000	AKT3	NM_005465.x-770s1c1	-3.04	33%	A549
10000	AKT3	NM_005465.x-1757s1c1	-1.83	47%	A549
10000	AKT3	NM_005465.x-569s1c1	-1.82	21%	A549
10154	PLXNC1	NM_005761.1-1236s1c1	-2.26	32%	Jurkat
10154	PLXNC1	NM_005761.1-3289s1c1	-2.25	31%	Jurkat
10519	CIB1	NM_006384.2-504s1c1	-2.80	7%	A549
10519	CIB1	NM_006384.2-376s1c1	-2.04	31%	A549
10783	NEK6	NM_014397.x-445s1c1	-2.40	3%	MCF7
10783	NEK6	NM_014397.x-484s1c1	-2.11	22%	MCF7
10966	RAB40B	NM_006822.1-513s1c1d2	-3.48	40%	A549
10966	RAB40B	NM_006822.1-354s1c1d1	-2.30	7%	A549
11021	RAB35	NM_006861.4-709s1c1d2	-3.93	37%	A549
11021	RAB35	NM_006861.4-486s1c1d2	-3.27	27%	A549
11021	RAB35	NM_006861.4-207s1c1d2	-2.58	19%	A549
11321	XAB1	NM_007266.1-835s1c1d2	2.33	4%	A549
11321	XAB1	NM_007266.1-220s1c1d2	2.73	18%	A549
11344	TWF2	NM_007284.3-522s1c1	-2.09	22%	A549
11344	TWF2	NM_007284.3-610s1c1	-1.50	9%	A549
25837	RAB26	NM_014353.4-721s1c1d2	-4.06	40%	A549
25837	RAB26	NM_014353.4-512s1c1d2	-2.21	48%	A549
26007	DAK	NM_015533.2-1015s1c1	-1.70	10%	A549
26007	DAK	NM_015533.2-1597s1c1	-1.51	0%	A549
29110	TBK1	NM_013254.x-1212s1c1	-2.46	35%	A549
29110	TBK1	NM_013254.x-1536s1c1	-1.75	33%	A549
51128	SAR1B	NM_016103.2-267s1c1d2	-3.50	9%	A549
51128	SAR1B	NM_016103.2-569s1c1d2	-1.95	8%	A549
51135	IRAK4	NM_016123.x-820s1c1	1.53	10%	A549
51135	IRAK4	NM_016123.x-374s1c1	1.88	29%	A549
51678	MPP6	NM_016447.x-528s1c1	-1.89	14%	A549
51678	MPP6	NM_016447.x-527s1c1	-1.57	27%	A549
55288	RHOT1	NM_018307.2-169s1c1d2	-3.02	23%	Jurkat
55288	RHOT1	NM_018307.2-900s1c1d2	-2.05	17%	Jurkat
55312	RFK	NM_018339.3-731s1c1	1.71	10%	A549
55312	RFK	NM_018339.3-550s1c1	1.87	5%	A549
55312	RFK	NM_018339.3-595s1c1	3.05	3%	A549
55577	NAGK	NM_017567.1-999s1c1	2.05	34%	A549
55577	NAGK	NM_017567.1-621s1c1	3.09	10%	A549
55750	AGK	NM_018238.2-1634s1c1	2.07	35%	Jurkat
55750	AGK	NM_018238.2-457s1c1	2.72	47%	Jurkat
55970	GNG12	NM_018841.2-272s1c1d1	1.79	32%	A549
55970	GNG12	NM_018841.2-238s1c1d1	2.21	4%	A549
56681	SAR1A	NM_020150.3-398s1c1d3	-2.29	34%	A549

56681	SAR1A	NM_020150.3-566s1c1d3	-2.07	9%	A549
56997	CABC1	NM_020247.3-683s1c1	-2.17	35%	MCF7
56997	CABC1	NM_020247.3-1093s1c1	-1.93	0%	MCF7
56997	CABC1	NM_020247.3-1678s1c1	-1.56	47%	MCF7
57111	RAB25	NM_020387.1-387s1c1d1	-3.65	14%	MCF7
57111	RAB25	NM_020387.1-706s1c1d1	-3.05	2%	MCF7
57111	RAB25	NM_020387.1-571s1c1d1	-2.66	2%	MCF7
57521	RAPTOR	NM_020761.1-2564s1c1d1	2.52	35%	A549
57521	RAPTOR	NM_020761.1-4689s1c1d1	2.53	28%	A549
60493	FASTKD5	NM_021826.4-1341s1c1	-2.47	7%	A549
60493	FASTKD5	NM_021826.4-1602s1c1	-2.00	5%	A549
79109	MAPKAP1	NM_024117.x-526s1c1d1	-1.94	23%	MCF7
79109	MAPKAP1	NM_024117.x-1308s1c1d1	-1.50	19%	MCF7
79675	FASTKD1	NM_024622.2-770s1c1	-1.65	28%	Jurkat
79675	FASTKD1	NM_024622.2-862s1c1	-1.61	42%	Jurkat
79877	DCAKD	NM_024819.3-997s1c1	1.55	10%	Jurkat
79877	DCAKD	NM_024819.3-590s1c1	3.06	21%	Jurkat
79877	DCAKD	NM_024819.3-419s1c1	3.28	35%	Jurkat
79877	DCAKD	NM_024819.3-420s1c1	3.44	22%	Jurkat
80347	COASY	NM_025233.4-2299s1c1	-2.74	7%	A549
80347	COASY	NM_025233.4-547s1c1	-2.01	37%	A549
81876	RAB1B	NM_030981.1-374s1c1d1	-2.51	3%	A549
81876	RAB1B	NM_030981.1-260s1c1d2	-2.11	2%	A549
81876	RAB1B	NM_030981.1-290s1c1d1	-1.93	47%	A549
83440	ADPGK	NM_031284.3-995s1c1	-3.55	3%	A549
83440	ADPGK	NM_031284.3-507s1c1	-3.50	8%	A549
83440	ADPGK	NM_031284.3-1498s1c1	-2.18	6%	A549
84284	C1orf57	NM_032324.1-561s1c1	2.66	26%	Jurkat
84284	C1orf57	NM_032324.1-569s1c1	2.68	20%	Jurkat
84451		NM_032435.x-1423s1c1	-3.68	0%	MCF7
84451		NM_032435.x-4199s1c1	-2.02	14%	MCF7
84451		NM_032435.x-2263s1c1	-1.58	26%	MCF7
84930	MASTL	NM_032844.x-1818s1c1	-1.95	17%	A549
84930	MASTL	NM_032844.x-2725s1c1	-1.93	16%	A549
89941	RHOT2	NM_138769.1-499s1c1d1	-3.56	ND	A549
89941	RHOT2	NM_138769.1-1585s1c1d1	-2.50	13%	A549
89941	RHOT2	NM_138769.1-227s1c1d1	-1.84	32%	A549
139728	PNCK	NM_198452.1-1391s1c1	1.64	27%	MCF7
139728	PNCK	NM_198452.1-229s1c1	2.22	21%	MCF7
143098	MPP7	NM_173496.2-610s1c1	-2.44	44%	MCF7
143098	MPP7	NM_173496.2-493s1c1	-1.87	37%	MCF7
197258	FUK	NM_145059.1-525s1c1	-3.21	16%	Jurkat

197258	FUK	NM_145059.1-1966s1c1	-2.54	23%	Jurkat
197258	FUK	NM_145059.1-3135s1c1	-2.34	9%	Jurkat
204851	HIPK1	NM_152696.3-2649s1c1	-1.78	29%	MCF7
260425	MAGI3	NM_020965.2-2984s1c1	-3.05	15%	A549
260425	MAGI3	NM_020965.2-1964s1c1	-2.08	8%	A549
282974	STK32C	NM_173575.2-311s1c1	-2.72	16%	A549
282974	STK32C	NM_173575.2-839s1c1	-2.04	29%	A549
282974	STK32C	NM_173575.2-1386s1c1	-1.93	21%	A549
282974	STK32C	NM_173575.2-1898s1c1	-1.84	23%	A549
326624	RAB37	NM_175738.2-711s1c1d2	-3.07	36%	Jurkat
326624	RAB37	NM_175738.2-1059s1c1d2	-2.67	36%	Jurkat

APPENDIX D: 48 hit genes from Table S4 that are not known to be associated with PI3K/AKT signaling whose expression is not tissue-specific. nd, no data.

NCBI ID	SYMBOL	Expressed widely?	Result of KD?
5575	PRKAR1B	Yes	↑ phospho-AKT
6011	GRK1	Yes	↑ phospho-AKT
9943	OXSR1	Yes	↑ phospho-AKT
55312	RFK	Yes	↑ phospho-AKT
79877	DCAKD	Yes	↑ phospho-AKT
1163	CKS1B	nd	↓ phospho-AKT
3706	ITPKA	Yes	↓ phospho-AKT
5394	EXOSC10	Yes	↓ phospho-AKT
5586	PKN2	Yes	↓ phospho-AKT
5881	RAC3	Yes	↓ phospho-AKT
6729	SRP54	Yes	↓ phospho-AKT
6872	TAF1	Yes	↓ phospho-AKT
7083	TK1	Yes	↓ phospho-AKT
9064	MAP3K6	nd	↓ phospho-AKT
11021	RAB35	Yes	↓ phospho-AKT
11158	RABL2B	nd	↓ phospho-AKT
11159	RABL2A	nd	↓ phospho-AKT
26164	GTPBP5	Yes	↓ phospho-AKT
27289	RND1	nd	↓ phospho-AKT
54676	GTPBP2	nd	↓ phospho-AKT
54734	RAB39	nd	↓ phospho-AKT
56997	CABC1	nd	↓ phospho-AKT
57538	ALPK3	Yes	↓ phospho-AKT
57551	TAOK1	Yes	↓ phospho-AKT
64122	FN3K	Yes	↓ phospho-AKT
64792	RABL5	Yes	↓ phospho-AKT
79646	PANK3	Yes	↓ phospho-AKT
80216	ALPK1	Yes	↓ phospho-AKT
81876	RAB1B	Yes	↓ phospho-AKT
83440	ADPGK	Yes	↓ phospho-AKT
83903	GSG2	Yes	↓ phospho-AKT
84100	ARL6	Yes	↓ phospho-AKT
84197	POMK	Yes	↓ phospho-AKT
89941	RHOT2	Yes	↓ phospho-AKT
91461	PKDCC	Yes	↓ phospho-AKT
127933	UHMK1	Yes	↓ phospho-AKT
130106	CIB4	Yes	↓ phospho-AKT
158158	RASEF	Yes	↓ phospho-AKT
197258	FUK	Yes	↓ phospho-AKT
203447	NRK	low	↓ phospho-AKT
282974	STK32C	Yes	↓ phospho-AKT

283629	TSSK4	Yes	↓ phospho-AKT
284086	NEK8	Yes	↓ phospho-AKT
285282	RABL3	Yes	↓ phospho-AKT
347736	TXNDC6	Yes	↓ phospho-AKT
374872	C19orf35	nd	↓ phospho-AKT
402679	MARK2P10	nd	↓ phospho-AKT
440345	NPIPB4	nd	↓ phospho-AKT

BIBLIOGRAPHY

1. Laplante, M. and D.M. Sabatini, *mTOR signaling in growth control and disease.* Cell, 2012. **149**: p. 274-293.
2. Viglietto, G., et al., *Contribution of PKB/AKT signaling to thyroid cancer.* Front Biosci (Landmark Ed), 2011. **16**: p. 1461-87.
3. Wheeler, D.B., A.E. Carpenter, and D.M. Sabatini, *Cell microarrays and RNA interference chip away at gene function.* Nat Genet, 2005. **37 Suppl**: p. S25-30.
4. Wheeler, D.B., et al., *RNAi living-cell microarrays for loss-of-function screens in Drosophila melanogaster cells.* Nat Methods, 2004. **1**(2): p. 127-32.
5. Ruderman, N.B., et al., *Activation of phosphatidylinositol 3-kinase by insulin.* Proc Natl Acad Sci U S A, 1990. **87**: p. 1411-1415.
6. Cantley, L.C., et al., *Oncogenes and signal transduction.* Cell, 1991: p. 281-302.
7. Soltoff, S.P., et al., *Phosphatidylinositol-3 kinase and growth regulation.* Cold Spring Harb Symp Quant Biol, 1992. **57**: p. 75-80.
8. Auger, K.R., et al., *Polyoma virus middle T antigen-pp60c-src complex associates with purified phosphatidylinositol 3-kinase in vitro.* J Biol Chem, 1992. **267**: p. 5408-5415.
9. Auger, K.R., et al., *Phosphatidylinositol 3-kinase and its novel product, phosphatidylinositol 3-phosphate, are present in Saccharomyces cerevisiae.* J Biol Chem, 1989. **264**: p. 20181-20184.
10. Whitman, M., et al., *Type I phosphotidylinositol kinase makes a novel inositol phospholipid.* Nature, 1988. **332**: p. 644-646.
11. Auger, K.R., et al., *PDGF-dependent tyrosine phosphorylation stimulates production of novel polyphosphoinositides in intact cells.* Cell, 1989. **57**: p. 167-175.
12. Vanhaesebroeck, B., et al., *Phosphoinositide 3-kinases: a conserved family of signal transducers.* Trends Biochem Sci, 1997. **22**(7): p. 267-72.
13. Wymann, M.P. and L. Pirola, *Structure and function of phosphoinositide 3-kinases.* Biochimica et biophysica acta, 1998. **1436**: p. 127-50.
14. Leevers, S.J., B. Vanhaesebroeck, and M.D. Waterfield, *Signalling through phosphoinositide 3-kinases: the lipids take centre stage.* Curr Opin Cell Biol, 1999. **11**(2): p. 219-25.
15. Knight, Z.A., et al., *A pharmacological map of the PI3-K family defines a role for p110alpha in insulin signaling.* Cell, 2006. **125**: p. 733-47.
16. Okkenhaug, K. and B. Vanhaesebroeck, *New responsibilities for the PI3K regulatory subunit p85 alpha.* Sci STKE, 2001. **2001**(65): p. pe1.
17. Klippel, A., et al., *The interaction of small domains between the subunits of phosphatidylinositol 3-kinase determines enzyme activity.* Mol Cell Biol, 1994. **14**: p. 2675-2685.
18. Karlsson, T., et al., *Molecular interactions of the Src homology 2 domain protein Shb with phosphotyrosine residues, tyrosine kinase*

receptors and Src homology 3 domain proteins. Oncogene, 1995. **10**: p. 1475-1483.
19. White, M.F., *The IRS-signaling system: a network of docking proteins that mediate insulin and cytokine action.* Recent Prog Horm Res, 1998. **53**: p. 119-38.
20. Ueki, K., et al., *Molecular balance between the regulatory and catalytic subunits of phosphoinositide 3-kinase regulates cell signaling and survival.* Mol Cell Biol, 2002. **22**: p. 965-977.
21. Mauvais-Jarvis, F., et al., *Reduced expression of the murine p85alpha subunit of phosphoinositide 3-kinase improves insulin signaling and ameliorates diabetes.* J Clin Invest, 2002. **109**: p. 141-149.
22. Ueki, K., et al., *Positive and negative roles of p85 alpha and p85 beta regulatory subunits of phosphoinositide 3-kinase in insulin signaling.* J Biol Chem, 2003. **278**: p. 48453-48466.
23. Taniguchi, C.M., et al., *Phosphoinositide 3-kinase regulatory subunit p85alpha suppresses insulin action via positive regulation of PTEN.* Proc Natl Acad Sci U S A, 2006. **103**: p. 12093-12097.
24. Stoyanov, B., et al., *Cloning and characterization of a G protein-activated human phosphoinositide-3 kinase.* Science, 1995. **269**: p. 690-693.
25. Hooshmand-Rad, R., et al., *The PI 3-kinase isoforms p110(alpha) and p110(beta) have differential roles in PDGF- and insulin-mediated signaling.* J Cell Sci, 2000. **113 Pt 2**: p. 207-14.
26. Arcaro, A., et al., *Two distinct phosphoinositide 3-kinases mediate polypeptide growth factor-stimulated PKB activation.* EMBO J, 2002. **21**(19): p. 5097-108.
27. Jia, S., et al., *Essential roles of PI(3)K-p110beta in cell growth, metabolism and tumorigenesis.* Nature, 2008. **454**: p. 776-9.
28. Jiang, X., et al., *Phosphoinositide 3-kinase pathway activation in phosphate and tensin homolog (PTEN)-deficient prostate cancer cells is independent of receptor tyrosine kinases and mediated by the p110beta and p110delta catalytic subunits.* J Biol Chem, 2010. **285**(20): p. 14980-9.
29. Foukas, L.C., et al., *Activity of any class IA PI3K isoform can sustain cell proliferation and survival.* Proc Natl Acad Sci U S A, 2010. **107**(25): p. 11381-6.
30. Berenjeno, I.M., et al., *Both p110alpha and p110beta isoforms of PI3K can modulate the impact of loss-of-function of the PTEN tumour suppressor.* Biochem J, 2012. **442**(1): p. 151-9.
31. Kang, S., et al., *Oncogenic transformation induced by the p110beta, -gamma, and -delta isoforms of class I phosphoinositide 3-kinase.* Proc Natl Acad Sci U S A, 2006. **103**(5): p. 1289-94.
32. Vanhaesebroeck, B., et al., *P110delta, a novel phosphoinositide 3-kinase in leukocytes.* Proc Natl Acad Sci U S A, 1997. **94**: p. 4330-4335.

33. Aksoy, E., et al., *The p110delta isoform of the kinase PI(3)K controls the subcellular compartmentalization of TLR4 signaling and protects from endotoxic shock.* Nat Immunol, 2012. **13**(11): p. 1045-54.
34. Okkenhaug, K. and B. Vanhaesebroeck, *PI3K in lymphocyte development, differentiation and activation.* Nat Rev Immunol, 2003. **3**(4): p. 317-30.
35. Okkenhaug, K. and B. Vanhaesebroeck, *PI3K-signalling in B- and T-cells: insights from gene-targeted mice.* Biochem Soc Trans, 2003. **31**(Pt 1): p. 270-4.
36. Okkenhaug, K., et al., *Impaired B and T cell antigen receptor signaling in p110delta PI 3-kinase mutant mice.* Science, 2002. **297**(5583): p. 1031-4.
37. Maxwell, M.J., et al., *Attenuation of phosphoinositide 3-kinase delta signaling restrains autoimmune disease.* J Autoimmun, 2012. **38**(4): p. 381-91.
38. Yamany, T., et al., *Erythema multiforme-like reaction with mucosal involvement following administration of idelalisib for relapse of chronic lymphocytic leukemia.* Leuk Lymphoma, 2014: p. 1-2.
39. Chung, C. and R. Lee, *Ibrutinib, obinutuzumab, idelalisib, and beyond: review of novel and evolving therapies for chronic lymphocytic leukemia.* Pharmacotherapy, 2014. **34**(12): p. 1298-316.
40. Brown, J.R., *Idelalisib for chronic lymphocytic leukemia.* Clin Adv Hematol Oncol, 2014. **12**(12): p. 846-8.
41. Khan, M., et al., *Idelalisib for the treatment of chronic lymphocytic leukemia.* ISRN Oncol, 2014. **2014**: p. 931858.
42. Brown, J.R., et al., *Idelalisib, an inhibitor of phosphatidylinositol 3-kinase p110delta, for relapsed/refractory chronic lymphocytic leukemia.* Blood, 2014. **123**(22): p. 3390-7.
43. Stephens, L., et al., *A heterotrimeric GTPase-regulated isoform of PI3K and the regulation of its potential effectors.* Philosophical transactions of the Royal Society of London. Series B, Biological sciences, 1996. **351**: p. 211-5.
44. Lopez-Ilasaca, M., et al., *Linkage of G protein-coupled receptors to the MAPK signaling pathway through PI 3-kinase gamma.* Science, 1997. **275**: p. 394-397.
45. Stephens, L.R., et al., *The G beta gamma sensitivity of a PI3K is dependent upon a tightly associated adaptor, p101.* Cell, 1997. **89**(1): p. 105-14.
46. Voigt, P., M.B. Dorner, and M. Schaefer, *Characterization of p87PIKAP, a novel regulatory subunit of phosphoinositide 3-kinase gamma that is highly expressed in heart and interacts with PDE3B.* J Biol Chem, 2006. **281**(15): p. 9977-86.
47. Brock, C., et al., *Roles of G beta gamma in membrane recruitment and activation of p110 gamma/p101 phosphoinositide 3-kinase gamma.* J Cell Biol, 2003. **160**(1): p. 89-99.

48. Czupalla, C., et al., *Identification and characterization of the autophosphorylation sites of phosphoinositide 3-kinase isoforms beta and gamma.* J Biol Chem, 2003. **278**(13): p. 11536-45.
49. Steck, P.A., et al., *Identification of a candidate tumour suppressor gene, MMAC1, at chromosome 10q23.3 that is mutated in multiple advanced cancers.* Nat Genet, 1997. **15**(4): p. 356-62.
50. Tashiro, H., et al., *Mutations in PTEN are frequent in endometrial carcinoma but rare in other common gynecological malignancies.* Cancer Res, 1997. **57**(18): p. 3935-40.
51. Rasheed, B.K., et al., *PTEN gene mutations are seen in high-grade but not in low-grade gliomas.* Cancer Res, 1997. **57**(19): p. 4187-90.
52. Wang, S.I., et al., *Somatic mutations of PTEN in glioblastoma multiforme.* Cancer Res, 1997. **57**(19): p. 4183-6.
53. Li, J., et al., *PTEN, a putative protein tyrosine phosphatase gene mutated in human brain, breast, and prostate cancer.* Science, 1997. **275**(5308): p. 1943-7.
54. Li, J., et al., *The PTEN/MMAC1 tumor suppressor induces cell death that is rescued by the AKT/protein kinase B oncogene.* Cancer Res, 1998. **58**(24): p. 5667-72.
55. Simpson, L. and R. Parsons, *PTEN: life as a tumor suppressor.* Exp Cell Res, 2001. **264**(1): p. 29-41.
56. Sulis, M.L. and R. Parsons, *PTEN: from pathology to biology.* Trends Cell Biol, 2003. **13**(9): p. 478-83.
57. Parsons, R. and L. Simpson, *PTEN and cancer.* Methods Mol Biol, 2003. **222**: p. 147-66.
58. Parsons, R., *Human cancer, PTEN and the PI-3 kinase pathway.* Semin Cell Dev Biol, 2004. **15**(2): p. 171-6.
59. Gericke, A., M. Munson, and A.H. Ross, *Regulation of the PTEN phosphatase.* Gene, 2006. **374**: p. 1-9.
60. Georgescu, M.M., et al., *Stabilization and productive positioning roles of the C2 domain of PTEN tumor suppressor.* Cancer Res, 2000. **60**(24): p. 7033-8.
61. Wisniewski, D., et al., *A novel SH2-containing phosphatidylinositol 3,4,5-trisphosphate 5-phosphatase (SHIP2) is constitutively tyrosine phosphorylated and associated with src homologous and collagen gene (SHC) in chronic myelogenous leukemia progenitor cells.* Blood, 1999. **93**(8): p. 2707-20.
62. Hejna, J.A., et al., *Cloning and characterization of a human cDNA (INPPL1) sharing homology with inositol polyphosphate phosphatases.* Genomics, 1995. **29**(1): p. 285-7.
63. Pesesse, X., et al., *The SH2 domain containing inositol 5-phosphatase SHIP2 displays phosphatidylinositol 3,4,5-trisphosphate and inositol 1,3,4,5-tetrakisphosphate 5-phosphatase activity.* FEBS Lett, 1998. **437**(3): p. 301-3.

64. Habib, T., et al., *Growth factors and insulin stimulate tyrosine phosphorylation of the 51C/SHIP2 protein.* J Biol Chem, 1998. **273**(29): p. 18605-9.
65. Bruyns, C., et al., *The two SH2-domain-containing inositol 5-phosphatases SHIP1 and SHIP2 are coexpressed in human T lymphocytes.* Biol Chem, 1999. **380**(7-8): p. 969-74.
66. Blero, D., et al., *The SH2 domain containing inositol 5-phosphatase SHIP2 controls phosphatidylinositol 3,4,5-trisphosphate levels in CHO-IR cells stimulated by insulin.* Biochem Biophys Res Commun, 2001. **282**(3): p. 839-43.
67. Pesesse, X., et al., *The Src homology 2 domain containing inositol 5-phosphatase SHIP2 is recruited to the epidermal growth factor (EGF) receptor and dephosphorylates phosphatidylinositol 3,4,5-trisphosphate in EGF-stimulated COS-7 cells.* J Biol Chem, 2001. **276**(30): p. 28348-55.
68. Clement, S., et al., *The lipid phosphatase SHIP2 controls insulin sensitivity.* Nature, 2001. **409**(6816): p. 92-7.
69. Leahey, A.M., L.R. Charnas, and R.L. Nussbaum, *Nonsense mutations in the OCRL-1 gene in patients with the oculocerebrorenal syndrome of Lowe.* Hum Mol Genet, 1993. **2**(4): p. 461-3.
70. Ungewickell, A., et al., *The inositol polyphosphate 5-phosphatase Ocrl associates with endosomes that are partially coated with clathrin.* Proc Natl Acad Sci U S A, 2004. **101**(37): p. 13501-6.
71. Razidlo, G.L., D. Katafiasz, and G.S. Taylor, *Myotubularin regulates Akt-dependent survival signaling via phosphatidylinositol 3-phosphate.* The Journal of biological chemistry, 2011. **286**: p. 20005-19.
72. Karnoub, A.E. and R.A. Weinberg, *Ras oncogenes: split personalities.* Nat Rev Mol Cell Biol, 2008. **9**(7): p. 517-31.
73. Marengere, L.E., et al., *SH2 domain specificity and activity modified by a single residue.* Nature, 1994. **369**: p. 502-505.
74. Sakaue, M., D. Bowtell, and M. Kasuga, *A dominant-negative mutant of mSOS1 inhibits insulin-induced Ras activation and reveals Ras-dependent and -independent insulin signaling pathways.* Mol Cell Biol, 1995. **15**: p. 379-388.
75. Wood, K.W., et al., *ras mediates nerve growth factor receptor modulation of three signal-transducing protein kinases: MAP kinase, Raf-1, and RSK.* Cell, 1992. **68**(6): p. 1041-50.
76. Avruch, J., X.F. Zhang, and J.M. Kyriakis, *Raf meets Ras: completing the framework of a signal transduction pathway.* Trends Biochem Sci, 1994. **19**(7): p. 279-83.
77. Macdonald, S.G., et al., *Reconstitution of the Raf-1-MEK-ERK signal transduction pathway in vitro.* Mol Cell Biol, 1993. **13**(11): p. 6615-20.
78. Crews, C.M., A.A. Alessandrini, and R.L. Erikson, *Mouse Erk-1 gene product is a serine/threonine protein kinase that has the potential to phosphorylate tyrosine.* Proc Natl Acad Sci U S A, 1991. **88**: p. 8845-8849.

79. Crews, C.M., A. Alessandrini, and R.L. Erikson, *Erks: their fifteen minutes has arrived.* Cell Growth Differ, 1992. **3**: p. 135-142.
80. Crews, C.M., A. Alessandrini, and R.L. Erikson, *The primary structure of MEK, a protein kinase that phosphorylates the ERK gene product.* Science, 1992. **258**(5081): p. 478-80.
81. Marais, R., J. Wynne, and R. Treisman, *The SRF accessory protein Elk-1 contains a growth factor-regulated transcriptional activation domain.* Cell, 1993. **73**(2): p. 381-93.
82. Cruzalegui, F.H., E. Cano, and R. Treisman, *ERK activation induces phosphorylation of Elk-1 at multiple S/T-P motifs to high stoichiometry.* Oncogene, 1999. **18**(56): p. 7948-57.
83. Grove, J.R., et al., *Regulation of an epitope-tagged recombinant Rsk-1 S6 kinase by phorbol ester and erk/MAP kinase.* Biochemistry, 1993. **32**: p. 7727-7738.
84. Dalby, K.N., et al., *Identification of regulatory phosphorylation sites in mitogen-activated protein kinase (MAPK)-activated protein kinase-1a/p90rsk that are inducible by MAPK.* J Biol Chem, 1998. **273**(3): p. 1496-505.
85. Deak, M., et al., *Mitogen- and stress-activated protein kinase-1 (MSK1) is directly activated by MAPK and SAPK2/p38, and may mediate activation of CREB.* EMBO J, 1998. **17**(15): p. 4426-41.
86. Guan, K.L., et al., *Negative regulation of the serine/threonine kinase B-Raf by Akt.* J Biol Chem, 2000. **275**(35): p. 27354-9.
87. Chen, B., et al., *BRAFV600E negatively regulates the AKT pathway in melanoma cell lines.* PLoS One, 2012. **7**(8): p. e42598.
88. Hayashi, H., et al., *Down-regulation of the PI3-kinase/Akt pathway by ERK MAP kinase in growth factor signaling.* Genes Cells, 2008. **13**(9): p. 941-7.
89. Naegele, S. and S.J. Morley, *Molecular cross-talk between MEK1/2 and mTOR signaling during recovery of 293 cells from hypertonic stress.* J Biol Chem, 2004. **279**: p. 46023-46034.
90. Ma, L., et al., *Phosphorylation and functional inactivation of TSC2 by Erk implications for tuberous sclerosis and cancer pathogenesis.* Cell, 2005. **121**: p. 179-193.
91. Arvisais, E.W., et al., *AKT-independent phosphorylation of TSC2 and activation of mTOR and ribosomal protein S6 kinase signaling by prostaglandin F2alpha.* J Biol Chem, 2006. **281**: p. 26904-26913.
92. Ma, L., et al., *Identification of S664 TSC2 phosphorylation as a marker for extracellular signal-regulated kinase mediated mTOR activation in tuberous sclerosis and human cancer.* Cancer Res, 2007. **67**: p. 7106-7112.
93. Roux, P.P., et al., *Tumor-promoting phorbol esters and activated Ras inactivate the tuberous sclerosis tumor suppressor complex via p90 ribosomal S6 kinase.* Proc Natl Acad Sci U S A, 2004. **101**: p. 13489-13494.

94. Rodriguez-Viciana, P., et al., *Phosphatidylinositol-3-OH kinase as a direct target of Ras.* Nature, 1994. **370**: p. 527-532.
95. Kodaki, T., et al., *The activation of phosphatidylinositol 3-kinase by Ras.* Curr Biol, 1994. **4**: p. 798-806.
96. Downward, J., *KSR: a novel player in the RAS pathway [comment].* Cell, 1995. **83**: p. 831-834.
97. Rodriguez-Viciana, P., et al., *Activation of phosphoinositide 3-kinase by interaction with Ras and by point mutation.* EMBO J, 1996. **15**: p. 2442-2451.
98. Rodriguez-Viciana, P., et al., *Phosphatidylinositol 3' kinase: one of the effectors of Ras.* Philos Trans R Soc Lond B Biol Sci, 1996. **351**: p. 222-225.
99. Rubio, I., et al., *Interaction of Ras with phosphoinositide 3-kinase gamma.* Biochem J, 1997. **326**: p. 891-895.
100. Rodriguez-Viciana, P., et al., *Role of phosphoinositide 3-OH kinase in cell transformation and control of the actin cytoskeleton by Ras.* Cell, 1997. **89**: p. 457-467.
101. Gupta, S., et al., *Binding of ras to phosphoinositide 3-kinase p110alpha is required for ras-driven tumorigenesis in mice.* Cell, 2007. **129**: p. 957-68.
102. Alessi, D.R., et al., *3-Phosphoinositide-dependent protein kinase-1 (PDK1): structural and functional homology with the Drosophila DSTPK61 kinase.* Curr Biol, 1997. **7**: p. 776-789.
103. Alessi, D.R., et al., *Characterization of a 3-phosphoinositide-dependent protein kinase which phosphorylates and activates protein kinase Balpha.* Curr Biol, 1997. **7**: p. 261-269.
104. Cohen, P., D.R. Alessi, and D.A. Cross, *PDK1, one of the missing links in insulin signal transduction?* FEBS Lett, 1997. **410**: p. 3-10.
105. Alessi, D.R., et al., *Mechanism of activation of protein kinase B by insulin and IGF-1.* EMBO J, 1996. **15**: p. 6541-6551.
106. Datta, K., et al., *Akt is a direct target of the phosphatidylinositol 3-kinase. Activation by growth factors, v-src and v-Ha-ras, in Sf9 and mammalian cells.* J Biol Chem, 1996. **271**: p. 30835-30839.
107. Currie, R.A., et al., *Role of phosphatidylinositol 3,4,5-trisphosphate in regulating the activity and localization of 3-phosphoinositide-dependent protein kinase-1.* Biochem J, 1999. **337 (Pt 3)**: p. 575-83.
108. Williams, M.R., et al., *The role of 3-phosphoinositide-dependent protein kinase 1 in activating AGC kinases defined in embryonic stem cells.* Curr Biol, 2000. **10**: p. 439-48.
109. Frodin, M., et al., *A phosphoserine-regulated docking site in the protein kinase RSK2 that recruits and activates PDK1.* EMBO J, 2000. **19**(12): p. 2924-34.
110. Jensen, C.J., et al., *90-kDa ribosomal S6 kinase is phosphorylated and activated by 3-phosphoinositide-dependent protein kinase-1.* J Biol Chem, 1999. **274**: p. 27168-76.

111. Richards, S.A., et al., *Ribosomal S6 kinase 1 (RSK1) activation requires signals dependent on and independent of the MAP kinase ERK.* Curr Biol, 1999. **9**: p. 810-20.
112. Staal, S.P., *Molecular cloning of the akt oncogene and its human homologues AKT1 and AKT2: amplification of AKT1 in a primary human gastric adenocarcinoma.* Proc Natl Acad Sci U S A, 1987. **84**: p. 5034-5037.
113. Staal, S.P., et al., *The AKT1 proto-oncogene maps to human chromosome 14, band q32.* Genomics, 1988. **2**: p. 96-98.
114. Staal, S.P. and J.W. Hartley, *Thymic lymphoma induction by the AKT8 murine retrovirus.* J Exp Med, 1988. **167**: p. 1259-1264.
115. Dummler, B. and B.a. Hemmings, *Physiological roles of PKB/Akt isoforms in development and disease.* Biochemical Society transactions, 2007. **35**: p. 231-5.
116. Bellacosa, A., et al., *Structure, expression and chromosomal mapping of c-akt: relationship to v-akt and its implications.* Oncogene, 1993. **8**: p. 745-754.
117. Bellacosa, A., et al., *Akt activation by growth factors is a multiple-step process: the role of the PH domain.* Oncogene, 1998. **17**: p. 313-325.
118. Toker, A. and A.C. Newton, *Akt/protein kinase B is regulated by autophosphorylation at the hypothetical PDK-2 site.* J Biol Chem, 2000. **275**: p. 8271-8274.
119. Sarbassov, D.D., et al., *Phosphorylation and regulation of Akt/PKB by the rictor-mTOR complex.* Science, 2005. **307**: p. 1098-1101.
120. Guertin, D.A. and D.M. Sabatini, *Defining the role of mTOR in cancer.* Cancer Cell, 2007. **12**: p. 9-22.
121. Guertin, D.A., et al., *Ablation in mice of the mTORC components raptor, rictor, or mLST8 reveals that mTORC2 is required for signaling to Akt-FOXO and PKCalpha, but not S6K1.* Dev Cell, 2006. **11**: p. 859-871.
122. Zeigerer, A. and M. Lampson, *GLUT4 retention in adipocytes requires two intracellular insulin-regulated transport steps.* Molecular biology of …, 2002. **13**: p. 2421-2435.
123. Zhou, Q.L., et al., *Akt substrate TBC1D1 regulates GLUT1 expression through the mTOR pathway in 3T3-L1 adipocytes.* Biochem J, 2008. **411**: p. 647-655.
124. Ramm, G., et al., *A role for 14-3-3 in insulin-stimulated GLUT4 translocation through its interaction with the RabGAP AS160.* J Biol Chem, 2006. **281**(39): p. 29174-80.
125. Srivastava, A.K. and S.K. Pandey, *Potential mechanism(s) involved in the regulation of glycogen synthesis by insulin.* Mol Cell Biochem, 1998. **182**(1-2): p. 135-41.
126. Cross, D.A., et al., *Inhibition of glycogen synthase kinase-3 by insulin mediated by protein kinase B.* Nature, 1995. **378**: p. 785-789.
127. Brunet, A., et al., *Akt promotes cell survival by phosphorylating and inhibiting a Forkhead transcription factor.* Cell, 1999. **96**: p. 857-868.

128. Greer, E.L. and A. Brunet, *FOXO transcription factors in ageing and cancer.* Acta Physiol (Oxf), 2008. **192**(1): p. 19-28.
129. Greer, E.L. and A. Brunet, *FOXO transcription factors at the interface between longevity and tumor suppression.* Oncogene, 2005. **24**(50): p. 7410-25.
130. Franke, T.F. and L.C. Cantley, *Apoptosis. A Bad kinase makes good.* Nature, 1997. **390**: p. 116-117.
131. Datta, S.R., et al., *Akt phosphorylation of BAD couples survival signals to the cell-intrinsic death machinery.* Cell, 1997. **91**: p. 231-241.
132. Peterson, R.T. and S.L. Schreiber, *Kinase phosphorylation: Keeping it all in the family.* Curr Biol, 1999. **9**: p. R521-4.
133. Pearce, L.R., D. Komander, and D.R. Alessi, *The nuts and bolts of AGC protein kinases.* Nature reviews. Molecular cell biology, 2010. **11**: p. 9-22.
134. Biondi, R.M., et al., *The PIF-binding pocket in PDK1 is essential for activation of S6K and SGK, but not PKB.* EMBO J, 2001. **20**: p. 4380-90.
135. Brunet, A., et al., *Protein kinase SGK mediates survival signals by phosphorylating the forkhead transcription factor FKHRL1 (FOXO3a).* Mol Cell Biol, 2001. **21**: p. 952-965.
136. Vasudevan, K.M., et al., *AKT-independent signaling downstream of oncogenic PIK3CA mutations in human cancer.* Cancer cell, 2009. **16**: p. 21-32.
137. Vezina, C., A. Kudelski, and S.N. Sehgal, *Rapamycin (AY-22,989), a new antifungal antibiotic. I. Taxonomy of the producing streptomycete and isolation of the active principle.* J Antibiot (Tokyo), 1975. **28**: p. 721-726.
138. Sehgal, S.N., H. Baker, and C. Vezina, *Rapamycin (AY-22,989), a new antifungal antibiotic. II. Fermentation, isolation and characterization.* J Antibiot (Tokyo), 1975. **28**: p. 727-732.
139. Baker, H., et al., *Rapamycin (AY-22,989), a new antifungal antibiotic. III. In vitro and in vivo evaluation.* J Antibiot (Tokyo), 1978. **31**: p. 539-545.
140. Singh, K., S. Sun, and C. Vezina, *Rapamycin (AY-22,989), a new antifungal antibiotic. IV. Mechanism of action.* J Antibiot (Tokyo), 1979. **32**: p. 630-645.
141. Martel, R.R., J. Klicius, and S. Galet, *Inhibition of the immune response by rapamycin, a new antifungal antibiotic.* Can J Physiol Pharmacol, 1977. **55**: p. 48-51.
142. Brown, E.J., et al., *A mammalian protein targeted by G1-arresting rapamycin-receptor complex.* Nature, 1994. **369**: p. 756-758.
143. Sabatini, D.M., et al., *RAFT1: a mammalian protein that binds to FKBP12 in a rapamycin-dependent fashion and is homologous to yeast TORs.* Cell, 1994. **78**: p. 35-43.
144. Koser, P.L., et al., *The tyrosine89 residue of yeast FKBP12 is required for rapamycin binding.* Gene, 1993. **129**: p. 159-165.

145. Chiu, M.I., H. Katz, and V. Berlin, *RAPT1, a mammalian homolog of yeast Tor, interacts with the FKBP12/rapamycin complex.* Proc Natl Acad Sci U S A, 1994. **91**: p. 12574-12578.
146. Stan, R., et al., *Interaction between FKBP12-rapamycin and TOR involves a conserved serine residue.* J Biol Chem, 1994. **269**: p. 32027-32030.
147. Heitman, J., et al., *FK506-binding protein proline isomerase is a target for the immunosuppressant rapamycin.* Proc. Natl. Acad. Sci., 1991. **88**: p. 1948-1952.
148. Lempiainen, H. and T.D. Halazonetis, *Emerging common themes in regulation of PIKKs and PI3Ks.* EMBO J, 2009. **28**(20): p. 3067-73.
149. Sabatini, D.M., et al., *The rapamycin and FKBP12 target (RAFT) displays phosphatidylinositol 4-kinase activity.* J Biol Chem, 1995. **270**: p. 20875-20878.
150. Kunz, J., et al., *Target of rapamycin in yeast, TOR2, is an essential phosphatidylinositol kinase homolog required for G1 progression.* Cell, 1993. **73**: p. 585-596.
151. Burnett, P.E., et al., *RAFT1 phosphorylation of the translational regulators p70 S6 kinase and 4E-BP1.* PNAS, 1998. **95**: p. 1432-1437.
152. Hara, K., et al., *Raptor, a Binding Partner of Target of Rapamycin (TOR), Mediates TOR Action.* Cell, 2002. **110**: p. 177-89.
153. Kim, D.-H.H., et al., *mTOR Interacts with Raptor to Form a Nutrient-Sensitive Complex that Signals to the Cell Growth Machinery.* Cell, 2002. **110**: p. 163-175.
154. Lee-Fruman, K.K., et al., *Characterization of S6K2, a novel kinase homologous to S6K1.* Oncogene, 1999. **18**: p. 5108-14.
155. Dufner, a. and G. Thomas, *Ribosomal S6 kinase signaling and the control of translation.* Experimental cell research, 1999. **253**: p. 100-9.
156. Khaleghpour, K., et al., *Translational homeostasis: eukaryotic translation initiation factor 4E control of 4E-binding protein 1 and p70 S6 kinase activities.* Molecular and cellular biology, 1999. **19**: p. 4302-10.
157. Iiboshi, Y., et al., *Amino acid-dependent control of p70(s6k). Involvement of tRNA aminoacylation in the regulation.* J Biol Chem, 1999. **274**: p. 1092-9.
158. Fingar, D.C., et al., *Mammalian cell size is controlled by mTOR and its downstream targets S6K1 and 4EBP1/eIF4E.* Genes Dev, 2002. **16**: p. 1472-87.
159. Clohessy, J.G., M. Reschke, and P.P. Pandolfi, *Found in translation of mTOR signaling.* Cell Res, 2012. **22**: p. 1315-1318.
160. Thoreen, C.C., et al., *A unifying model for mTORC1-mediated regulation of mRNA translation.* Nature, 2012. **485**: p. 109-113.
161. Thomas, G. and M.N. Hall, *TOR signalling and control of cell growth.* Curr Opin Cell Biol, 1997. **9**: p. 782-7.

162. Ohanna, M., et al., *Atrophy of S6K1(-/-) skeletal muscle cells reveals distinct mTOR effectors for cell cycle and size control.* Nat Cell Biol, 2005. **7**: p. 286-294.
163. Stocker, H., et al., *Rheb is an essential regulator of S6K in controlling cell growth in Drosophila.* Nat Cell Biol, 2003. **5**: p. 559-565.
164. Kozma, S.C. and G. Thomas, *Regulation of cell size in growth, development and human disease: PI3K, PKB and S6K.* Bioessays, 2002. **24**: p. 65-71.
165. Potter, C.J., L.G. Pedraza, and T. Xu, *Akt regulates growth by directly phosphorylating Tsc2.* Nat Cell Biol, 2002. **4**: p. 658-65.
166. Inoki, K., et al., *TSC2 is phosphorylated and inhibited by Akt and suppresses mTOR signalling.* Nat Cell Biol, 2002. **12**: p. 12.
167. Castro, A.F., et al., *Rheb binds tuberous sclerosis complex 2 (TSC2) and promotes S6 kinase activation in a rapamycin- and farnesylation-dependent manner.* J Biol Chem, 2003. **278**: p. 32493-32496.
168. Manning, B.D. and L.C. Cantley, *Rheb fills a GAP between TSC and TOR.* Trends Biochem Sci, 2003. **28**: p. 573-576.
169. Kwiatkowski, D.J., *Rhebbing up mTOR: new insights on TSC1 and TSC2, and the pathogenesis of tuberous sclerosis.* Cancer Biol Ther, 2003. **2**: p. 471-476.
170. Inoki, K., et al., *Rheb GTPase is a direct target of TSC2 GAP activity and regulates mTOR signaling.* Genes Dev, 2003. **17**: p. 1829-1834.
171. Zhang, Y., et al., *Rheb is a direct target of the tuberous sclerosis tumour suppressor proteins.* Nat Cell Biol, 2003. **5**: p. 578-581.
172. Tee, A.R., et al., *Tuberous sclerosis complex gene products, Tuberin and Hamartin, control mTOR signaling by acting as a GTPase-activating protein complex toward Rheb.* Curr Biol, 2003. **13**: p. 1259-1268.
173. Saucedo, L.J., et al., *Rheb promotes cell growth as a component of the insulin/TOR signalling network.* Nat Cell Biol, 2003. **5**: p. 566-571.
174. Garami, A., et al., *Insulin activation of Rheb, a mediator of mTOR/S6K/4E-BP signaling, is inhibited by TSC1 and 2.* Mol Cell, 2003. **11**: p. 1457-1466.
175. Long, X., et al., *Rheb binds and regulates the mTOR kinase.* Curr Biol, 2005. **15**: p. 702-713.
176. Tee, A.R., J. Blenis, and C.G. Proud, *Analysis of mTOR signaling by the small G-proteins, Rheb and RhebL1.* FEBS Lett, 2005. **579**: p. 4763-4768.
177. Thedieck, K., et al., *PRAS40 and PRR5-like protein are new mTOR interactors that regulate apoptosis.* PloS one, 2007. **2**: p. e1217.
178. Sancak, Y., et al., *PRAS40 is an insulin-regulated inhibitor of the mTORC1 protein kinase.* Mol Cell, 2007. **25**: p. 903-915.
179. Oshiro, N., et al., *The proline-Rich Akt substrate of 40 kDa (PRAS40) is a physiological substrate of mTOR complex 1.* J Biol Chem, 2007.

180. Fonseca, B.D., et al., *PRAS40 is a target for mammalian target of rapamycin complex 1 and is required for signaling downstream of this complex.* The Journal of biological chemistry, 2007. **282**: p. 24514-24.
181. Laplante, M. and D.M. Sabatini, *mTOR Signaling.* Cold Spring Harb Perspect Biol, 2012. **4**.
182. Efeyan, A., R. Zoncu, and D.M. Sabatini, *Amino acids and mTORC1: from lysosomes to disease.* Trends Mol Med, 2012. **18**: p. 524-533.
183. Sancak, Y., et al., *The Rag GTPases bind raptor and mediate amino acid signaling to mTORC1.* Science (New York, N.Y.), 2008. **320**: p. 1496-501.
184. Sancak, Y., et al., *Ragulator-Rag complex targets mTORC1 to the lysosomal surface and is necessary for its activation by amino acids.* Cell, 2010. **141**: p. 290-303.
185. Zoncu, R., et al., *mTORC1 senses lysosomal amino acids through an inside-out mechanism that requires the vacuolar H(+)-ATPase.* Science, 2011. **334**: p. 678-683.
186. Bar-Peled, L., et al., *A Tumor suppressor complex with GAP activity for the Rag GTPases that signal amino acid sufficiency to mTORC1.* Science, 2013. **340**(6136): p. 1100-6.
187. Balendran, A., et al., *PDK1 acquires PDK2 activity in the presence of a synthetic peptide derived from the carboxyl terminus of PRK2.* Curr Biol, 1999. **9**: p. 393-404.
188. Chan, T.O. and P.N. Tsichlis, *PDK2: a complex tail in one Akt.* Sci STKE, 2001. **2001**: p. PE1.
189. Hresko, R.C., H. Murata, and M. Mueckler, *Phosphoinositide-dependent kinase-2 is a distinct protein kinase enriched in a novel cytoskeletal fraction associated with adipocyte plasma membranes.* J Biol Chem, 2003. **278**: p. 21615-21622.
190. Partovian, C. and M. Simons, *Regulation of protein kinase B/Akt activity and Ser473 phosphorylation by protein kinase Calpha in endothelial cells.* Cellular signalling, 2004. **16**: p. 951-7.
191. Viniegra, J.G., et al., *Full activation of PKB/Akt in response to insulin or ionizing radiation is mediated through ATM.* The Journal of biological chemistry, 2005. **280**: p. 4029-36.
192. Feng, J., et al., *Identification of a PKB/Akt Hydrophobic Motif Ser-473 Kinase as DNA-dependent Protein Kinase.* J Biol Chem, 2004. **279**: p. 41189-41196.
193. Persad, S., et al., *Regulation of protein kinase B/Akt-serine 473 phosphorylation by integrin-linked kinase: critical roles for kinase activity and amino acids arginine 211 and serine 343.* J Biol Chem, 2001. **276**: p. 27462-27469.
194. Persad, S., et al., *Inhibition of integrin-linked kinase (ILK) suppresses activation of protein kinase B/Akt and induces cell cycle arrest and apoptosis of PTEN-mutant prostate cancer cells.* Proceedings of the National Academy of Sciences of the United States of America, 2000. **97**: p. 3207-12.

195. Hresko, R.C. and M. Mueckler, *mTOR/RICTOR is the Ser473 kinase for Akt/PKB in 3T3-L1 adipocytes.* J Biol Chem, 2005. **280**: p. 40406-40416.
196. Sarbassov, D.D., et al., *Rictor, a novel binding partner of mTOR, defines a rapamycin-insensitive and raptor-independent pathway that regulates the cytoskeleton.* Curr Biol, 2004. **14**(14): p. 1296-302.
197. Yan, L., V. Mieulet, and R.F. Lamb, *mTORC2 is the hydrophobic motif kinase for SGK1.* The Biochemical journal, 2008. **416**: p. e19-21.
198. Kim, D.-H.H., et al., *GbetaL, a positive regulator of the rapamycin-sensitive pathway required for the nutrient-sensitive interaction between raptor and mTOR.* Molecular cell, 2003. **11**: p. 895-904.
199. Yang, Q., et al., *Identification of Sin1 as an essential TORC2 component required for complex formation and kinase activity.* Genes Dev, 2006. **20**: p. 2820-2832.
200. Jacinto, E., et al., *SIN1/MIP1 maintains rictor-mTOR complex integrity and regulates Akt phosphorylation and substrate specificity.* Cell, 2006. **127**: p. 125-37.
201. Frias, M.a., et al., *mSin1 is necessary for Akt/PKB phosphorylation, and its isoforms define three distinct mTORC2s.* Current biology : CB, 2006. **16**: p. 1865-70.
202. Lu, M., et al., *mSIN1 protein mediates SGK1 protein interaction with mTORC2 protein complex and is required for selective activation of the epithelial sodium channel.* J Biol Chem, 2011. **286**(35): p. 30647-54.
203. Facchinetti, V., et al., *The mammalian target of rapamycin complex 2 controls folding and stability of Akt and protein kinase C.* The EMBO journal, 2008. **27**: p. 1932-43.
204. Hall, M.N., *mTOR-what does it do?* Transplant Proc, 2008. **40**: p. S5-8.
205. Woo, S.-Y.Y., et al., *PRR5, a novel component of mTOR complex 2, regulates platelet-derived growth factor receptor beta expression and signaling.* J Biol Chem, 2007. **282**: p. 25604-25612.
206. Pearce, L.R., et al., *Identification of Protor as a novel Rictor-binding component of mTOR complex-2.* Biochem J, 2007. **405**: p. 513-522.
207. Pearce, L.R., et al., *Protor-1 is required for efficient mTORC2-mediated activation of SGK1 in the kidney.* Biochem J, 2011. **436**(1): p. 169-79.
208. Peterson, T.R., et al., *DEPTOR is an mTOR inhibitor frequently overexpressed in multiple myeloma cells and required for their survival.* Cell, 2009. **137**: p. 873-886.
209. Laplante, M., et al., *DEPTOR cell-autonomously promotes adipogenesis, and its expression is associated with obesity.* Cell Metab, 2012. **16**: p. 202-212.
210. Pederson, T.M., D.L. Kramer, and C.M. Rondinone, *Serine/threonine phosphorylation of IRS-1 triggers its degradation: possible regulation by tyrosine phosphorylation.* Diabetes, 2001. **50**(1): p. 24-31.
211. Sun, X.J., et al., *Insulin-induced insulin receptor substrate-1 degradation is mediated by the proteasome degradation pathway.* Diabetes, 1999. **48**: p. 1359-1364.

212. Tzatsos, A. and K.V. Kandror, *Nutrients suppress phosphatidylinositol 3-kinase/Akt signaling via raptor-dependent mTOR-mediated insulin receptor substrate 1 phosphorylation.* Mol Cell Biol, 2006. **26**: p. 63-76.
213. Gual, P., et al., *MAP kinases and mTOR mediate insulin-induced phosphorylation of insulin receptor substrate-1 on serine residues 307, 612 and 632.* Diabetologia, 2003. **46**: p. 1532-1542.
214. Carlson, C.J., M.F. White, and C.M. Rondinone, *Mammalian target of rapamycin regulates IRS-1 serine 307 phosphorylation.* Biochem Biophys Res Commun, 2004. **316**: p. 533-539.
215. Hiratani, K., et al., *Roles of mTOR and JNK in serine phosphorylation, translocation, and degradation of IRS-1.* Biochem Biophys Res Commun, 2005. **335**: p. 836-842.
216. Yu, Y., et al., *Phosphoproteomic analysis identifies Grb10 as an mTORC1 substrate that negatively regulates insulin signaling.* Science, 2011. **332**: p. 1322-1326.
217. Yea, S.S. and D.A. Fruman, *Cell signaling. New mTOR targets Grb attention.* Science, 2011. **332**: p. 1270-1271.
218. Yu, Y., S. Yoon, and G. Poulogiannis, *Quantitative Phosphoproteomic Analysis Identifies the Adaptor Protein Grb10 as an mTORC1 Substrate that Negatively Regulates Insulin Signaling.* Science (New York, …, 2011. **332**: p. 1322-1326.
219. O'Reilly, K.E., et al., *mTOR inhibition induces upstream receptor tyrosine kinase signaling and activates Akt.* Cancer Res, 2006. **66**: p. 1500-1508.
220. Easton, J.B., R.T. Kurmasheva, and P.J. Houghton, *IRS-1: auditing the effectiveness of mTOR inhibitors.* Cancer Cell, 2006. **9**: p. 153-155.
221. Sawyers, C.L., *Will mTOR inhibitors make it as cancer drugs?* Cancer Cell, 2003. **4**: p. 343-348.
222. Gera, J.F., et al., *AKT activity determines sensitivity to mammalian target of rapamycin (mTOR) inhibitors by regulating cyclin D1 and c-myc expression.* J Biol Chem, 2004. **279**: p. 2737-2746.
223. Hanahan, D. and R.a. Weinberg, *Hallmarks of cancer: the next generation.* Cell, 2011. **144**: p. 646-74.
224. Bader, A.G., S. Kang, and P.K. Vogt, *Cancer-specific mutations in PIK3CA are oncogenic in vivo.* Proc Natl Acad Sci U S A, 2006. **103**(5): p. 1475-9.
225. Vivanco, I. and C.L. Sawyers, *The phosphatidylinositol 3-Kinase AKT pathway in human cancer.* Nat Rev Cancer, 2002. **2**: p. 489-501.
226. Philp, A.J., et al., *The phosphatidylinositol 3'-kinase p85alpha gene is an oncogene in human ovarian and colon tumors.* Cancer Res, 2001. **61**(20): p. 7426-9.
227. Jimenez, C., et al., *Identification and characterization of a new oncogene derived from the regulatory subunit of phosphoinositide 3-kinase.* EMBO J, 1998. **17**: p. 743-753.
228. Ndubaku, C.O., et al., *Discovery of 2-{3-[2-(1-isopropyl-3-methyl-1H-1,2-4-triazol-5-yl)-5,6-dihydrobenzo[f]imidazo[1 ,2-d][1,4]oxazepin-9-yl]-*

1H-pyrazol-1-yl}-2-methylpropanamide (GDC-0032): a beta-sparing phosphoinositide 3-kinase inhibitor with high unbound exposure and robust in vivo antitumor activity. J Med Chem, 2013. **56**(11): p. 4597-610.
229. Mueller, S., et al., *PTEN promoter methylation and activation of the PI3K/Akt/mTOR pathway in pediatric gliomas and influence on clinical outcome.* Neuro Oncol, 2012. **14**: p. 1146-1152.
230. Vlietstra, R.J., et al., *Frequent inactivation of PTEN in prostate cancer cell lines and xenografts.* Cancer Res, 1998. **58**: p. 2720-2723.
231. Liaw, D., et al., *Germline mutations of the PTEN gene in Cowden disease, an inherited breast and thyroid cancer syndrome.* Nat Genet, 1997. **16**(1): p. 64-7.
232. Dahia, P.L., et al., *Somatic deletions and mutations in the Cowden disease gene, PTEN, in sporadic thyroid tumors.* Cancer Res, 1997. **57**(21): p. 4710-3.
233. Trotman, L.C., et al., *Pten dose dictates cancer progression in the prostate.* PLoS biology, 2003. **1**: p. E59.
234. Ma, L., et al., *Genetic analysis of Pten and Tsc2 functional interactions in the mouse reveals asymmetrical haploinsufficiency in tumor suppression.* Genes Dev, 2005. **19**: p. 1779-1786.
235. Hopkins, B.D., et al., *A secreted PTEN phosphatase that enters cells to alter signaling and survival.* Science, 2013. **341**(6144): p. 399-402.
236. Kadota, M., et al., *Identification of novel gene amplifications in breast cancer and coexistence of gene amplification with an activating mutation of PIK3CA.* Cancer Res, 2009. **69**(18): p. 7357-65.
237. Lee, J.C., et al., *Epidermal growth factor receptor activation in glioblastoma through novel missense mutations in the extracellular domain.* PLoS medicine, 2006. **3**: p. e485.
238. Gong, H., et al., *A comparative study of affibody, panitumumab, and EGF for near-infrared fluorescence imaging of EGFR- and EGFRvIII-expressing tumors.* Cancer Biol Ther, 2013. **15**(2).
239. Tanaka, K., et al., *Oncogenic EGFR signaling activates an mTORC2-NF-κB pathway that promotes chemotherapy resistance.* Cancer discovery, 2011. **1**: p. 524-38.
240. Carpten, J.D., et al., *A transforming mutation in the pleckstrin homology domain of AKT1 in cancer.* Nature, 2007. **448**: p. 439-44.
241. Bleeker, F.E., et al., *AKT1(E17K) in human solid tumours.* Oncogene, 2008. **27**: p. 5648-50.
242. Malanga, D., et al., *Activating E17K mutation in the gene encoding the protein kinase AKT1 in a subset of squamous cell carcinoma of the lung.* Cell Cycle, 2008: p. 665-669.
243. Lauring, J., et al., *Knock in of the AKT1 E17K mutation in human breast epithelial cells does not recapitulate oncogenic PIK3CA mutations.* Oncogene, 2010. **29**(16): p. 2337-45.

244. Murugan, A.K., A. Alzahrani, and M. Xing, *Mutations in critical domains confer the human mTOR gene strong tumorigenicity.* J Biol Chem, 2013. **288**(9): p. 6511-21.
245. Brian Grabiner and David M. Sabatini`, personal communication.
246. Leyland-Jones, B., *Trastuzumab: hopes and realities.* Lancet Oncol, 2002. **3**(3): p. 137-44.
247. Hegedus, C., et al., *Interaction of nilotinib, dasatinib and bosutinib with ABCB1 and ABCG2: implications for altered anti-cancer effects and pharmacological properties.* Br J Pharmacol, 2009. **158**(4): p. 1153-64.
248. Redaelli, S., et al., *Activity of bosutinib, dasatinib, and nilotinib against 18 imatinib-resistant BCR/ABL mutants.* J Clin Oncol, 2009. **27**(3): p. 469-71.
249. Remsing Rix, L.L., et al., *Global target profile of the kinase inhibitor bosutinib in primary chronic myeloid leukemia cells.* Leukemia, 2009. **23**(3): p. 477-85.
250. Perry, C.M. and L.R. Wiseman, *Trastuzumab.* BioDrugs, 1999. **12**(2): p. 129-35.
251. Albanell, J. and J. Baselga, *Trastuzumab, a humanized anti-HER2 monoclonal antibody, for the treatment of breast cancer.* Drugs Today (Barc), 1999. **35**(12): p. 931-46.
252. Gong, S.J., et al., *Growth inhibitory effects of trastuzumab and chemotherapeutic drugs in gastric cancer cell lines.* Cancer Lett, 2004. **214**(2): p. 215-24.
253. Rebischung, C., et al., *The effectiveness of trastuzumab (Herceptin) combined with chemotherapy for gastric carcinoma with overexpression of the c-erbB-2 protein.* Gastric Cancer, 2005. **8**(4): p. 249-52.
254. Nahta, R., M.C. Hung, and F.J. Esteva, *The HER-2-targeting antibodies trastuzumab and pertuzumab synergistically inhibit the survival of breast cancer cells.* Cancer Res, 2004. **64**(7): p. 2343-6.
255. Kawaguchi, Y., et al., *Targeting EGFR and HER-2 with cetuximab- and trastuzumab-mediated immunotherapy in oesophageal squamous cell carcinoma.* Br J Cancer, 2007. **97**(4): p. 494-501.
256. Tyagi, P., *Recent results and ongoing trials with panitumumab (ABX-EGF), a fully human anti-epidermal growth factor receptor antibody, in metastatic colorectal cancer.* Clin Colorectal Cancer, 2005. **5**(1): p. 21-3.
257. Konecny, G.E., et al., *Activity of the dual kinase inhibitor lapatinib (GW572016) against HER-2-overexpressing and trastuzumab-treated breast cancer cells.* Cancer Res, 2006. **66**(3): p. 1630-9.
258. Herbst, R.S., et al., *TRIBUTE: a phase III trial of erlotinib hydrochloride (OSI-774) combined with carboplatin and paclitaxel chemotherapy in advanced non-small-cell lung cancer.* Journal of clinical oncology : official journal of the American Society of Clinical Oncology, 2005. **23**: p. 5892-9.

259. Paez, J.G., et al., *EGFR mutations in lung cancer: correlation with clinical response to gefitinib therapy.* Science (New York, N.Y.), 2004. **304**: p. 1497-500.
260. Owonikoko, T.K. and F.R. Khuri, *Targeting the PI3K/AKT/mTOR Pathway.* Am Soc Clin Oncol Educ Book, 2013: p. 395-401.
261. Furet, P., et al., *Discovery of NVP-BYL719 a potent and selective phosphatidylinositol-3 kinase alpha inhibitor selected for clinical evaluation.* Bioorg Med Chem Lett, 2013. **23**(13): p. 3741-8.
262. Sturgeon, S.A., et al., *Advantages of a selective beta-isoform phosphoinositide 3-kinase antagonist, an anti-thrombotic agent devoid of other cardiovascular actions in the rat.* Eur J Pharmacol, 2008. **587**(1-3): p. 209-15.
263. Martini, M., et al., *Targeting PI3K in Cancer: Any Good News?* Front Oncol, 2013. **3**: p. 108.
264. Hudis, C., et al., *A phase 1 study evaluating the combination of an allosteric AKT inhibitor (MK-2206) and trastuzumab in patients with HER2-positive solid tumors.* Breast Cancer Res, 2013. **15**(6): p. R110.
265. LoPiccolo, J., et al., *Targeting the PI3K/Akt/mTOR pathway: effective combinations and clinical considerations.* Drug Resist Updat, 2008. **11**: p. 32-50.
266. Lin, J., et al., *Targeting activated Akt with GDC-0068, a novel selective Akt inhibitor that is efficacious in multiple tumor models.* Clin Cancer Res, 2013. **19**(7): p. 1760-72.
267. Blake, J.F., et al., *Discovery and preclinical pharmacology of a selective ATP-competitive Akt inhibitor (GDC-0068) for the treatment of human tumors.* J Med Chem, 2012. **55**(18): p. 8110-27.
268. Cho, D.C., et al., *Two phase 2 trials of the novel Akt inhibitor perifosine in patients with advanced renal cell carcinoma after progression on vascular endothelial growth factor-targeted therapy.* Cancer, 2012. **118**(24): p. 6055-62.
269. Yan, Y., et al., *Evaluation and Clinical Analyses of Downstream Targets of the Akt Inhibitor GDC-0068.* Clin Cancer Res, 2013.
270. Hudes, G., et al., *Temsirolimus, interferon alfa, or both for advanced renal-cell carcinoma.* The New England journal of medicine, 2007. **356**: p. 2271-81.
271. Voss, M.H., A.M. Molina, and R.J. Motzer, *mTOR inhibitors in advanced renal cell carcinoma.* Hematol Oncol Clin North Am, 2011. **25**: p. 835-852.
272. Wheler, J.J., et al., *Anastrozole and everolimus in advanced gynecologic and breast malignancies: activity and molecular alterations in the PI3K/AKT/mTOR pathway.* Oncotarget, 2014. **5**(10): p. 3029-38.
273. Piccart, M., et al., *Everolimus plus exemestane for hormone-receptor-positive, human epidermal growth factor receptor-2-negative advanced breast cancer: overall survival results from BOLERO-2dagger.* Ann Oncol, 2014. **25**(12): p. 2357-62.

274. Rugo, H.S., et al., *Incidence and time course of everolimus-related adverse events in postmenopausal women with hormone receptor-positive advanced breast cancer: insights from BOLERO-2.* Ann Oncol, 2014. **25**(4): p. 808-15.
275. Bachelot, T., et al., *Comparative efficacy of everolimus plus exemestane versus fulvestrant for hormone-receptor-positive advanced breast cancer following progression/recurrence after endocrine therapy: a network meta-analysis.* Breast Cancer Res Treat, 2014. **143**(1): p. 125-33.
276. Burgess, M.R. and C.L. Sawyers, *Treating imatinib-resistant leukemia: the next generation targeted therapies.* TheScientificWorldJournal, 2006. **6**: p. 918-30.
277. Furic, L., et al., *Targeting mTOR-dependent tumours with specific inhibitors: a model for personalized medicine based on molecular diagnoses.* Curr Oncol, 2009. **16**: p. 59-61.
278. Carter, T.a., et al., *Inhibition of drug-resistant mutants of ABL, KIT, and EGF receptor kinases.* Proceedings of the National Academy of Sciences of the United States of America, 2005. **102**: p. 11011-6.
279. Young, M.a., et al., *Structure of the kinase domain of an imatinib-resistant Abl mutant in complex with the Aurora kinase inhibitor VX-680.* Cancer research, 2006. **66**: p. 1007-14.
280. Skaggs, B.J., et al., *Phosphorylation of the ATP-binding loop directs oncogenicity of drug-resistant BCR-ABL mutants.* Proceedings of the National Academy of Sciences of the United States of America, 2006. **103**: p. 19466-71.
281. Ercan, D., et al., *Reactivation of ERK signaling causes resistance to EGFR kinase inhibitors.* Cancer Discov, 2012. **2**(10): p. 934-47.
282. Bivona, T.G., et al., *FAS and NF-κB signalling modulate dependence of lung cancers on mutant EGFR.* Nature, 2011. **471**: p. 523-6.
283. Hunter, C.P., *Genetics: a touch of elegance with RNAi.* Curr Biol, 1999. **9**(12): p. R440-2.
284. Sharp, P.A., *RNAi and double-strand RNA.* Genes Dev, 1999. **13**(2): p. 139-41.
285. Murchison, E.P. and G.J. Hannon, *miRNAs on the move: miRNA biogenesis and the RNAi machinery.* Curr Opin Cell Biol, 2004. **16**(3): p. 223-9.
286. Tijsterman, M. and R.H. Plasterk, *Dicers at RISC; the mechanism of RNAi.* Cell, 2004. **117**(1): p. 1-3.
287. Hutvagner, G., *Small RNA asymmetry in RNAi: function in RISC assembly and gene regulation.* FEBS Lett, 2005. **579**(26): p. 5850-7.
288. Filipowicz, W., *RNAi: the nuts and bolts of the RISC machine.* Cell, 2005. **122**(1): p. 17-20.
289. Brummelkamp, T.R., R. Bernards, and R. Agami, *A system for stable expression of short interfering RNAs in mammalian cells.* Science (New York, N.Y.), 2002. **296**: p. 550-3.

290. Paddison, P.J., A.A. Caudy, and G.J. Hannon, *Stable suppression of gene expression by RNAi in mammalian cells.* Proc Natl Acad Sci U S A, 2002. **99**(3): p. 1443-8.
291. Stewart, S.A., et al., *Lentivirus-delivered stable gene silencing by RNAi in primary cells.* RNA, 2003. **9**: p. 493-501.
292. Rubinson, D.A., et al., *A lentivirus-based system to functionally silence genes in primary mammalian cells, stem cells and transgenic mice by RNA interference.* Nat Genet, 2003. **33**: p. 401-406.
293. Shi, Y., *Mammalian RNAi for the masses.* Trends Genet, 2003. **19**(1): p. 9-12.
294. Sumimoto, H. and Y. Kawakami, *Lentiviral vector-mediated RNAi and its use for cancer research.* Future Oncol, 2007. **3**(6): p. 655-64.
295. Berns, K., et al., *A large-scale RNAi screen in human cells identifies new components of the p53 pathway.* Nature, 2004. **428**: p. 431-7.
296. Brummelkamp, T.R., et al., *Loss of the cylindromatosis tumour suppressor inhibits apoptosis by activating NF-kappaB.* Nature, 2003. **424**: p. 797-801.
297. Brummelkamp, T.R. and R. Bernards, *New tools for functional mammalian cancer genetics.* Nat Rev Cancer, 2003. **3**: p. 781-789.
298. Friedman, A. and N. Perrimon, *A functional RNAi screen for regulators of receptor tyrosine kinase and ERK signalling.* Nature, 2006. **444**: p. 230-4.
299. Philips, J.a., E.J. Rubin, and N. Perrimon, *Drosophila RNAi screen reveals CD36 family member required for mycobacterial infection.* Science (New York, N.Y.), 2005. **309**: p. 1251-3.
300. Boutros, M., et al., *Genome-wide RNAi analysis of growth and viability in Drosophila cells.* Science, 2004. **303**: p. 832-835.
301. Kiger, A., et al., *A functional genomic analysis of cell morphology using RNA interference.* J Biol, 2003. **2**: p. 27.
302. Moffat, J. and D.M. Sabatini, *Building mammalian signalling pathways with RNAi screens.* Nat Rev Mol Cell Biol, 2006. **7**: p. 177-187.
303. Moffat, J., et al., *A lentiviral RNAi library for human and mouse genes applied to an arrayed viral high-content screen.* Cell, 2006. **124**: p. 1283-1298.
304. Brummelkamp, T.R., et al., *An shRNA barcode screen provides insight into cancer cell vulnerability to MDM2 inhibitors.* Nature chemical biology, 2006. **2**: p. 202-6.
305. Luo, B., et al., *Highly parallel identification of essential genes in cancer cells.* Proc Natl Acad Sci U S A, 2008. **105**: p. 20380-20385.
306. Zender, L., et al., *An oncogenomics-based in vivo RNAi screen identifies tumor suppressors in liver cancer.* Cell, 2008. **135**: p. 852-64.
307. Hannon, G.J. and J.J. Rossi, *Unlocking the potential of the human genome with RNA interference.* Nature, 2004. **431**: p. 371-378.
308. Paddison, P.J., et al., *A resource for large-scale RNA-interference-based screens in mammals.* Nature, 2004. **428**: p. 427-431.

309. Mohr, S.E. and N. Perrimon, *RNAi screening: new approaches, understandings, and organisms.* Wiley Interdiscip Rev RNA, 2012. **3**(2): p. 145-58.
310. Possemato, R., et al., *Functional genomics reveal that the serine synthesis pathway is essential in breast cancer.* Nature, 2011. **476**: p. 346-350.
311. Perrimon, N., J.Q. Ni, and L. Perkins, *In vivo RNAi: today and tomorrow.* Cold Spring Harb Perspect Biol, 2010. **2**(8): p. a003640.
312. Lee, A.J., R. Kolesnick, and C. Swanton, *RNAi-mediated functional analysis of pathways influencing cancer cell drug resistance.* Expert Rev Mol Med, 2009. **11**: p. e15.
313. Friedman, A. and N. Perrimon, *Genetic screening for signal transduction in the era of network biology.* Cell, 2007. **128**: p. 225-31.
314. Perrimon, N., et al., *Drug-target identification in Drosophila cells: combining high-throughout RNAi and small-molecule screens.* Drug discovery today, 2007. **12**: p. 28-33.
315. Root, D.E., et al., *Genome-scale loss-of-function screening with a lentiviral RNAi library.* Nat Methods, 2006. **3**: p. 715-719.
316. Shaw, R.J. and L.C. Cantley, *Ras, PI(3)K and mTOR signalling controls tumour cell growth.* Nature, 2006. **441**: p. 424-430.
317. Cantley, L.C., *The phosphoinositide 3-kinase pathway.* Science, 2002. **296**: p. 1655-1657.
318. Katso, R., et al., *Cellular function of phosphoinositide 3-kinases: implications for development, homeostasis, and cancer.* Annu Rev Cell Dev Biol, 2001. **17**: p. 615-75.
319. Hennessy, B.T., et al., *Exploiting the PI3K/AKT pathway for cancer drug discovery.* Nature reviews. Drug discovery, 2005. **4**: p. 988-1004.
320. Zhang, J.-h.H., T.D.Y. Chung, and K.R. Oldenburg, *A Simple Statistical Parameter for Use in Evaluation and Validation of High Throughput Screening Assays.* J Biomol Screen, 1999. **4**: p. 67-73.
321. Gao, J., et al., *Integrative Analysis of Complex Cancer Genomics and Clinical Profiles Using the cBioPortal.* Science Signaling, 2013. **6**: p. pl1-pl1.
322. Cerami, E., et al., *The cBio cancer genomics portal: an open platform for exploring multidimensional cancer genomics data.* Cancer discovery, 2012. **2**: p. 401-4.
323. Forbes, S.A., et al., *COSMIC: mining complete cancer genomes in the Catalogue of Somatic Mutations in Cancer.* Nucleic Acids Res, 2011. **39**(Database issue): p. D945-50.
324. Forbes, S.A., et al., *COSMIC (the Catalogue of Somatic Mutations in Cancer): a resource to investigate acquired mutations in human cancer.* Nucleic Acids Res, 2010. **38**(Database issue): p. D652-7.
325. Forbes, S.A., et al., *The Catalogue of Somatic Mutations in Cancer (COSMIC).* Curr Protoc Hum Genet, 2008. **Chapter 10**: p. Unit 10 11.
326. Bamford, S., et al., *The COSMIC (Catalogue of Somatic Mutations in Cancer) database and website.* Br J Cancer, 2004. **91**(2): p. 355-8.

327. Sonkin, D., et al., *Tumor suppressors status in cancer cell line encyclopedia.* Mol Oncol, 2013. **7**(4): p. 791-8.
328. Marum, L., *Cancer Cell Line Encyclopedia launched by Novartis and Broad Institute.* Future Med Chem, 2012. **4**(8): p. 947.
329. Barretina, J., et al., *The Cancer Cell Line Encyclopedia enables predictive modelling of anticancer drug sensitivity.* Nature, 2012. **483**(7391): p. 603-7.
330. Sancak, Y., et al., *The Rag GTPases Bind Raptor and Mediate Amino Acid Signaling to mTORC1.* Science, 2008. **320**: p. 1496-1501.
331. Ali, S.M. and D.M. Sabatini, *Structure of S6 kinase 1 determines whether raptor-mTOR or rictor-mTOR phosphorylates its hydrophobic motif site.* J Biol Chem, 2005. **280**: p. 19445-19448.
332. Zhao, J.J., et al., *Human mammary epithelial cell transformation through the activation of phosphatidylinositol 3-kinase.* Cancer cell, 2003. **3**: p. 483-95.
333. Sarbassov, D.D., et al., *Isolation of the mTOR complexes by affinity purification.* Methods Mol Biol, 2012. **821**: p. 59-74.
334. Clark, G.J., et al., *Biological assays for Ras transformation.* Methods Enzymol, 1995. **255**: p. 395-412.
335. Cox, A.D. and C.J. Der, *Biological assays for cellular transformation.* Methods Enzymol, 1994. **238**: p. 277-94.
336. Dambournet, D., et al., *Rab35 GTPase and OCRL phosphatase remodel lipids and F-actin for successful cytokinesis.* Nat Cell Biol, 2011. **13**: p. 981-988.
337. Allaire, P.D., et al., *The Connecdenn DENN domain: a GEF for Rab35 mediating cargo-specific exit from early endosomes.* Mol Cell, 2010. **37**: p. 370-382.
338. Chua, C.E., Y.S. Lim, and B.L. Tang, *Rab35--a vesicular traffic-regulating small GTPase with actin modulating roles.* FEBS Lett, 2010. **584**: p. 1-6.
339. Zhang, J., et al., *Rab35 controls actin bundling by recruiting fascin as an effector protein.* Science, 2009. **325**: p. 1250-1254.
340. Chaineau, M., M.S. Ioannou, and P.S. McPherson, *Rab35: GEFs, GAPs and Effectors.* Traffic, 2013.
341. Bayascas, J.R. and D.R. Alessi, *Regulation of Akt/PKB Ser473 phosphorylation.* Mol Cell, 2005. **18**(2): p. 143-5.
342. Mora, A., et al., *PDK1, the master regulator of AGC kinase signal transduction.* Semin Cell Dev Biol, 2004. **15**: p. 161-170.
343. Huang, J., *An in vitro assay for the kinase activity of mTOR complex 2.* Methods Mol Biol, 2012. **821**: p. 75-86.
344. Sarbassov, D.D., et al., *Prolonged rapamycin treatment inhibits mTORC2 assembly and Akt/PKB.* Mol Cell, 2006. **22**: p. 159-168.
345. Sarbassov, D.D., et al., *Phosphorylation and regulation of Akt/PKB by the rictor-mTOR complex.* Science, 2005. **307**(5712): p. 1098-101.

346. Scheid, M.P., P.A. Marignani, and J.R. Woodgett, *Multiple phosphoinositide 3-kinase-dependent steps in activation of protein kinase B.* Mol Cell Biol, 2002. **22**: p. 6247-6260.
347. Zhao, Y., X. Xiong, and Y. Sun, *DEPTOR, an mTOR inhibitor, is a physiological substrate of SCF(betaTrCP) E3 ubiquitin ligase and regulates survival and autophagy.* Mol Cell, 2011. **44**: p. 304-316.
348. Kazi, A.A., et al., *Deptor knockdown enhances mTOR Activity and protein synthesis in myocytes and ameliorates disuse muscle atrophy.* Mol Med, 2011. **17**: p. 925-936.
349. Gao, D., et al., *mTOR drives its own activation via SCF(betaTrCP)-dependent degradation of the mTOR inhibitor DEPTOR.* Mol Cell, 2011. **44**: p. 290-303.
350. Sun, S.-Y.Y., et al., *Activation of Akt and eIF4E survival pathways by rapamycin-mediated mammalian target of rapamycin inhibition.* Cancer Res, 2005. **65**: p. 7052-7058.
351. Harrington, L.S., G.M. Findlay, and R.F. Lamb, *Restraining PI3K: mTOR signalling goes back to the membrane.* Trends Biochem Sci, 2005. **30**: p. 35-42.
352. Manning, B.D., et al., *Feedback inhibition of Akt signaling limits the growth of tumors lacking Tsc2.* Genes Dev, 2005. **19**: p. 1773-1778.
353. Wan, X., et al., *Rapamycin induces feedback activation of Akt signaling through an IGF-1R-dependent mechanism.* Oncogene, 2007. **26**: p. 1932-40.
354. Hsu, P.P., et al., *The mTOR-regulated phosphoproteome reveals a mechanism of mTORC1-mediated inhibition of growth factor signaling.* Science, 2011. **332**: p. 1317-1322.
355. Liu, Q., et al., *Development of ATP-competitive mTOR inhibitors.* Methods Mol Biol, 2012. **821**: p. 447-460.
356. Schenone, S., et al., *ATP-competitive inhibitors of mTOR: an update.* Curr Med Chem, 2011. **18**: p. 2995-3014.
357. Tyner, J.W., et al., *High-throughput sequencing screen reveals novel, transforming RAS mutations in myeloid leukemia patients.* Blood, 2009. **113**(8): p. 1749-55.
358. Janakiraman, M., et al., *Genomic and biological characterization of exon 4 KRAS mutations in human cancer.* Cancer Res, 2010. **70**(14): p. 5901-11.
359. Folkes, A.J., et al., *The identification of 2-(1H-indazol-4-yl)-6-(4-methanesulfonyl-piperazin-1-ylmethyl)-4-morpholin-4-yl-t hieno[3,2-d]pyrimidine (GDC-0941) as a potent, selective, orally bioavailable inhibitor of class I PI3 kinase for the treatment of cancer.* J Med Chem, 2008. **51**(18): p. 5522-32.
360. Wheeler et. al`, IDENTIFICATION OF AN ONCOGENIC RAB PROTEIN`, in submission
361. Davey, J.R., et al., *TBC1D13 is a RAB35 specific GAP that plays an important role in GLUT4 trafficking in adipocytes.* Traffic (Copenhagen, Denmark), 2012. **13**: p. 1429-41.

362. Davey, J.R., et al., *TBC1D13 is a RAB35 specific GAP that plays an important role in GLUT4 trafficking in adipocytes.* Traffic, 2012. **13**(10): p. 1429-41.
363. Zoncu, R., et al., *mTORC1 senses lysosomal amino acids through an inside-out mechanism that requires the vacuolar H(+)-ATPase.* Science, 2011. **334**(6056): p. 678-83.
364. Sarbassov, D.D., et al., *Rictor, a novel binding partner of mTOR, defines a rapamycin-insensitive and raptor-independent pathway that regulates the cytoskeleton.* Curr Biol, 2004. **14**: p. 1296-1302.
365. Lockwood, W.W., et al., *The novel ubiquitin ligase complex, SCF(Fbxw4), interacts with the COP9 signalosome in an F-box dependent manner, is mutated, lost and under-expressed in human cancers.* PLoS One, 2013. **8**(5): p. e63610.
366. Moulick, K., et al., *Affinity-based proteomics reveal cancer-specific networks coordinated by Hsp90.* Nat Chem Biol, 2011. **7**(11): p. 818-26.
367. Downward, J., *Ras signalling and apoptosis.* Current Opinion in Genetics and Development, 1998. **8**: p. 49-54.
368. Downward, J., *Role of phosphoinositide-3-OH kinase in Ras signaling.* Adv Second Messenger Phosphoprotein Res, 1997. **31**: p. 1-10.
369. Khwaja, A., et al., *Matrix adhesion and Ras transformation both activate a phosphoinositide 3-OH kinase and protein kinase B/Akt cellular survival pathway.* EMBO J, 1997. **16**: p. 2783-2793.
370. Marte, B.M., et al., *R-Ras can activate the phosphoinositide 3-kinase but not the MAP kinase arm of the Ras effector pathways [published erratum appears in Curr Biol 1997 Mar 1; 7(3):197].* Curr Biol, 1997. **7**: p. 63-70.
371. Bar-Peled, L., et al., *Ragulator is a GEF for the rag GTPases that signal amino acid levels to mTORC1.* Cell, 2012. **150**: p. 1196-1208.
372. Chamberlain, M.D., et al., *The p85alpha subunit of phosphatidylinositol 3'-kinase binds to and stimulates the GTPase activity of Rab proteins.* The Journal of biological chemistry, 2004. **279**: p. 48607-14.
373. Patino-Lopez, G., et al., *Rab35 and its GAP EPI64C in T cells regulate receptor recycling and immunological synapse formation.* J Biol Chem, 2008. **283**: p. 18323-18330.
374. Kazlauskas, A. and J.A. Cooper, *Autophosphorylation of the PDGF receptor in the kinase insert region regulates interactions with cell proteins.* Cell, 1989. **58**(6): p. 1121-33.
375. Cama, A., et al., *Substitution of glutamic acid for alanine 1135 in the putative "catalytic loop" of the tyrosine kinase domain of the human insulin receptor. A mutation that impairs proteolytic processing into subunits and inhibits receptor tyrosine kinase activity.* J Biol Chem, 1993. **268**(11): p. 8060-9.
376. Ward, W.H., et al., *Epidermal growth factor receptor tyrosine kinase. Investigation of catalytic mechanism, structure-based searching and discovery of a potent inhibitor.* Biochem Pharmacol, 1994. **48**(4): p. 659-66.

377. Xu, B., V.G. Bird, and W.T. Miller, *Substrate specificities of the insulin and insulin-like growth factor 1 receptor tyrosine kinase catalytic domains.* J Biol Chem, 1995. **270**(50): p. 29825-30.
378. Songyang, Z., et al., *Catalytic specificity of protein-tyrosine kinases is critical for selective signalling.* Nature, 1995. **373**(6514): p. 536-9.
379. Sawyers, C.L., et al., *Imatinib induces hematologic and cytogenetic responses in patients with chronic myelogenous leukemia in myeloid blast crisis: results of a phase II study.* Blood, 2002. **99**: p. 3530-9.
380. Holtz, M.S., et al., *Imatinib mesylate (STI571) inhibits growth of primitive malignant progenitors in chronic myelogenous leukemia through reversal of abnormally increased proliferation.* Blood, 2002. **99**: p. 3792-800.
381. Fabian, M.A., et al., *A small molecule-kinase interaction map for clinical kinase inhibitors.* Nat Biotechnol, 2005. **23**: p. 329-336.
382. Chintalgattu, V., et al., *Coronary microvascular pericytes are the cellular target of sunitinib malate-induced cardiotoxicity.* Sci Transl Med, 2013. **5**(187): p. 187ra69.
383. Heinrich, M.C., et al., *Crenolanib inhibits the drug-resistant PDGFRA D842V mutation associated with imatinib-resistant gastrointestinal stromal tumors.* Clin Cancer Res, 2012. **18**(16): p. 4375-84.
384. Fathi, A.T., *Emergence of crenolanib for FLT3-mutant AML.* Blood, 2013. **122**(22): p. 3547-8.
385. Galanis, A., et al., *Crenolanib is a potent inhibitor of FLT3 with activity against resistance-conferring point mutants.* Blood, 2013.
386. *Crenolanib Is Effective Against Secondary FLT3 Mutations in AML.* Cancer Discov, 2013. **3**(11): p. 1215.
387. Zimmerman, E.I., et al., *Crenolanib is active against models of drug-resistant FLT3-ITD-positive acute myeloid leukemia.* Blood, 2013. **122**(22): p. 3607-15.
388. Haugh, J.M., et al., *Effect of epidermal growth factor receptor internalization on regulation of the phospholipase C-gamma1 signaling pathway.* The Journal of biological chemistry, 1999. **274**: p. 8958-65.
389. Burke, P., K. Schooler, and H.S. Wiley, *Regulation of epidermal growth factor receptor signaling by endocytosis and intracellular trafficking.* Molecular biology of the cell, 2001. **12**: p. 1897-910.
390. Wang, Y., et al., *Platelet-derived growth factor receptor-mediated signal transduction from endosomes.* The Journal of biological chemistry, 2004. **279**: p. 8038-46.
391. McCaffrey, G., et al., *High-resolution fractionation of signaling endosomes containing different receptors.* Traffic (Copenhagen, Denmark), 2009. **10**: p. 938-50.
392. Stenmark, H. and V. Olkkonen, *The Rab GTPase family.* Genome Biol, 2001: p. 1-7.
393. Jean, S. and A.A. Kiger, *Coordination between RAB GTPase and phosphoinositide regulation and functions.* Nat Rev Mol Cell Biol, 2012. **13**(7): p. 463-70.

394. Zerial, M. and H. Stenmark, *Rab GTPases in vesicular transport.* Curr Opin Cell Biol, 1993. **5**(4): p. 613-20.
395. Stenmark, H., *Rab GTPases as coordinators of vesicle traffic.* Nat Rev Mol Cell Biol, 2009. **10**(8): p. 513-25.
396. Gorvel, J.P., et al., *rab5 controls early endosome fusion in vitro.* Cell, 1991. **64**(5): p. 915-25.
397. Li, G. and P.D. Stahl, *Post-translational processing and membrane association of the two early endosome-associated rab GTP-binding proteins (rab4 and rab5).* Arch Biochem Biophys, 1993. **304**(2): p. 471-8.
398. Barbieri, M.A., et al., *Rab5, an early acting endosomal GTPase, supports in vitro endosome fusion without GTP hydrolysis.* J Biol Chem, 1994. **269**(29): p. 18720-2.
399. Li, G., et al., *Evidence for phosphatidylinositol 3-kinase as a regulator of endocytosis via activation of Rab5.* Proc Natl Acad Sci U S A, 1995. **92**: p. 10207-10211.
400. Barbieri, M.A., et al., *Rab5 regulates the dynamics of early endosome fusion.* Biocell, 1996. **20**(3): p. 331-8.
401. Gaullier, J.-m., et al., *EEA1 links PI(3)K function to Rab5 regulation of endosome fusion.* Nature, 1998. **394**: p. 2-6.
402. Christoforidis, S., et al., *Phosphatidylinositol-3-OH kinases are Rab5 effectors.* Nature cell biology, 1999. **1**: p. 249-52.
403. Lebrand, C., et al., *Late endosome motility depends on lipids via the small GTPase Rab7.* EMBO J, 2002. **21**(6): p. 1289-300.
404. Ceresa, B.P. and S.J. Bahr, *rab7 activity affects epidermal growth factor:epidermal growth factor receptor degradation by regulating endocytic trafficking from the late endosome.* J Biol Chem, 2006. **281**(2): p. 1099-106.
405. Urbe, S., et al., *Rab11, a small GTPase associated with both constitutive and regulated secretory pathways in PC12 cells.* FEBS letters, 1993. **334**: p. 175-182.
406. Ren, M., et al., *Hydrolysis of GTP on rab11 is required for the direct delivery of transferrin from the pericentriolar recycling compartment to the cell surface but not from sorting endosomes.* Proceedings of the National Academy of Sciences of the United States of America, 1998. **95**: p. 6187-92.
407. Chen, W., et al., *Rab11 is required for trans-golgi network-to-plasma membrane transport and a preferential target for GDP dissociation inhibitor.* Molecular biology of the cell, 1998. **9**: p. 3241-57.
408. Casanova, J.E., et al., *Association of Rab25 and Rab11a with the apical recycling system of polarized Madin-Darby canine kidney cells.* Molecular biology of the cell, 1999. **10**: p. 47-61.
409. Wang, X., et al., *Regulation of vesicle trafficking in madin-darby canine kidney cells by Rab11a and Rab25.* The Journal of biological chemistry, 2000. **275**: p. 29138-46.

410. Hales, C.M., et al., *Identification and characterization of a family of Rab11-interacting proteins.* The Journal of biological chemistry, 2001. **276**: p. 39067-75.
411. Lapierre, L.a., et al., *Rab11b resides in a vesicular compartment distinct from Rab11a in parietal cells and other epithelial cells.* Experimental Cell Research, 2003. **290**: p. 322-331.
412. Kannan, K., et al., *Lysosome-associated membrane proteins h-LAMP1 (CD107a) and h-LAMP2 (CD107b) are activation-dependent cell surface glycoproteins in human peripheral blood mononuclear cells which mediate cell adhesion to vascular endothelium.* Cell Immunol, 1996. **171**(1): p. 10-9.
413. Cook, N.R., P.E. Row, and H.W. Davidson, *Lysosome associated membrane protein 1 (Lamp1) traffics directly from the TGN to early endosomes.* Traffic, 2004. **5**(9): p. 685-99.
414. Chamberlain, M.D., et al., *Deregulation of Rab5 and Rab4 proteins in p85R274A-expressing cells alters PDGFR trafficking.* Cell Signal, 2010. **22**(10): p. 1562-75.
415. Bucci, C., et al., *Rab7: a key to lysosome biogenesis.* Mol Biol Cell, 2000. **11**(2): p. 467-80.
416. Abe, Y., et al., *A Small Ras-like protein Ray/Rab1c modulates the p53-regulating activity of PRPK.* Biochemical and biophysical research communications, 2006. **344**: p. 377-85.
417. Zhao, H., O. Ettala, and H.K. Vaananen, *Intracellular membrane trafficking pathways in bone-resorbing osteoclasts revealed by cloning and subcellular localization studies of small GTP-binding rab proteins.* Biochem Biophys Res Commun, 2002. **293**(3): p. 1060-5.
418. Mihai Gazdag, E., et al., *Mechanism of Rab1b deactivation by the Legionella pneumophila GAP LepB.* EMBO Rep, 2013. **14**(2): p. 199-205.
419. Nuoffer, C., et al., *A GDP-bound of rab1 inhibits protein export from the endoplasmic reticulum and transport between Golgi compartments.* J Cell Biol, 1994. **125**(2): p. 225-37.
420. Pind, S.N., et al., *Rab1 and Ca2+ are required for the fusion of carrier vesicles mediating endoplasmic reticulum to Golgi transport.* J Cell Biol, 1994. **125**(2): p. 239-52.
421. Kouranti, I., et al., *Rab35 regulates an endocytic recycling pathway essential for the terminal steps of cytokinesis.* Curr Biol, 2006. **16**: p. 1719-1725.
422. Echard, A., *Membrane traffic and polarization of lipid domains during cytokinesis.* Biochem Soc Trans, 2008. **36**(Pt 3): p. 395-9.
423. Hsu, C., et al., *Regulation of exosome secretion by Rab35 and its GTPase-activating proteins TBC1D10A-C.* J Cell Biol, 2010. **189**: p. 223-232.
424. Charrasse, S., et al., *Rab35 regulates cadherin-mediated adherens junction formation and myoblast fusion.* Molecular biology of the cell, 2013. **24**: p. 234-45.

425. Allaire, P.D., et al., *Interplay between Rab35 and Arf6 controls cargo recycling to coordinate cell adhesion and migration.* J Cell Sci, 2013. **126**(Pt 3): p. 722-31.
426. Allaire, P.D., et al., *Interplay between Rab35 and Arf6 controls cargo recycling to coordinate cell adhesion and recycling.* Journal of cell science, 2012.
427. Yoshimura, S.-i., et al., *Family-wide characterization of the DENN domain Rab GDP-GTP exchange factors.* The Journal of cell biology, 2010. **191**: p. 367-81.
428. Uytterhoeven, V., et al., *Loss of skywalker reveals synaptic endosomes as sorting stations for synaptic vesicle proteins.* Cell, 2011. **145**(1): p. 117-32.
429. Kobayashi, H. and M. Fukuda, *Rab35 regulates Arf6 activity through centaurin beta2/ACAP2 during neurite outgrowth.* J Cell Sci, 2012.
430. Chesneau, L., et al., *An ARF6/Rab35 GTPase cascade for endocytic recycling and successful cytokinesis.* Curr Biol, 2012. **22**: p. 147-153.
431. Kobayashi, H., et al., *Rab35 promotes the recruitment of Rab8, Rab13 and Rab36 to recycling endosomes through MICAL-L1 during neurite outgrowth.* Biol Open, 2014. **3**(9): p. 803-14.
432. Shim, J., et al., *Rab35 mediates transport of Cdc42 and Rac1 to the plasma membrane during phagocytosis.* Molecular and cellular biology, 2010. **30**: p. 1421-33.
433. Marat, A.L., M.S. Ioannou, and P.S. McPherson, *Connecdenn 3/DENND1C binds actin linking Rab35 activation to the actin cytoskeleton.* Mol Biol Cell, 2012. **23**: p. 163-175.
434. Prekeris, R., *Actin regulation during abscission: unexpected roles of Rab35 and endocytic transport.* Cell Res, 2011. **21**: p. 1283-1285.
435. Chevallier, J., et al., *Rab35 regulates neurite outgrowth and cell shape.* FEBS Lett, 2009. **583**: p. 1096-1101.
436. Vandenbroere, I., et al., *The c-Cbl-associated protein and c-Cbl are two new partners of the SH2-containing inositol polyphosphate 5-phosphatase SHIP2.* Biochem Biophys Res Commun, 2003. **300**(2): p. 494-500.
437. Grossmann, A.H., et al., *Catalytic domains of tyrosine kinases determine the phosphorylation sites within c-Cbl.* FEBS Lett, 2004. **577**(3): p. 555-62.
438. Muthuswamy, S.K., M. Gilman, and J.S. Brugge, *Controlled dimerization of ErbB receptors provides evidence for differential signaling by homo- and heterodimers.* Mol Cell Biol, 1999. **19**(10): p. 6845-57.
439. Sehat, B., et al., *Identification of c-Cbl as a new ligase for insulin-like growth factor-I receptor with distinct roles from Mdm2 in receptor ubiquitination and endocytosis.* Cancer Res, 2008. **68**(14): p. 5669-77.
440. Miyake, S., et al., *The tyrosine kinase regulator Cbl enhances the ubiquitination and degradation of the platelet-derived growth factor receptor alpha.* Proc Natl Acad Sci U S A, 1998. **95**(14): p. 7927-32.

441. Miyake, S., et al., *Cbl-mediated negative regulation of platelet-derived growth factor receptor-dependent cell proliferation. A critical role for Cbl tyrosine kinase-binding domain.* J Biol Chem, 1999. **274**(23): p. 16619-28.
442. Peschard, P., et al., *A conserved DpYR motif in the juxtamembrane domain of the Met receptor family forms an atypical c-Cbl/Cbl-b tyrosine kinase binding domain binding site required for suppression of oncogenic activation.* J Biol Chem, 2004. **279**(28): p. 29565-71.
443. Zeng, S., et al., *Regulation of stem cell factor receptor signaling by Cbl family proteins (Cbl-b/c-Cbl).* Blood, 2005. **105**(1): p. 226-32.
444. Duval, M., et al., *Vascular endothelial growth factor-dependent down-regulation of Flk-1/KDR involves Cbl-mediated ubiquitination. Consequences on nitric oxide production from endothelial cells.* J Biol Chem, 2003. **278**(22): p. 20091-7.
445. Truitt, L., et al., *The EphB6 receptor cooperates with c-Cbl to regulate the behavior of breast cancer cells.* Cancer Res, 2010. **70**(3): p. 1141-53.
446. Sharfe, N., et al., *Ephrin-A1 induces c-Cbl phosphorylation and EphA receptor down-regulation in T cells.* J Immunol, 2003. **170**(12): p. 6024-32.
447. Stasyk, T., et al., *Identification of endosomal epidermal growth factor receptor signaling targets by functional organelle proteomics.* Molecular & cellular proteomics : MCP, 2007. **6**: p. 908-22.
448. Murphy, J.E., et al., *Endosomes: a legitimate platform for the signaling train.* Proceedings of the National Academy of Sciences of the United States of America, 2009. **106**: p. 17615-22.
449. Wang, Y., et al., *Endosomal Signaling of Epidermal Growth Factor Receptor Stimulates Signal Transduction Pathways Leading to Cell Survival.* Molecular & Cellular Biology, 2002. **22**: p. 7279-7290.
450. Girard, E., et al., *The dynamin chemical inhibitor dynasore impairs cholesterol trafficking and sterol-sensitive genes transcription in human HeLa cells and macrophages.* PLoS One, 2011. **6**(12): p. e29042.
451. Douthitt, H.L., et al., *Dynasore, an inhibitor of dynamin, increases the probability of transmitter release.* Neuroscience, 2011. **172**: p. 187-95.
452. Young, A., et al., *Dynasore inhibits removal of wild-type and DeltaF508 cystic fibrosis transmembrane conductance regulator (CFTR) from the plasma membrane.* Biochem J, 2009. **421**(3): p. 377-85.
453. Chung, C.L., et al., *Dynasore, a dynamin inhibitor, induces PAI-1 expression in MeT-5A human pleural mesothelial cells.* Am J Respir Cell Mol Biol, 2009. **40**(6): p. 692-700.
454. Hay, J.C. and R.H. Scheller, *SNAREs and NSF in targeted membrane fusion.* Current opinion in cell biology, 1997. **9**: p. 505-12.
455. Subramaniam, V.N., E. Loh, and W. Hong, *N-Ethylmaleimide-sensitive factor (NSF) and alpha-soluble NSF attachment proteins (SNAP) mediate dissociation of GS28-syntaxin 5 Golgi SNAP receptors (SNARE) complex.* J Biol Chem, 1997. **272**(41): p. 25441-4.

456. Sollner, T., et al., *SNAP receptors implicated in vesicle targeting and fusion.* Nature, 1993. **362**(6418): p. 318-24.
457. Tibaldi, E., et al., *The tyrosine phosphatase SHP-1 inhibits proliferation of activated hepatic stellate cells by impairing PDGF receptor signaling.* Biochim Biophys Acta, 2013.
458. Bonita, D.P., et al., *Phosphotyrosine binding domain-dependent upregulation of the platelet-derived growth factor receptor alpha signaling cascade by transforming mutants of Cbl: implications for Cbl's function and oncogenicity.* Mol Cell Biol, 1997. **17**(8): p. 4597-610.
459. Zhang, H., et al., *PDGFRs are critical for PI3K/Akt activation and negatively regulated by mTOR.* J Clin Invest, 2007. **117**: p. 730-738.
460. Rosenkranz, S., et al., *Src family kinases negatively regulate platelet-derived growth factor alpha receptor-dependent signaling and disease progression.* The Journal of biological chemistry, 2000. **275**: p. 9620-7.
461. Bae, Y.S., et al., *Platelet-derived growth factor-induced H(2)O(2) production requires the activation of phosphatidylinositol 3-kinase.* The Journal of biological chemistry, 2000. **275**: p. 10527-31.
462. Baxter, R.M., et al., *Full activation of the platelet-derived growth factor beta-receptor kinase involves multiple events.* The Journal of biological chemistry, 1998. **273**: p. 17050-5.
463. Lei, H. and A. Kazlauskas, *Growth factors outside of the platelet-derived growth factor (PDGF) family employ reactive oxygen species/Src family kinases to activate PDGF receptor alpha and thereby promote proliferation and survival of cells.*, in *The Journal of biological chemistry*. 2009. p. 6329-36.
464. Saito, Y., et al., *Receptor heterodimerization: essential mechanism for platelet-derived growth factor-induced epidermal growth factor receptor transactivation.* Mol Cell Biol, 2001. **21**(19): p. 6387-94.
465. Meneely, P.M. and M.R. Willmann, *Advanced genetic analysis : genes, genomes, and networks in eukaryotes*. 2009, Oxford: Oxford University Press. xxvii, 542 p.
466. Cheung, L.W., et al., *Naturally occurring neomorphic PIK3R1 mutations activate the MAPK pathway, dictating therapeutic response to MAPK pathway inhibitors.* Cancer Cell, 2014. **26**(4): p. 479-94.
467. Quilliam, L.A., et al., *Biological and structural characterization of a Ras transforming mutation at the phenylalanine-156 residue, which is conserved in all members of the Ras superfamily.* Proc Natl Acad Sci U S A, 1995. **92**(5): p. 1272-6.
468. Poulikakos, P.I., et al., *RAF inhibitor resistance is mediated by dimerization of aberrantly spliced BRAF(V600E).* Nature, 2011. **480**: p. 387-90.
469. Atefi, M., et al., *Reversing melanoma cross-resistance to BRAF and MEK inhibitors by co-targeting the AKT/mTOR pathway.* PLoS One, 2011. **6**: p. e28973.

470. Poulikakos, P.I., et al., *RAF inhibitor resistance is mediated by dimerization of aberrantly spliced BRAF(V600E).* Nature, 2011. **480**(7377): p. 387-90.
471. Tuchman, M., et al., *The ornithine transcarbamylase gene: new "private" mutations in four patients and study of a polymorphism.* Hum Mutat, 1994. **3**(3): p. 318-20.
472. Tuchman, M., et al., *Identification of 'private' mutations in patients with ornithine transcarbamylase deficiency.* J Inherit Metab Dis, 1997. **20**(4): p. 525-7.
473. Hoglund, P., et al., *Clustering of private mutations in the congenital chloride diarrhea/down-regulated in adenoma gene.* Hum Mutat, 1998. **11**(4): p. 321-7.
474. Sawyers`, C.L.`; personal communication
475. Rahner, N., et al., *Nine novel pathogenic germline mutations in MLH1, MSH2, MSH6 and PMS2 in families with Lynch syndrome.* Acta Oncol, 2007. **46**(6): p. 763-9.
476. Mosesson, Y., G.B. Mills, and Y. Yarden, *Derailed endocytosis: an emerging feature of cancer.* Nat Rev Cancer, 2008. **8**(11): p. 835-50.
477. Yan, Z.F., et al., *Oncogenic c-Ki-ras but not oncogenic c-Ha-ras up-regulates CEA expression and disrupts basolateral polarity in colon epithelial cells.* Journal of Biological Chemistry, 1997. **272**(44): p. 27902-27907.
478. Rossi, F. and C. Gonzalez, *Synergism between altered cortical polarity and the PI3K/TOR pathway in the suppression of tumour growth.* EMBO Rep, 2012. **13**(2): p. 157-62.
479. Larue, L. and A. Bellacosa, *Epithelial-mesenchymal transition in development and cancer: role of phosphatidylinositol 3' kinase/AKT pathways.* Oncogene, 2005. **24**(50): p. 7443-54.
480. Joffre, C., et al., *A direct role for Met endocytosis in tumorigenesis.* Nature cell biology, 2011. **13**: p. 827-37.